Analyse et modélisation des trajectoires des dispositifs à concentration de poissons dérivants (DCP) dans les zones océaniques tropicales et estimation des risques associés à leur déploiement

Taha Imzilen

Sorbonne Université

École doctorale des sciences de l'environnement d'Île de France (N° 129)

IRD - Unité mixte de recherche MARBEC

Analyse et modélisation des trajectoires des dispositifs à concentration de poissons dérivants (DCP) dans les zones océaniques tropicales et estimation des risques associés à leur déploiement

Mesures de mitigation pour atténuer les risques de perte et échouage des DCP

Par Taha IMZILEN

Thèse de doctorat en Sciences de la mer

Dirigée par Christophe Lett et David Kaplan

Présentée et soutenue publiquement le 15 Décembre 2021

Devant un jury composé de :

Lars Stemmann, Professeur, Sorbonne Université	Président du jury
Christophe Maes, Chargé de Recherche, IRD, LOPS	Rapporteur
David Jose Die, Professeur associé, University of Miami	Rapporteur
Christophe Lett, Directeur de Recherche, IRD, MARBEC	Co-directeur de thèse
David Kaplan, Directeur de Recherche, IRD, MARBEC	Co-directeur de thèse
Alexandra Maufroy, Chargée de mission, ORTHONGEL	Invitée

Remerciements

Le doctorat est sans doute un travail difficile que rencontre un étudiant, et qui demande beaucoup d'engagement et d'autonomie. Pendant cette période, l'étudiant connaît certainement des moments de détermination et de gloire, mais il y a aussi des moments où l'hésitation et le doute se présentent. *De nombreuses personnes se retrouvent, pour le pire ou le meilleur, entre le doctorant et son doctorat. Ce sont certaines de ces personnes que j'aimerais mettre en avant dans ces remerciements.*

Je commencerais par remercier chaleureusement mes deux directeurs Christophe Lett et David Kaplan pour leur confiance, leur soutien et leur grande disponibilité. Avant de commencer ce projet ils ont consacré beaucoup de temps et d'effort dans le but de trouver un moyen de financement. Je tiens à leur témoigner ma gratitude aussi pour leur grande disponibilité, pour les nombreux conseils scientifiques et pour leur savoir et expertise qu'ils mont transmis durant ces trois ans de travail. J'aimerais également insister sur le coté humain, particulièrement pendant la période de la pandémie mondiale de Covid-19 qui n'a pas été facile pour moi et que j'ai surmonté grâce à leur soutien, merci.

Je remercie l'Institut de Recherche pour le Développement (IRD)-UMR MARBEC qui m'a permis de réaliser cette thèse au sein de la station marine de Sète. Ce travail a été co-financé par les projets européens de recherche CECOFAD2 (Specific Contract No 9 of EASME/EMFF/ 2016/008) et INNOV-FAD (European Maritime and Fisheries Fund, measure n ◦ 39, OSIRIS #PFEA390017FA1000004, and France Filière Pêche), et de L'Observatoire des Écosystèmes Pélagiques Tropicaux exploités (Ob7) de l'IRD.

Je tiens également à communiquer ma reconnaissance à Emmanuel Chassot qui a co-encadré cette thèse et qui, malgré la distance, m'a toujours soutenu par mail et en visio. Je remercie également Laurent Dagorn, Daniel Gaertner, Nicolas Barrier, Laurent Floch, Julien Lebranchu, Alexandra Maufroy et Michel Goujon pour m'avoir supporté et avoir contribué au bon avancement de ce travail. Je n'oublierai pas Hassan Rhinane, Aissa Benazzouz et Hervé Demarcq qui m'ont permis de rejoindre pour la première fois l'IRD pour faire mon stage de Master en 2013, et particulièrement Julien Barde qui ensuite m'a fait confiance et m'as permis de rester travailler à l'IRD et ainsi contribuer au développent de mes connaissances et mes compétences.

Un grand merci à chacune des personnes rencontrées à l'IRD et à Ifremer de Sète. Merci aux doctorants et aux collègues, malheureusement je ne pourrais pas vous citer tous mais sachez que vous avez rendu ces trois années mémorables. Merci au Docteur Audrey Hoarau pour ton soutien pendant les moments difficiles du confinement et durant la rédaction de ma thèse.

Au terme de ce parcours, je remercie enfin celles et ceux qui me sont chers et que j'ai beaucoup délaissés ces derniers années pour achever cette thèse. Leurs attentions et encouragements m'ont accompagnée tout au long de ces années. Je suis redevable à mes parents, Malika et Abdeslam, mon frère et mes sœurs, Nizar, Meryem et Zineb pour leur soutien moral et leur confiance indéfectible dans mes choix.

Sommaire

Table des matières

Introduction générale

1. La pollution engendrée par la pêche, une menace pour les océans

1.1. L'importance du milieu océanique

L’océan recouvre environ 70% de la surface de la terre et produit plus de la moitié de l’oxygène que nous respirons (Environment 2017). En interagissant avec l’atmosphère, il joue un rôle indispensable de contrôle et de régulation des grands équilibres naturels qui rendent notre planète habitable. L’océan abrite également une immense variété de ressources vivantes qui ont été exploitées depuis longtemps par l’être humain (Yellen et al. 1995; Caddy & Majkowski 1996) et représentent la ressource principale d’alimentation pour environ 3.5 milliards de personnes. L’océan a aussi un impact économique considérable sur plusieurs secteurs comme le transport, l’énergie ou le tourisme. La préservation de l’océan est donc un impératif autant écologique qu’économique. Mais les activités humaines, qu’elles soient maritimes ou terrestres, conduisent à divers changements ecolo-physico-chimiques qui perturbent et dégradent l’océan, comme par exemple le réchauffement et l’acidification des eaux qui engendrent des zones désoxygénées où la vie sous-marine ne se développe plus.

1.2. La pollution marine

La pollution est l’une des principales menaces qui pèsent sur les océans et les eaux côtières qui reçoivent un grand nombre de déchets constitués majoritairement de plastique. Les déchets marins sont définis comme toute matière solide persistante, fabriquée ou transformée, et rejetée ou abandonnée dans l'environnement marin et côtier (United Nations Environment Programme 2005; Galgani et al. 2010). Les organismes marins ingèrent ces déchets ou bien s'emmêlent dedans, souvent avec des conséquences fatales (Derraik 2002). Il existe de nombreuses mesures régionales, nationales et internationales visant à prévenir et à atténuer l’impact de ces déchets, mais elles ne permettent pas de faire face à l'ampleur et à l'accélération du phénomène (Borrelle et al. 2017). La plupart des déchets et polluants marins sont d'origine terrestre, avec une masse totale qui atteint jusqu’à 12,7 millions de tonnes métriques de plastique entrant dans l'océan chaque année (Jambeck et al. 2015; Haward 2018). Cependant, une partie importante des déchets et polluants marins provient des activités maritimes, en particulier la pêche, en raison d'équipements jetés, abandonnés, ou perdus (United Nations Environment Programme 2017; Lebreton et al. 2018; Richardson et al. 2019)

2. Les DCP dérivants, un équipement de pêche qui impacte les océans

2.1. La pêche au thon tropical

La pêche au thon fait partie des pêcheries les plus lucratives au monde, avec une valeur marchande estimée à plus de 42 milliards de dollars par an (Galland et al. 2016). Elle a émergé vers la fin des années 1940 suite à la demande croissante en thon en conserve (Miyake et al. 2004) et s'est développée depuis afin de soutenir la sécurité alimentaire, créer des emplois, et contribuer à la croissance économique dans de nombreux pays (Bell et al. 2009; ISSF 2019). Bien que la pêche au thon était au départ artisanale et locale, la pêche industrielle s'est rapidement développée.

Sept espèces de thons ont un grand intérêt commercial à l'échelle mondiale, le germon (*Thunnus alalunga*), le thon rouge (*Thunnus thynnus*), le thon bleu du Pacifique (*Thunnus orientalis*), le thon rouge du sud (*Thunnus maccoyii*), la bonite à ventre rayé ou listao (*Katsuwonus pelamis*), le thon albacore ou thon à nageoires jaunes (*Thunnus albacares*) et le thon obèse ou patudo (*Thunnus obesos*). Ces espèces représentaient une capture totale estimée à 4.9 millions de tonnes en 2017, majoritairement constituée de trois espèces : le listao (58% de la capture totale), l'albacore (28%) et le patudo (8%) (ISSF 2019).

De multiples engins de pêche sont utilisés dans la pêche au thon. Au début, la palangre et la pêche à la ligne étaient les principaux engins utilisés, mais actuellement c'est la pêche à la senne (Fig. I.1) qui est la technique employée majoritairement pour capturer le thon tropical (« Purse seine », environ 65% de la capture totale ; Fig. I.2). Ce changement s'est produit dans les années 1980, notamment en raison du développement rapide de l'utilisation des objets flottants dérivants sous lesquels les thons s'agrègent (Fonteneau et al. 2000; Castro et al. 2002).

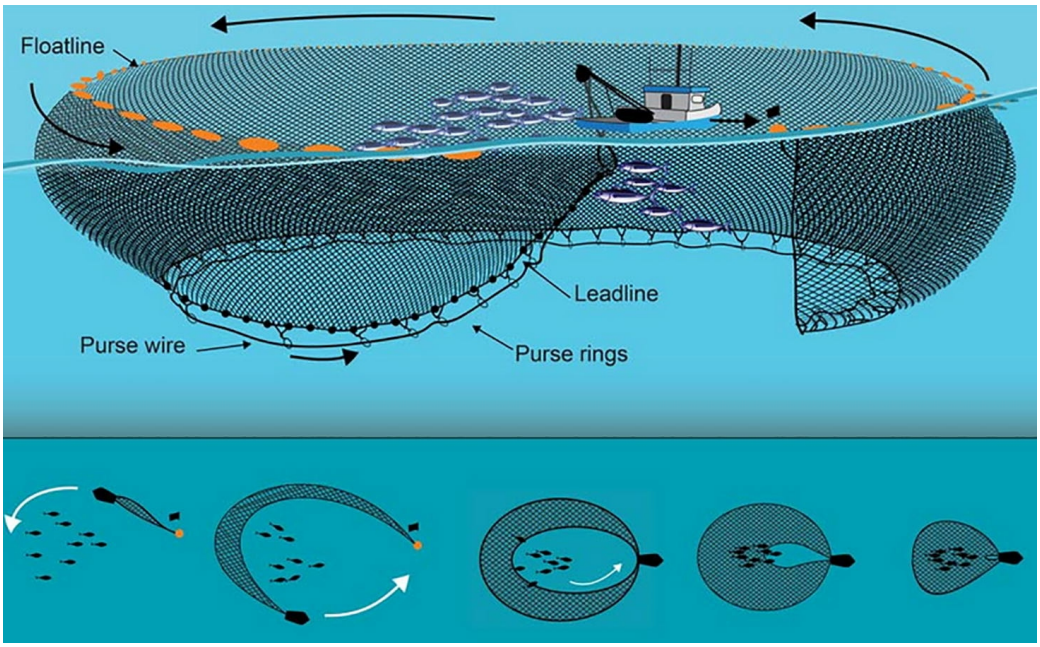

***Figure I.1**: Pêche à la senne coulissante (© Australian Fisheries Management Authority).*

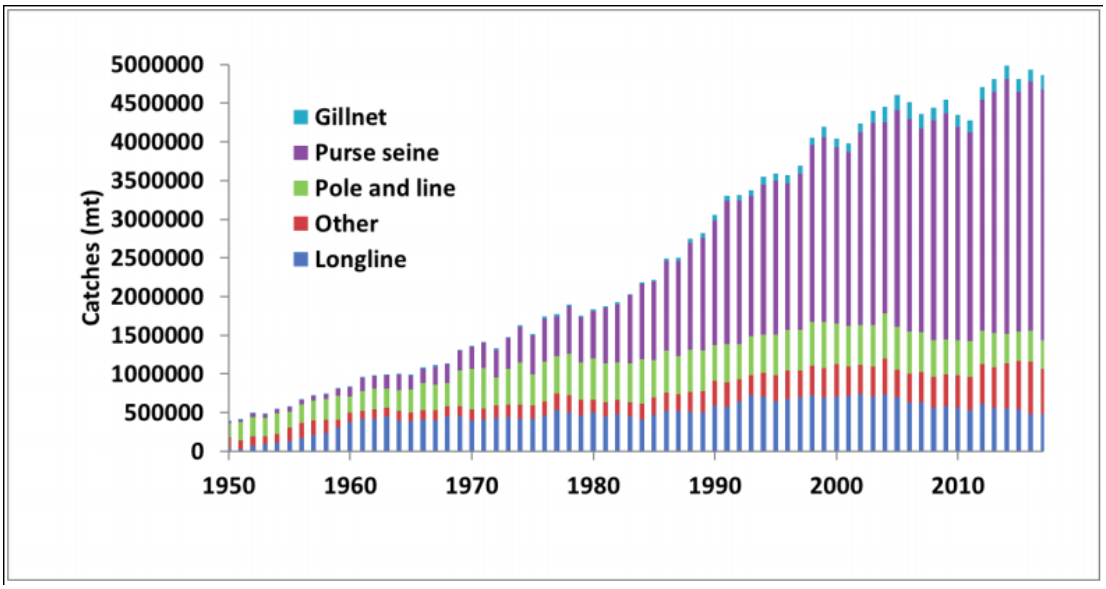

***Figure I.2:** Captures totales par année et par engin de pêche des principales espèces de thonidés pêchés sur la période 1950-2017 (ISSF 2019, « Purse seine » = pêche à la senne.).*

2.2. Le comportement d'agrégation des thons sous les objets flottants

Les objets qui flottent à la surface ainsi que certains grands êtres vivants peuvent concentrer naturellement le poisson et les pêcheurs profitent de ce comportement d'agrégation pour augmenter leurs captures et diminuer le temps de la recherche des bancs de poissons dits libres (Fréon & Dagorn 2000; Castro et al. 2002; Dempster & Taquet 2004). Ce phénomène

n’est pas récent. Il date d’au moins le 18ème siècle av. J.-C, d’après une représentation peinte sur un vase grec trouvé sur l'île d'Ischia en Italie (Viñuales-Solé 1996). Les agrégations sous objets flottants, ancrés ou dérivants, concernent des centaines d’espèces marines, et pas seulement les espèces cibles de la pêche au thon (Fréon & Dagorn 2000; Castro et al. 2002). Plusieurs hypothèses ont été avancées pour expliquer ce comportement, suggérant que les objets flottants représenteraient un endroit favorable pour la recherche alimentaire (Hunter & Mitchell 1967), une zone de refuge contre les prédateurs (Gooding & Magnuson 1967), un point de rencontre facilitant la formation des bancs (Dagorn & Fréon 1999; Fréon & Dagorn 2000) ou un indicateur de zone riche en nutriments (Hall 1992). Ces deux dernières hypothèses semblent être les plus privilégiées par la communauté scientifique.

2.3. L’utilisation des DCP et son développement dans la pêche au thon tropical à la senne

Au début des années 1960, les pêcheurs ont commencé à fortement s'intéresser au comportement d’agrégation des thons sous les objets flottants. Ils ont ainsi considérablement focalisé leurs efforts de pêche sur les bancs associés (c’est-à-dire les bancs regroupés sous des objets flottants, au contraire des bancs libres), en particulier dans les Océans Pacifique Est et Atlantique. Au début, les pêcheurs suivaient les objets flottants et attendaient que suffisamment de thons s'agrègent en dessous avant de déployer leur filet (Greenblatt 1979). Les objets flottants étaient initialement naturels, par exemple des amas d’algues, des mammifères marins ou des débris de bois terrestres entrés dans l'océan par l'embouchure des fleuves (Greenblatt 1979; Fig. I.3 A-C). Au fil du temps, les objets flottants artificiels sont devenus prépondérants, suivant l’augmentation des débris issus des activités terrestres et marines rejetés dans les océans (Caddy & Majkowski 1996; Fig. I.3 D-F).

Devant l’efficacité de la pêche sous ces divers objets, la communauté des pêcheurs a commencé à développer ses propres dispositifs, appelés Dispositifs de Concentration de Poissons (DCP) (Fig I.3 G-I), qui peuvent être ancrés ou dérivants . Les DCP ancrés ont été déployés pour la première fois à la fin des années 1960 aux Philippines et en Indonésie pour soutenir la pêche au thon tropical à la ligne (Itano et al. 2004). L’efficacité de ces DCP ancrés a rapidement encouragé les senneurs à déployer leurs propres DCP dérivants partout dans le monde (Fonteneau et al. 2000; Bromhead et al. 2003).

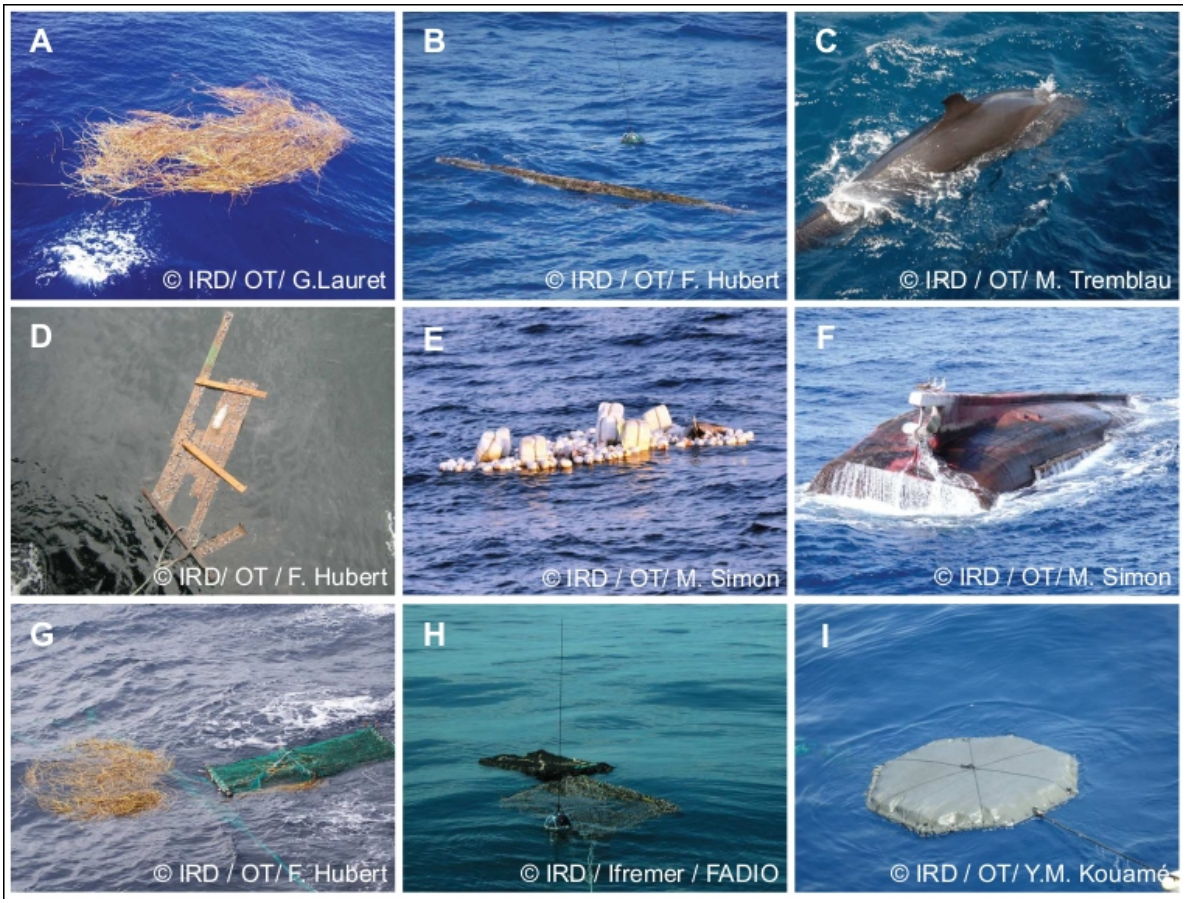

Figure I.3: Typologie des objets flottants dérivants utilisés par les thoniers senneurs tropicaux. A : tas de paille – B : bûche de bois – C : grands êtres vivants (mammifère marin) – D : débris d'activités terrestres – E : débris d'activités marines – F : épave – G : bûche naturelle rehaussée d'un DCP – H et I : différents types de DCP (bambou ou radeau plastique) (Maufroy 2016)

Plusieurs études ont démontré l'efficacité des DCP dérivants pour la pêche au thon tropical à la senne (e.g., Marsac et al. 2000). Des experts scientifiques ont recommandé cette technique qui semblait être, à l'époque, une solution durable et un outil prometteur pour améliorer la capture des thons, notamment les bancs de thons trop profonds (Ariz et al. 1999) ou trop rapides (Bard et al. 1985) qui posaient problème aux senneurs. Ainsi, les DCP dérivants sont devenus un engin utilisé de façon récurrente par la pêche industrielle à la senne (Dagorn et al. 2013). Toutefois, leur utilisation va particulièrement s'étendre à l'arrivée des nouvelles technologies comme les balises radio au milieu des années 1980 et 1990, puis les bouées équipées de GPS à partir du début des années 2000 (Castro et al. 2002; Fonteneau et al. 2013). Le développement et l'utilisation de bouées GPS attachées aux objets flottants dérivants a permis de suivre leurs positions en temps réel à distance et ainsi d'élargir les zones

de pêche (Itano et al. 2004). Plus récemment, l'intégration d'échosondeurs dans ces bouées a encore augmenté l'efficacité de la pêche en permetant aux senneurs d'avoir une estimation de la quantité de poissons agrégés sous un objet flottant donné et de ne se diriger vers ce dernier que lorsque cette quantité est suffisamment importante pour procéder à une opération de pêche (Chassot et al. 2014; Lopez et al. 2014; Baidai et al. 2020).

Parallèlement à l'intégration des nouvelles technologies aux DCP dérivants, l'évolution d'autres équipements de pêche a également joué un rôle dans le développement de la pêche sous DCP. La taille moyenne des bateaux senneurs est passée de 40 m environ pour les bateaux construits dans les années 1960 à plus de 90 m dans les années 2000 (Maufroy 2016). La taille des sennes coulissantes a également augmenté (Torres-Irineo et al. 2014). De plus, les flottilles des senneurs ont adopté l'utilisation des «navires supports» qui sont chargés d'assister les senneurs dans différentes activités liées aux DCP comme leur déploiement ou le remplacement des bouées GPS (Ariz et al. 1999; Fonteneau et al. 2000; Arrizabalaga et al. 2001). Ainsi, bien qu' historiquement les senneurs répartissaient leur effort de pêche entre les bancs de thons libres et les bancs associés à des objets flottants, plusieurs flottes se concentrent maintenant presque exclusivement sur la pêche sous DCP dérivants (Galland et al. 2016; Taconet et al. 2018), avec un nombre de DCP déployés par an qui dépasse maintenant 100 000 au niveau mondial (Scott & Lopez 2014).

2.4. La structure d'un DCP dérivant

Les DCP dérivants utilisés par les flottilles des senneurs sont généralement constitués de radeaux rectangulaires en bambou, plastique ou métal d'environ 4 à 6 m² recouverts de vieux filets de pêche ou plus récemment de matériaux non maillants pour rendre le DCP moins visible à la surface et empêcher leur vol (Fig. I.4 ; Franco et al. 2009; Maufroy et al. 2015). Des flotteurs en plastique ou en éthylène-acétate de vinyle sont généralement attachés sous les radeaux pour assurer leur flottabilité. Les DCP comportent aussi une structure verticale constituée de vieux filets de pêche pouvant atteindre plus de 80 m en profondeur, attachés à un poids pour maintenir une position verticale et ralentir la dérive de l'ensemble du dispositif, mais aussi pour faciliter l'agrégation des poissons, bien qu'aucune étude scientifique n'ait prouvé cet effet (Dagorn et al. 2013). La structure verticale des DCP a évolué au fil du temps, passant de filets suspendus en forme de «rideaux» (Fig. I.5 - à gauche) à des cordes ou filets en forme de «boudins» (Fig. I.5 - à droite) depuis le début des années 2010 ; principalement pour empêcher les maillages des tortues et des requins pendant

la dérive du DCP (Filmalter et al. 2013; ISSF 2019) et la pêche dite fantôme (c'est-à-dire capture intervenant en dehors des activités de pêche; Anderson 2009; Filmalter et al. 2013).

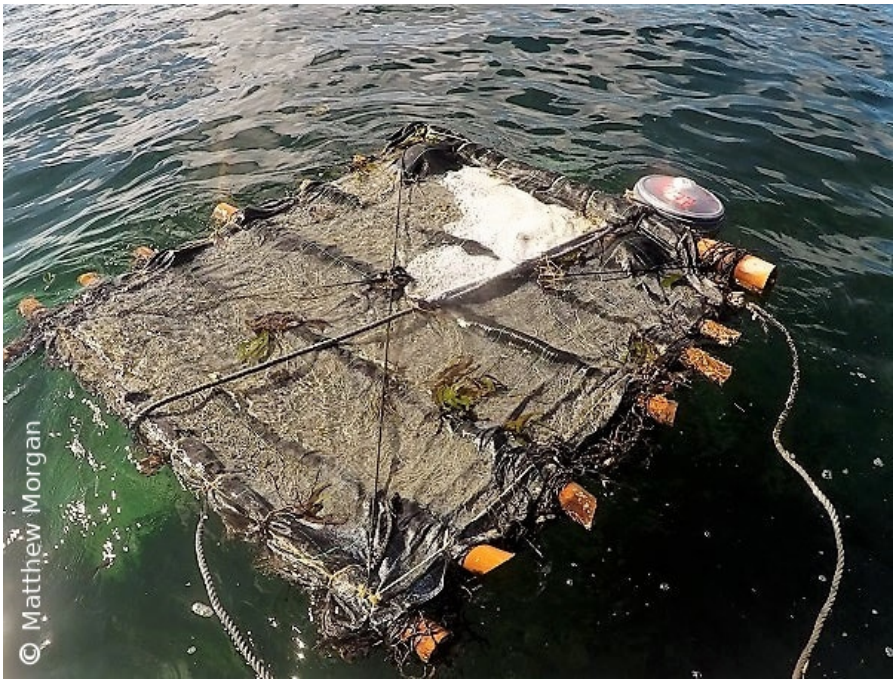

***Figure I.4**: Photo d'un DCP dérivant constitué de radeau rectangulaire en bambou*

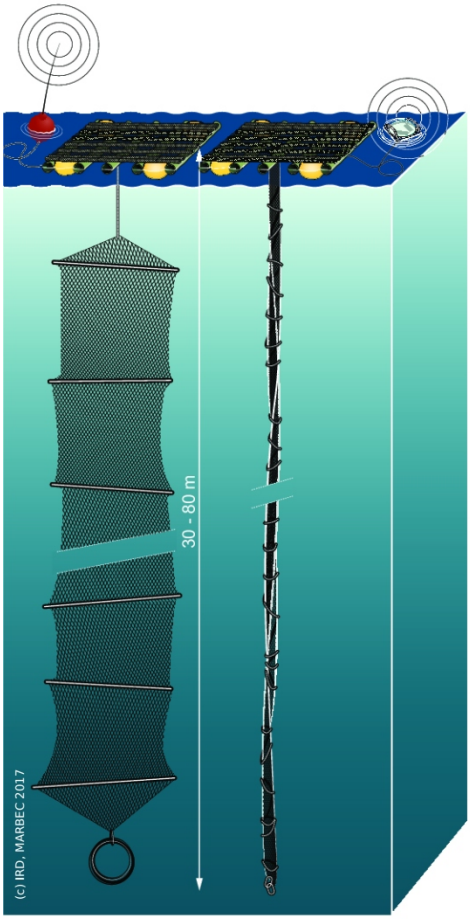

Figure I.5*: Représentation schématique d'un Dispositif de Concentration de Poissons (DCP) dérivant utilisé dans les pêcheries à la senne coulissante, avec une structure verticale constituée de filets en forme de «rideau» (à gauche) et des cordes ou filets en forme de «boudins» (à droite).*

2.5. Les impacts négatifs des DCP dérivants éveillent les inquiétudes

L'augmentation du nombre de DCP dérivants déployés par les senneurs et leur efficacité a clairement augmenté la productivité de la pêcherie aux thons tropicaux. La pêche sous DCP est ainsi devenue le mode de pêche dominant pour cette pêcherie (Fonteneau et al. 2013), avec une capture annuelle mondiale dépassant les 2 millions de tonnes ces dernières années (ISSF 2019). Cependant, l'augmentation du nombre de DCP a engendré des préoccupations concernant la surpêche de la ressource et l'augmentation des captures d'espèces non ciblées, dont des espèces sensibles comme les requins (Amandè et al. 2010; Dagorn et al. 2013; Filmalter et al. 2013; Maufroy et al. 2015). En effet, l'exploitation des

thons sous DCP a conduit à une diminution de la taille moyenne des thons capturés par rapport à ceux capturés sur bancs libres (Fonteneau et al. 2000; Marsac et al. 2000; Chassot et al. 2014). Ces thons de petite tailles sont majoritairement immatures (40 à 60 cm) pour deux des espèces cibles (thon obèse et albacore) (Fonteneau et al. 2013; Sun et al. 2013); contrairement au listao, la troisième espèce majeure ciblée par les thoniers senneurs tropicaux. (Grande et al. 2014). De ce fait, la capture sous DCP peut contribuer à dégrader les stocks par deux mécanismes : une perte du potentiel de reproduction, et donc de recrutement pour l'albacore et le patudo (surexploitation de croissance), ainsi qu'une diminution de la biomasse du stock en prélevant des individus en trop grande quantité (surpêche) (Fonteneau et al. 2013). En outre, l'augmentation rapide du nombre de DCP pourrait avoir un effet de « piège écologique » en modifiant le comportement naturel des thons et en les « piégeant » dans un environnement de plus faible qualité que leur environnement naturel, engendrant ainsi une plus faible croissance et une augmentation de la mortalité (Marsac et al. 2000; Hallier & Gaertner 2008), même si l'hypothèse de piège écologique fait encore sujet de débat (Dagorn et al. 2013; ISSF 2014). L'utilisation d'un grand nombre de DCP affecte les thons tropicaux mais également d'autres espèces non ciblées qui se retrouvent capturée accidentellement avec les thons ciblés. Bien que des captures accidentelles puissent se produire également sur banc libre, mais le taux supérieur de prises accidentelles sous DCP a amplifié le problème (Hall et al. 2000).

2.6. La perte et l'échouage des DCP, une menace pour les littoraux

Un autre problème lié à l'utilisation des DCP dérivants est qu'un pourcentage non négligeable de ceux-ci finissent par dériver loin des zones de pêche et se désagrègent, coulent ou s'échouent dans les zones côtières (Fig. I.6), ce dernier cas étant le plus préoccupant puisqu'il contribue à la pollution des littoraux et menace les habitats sensibles tels que les récifs coralliens (Balderson & Martin 2015; Stelfox et al. 2016; Zudaire et al. 2018).

Figure. I.6*: Photos de DCP échoués aux Seychelles sur l'atoll Farquhar (à gauche) et sur l'atoll Alphonse (à droite)*

L'inquiétude concernant la perte et l'échouage des DCP a augmenté ces dernières années parallèlement à la prise de conscience croissante de l'ampleur de la pollution marine et des engins et dispositifs de pêche abandonnés, qui se révèlent être une composante importante des déchets marins sur la planète. Maufroy et al. (2015) ont analysé les positions des DCP déployés par les senneurs français opérant dans les Océans Indien et Atlantique sur la période 2007-2011 et ils ont trouvé qu'environ 10% des DCP échouaient, mettant en lumière leur impact considérable sur les habitats côtiers fragiles. Cependant, étendre la période d'étude à une période plus récente dans ces deux océans semble nécessaire du fait de la forte croissance du nombre de DCP déployés depuis 2011 (Katara et al. 2018; Floch et al. 2019) et du changement potentiel de la distribution spatio-temporelle des DCP après l'intégration des échosondeurs (Chassot et al. 2014; Floch et al. 2019). Une analyse similaire à celle de Maufroy et al. (2015) mais conduite dans l'Océan Pacifique Occidental et Central a estimé qu'approximativement 6% des DCP s'étaient échoués sur la période 2016-2017 (Escalle et al. 2019). Toutefois, ces résultats sous-estiment potentiellement le taux réel des échouages car un nombre important des DCP pourraient être désactivés et leurs signaux perdus, empêchant ainsi d'examiner leur devenir en mer (Maufroy et al. 2015; Escalle et al. 2019, 2021). Des simulations de trajectoires de DCP ont aussi été effectuées pour aborder ce sujet, mais la question de la qualité et de la précision de ces simulations ont été relativement peu abordées, notamment en terne de volume de données observées utilisées pour évaluer les simulations (Imzilen et al. 2016; Davies et al. 2017; Phillips et al. 2019; Escalle et al. 2019; Curnick et al. 2021).

Plusieurs solutions ont été proposées pour réduire l'impact des échouage et de la perte des DCP (Moreno et al. 2018). La récupération en mer des DCP perdus semble être l'une des options les plus prometteuses. Ainsi en 2016 certains senneurs de l'UE, en collaboration avec l'ONG locale Island Conservation Society (ICS) et le Seychelles Fishing Authority (SFA), ont lancé un programme nommé «FAD Watch » dans le but de limiter les échouages des DCP dans certaines zones côtières des Seychelles (Zudaire et al. 2018). Un système de détection a été mis en place pour envoyer des alertes lorsque des DCP arrivaient dans un rayon de 3 à 5 mn au large de 6 îles de l'archipel des Seychelles, ce qui a permis de collecter au total 109 DCP risquant l'échouage sur la période 2016-2017. Toutefois, la possibilité d'étendre ce type de programme de surveillance à l'ensemble d'un bassin océanique reste difficile à envisager et nécessiterait d'abord une étude scientifique approfondie de la dérive des DCP.

Par ailleurs, les Organisations Régionales de Gestion de la Pêche (ORGP) responsables de la gestion des stocks des thons tropicaux ont également pris des mesures visant à réduire les impacts négatifs des DCP sur l'écosystème marin. Le nombre maximal de DCP équipés de bouées opérationnelles a ainsi été fixé à 300 DCP par bateau dans l'Océan Indien et dans l'Océan Atlantique (ICCAT 2019; IOTC 2019). D'autres mesures ont été instaurées, notamment dans l'Océan Atlantique, afin de suspendre toute activité liées aux DCP de janvier à mars. Les ORGP encouragent également l'utilisation de matériaux biodégradables dans la construction des DCP (ICCAT 2019; IOTC 2019; IATTC-WCPFC 2020), cet aspect étant aujourd'hui une composante systématique des plans nationaux de gestion des DCP (ORTHONGEL 2021a, 2021b). Toutefois, identifier et développer des matériaux appropriés pour remplacer les matériaux non biodégradables des DCP restent difficiles et il faudra probablement du temps afin de les tester et prouver leur efficacité (Lopez et al. 2019; Moreno et al. 2021; Zudaire et al. 2021). Force est de constater que les restrictions et incitations visant à réduire les impacts négatifs des DCP restent insuffisantes, en particulier en ce qui concerne l' échouage et la perte des DCP .

3. Objectifs de la thèse

Bien que les ORGP consacrent des efforts pour réduire les impacts négatifs des DCP, les incitations et mesures de gestion mises en place actuellement restent insuffisantes en ce qui concerne la réduction de l' échouage et la perte des DCP. En effet, ces mesures ne se basant pas sur une analyse spatio-temporelle de la dérive des DCP, leur efficacité pour limiter

ces événements reste inconnue. Une étude permettant d'approfondir les connaissances sur l' échouage et la perte des DCP, ainsi que d'identifier les mesures d'atténuation appropriées pour atténuer ces problèmes, est nécessaire. Dans ce contexte, l'objectif de ce travail de thèse est d'explorer trois mesures permettant respectivement d'éviter, d'empêcher et d'anticiper la perte et l'échouage des DCP dans les Océans Indien et Atlantique. Tout d'abord, nous avons étudié la possibilité de mettre en place des stratégies d'interdiction de déploiement des DCP dans des zones identifiées à haut risque d'échouage afin d'éviter ces événements. Dans un second temps, nous avons étudié la faisabilité de mettre en place des programmes de récupération des DCP en mer afin d'empêcher leur perte et leur échouage. Enfin, nous avons exploré la possibilité d'utiliser un modèle de transport Lagrangien pour simuler les trajectoires des DCP et anticiper leur perte et échouage. Cela pourrait potentiellement aboutir à utiliser des technologies permettant de contrôler à distance un DCP pour le dévier de sa trajectoire lorsqu'elle est jugée risquée (cf. le projet INNOV-FAD qui a financé partiellement le travail de cette thèse).

Ce manuscrit de thèse est articulé en plusieurs chapitres :

Dans le **Chapitre 1** je proposerai d'abord une méthode permettant d'identifier les événements d'échouage des DCP dérivants à partir de l'observation de leurs trajectoires, puis j'utiliserai cette méthode pour quantifier ces événements afin d'analyser leur variabilité temporelle et leur distribution spatiale. Je produirai ensuite une carte de risque d'échouage associée au déploiement d'un DCP et la combinaison de cette carte de risque et de celle des déploiements permettra d'identifier des zones risquées qui pourraient être interdites aux déploiements et d'estimer la quantité d'échouages qui seraient ainsi évités.

Dans le **Chapitre 2** je m'intéresserai particulièrement au sort des DCP qui dérivent en dehors des zones de pêche et finissent potentiellement perdus au milieu de l'océan ou échoués dans les zones côtières. J'analyserai les trajectoires suivies par ces DCP afin de déterminer les directions principales qu'ils suivent et leur passage potentiel à proximité de ports à partir desquels ils pourraient être interceptés si un programme de récupération des DCP en mer était mis en place.

Dans **le Chapitre 3** j'ai tenté de répondre à la question suivante :les DCP dérivent-ils comme les drifters qui sont utilisés en océanographie et qui sont conçus pour suivre les courant de la couche de surface ? Dans un premier temps, une comparaison des composantes de vitesses de DCP et de drifters qui se trouvaient par hasard proches dans l'espace et dans le temps permettra d'évaluer si les mouvements de ces deux engins sont similaires, malgré les

différences dans leurs structures, ou pas. Dans un second temps, une comparaison des vitesses de l'ensemble des DCP et des drifters avec un produit satellite de courant océanique (OSCAR) permettra de consolider les résultats précédents à plus grande échelle. J'ai effectué ce travail principalement avant le début de ma thèse, mais comme j'en ai réalisé une partie aussi pendant la thèse nous avons décidé de faire figurer ce chapitre dans ce manuscrit, ceci également afin que le manuscrit donne une vision d'ensemble des travaux que j'ai conduit sur le sujet.

Enfin, dans le **Chapitre 4** j'évaluerai la précision de simulations de trajectoires de DCP dérivants obtenues en utilisant un modèle Lagrangien dans le but d'explorer la possibilité d'utiliser cet outil en mode opérationnel dans le futur afin d'anticiper la perte et l'échouage des DCP. Les simulations seront forcées par des champs de courant issus d'un modèle hydrodynamique (GLORYS12V1) et de deux produits de courants dérivés de données satellites (OSCAR et GEKCO)

Finalement, la dernière partie du manuscrit sera consacrée à une discussion générale des résultats présentés précédemment afin de les comparer éventuellement aux précédentes études réalisées. Elle permettra également de mettre en exergue leur potentielles applications mais également leurs limites.

CHAPITRE 1

Spatial management can significantly reduce dFAD beachings in Indian and Atlantic Ocean tropical tuna purse seine fisheries

Les débris issus de la pêche sont une menace pesant sur l'écosystème marin côtier. La pêche au thon qui utilise majoritairement la senne coulissante, contribue à ce problème en construisant et déployant des milliers de DCP chaque année dont certains finissent par échouer sur le littoral. Dans ce premier chapitre, nous avons analysé un grand nombre de trajectoires de DCP dans l'Océan Indien et l'Océan Atlantique afin d'identifier les positions, les périodes et les origines des échouages. Nous avons constaté qu'en interdisant le déploiement de ces dispositifs dans des zones risquant fortement de conduire à des échouages, nous pourrions éviter bon nombre de ces évènements. De plus, dans les deux océans ces zones identifiées comme étant à haut risque ne correspondent pas aux zones de fort déploiement des DCP, ce qui suggérant que la mise en œuvre d'un tel programme de fermeture de zones n'aurait pas un gros impact sur la productivité de la pêcherie.

Ce chapitre 1 a été publié dans Biological Conservation :

Imzilen T, Lett C, Chassot E, Kaplan DM. 2021. Spatial management can significantly reduce dFAD beachings in Indian and Atlantic Ocean tropical tuna purse seine fisheries. Biological Conservation ***254****:108939. https://doi.org/10.1016/j.biocon.2020.108939*

1. Introduction

Debris from fisheries pose significant threats to coastal marine ecosystems worldwide (Tavares et al. 2017; Parton et al. 2019). Tropical tuna purse seine fisheries contribute to this problem via their extensive use of drifting fish aggregating devices (dFADs) (Consoli et al. 2020). Whereas historically purse seine vessels divided there fishing effort between free-swimming fish schools and schools associated with naturally-occurring floating objects (FOBs), they increasingly focus principally on FOB fishing (Galland et al. 2016; Taconet et al. 2018). The attachment to FOBs of, first, radio beacons in the mid-1980's and 1990's and then satellite-tracked, GPS-equipped buoys from the early 2000's, and most recently the integration of echo-sounders in satellite-tracked buoys have made this approach to catching tunas increasingly attractive to fishers (Chassot et al. 2014; Lopez et al. 2014). These technological developments have led purse seiners to manufacture and deploy large numbers of their own, man-made dFADs (Maufroy et al. 2017), and today it is believed that over 100 000 of these devices are deployed annually worldwide (Scott & Lopez 2014). dFADs typically consist of a floating structure and of a submerged substructure stretching up to 80 m below the surface (Imzilen et al. 2019). Some of the materials regularly used in dFAD construction include non-biodegradables such as PVC and metal tubes for the raft frames, ethylene vinyl acetate floats and plastic containers for buoyancy, and old nylon nets and pieces of salt bags for the subsurface structure. The massive increase in dFAD use poses a number of major concerns regarding ecological disturbance, overfishing, increased bycatch and creation of marine debris (Amandè et al. 2010; Dagorn et al. 2013; Filmalter et al. 2013; Maufroy et al. 2015). Most importantly for the context of this paper, a significant fraction of these dFADs end up beaching (i.e., stranding in coastal environments) (Maufroy et al. 2015), potentially damaging sensitive habitats such as coral reefs, and contributing to coastal marine debris and ghost fishing (Balderson & Martin 2015; Stelfox et al. 2016; Zudaire et al. 2018). This is of particular concern in a context of growing awareness of the extent of marine plastic pollution, with abandoned and lost fishing gears having been shown to be a major component of marine litter worldwide (Haward 2018; Lebreton et al. 2018; Richardson et al. 2019).

Given these concerns, dFAD beachings are a major area of interest for science, management and conservation. An initial examination of French dFAD spatio-temporal use in the tropical Indian Ocean (IO) and Atlantic Ocean (AO) over the period 2007-2011 indicated that ~10% of deployed dFADs ended up beached (Maufroy et al. 2015), highlighting the potential for considerable impacts on fragile coastal habitats due to these events. A similar examination in the Western and Central

Pacific Ocean found that ~6% of all trajectories were likely to have beached over a two year period (2016-2017; Escalle et al. 2019). However, given the significant differences in bathymetry and circulation between the western and central Pacific Ocean , IO and AO, and the more than four-fold increase in the number of dFADs deployed by purse seiners in the IO and AO since 2011 (Katara et al. 2018; Floch et al. 2019), the extent to which existing literature applies to current patterns of dFAD use is an important open question. Moreover, the French fleet switched to almost exclusively using echo-sounder equipped dFAD tracking buoys around 2012 (Chassot et al. 2014; Floch et al. 2019) and other major purse seine fleets also started using this new technology on or before this date, potentially altering the spatio-temporal distribution of dFAD deployments, fishing activity and associated beaching events. In parallel, management measures have been taken by the tuna regional fisheries management organizations to limit the total number of GPS buoys used by each purse seine vessel in both the AO and IO, but these measures have not directly addressed the spatial and temporal dynamics of beachings and, therefore, their efficacy for reducing this problem is unknown. A new analysis of dFAD beachings focused on spatio-temporal patterns that might be useful for identifying appropriate mitigation measures to avoid beachings is therefore urgently needed.

The goal of this paper is to quantify the impacts of dFAD beachings and identify strategies for mitigating these impacts in the tropical IO and AO. Using a large dataset of over 50 000 dFAD buoy trajectories, we first extend and improve upon the analysis of Maufroy et al. (2015, 2018), estimating beachings for the decade 2008-2017 for the IO and AO. We then identify deployment locations likely to lead to beaching events, and, using this information, we are able to estimate the impact of closing high beaching risk areas to dFAD deployments on the overall beaching rate under a pair of reasonable fishing effort redeployment strategies. Results indicate that there is indeed much promise in the IO and AO for reducing dFAD beachings by implementing sensible spatial limitations on deployment locations.

2. Materials and methods

2.1. Data collection

Through a collaboration with the French frozen tuna producers' organization (ORTHONGEL), the French Institute of Research on Development (IRD) has access to data on the locations of thousands of distinct GPS buoys attached to FOBs deployed by the French and associated flags (Mauritius, Italy, Seychelles) purse seine fleets operating in the tropical AO and IO

from ~2007 onward (coverage ~75-86% before 2010 and ~100% after that date; Maufroy et al. 2015). Though GPS buoys can be attached to both natural FOBs and man-made dFADs, the vast majority of FOBs in both oceans are now man-made dFADs (>90% of buoy deployments in both oceans based on observer data for 2013-2017), and, therefore, we will refer to these buoy trajectories as dFAD trajectories even though a small fraction of them are for other types of objects. GPS buoys are attached to dFADs deployed at sea by purse seine fishing vessels and their associated support vessels. Buoys can also be exchanged on FOBs encountered at sea and the buoys retrieved from the water are generally brought back to port where they can be recovered by the owner vessel for reuse. A single GPS buoy may therefore be redeployed several times, potentially on different dFADs. It is therefore important to note that, in this paper, we use the term 'dFAD' to refer to the entire device consisting of the floating object itself and the attached GPS buoy, whereas, the term 'buoy' designates solely the GPS buoy.

Buoy location data are transmitted with a periodicity that varies along the buoy trajectory, generally ranging from 15 minutes to 2 days. Buoy positions were filtered to remove those that were emitted while the buoy was onboard using a Random Forest classification algorithm that is an improvement over that developed in Maufroy et al. (2015) (Appendix A1). This improved classification algorithm is estimated to have an error rate of ~ 2% when predicting onboard positions and ~ 0.2% for at sea positions (Supplementary Table A1.4).

In this study, we used data of dFAD positions covering the decade 2008-2017. This data set consists of ~15 million IO positions representing a total of 38 845 distinct buoys and ~6 million AO positions representing a total of 12 147 distinct buoys. Separately, locations and times for dFAD deployments are available in French logbook data from 2013 onward.

2.2. Identification of dFAD beaching events

dFAD beachings were identified in two steps. The first step was to find dFADs that had an abnormally small rate of movement for an extended period of time, whereas the second step removed false positives (e.g., buoys onboard or at port) from this list of potential beachings. A given dFAD position was considered to be a potential beaching if: (1) at least 2 other later positions were within 200 m, and (2) all these close positions span a time period exceeding 1 day. The 200 m threshold is based on a dFAD snagged on the very bottom of its <100 m length nets hanging below

the dFAD swinging at most 100 m in each direction. The time span of at least 1 day is required to avoid identifying as beachings multiple position emissions from a single buoy over a short time period, such as occurs when the emission periodicity of dFAD positions is modified to 15 min to facilitate detection by vessels before a fishing set.

In the second step, the putative beachings identified in this first step were filtered to remove non-beaching events based on 4 tests: (1) the beaching is more than 10 km from a major fishing port to avoid cases where dFAD buoys are at a port; (2) the beaching event is <5 km from land or the water column depth is <100 m; (3) all positions are classified at sea and there are no gaps in location emission exceeding 2 days over the 5 days preceding the beaching; (4) greater than 90% of all positions of a given buoy within the time span of the potential beaching event are associated with the beaching event (i.e., meet the distance criteria described above; this condition avoids cases where a buoy happens to pass multiple times through the same area, because of an eddy for example). Only beaching events meeting these 4 conditions were considered for further analyses.

About half of the beachings identified by the conditions described above occurred in the water. The other half were generally located on land close to small fishing ports or coastal villages (Supplementary Fig. A2.2, Fig. A2.3 and Fig. A2.4). This suggests that these buoys were retrieved by small-scale boats, likely fishers. As these boats generally intercept dFADs in coastal areas and only collect the buoy for its valuable electronics, leaving the raft and netting to drift, it is entirely possible that these dFADs (without the buoy) later ended up beaching. Nevertheless, given the uncertainty regarding the fate of these dFADs, calculations in this paper have been carried out both including all beachings and including only beachings in the water. Unless otherwise stated, statistics reported in the paper are for all beachings including those on land. In the following sections of this paper, beachings located in water and on land are respectively referred to as “beachings along shore” and “recoveries displaced to shore”.

The number of beaching events per km of the continental shelf was calculated by counting all beachings occurring in each 5ºx5º grid cell and then dividing that number by the kilometers of continental shelf edge, defined by the 200 m isobath, within the cell. The continental shelf edge was used instead of the coastline to avoid anomalously high beaching rates for some very small islands surrounded by large continental shelf areas.

For identifying beachings, classifying beachings as on land or at sea and determining the continental shelf edge, coastline data were obtained from OpenStreetMap land polygons (available at https://osmdata.openstreetmap.de/data/land-polygons.html; accessed 2020-02-19) and bathymetry was obtained from the 30-arcsecond-resolution General Bathymetric Chart of the Oceans (GEBCO v.2014; available at https://www.gebco.net/data_and_products/gridded_bathymetry_data; accessed 2020-02-19).

2.3. Drift locations leading to beachings

In order to identify dFAD drift locations that had a high risk to lead to a beaching event, we calculated the fraction of buoys that beach within 3 months of a passage through a given 1°x1° grid cell. This analysis was carried out over the entire study period, but also by season to estimate seasonal variability in beaching risk. We selected 3 months as the time limit as it is intermediate between the mean timespan of at sea trajectories and that of the lifespan of a buoy in the dataset (i.e. 25 and 196 days, respectively), and because 3 months was considered a reasonable timespan over which fishers and managers could reasonably be expected to predict and mitigate for beaching likelihood. To ensure that results are not strongly sensitive to this choice, additional analyses were carried out to calculate the fraction of buoys that beach within 12 months. Note that individual buoy trajectories were separated into multiple in water trajectories using breaks defined by gaps of more than 2 days or positions classified as onboard representing more than 1 minute of trajectory time. The 1 minute limit was imposed to remove very short trajectory segments that were problematic for the classification algorithm (Appendix A1).

Since beachings threaten fragile marine habitats, especially coral habitats, we carried out the same analyses focusing exclusively on beachings in coral reef areas. Data on the global distribution of coral reefs were obtained from UNEP-WCMC, WorldFish Centre, WRI, TNC (2018 ,version 4.0; available at https://data.unep-wcmc.org/datasets/1; accessed April 30, 2019).

2.4. Deployment risk

To assess potential for reducing the dFAD beaching rate, we investigated closing areas of high beaching risk to dFAD deployments. Deployment locations were obtained from logbook data, whereas proportion of beaching was estimated as described above. Logbook deployment data was used instead of putative deployments from reconstructed dFAD trajectories because, though the random forest position classification model has a very high accuracy rate and predicted deployment locations do follow the spatial distribution of logbook deployment locations (Maufroy et al. 2015),

accurately predicting deployment locations is quite difficult and error prone given that a single error anywhere in the trajectory will split the trajectory, generating a new false deployment (Maufroy et al. 2015). Given the high quality of logbook data, it was considered that this was the most accurate estimate of recent dFAD deployment locations.

Multiplying dFAD deployments by the proportion of devices beaching allowed us to predict the reduction in beachings that would result from closing a given area. Different size areas corresponding to specific percentages of all pre-closure deployments were closed in order of beaching risk going from highest to lowest. Two hypotheses were considered regarding the number and spatial distribution of deployments after closing an area to deployments: (1) closures eliminate deployments that would have occurred in closed areas (i.e., fishing effort reduction occurs), and (2) closures displace deployments formerly in closed areas to remaining unclosed areas in proportion to the relative density of deployments prior to implementation of closures (i.e., “fishery squeeze” occurs; Halpern et al. 2004).

3. Results

The number of French and associated buoys deployed per year has increased dramatically and continuously over the decade 2008-2017, especially in the Indian Ocean (Fig. 1.1a). Over that period, more GPS buoys were deployed in the Indian Ocean (~ 40 000) than in the Atlantic Ocean (~ 12 000). The percentage of all deployed dFADs that ended up beaching has also dramatically increased from ~3.5% in 2008 to ~20% in 2013 (Fig. 1.1b; these numbers are roughly halved if we count only beachings along shore). After 2013, the percentage of dFADs that beached stabilizes at ~15-20% in the IO and ~19-22% in the AO. In total, we obtained 7187 beaching events for the IO and 2283 for the AO.

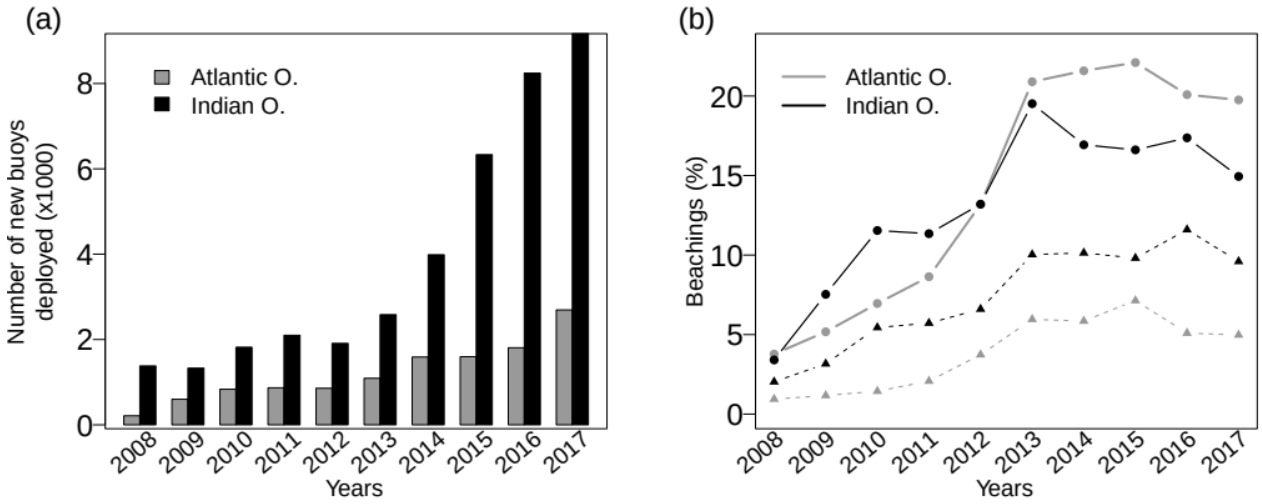

Figure 1.1: (a) Annual number of new buoys deployed by the French and associated flags purse seine fleet in the Atlantic (grey) and Indian (black) oceans over the period 2008-2017 and (b) percentage of these buoys that beached. The lines in (b) with solid circles include all beachings, whereas the lines with solid triangles include only beachings identified along shore. Beachings along shore and recoveries displaced to shore were separated via intersection with OpenStreetMap land polygons.

Maps of these 9470 beaching locations clearly identify coastal beaching hotspots (Fig. 1.2a and Supplementary Fig. A3.1a). Beachings occur in several zones in the IO, including southern Somalia, Kenya, Tanzania, Seychelles and the Maldives. In the AO, they occur mainly along the west African coast and the Gulf of Guinea between 20°N and 20°S. In both oceans, beachings also sporadically occur in more remote areas outside typical purse-seine fishing grounds (Maufroy et al. 2017), such as Indonesia, South Africa, Brazil and the Caribbean. Including only beachings that occur along the shore, the number of beaching decreases mostly along the western and north-eastern African coasts and in the Maldives (Fig. 1.2b and Supplementary Fig. A3.1b), which indicates that significant rates of putative recovery of dFAD buoys occur in those areas.

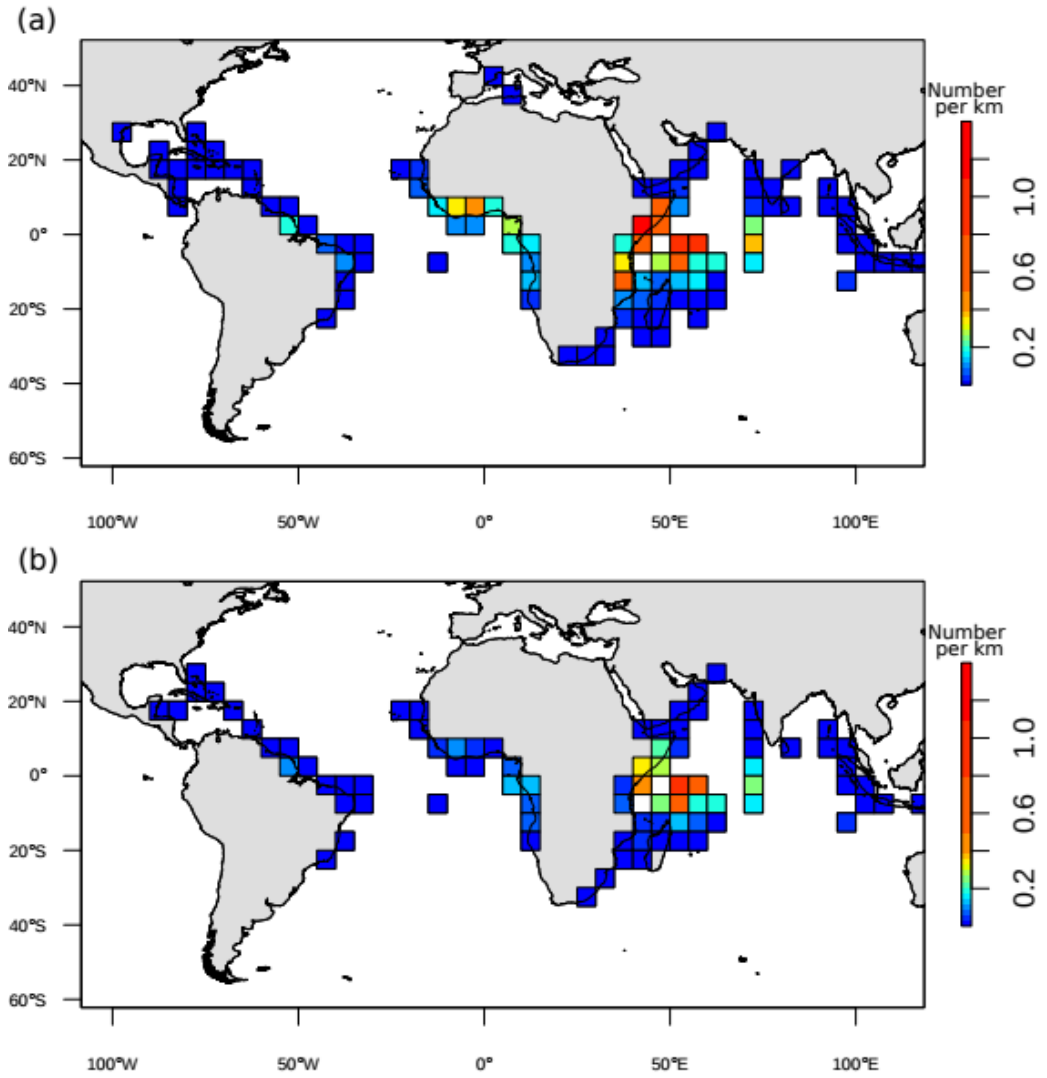

Figure 1.2: The number of French dFAD beachings recorded in our data per km of continental shelf edge in each 5°x5° grid cell for the period 2008-2017. Darker areas indicate higher rates of beaching. In (a), all beachings are considered, whereas in (b) only beachings along shore are included. Beachings along shore and recoveries displaced to shore were separated via intersection with OpenStreetMap land polygons. Note that our dFAD trajectory data is incomplete before ~2010, so the absolute number of beachings per kilometer is likely somewhat higher than values shown in the figure, though differences are likely to be small as the number of dFADs was far lower before 2010 than after 2010.

In both oceans, the proportion of dFADs beaching within 3 months of passing through a 1°x1° grid cell shows high spatial heterogeneity, with hotspots of beaching likelihood clearly visible (Fig. 1.3a). In the IO, the Gulf of Aden, Oman, Mozambique Channel, eastern and northern Madagascar, northern Maldives, western India, Sri Lanka and western Indonesia are all high risk areas for beaching. In the AO, the Gulf of Guinea, southern West Africa, the northern coast of South America and Caribbean have high proportion of beaching . Including only beachings that occur along shore reduces beaching proportions in all areas and reduces the importance of some coastal

areas characterized by a high density of small-scale fishers, such as in the vicinity of the Arabian Peninsula, the northern Gulf of Guinea and West Africa (Fig. 1.3b). Increasing the temporal window from 3 months to 12 months increases somewhat the spatial area over which proportion of beaching is non-negligible, but overall spatial patterns remain the same (Supplementary Fig. A3.2). Seasonal variability in dominant currents impacts beaching risk in predictable ways. For example, in the IO, during the winter monsoon, onshore currents create an area of high proportion of beaching east of Somalia, but this high risk area disappears during the upwelling favorable period of the summer monsoon (Supplementary Fig. A3.4). However, seasonal variability in the AO was weak. Finally, focusing exclusively on dFAD beachings on coral reefs narrowed the areas of high beaching risk to the north-west of the Maldives, Seychelles, northern Madagascar, the Mozambique channel and the Caribbean (Supplementary Fig. A3.5).

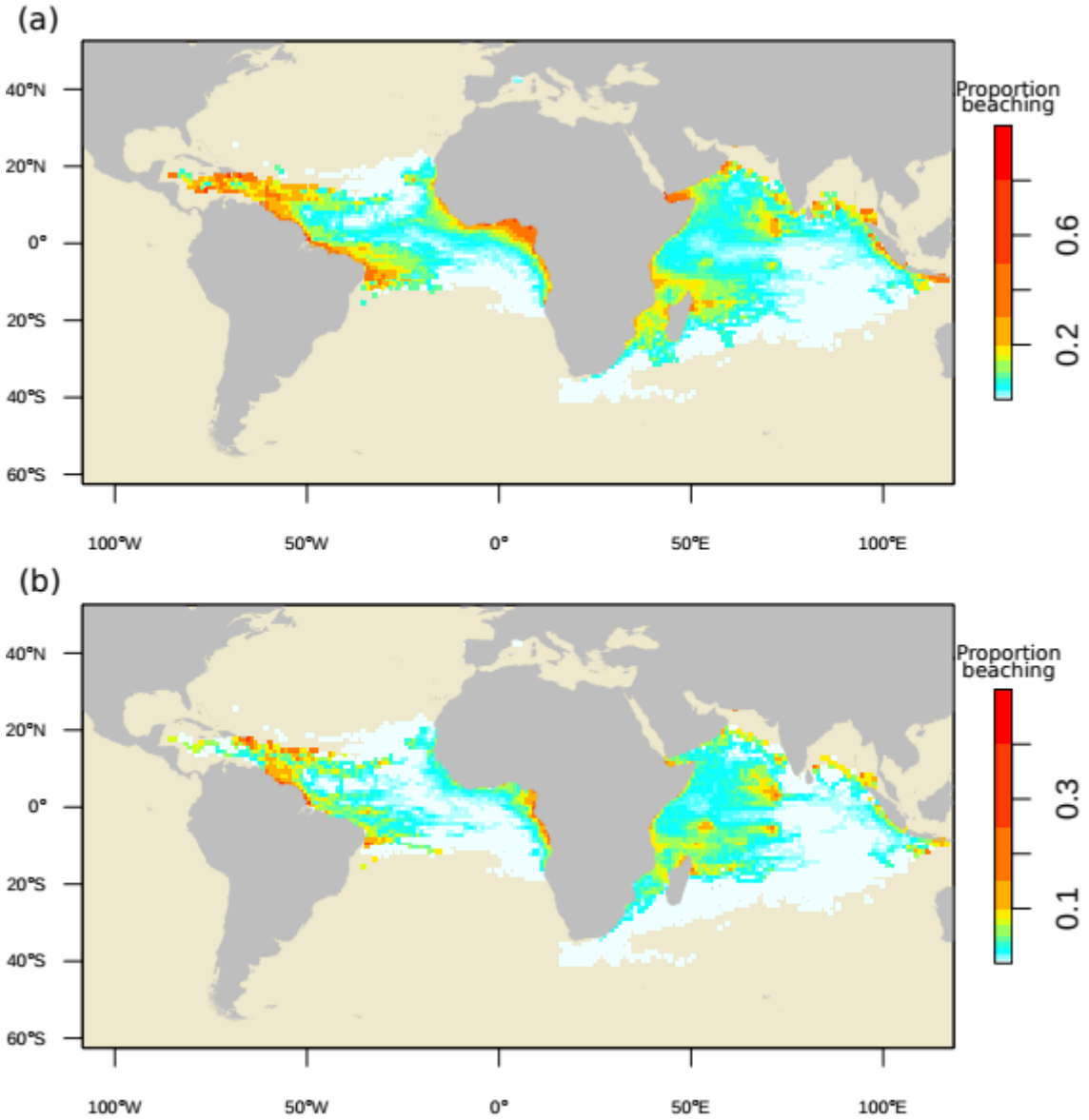

Figure 1.3: Maps of the proportion of dFADs that beached within 3 months after passing through each 1°x1° grid cell over the period 2008-2017. In (a), all beachings are considered, whereas in (b) only beachings along shore are included. Beachings along shore and recoveries displaced to shore were separated via intersection with OpenStreetMap land polygons. Note that the color intervals are unevenly distributed to highlight the low values.

Major areas of dFAD deployments during 2013-2017 spanned the whole fishing grounds of the French and associated flags purse seine fishery (Fig. 1.4a-b). In the AO, dFADs were deployed all along the coast of West Africa, from Mauritania down to Angola with the the most intense activity being observed along the equator and off the coasts of Mauritania, Gabon and Angola. In the IO, dFADs were deployed in the Western Indian Ocean, including the Exclusive Economic Zones of the Seychelles, Comoros, Kenya, French overseas territories and northwest of Madagascar

in the northern Mozambique Channel. dFADs deployments were particularly frequent North-West of the Seychelles.

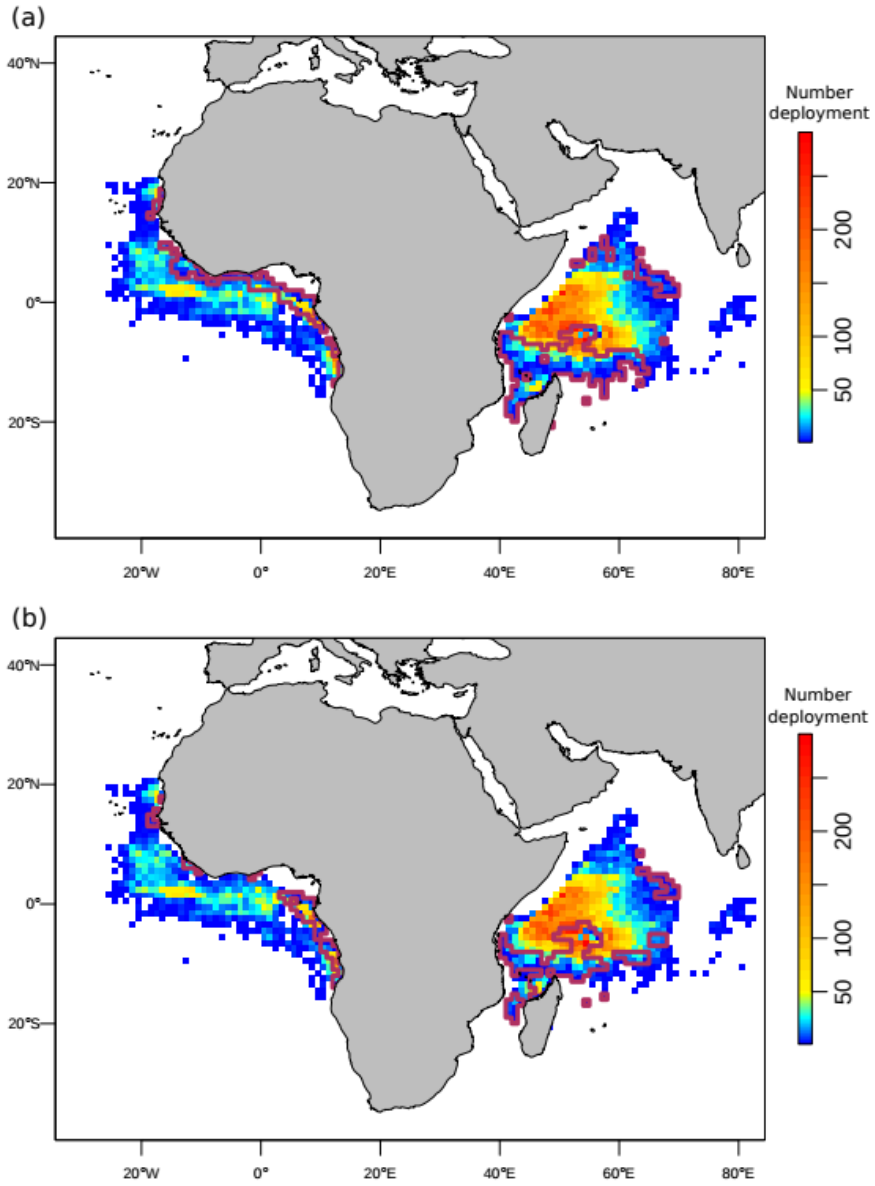

Figure 1.4: Density maps representing the number of dFAD deployments in each 1°x1° cell recorded in logbook data for the period 2013-2017. The thick, solid curves delimit areas representing the 20% of deployments most likely to produce a beaching within 3 months of a dFAD passing through those areas. In (a), all beachings are considered, whereas in (b), only beachings along shore are included. Beachings along shore and recoveries displaced to shore were separated via intersection with OpenStreetMap land polygons.

Combining spatial proportions of dFADs that beached (Fig. 1.3a-b) with observed dFAD deployment positions (Fig. 1.4a-b), we estimated the expected change in beachings and dFAD deployments due to prohibiting dFAD deployments in the highest risk areas for both oceans. Under all scenarios of dFAD deployment redistribution, spatial prohibitions are predicted to significantly

reduce beaching rates. For example, if we prohibit dFAD deployments in areas corresponding to the 20% of deployments with highest beaching risk, we can prevent 37% of beachings in the IO and 40% in the AO in the absence of dFAD deployment effort redistribution, and 21% and 25% of beachings in the IO and AO, respectively, even if we allow for dFAD deployment redistribution to areas with less beaching risk (Fig. 1.5a). These percentages are even higher when we focus on the proportion of beaching including only beachings that happen along shore, with up to a 52% reduction in beachings in the AO even if the total number of deployments is conserved via effort redistribution (grey dashed line in Fig. 1.5b).

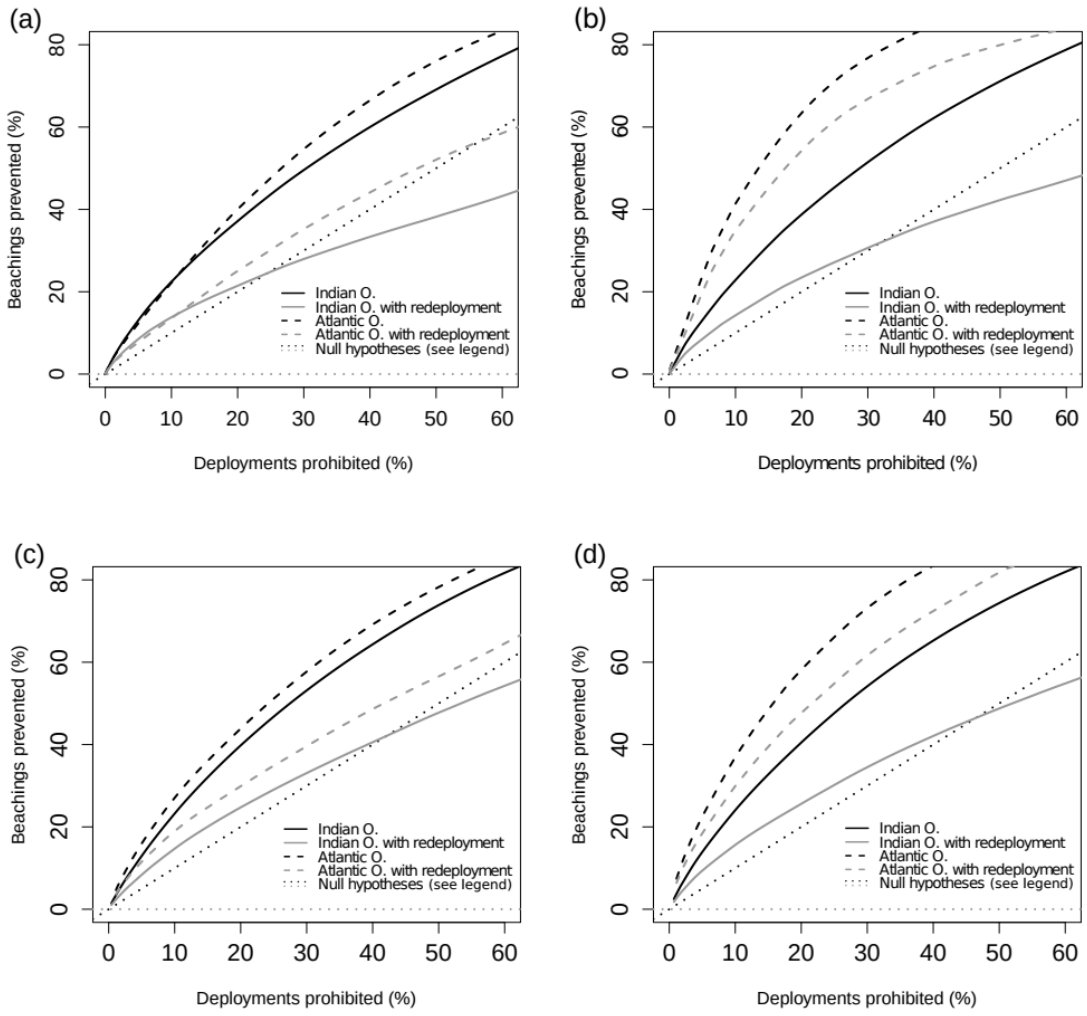

Figure 1.5: Predicted reduction in beaching rate as a function of the amount of area put aside in annual (a-b) or quarterly (c-d) closures to dFAD deployments. Areas are closed from most likely to least likely to produce a beaching within 3 months of deployment, with area being quantified along the x-axis in terms of the fraction of deployments that occurred in closed areas prior to their closure. Black and grey dotted lines correspond to the null expectation of what the corresponding black and grey curves would look like if all areas had the same beaching risk, and are the same in the IO and AO. In (a) and (c), all beachings are considered, whereas in (b) and (d), only beachings occurring along shore are included. Beachings along shore and recoveries displaced to shore were separated via intersection with OpenStreetMap land polygons.

Spatial prohibitions can be optimized to account for seasonal variability in beaching risk. For example, if areas corresponding to the 20% of deployments in areas with the highest beaching risk for each quarter are closed to dFAD deployments (Supplementary Fig. A3.6), we predict a 27% and 28% reduction in the IO and AO, respectively, even if dFAD deployment redistribution is allowed (Fig. 1.5c).

Focusing exclusively on beachings in coral reefs, prohibiting the 20% of deployments in the IO with the highest beaching risk to corals reduces coral reef beachings by 27% assuming dFAD deployment redistribution (Supplementary Fig. A3.7b), but the zones prohibited differ significantly from those that would be prohibited to reduce all beaching events (compare Fig. 1.4a and Supplementary Fig. A3.7a).

Closing the highest beaching risk areas to dFAD deployments is particularly effective at reducing beaching events in the south-western IO and in the eastern Gulf of Guinea in the AO (Fig. 1.6). If one focuses exclusively on coral reef beaching, then significant beaching reductions in the IO are also seen in the Maldives and off Indonesia (Supplementary Fig. A3.8). These results apply to both with and without dFAD deployment redistribution scenarios.

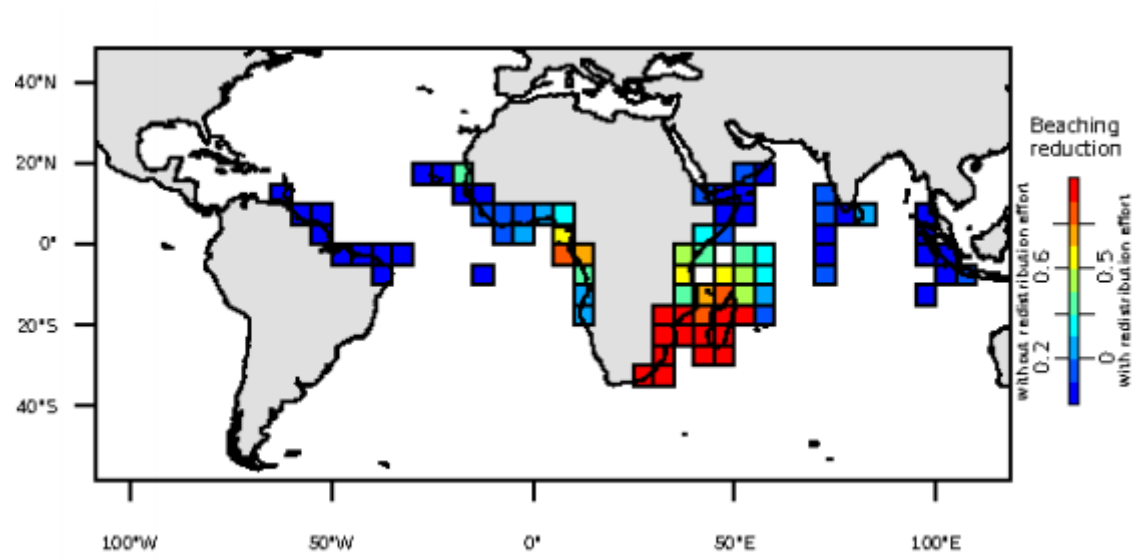

Figure 1.6: Map representing the predicted reduction in beaching when the 20% of dFAD deployments most likely to produce a beaching within 3 months are prohibited (see areas in Fig 1.4a), without (values on the left of the colorbar) and with (values on the right of the colorbar) dFAD deployment effort redistribution to non-prohibited areas.

4. Discussion

The overriding conclusion to be drawn from our results is that there is potentially a lot to be gained in terms of reduction in the rate of dFAD beachings from spatio-temporal closures for dFAD deployments by purse seine fishing vessels in the IO and AO. We examined a wide range of scenarios for closure objectives, implementation, and post-closure effects: considering all beachings versus just strandings along shore; considering all coastal zones versus just coral reefs; implementing static versus quarterly varying closures; and post-closure effort reduction versus effort redistribution to remaining open areas. In all cases, closing the riskiest areas to beaching is predicted to produce a tremendous reduction in beachings. Analyses of recent dFAD deployments in the IO by the Spanish fleet (the dominant other fleet in both oceans) indicate that Spanish and French deployments have quite similar spatial distributions. This suggests that our results may be applicable to all fleets (Katara et al. 2018), though access to dFAD trajectory data should be enhanced to confirm this. Perhaps most encouraging, high risk areas generally are relatively coherent in space so that it should be feasible from a management perspective to implement closures (e.g., south of 8°S in the IO and coastal zones in the Gulf of Guinea in the AO). In both oceans, the riskiest areas for beaching are not coincident with areas of high dFAD deployment activity nor fishing activities (Maufroy et al. 2015), suggesting that these closures could be implemented with relatively minimal impact to fisheries. The beaching reduction across coastal areas spared by the closures for dFAD deployment is highest in the south-western IO and in the eastern Gulf of Guinea in the AO, suggesting that our proposed deployment closure strategy is particularly efficient to protect these areas. The north-western IO and the northern Gulf of Guinea, which both represent hotspots of beaching, are less protected by the closures for dFAD deployments. However, high rates of putative recovery of dFAD buoys by coastal boats in these areas indicate that beaching early warning systems and dFAD recovery programs may be effective in areas that cannot be protected via closures if appropriate incentives can be provided to local partners for participating in these programs

As reported elsewhere (Maufroy et al. 2015; Floch et al. 2017, 2019), the number of dFADs deployed in both oceans has dramatically increased over the last decade. More surprising, the fraction of dFADs that end up beaching increased significantly over the period 2008-2013, after which time the fraction stabilizes. As this 2008-2013 period is coincident with a number of changes in the fishery, such as the switch to echosounder buoys (2010-2012), an increase in the prevalence

of dFAD fishing as opposed to fishing on free-swimming schools (Assan et al. 2019; Floch et al. 2019) and the fallout from Somali piracy (~2007-2011), it is hard to assign a specific cause to this pattern. One hypothesis is that as the number of dFADs has increased, the fraction of dFADs that are never fished upon has become more and more important to the point that after 2013 the fraction beaching simply reflects the balance one would expect in the absence of fishing between dFADs that beach versus dFADs that sink at sea. The stabilization of the beaching rate after 2013 may also be partially due to the implementation after 2014 of industry and/or regional fisheries management organizations limit on the number of buoys monitored by purse seine vessels (ICCAT 2019; IOTC 2019a) as fishers may remotely deactivate non-productive dFADs to remain under industry limits, resulting in the loss of location information for these FADs that continue to drift at sea and may later beach.

The risk of beaching depends strongly on the upper ocean circulation and its seasonal variability. In the IO, the southern African coast represents a high beaching risk area throughout the year due to the westward flowing Northern Equatorial Madagascar Current (Schott et al. 2009) that drives dFADs to the coasts of Mozambique and Tanzania. In the northern IO, high beaching risk areas change with monsoon regimes. The Somali coast represents a high beaching risk area in the winter when the Somali Current flows westwards (Schott & McCreary 2001), but not during the summer, when the western Maldives become a high risk area due to monsoon driven eastward circulation. There is less effect of seasonality on beaching risk in the AO, where areas of high beaching risk are driven by more-stable dominant circulation patterns. Along the western coast of Africa, beachings are related to the North Equatorial Countercurrent and the Guinea Current flowing eastwards, whereas high risk areas along the northern coast of South America and the Caribbean are linked to the South Equatorial, North Equatorial, North Brazil and Caribbean Currents flowing westwards (Bourles et al. 1999).

Our estimates of dFAD beaching rates after 2013 are higher than those estimated in the western central Pacific (Escalle et al. 2019) and in previous examinations in the IO and AO (Maufroy et al. 2015; Zudaire et al. 2018). Escalle et al. (2019) examined an area of the Pacific characterized principally by many small island chains, perhaps explaining lower beaching rates with respect to the continental land masses of the IO and AO. In the IO and AO, Maufroy et al. (2015) examined the period prior to 2013 for which we also find lower beaching rates. Zudaire et al. (2018) were principally concerned with the more-limited area of the Seychelles Archipelago, which is

composed of a large set of small islands similar to the area examined by Escalle et al. (2019) in the western central Pacific, and they considered a somewhat more restrictive definition of beaching.

There have been several recent management changes regarding the use of dFADs that may alter future dFAD beaching patterns, highlighting the importance of continuous monitoring of dFAD trajectories. The Indian Ocean Tuna Commission (IOTC) and the International Commission for the Conservation of Atlantic Tunas (ICCAT) currently limit the number of buoys monitored by an individual purse seine vessel at any given time to 300 (ICCAT 2019) and 350 (IOTC 2019a) buoys in the AO and IO, respectively, and these limits are likely to decrease over time. The IOTC has also implemented a resolution to progressively reduce and phase out the number of support vessels that assist the purse seiners with the management of dFADs (IOTC 2019b). These changes may lead purse seine vessels to optimize their use of dFADs in a number of ways. One potential outcome would be that fishers remotely deactivate dFADs that are likely to beach or drift outside of areas of interest so as to remain under industry limits. This practice is of much concern as it would result in the loss of information on the extent and location of dFAD beachings currently made available via fishing companies on a voluntary basis. Tuna regional fisheries management organizations should put in place appropriate incentives or other measures to assure that this information loss does not occur.

This study would not have been possible without access to a long and extensive time series of data on French dFAD trajectories. Though access to these extensive datasets is still quite limited for most fishing fleets worldwide, there are a number of encouraging signs of increased reporting of dFAD deployments and other dFAD activities to tuna regional fisheries management organizations (IOTC 2019a). We are hopeful that comprehensive datasets from all purse seine fishing fleets will be available in the near future, permitting better estimates of the impacts of management options and the development of real-time tools for the management of dFAD impacts on marine ecosystems.

Appendix A1 - New Classification model for onboard and at sea states of dFAD trajectory data

Overview

French dFAD trajectory data contain a mixture of geographic positions that were emitted while the transmitting buoy was onboard a boat and while the buoy was in the water. The onboard positions must be eliminated to recover the at sea trajectories useful for identifying beaching events. We accomplished this using a random forest classification algorithm. The algorithm used here is an improvement over that presented by Maufroy et al. (2015). In particular, it is distinguished with respect to the previous algorithm by:

1) The inclusion of additional training data derived from more recent dFAD trajectories

2) The use of new predictor variables based on variability in buoy speed or temperature for a set of positions immediately temporally before and after the position to be classified

New training dataset

The original classification algorithm developed by Maufroy et al. (2015) was based on a training dataset consisting of 204 buoys and 18,357 classified positions (Table A1.1). Data was manually classified based on buoy speed and temperature and data on nearby fishing activity. In this original dataset, classified buoys were randomly drawn from the period 2009-2010. Since the time that this training dataset was developed, the number and type of French dFAD buoys has considerably changed. In particular, the buoy manufacturer is now Marine Instruments. These buoys contain echosounders and have a higher maximum emission rate than previous models (<15 minutes versus 1 hour or more in previous models). As these technological changes potentially impact both classification success and dFAD deployment and use, we decided to include additional training data drawn from more recent time periods in our classification model. New training data was classified manually with the aid of a Shiny application in R that permitted simultaneous visualization of buoy speed, temperature, direction, emission rate and echosounder information, as well as dFAD deployment, visit and recovery data drawn from recent fisher logbooks and observer data. This additional training data consisted of 172 buoys and 61,419 classified positions drawn from the time period 2012-2018 (Table A1.2). Though classified buoy trajectories were largely randomly drawn from the set of buoy trajectories that possessed both logbook and observer data, 10-20 trajectories were specifically selected because they possessed data in the vicinity of Sri Lanka

during periods when the buoy had been recovered by artisanal fishers and was transported to a Sri Lankan port. This data was known to be difficult to properly classify due to the low speed of artisanal fishing boats, and additional classification data from this area was found to visually improve classification success in this region.

New classification model

In addition to including both new and old training data, the classification algorithm we used included a different set of predictor variables. Some predictor variables that were found to have little predictive power by Maufroy et al. (2015), such as rate of change in temperature, were removed, and new variables based on a temporal window around the position to be classified were added.

1.New predictor variables

New predictor variables included:

- the amount of time before and after a given position that buoy speed was less than 3 m/s
- the standard deviation of speed and temperature in a 7 position window around a given position (3 before, 3 after and the given position)

The first of these was included because speeds greater than 3 m/s were extremely rare in water positions, but common in boat positions (Fig. A1.1), so even though an individual boat position may have a low speed, subsequent or preceding positions were likely to have high speed (Fig. A1.2). Similarly, both speed and temperature were observed to be more variable when buoys were onboard, and therefore the standard deviation of these variables in a small temporal window around a position to be classified was found to be effective at separating onboard and at sea positions (Figs. A1.3 & A1.4).

The full set of predictor variables is presented in Table A1.3.

2.Model description

The final classification model as executed in R is presented below.

```
randomForest(formula = class ~ lt_5km_land + dist_port_km +
mean_time_change_s +
    mean_speed_ms + abs_azimuth_change_180 + acceleration_ms2 +
    local_speed_ms_stddev + local_water_temp_stddev + time_lt_3ms_s +
    before_time_lt_3ms_s + after_time_lt_3ms_s + is_mi_buoy,
    data = themodel$training.data, ntree = 1500, mtry = 4)
```

The meanings of the different predictor variables are given in Table A1.3.

3.Model diagnostics

Not surprisingly, the classification model has prefect prediction success when applied to the training data used to calibrate the model (Table A1.4; note, however, that this was not the case for the model used in Maufroy et al. 2015, which had imperfect prediction success even when applied to the training data used to construct the model). However, internal cross validation in the random forest model suggests that there is an ~2.3% error rate when predicting onboard positions and an ~0.2% error rate when predicting at sea positions (Table A1.5). These error rates are considerably lower than those estimated by Maufroy et al. (2015), which predicted a mean error rate over both position classes (i.e., onboard and at sea) of ~2.2%. The superior performance of the new model was further confirmed by cross-application of the new model to the old training data and the old model to the new training data, which indicated at least a 50% reduction in error rate with the new classification model. Model internal error rate indicates that the number of trees used is more than sufficient to reach model predictive stability (Fig. A1.5). By far the most important predictor variables for prediction success were the standard deviation of speed in a 7-position window around a given position (i.e., local_speed_ms_stddev), total time around a position for which buoy speed was less than 3 m/s (i.e., time_lt_3ms_s) and the speed of the buoy at a given position (i.e., mean_speed_ms) (Fig. A1.6). Though other variables contributed to model estimations, their impact was far weaker.

In Maufroy et al. (2015), a post-processing step was used to reclassify isolated pairs of consecutive onboard (B) positions as at sea (W) positions, which improved the overall classification success. Tests indicated that this post-processing step produced no significant improvement for the new classification model, likely due to the inclusion of new predictor variables that already take into account the temporal context of a given position. We, therefore, decided not to use this post-processing step with the new classification model.

Problem of positions with very short time steps

A small number of buoys in the dFAD trajectory database possessed a small number of positions that were less than 60 seconds (most often less than 5 seconds) after the position immediately preceding it (3,387 buoys out of 64,613 buoys in the entire database). These are generally associated with recent buoys transmitting multiple sets of echosounder data, one set

immediately after the other (e.g., due to multiple echosounder frequencies). The buoy speeds associated with these very small time steps were often anomalously large as they were presumably dominated by the noise in GPS position acquisition, which would be large relative to the small size of the time step. Given the large and rapidly varying velocities associated with these positions, they were often erroneously classified as on board a vessel. To correct for this, time periods less than 1 minute that were classified as on a vessel were ignored when dividing trajectories into at sea and onboard portions.

References

Maufroy A, Chassot E, Joo R, Kaplan DM (2015) Large-Scale Examination of Spatio-Temporal Patterns of Drifting Fish Aggregating Devices (dFADs) from Tropical Tuna Fisheries of the Indian and Atlantic Oceans. PLoS ONE 10:e0128023. doi:10.1371/journal.pone.0128023

Table A1.1: Number of buoys and positions by class in training dataset used in Maufroy et al. (2015). Position classification B indicates onboard (i.e., boat) positions, whereas classification W indicates at sea (i.e., water) positions. Note that the 'Number of buoys' column indicates the number of classified buoys that possess at least one position of a given class, and, therefore, an individual buoy can be counted in both the B and W classes.

Position classification	Number of buoys	Number of positions	Percent of positions
B	197	2677	14.6
W	201	15680	85.4
Total	**204**	**18357**	**100.0**

Table A1.2: Number of buoys and positions by class in new training dataset. Position classification B indicates onboard (i.e., boat) positions, whereas classification W indicates at sea (i.e., water) positions. Note that the 'Number of buoys' column indicates the number of classified buoys that possess at least one position of a given class, and, therefore, an individual buoy can be counted in both the B and W classes.

Position classification	Number of buoys	Number of positions	Percent of positions
B	147	4893	8
W	167	56526	92
Total	**172**	**61419**	**100.0**

Table A1.3: Names and descriptions of the predictor variables used in the classification model.

Predictor variable	Description
lt_5km_land	A boolean (true/false) indicating whether or not the buoy is within 5 km of the coast as determined by the GSHHS high resolution coastline data (http://www.soest.hawaii.edu/pwessel/gshhg/)
dist_port_km	Distance in kilometers to the nearest tuna fishing port
mean_time_change_s	Mean of the time step in seconds for the trajectory segment proceding a given buoy position and for the trajectory segement after the position
mean_speed_ms	Mean of the buoy speed in m/s over the trajectory segment proceding a given position and over the trajectory segement after the position
abs_azimuth_change_180	Heading change in degrees between the trajectory segments proceding and immediately after the position
acceleration_ms2	The linear acceleration (i.e., change in direction is *not* accounted for) of the buoy over the trajectory segements immediately proceding and after the position
local_speed_ms_stddev	The standard deviation of the buoy speeds in m/s over the trajectory segments immediately proceeding a set of 7 buoy positions in a window centered on the given position (3 before, 3 after and the central position)
local_water_temp_stddev	The standard deviation of the water temperature measurements in degrees Celcius at 7 buoy positions in a window centered on the given position (3 before, 3 after and the central position)
before_time_lt_3ms_s	The time period in seconds proceding a given position that the buoy speed was consistently less than 3 m/s
after_time_lt_3ms_s	The time period in seconds after a given position that the buoy speed was consistently less than 3 m/s
time_lt_3ms_s	The total time period in seconds before and after a given position that the buoy speed was consistently less than 3 m/s
is_mi_buoy	A boolean (true/false) indicating if the buoy in question was manufactured by Marine Instruments or not. Marine Instruments data corresponds to newer buoys typically including an echosounder

Table A1.4: Confusion matrix for the new classification model when predicting on the combined training dataset used to construct the model. Position classification B indicates onboard (i.e., boat) positions, whereas classification W indicates at sea (i.e., water) positions.

	Predicted B	Predicted W
Observed B	7,570	0
Observed W	0	72,206

Table A1.5: Internal confusion matrix for new classification model. This confusion matrix is the result of internal cross-validation of the random forest model. Position classification B indicates onboard (i.e., boat) positions, whereas classification W indicates at sea (i.e.,water) positions.

	Predicted B	Predicted W	Classification error rate
Observed B	7,393	177	0.0234
Observed W	158	72,048	0.0022

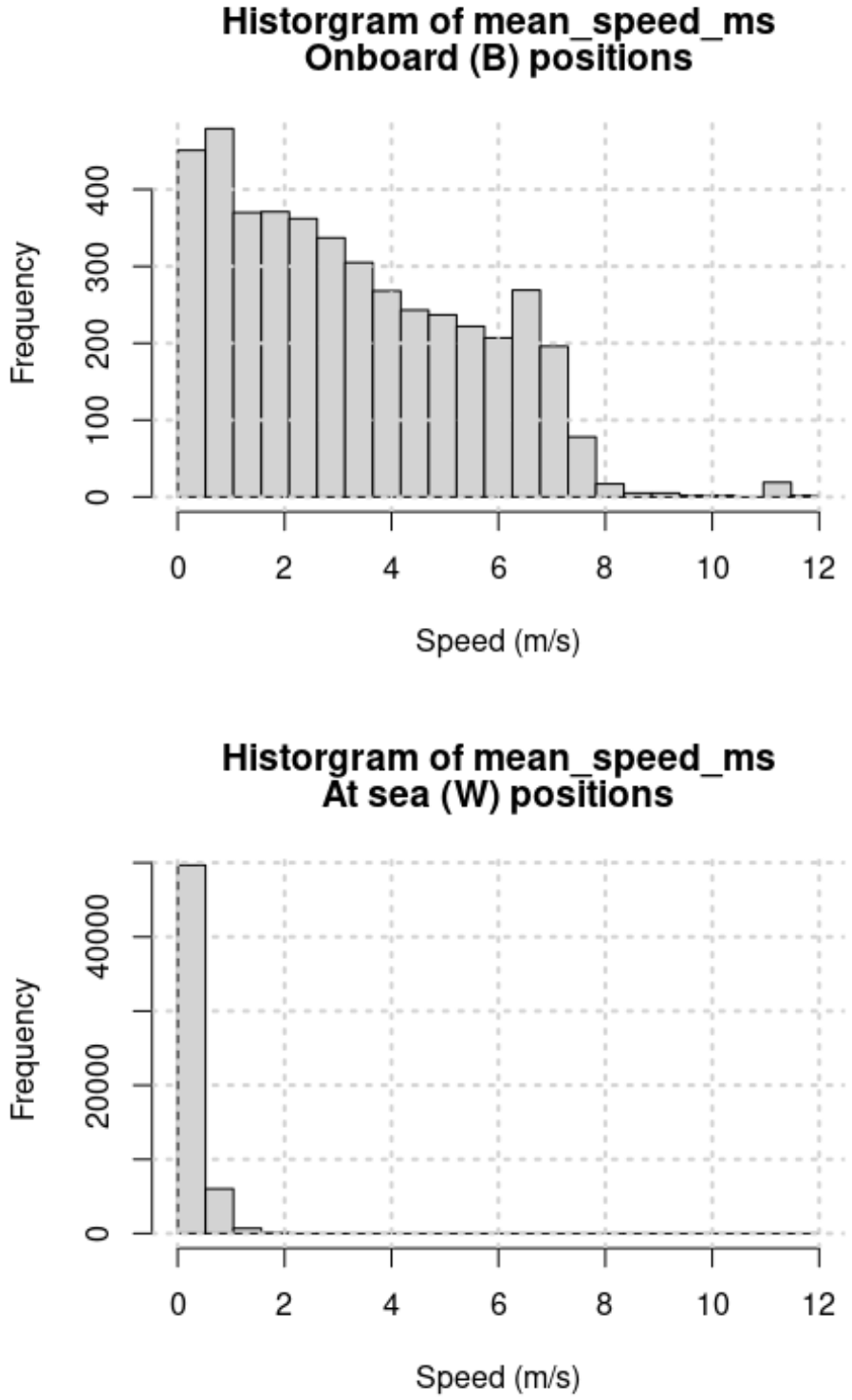

Figure A1.1: Histogram of mean_speed_ms, i.e., the mean of the two buoy speeds over the trajectory segments immediatiely proceding and immediately after a given buoy position (see Table A1.3 for more details). The top panel is for positions classified as onboard, whereas the bottom panel is for at sea positions.

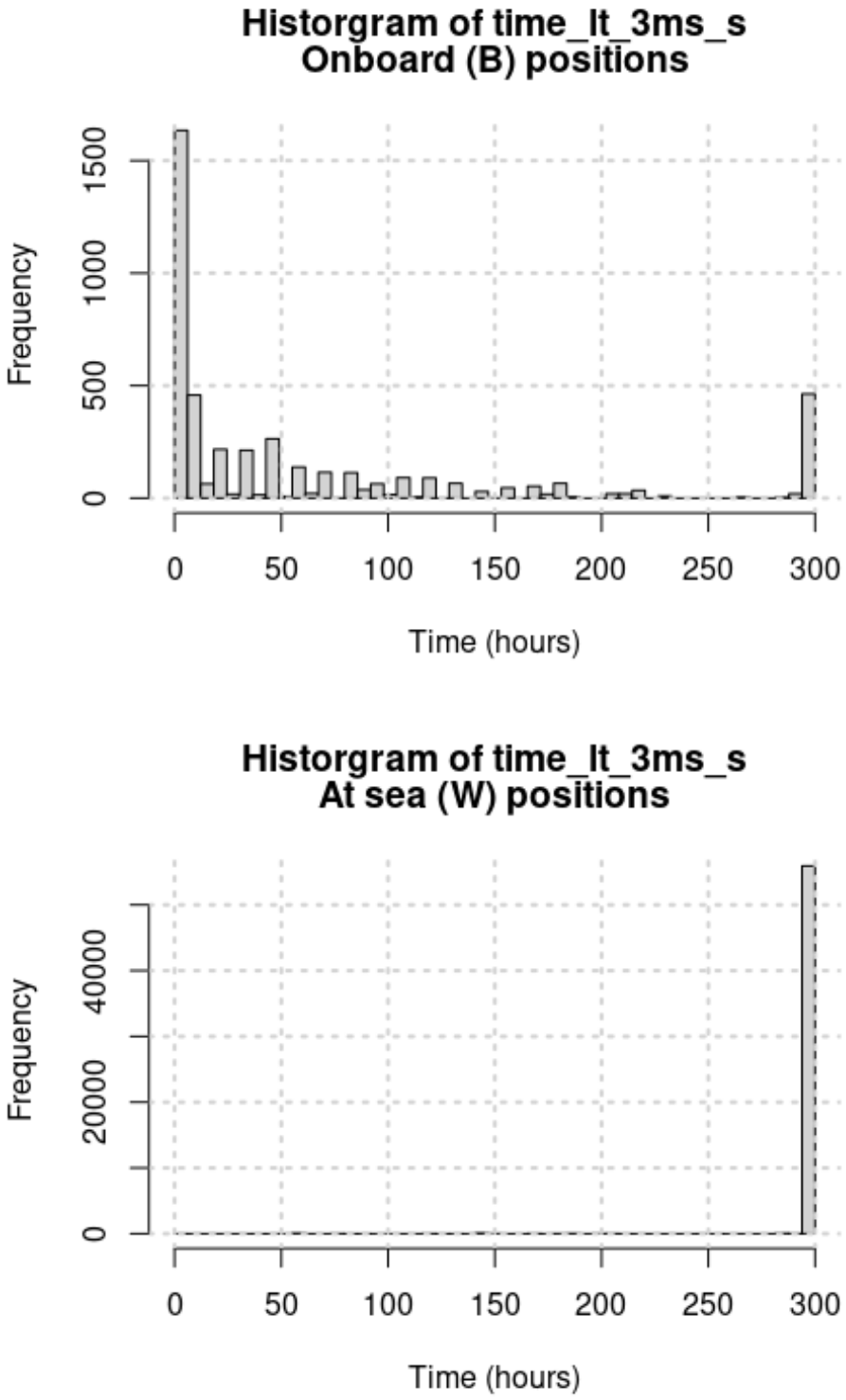

Figure A1.2: Histogram of time_lt_3ms_s, i.e., the time period around a given position for which buoy speed was inferior to 3 m/s (see Table A1.3 for more details). The top panel is for positions classified as onboard, whereas the bottom panel is for at sea positions. Values have been divided by 3600 to present results in units of hours instead of seconds.

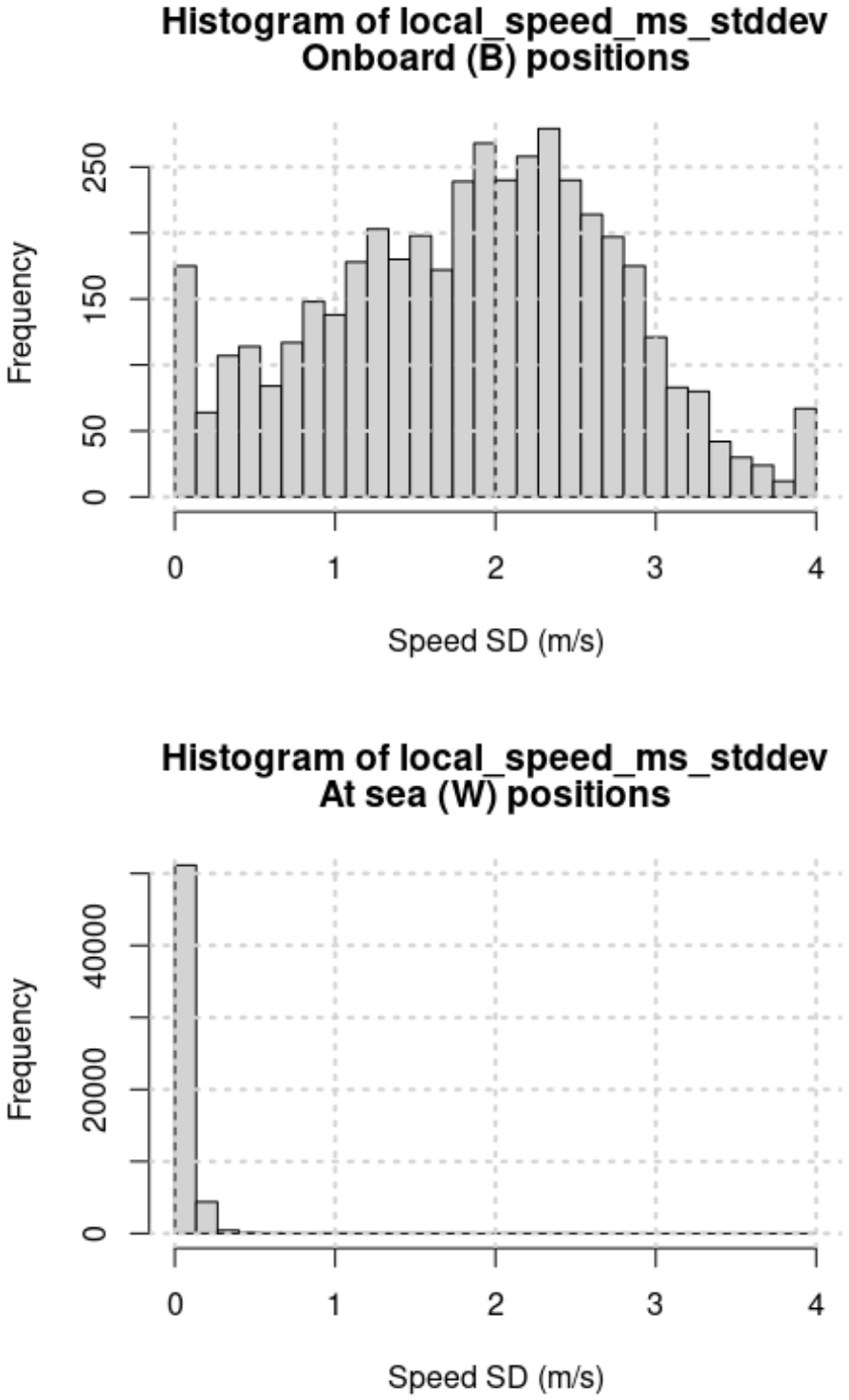

Figure A1.3: Histograms of local_speed_ms_stddev, i.e., the standard deviation of the buoy speed for a set of 7 consecutive buoy positions centered around a given position (see Table A1.3 for more details). The top panel is for positions classified as onboard, whereas the bottom is for at sea positions.

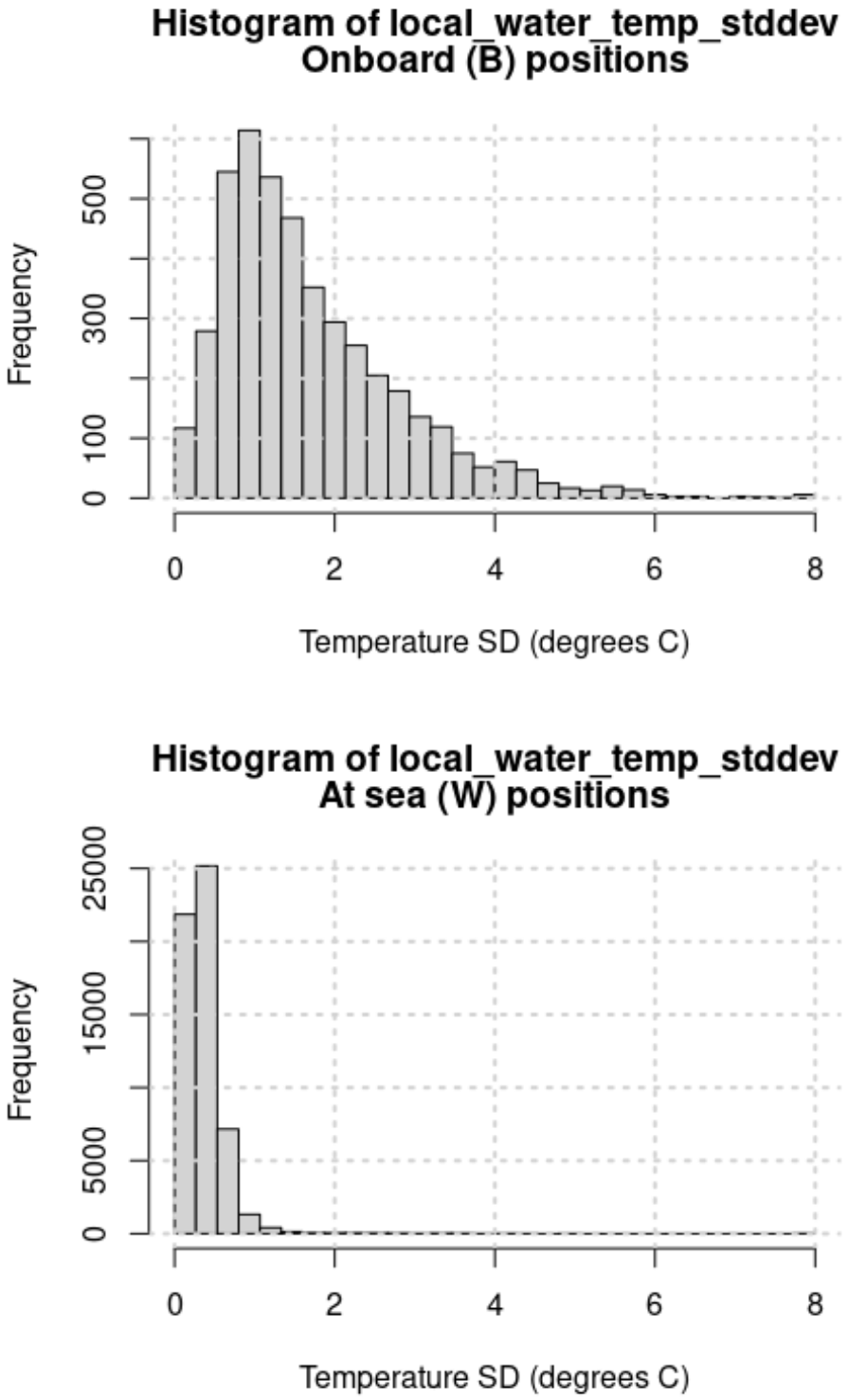

Figure A1.4: Histograms of local_water_temp_stddev, i.e., the standard deviation of water temperature measurements for a set of 7 consecutive buoy positions centered around a given position (see Table A1.3 for more details). The top panel is for positions classified as onboard, whereas the bottom is for at sea positions.

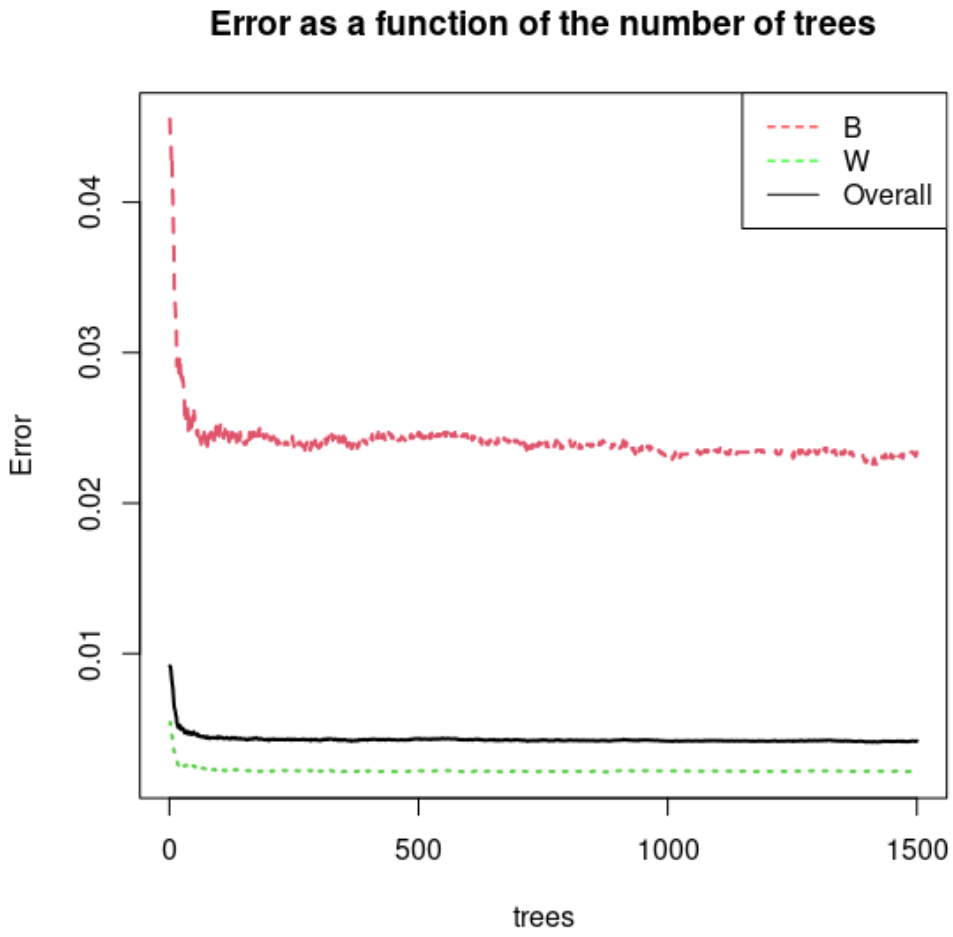

Figure A1.5: Error rate as a function of the number of trees included in the random forest model. Position classification B indicates onboard (i.e., boat) positions, whereas classification W indicates at sea (i.e., water) positions.

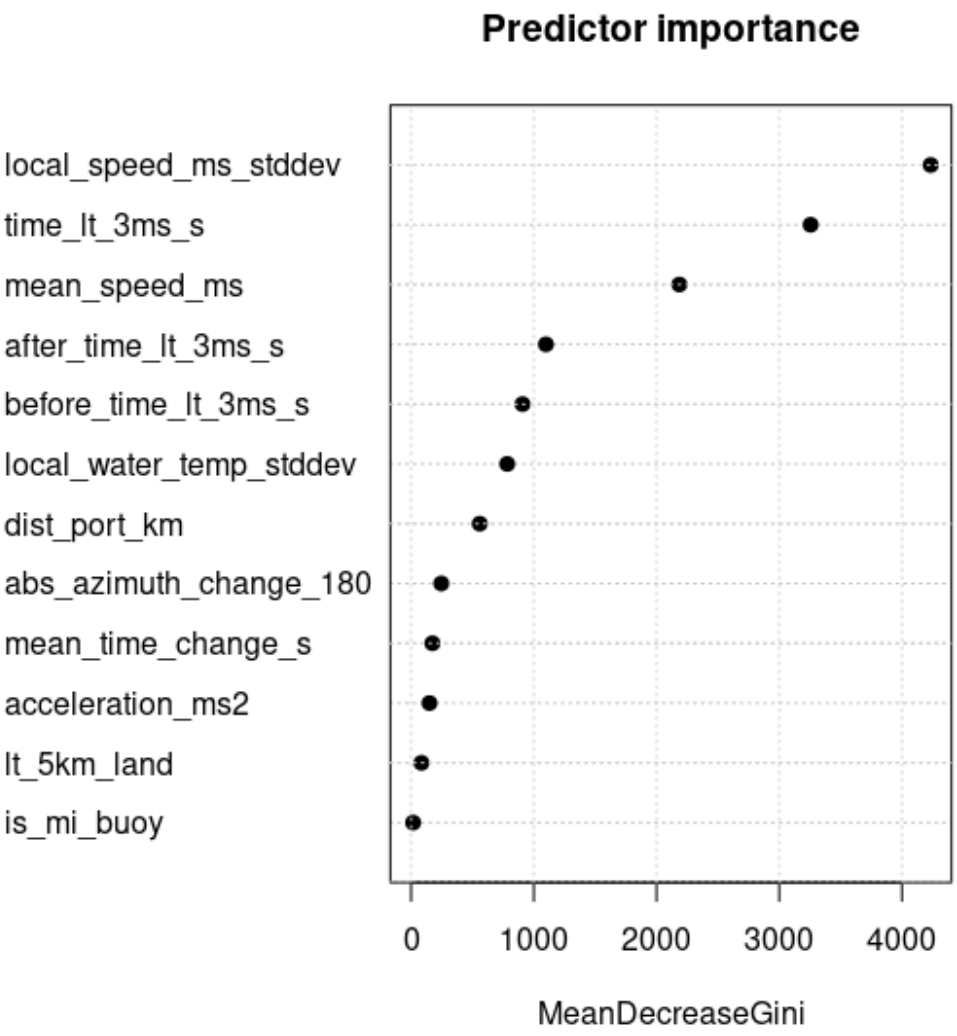

Figure A1.6: Predictor variable importance in new random forest classification model. See Table A1.3 for the meaning of the different explanatory variables. MeanDecreaseGini, the estimate used to quantify the importance of each predictor variable, is based on the average over all classification trees in the model of the reduction in node impurity at each node for which a given predictor variable was chosen. Impurity measures the probability of randomly assigning a measurement in a given branch of a classification tree to the wrong class (i.e., branches that are perfectly homogeneous in class will have an impurity of zero, whereas if a branch is split 50/50 between classes then the impurity is 0.5), and the reduction in impurity at a node is the difference in the impurity of the branch preceding a node and the weighted average impurities of the two branches immediately after a node. The scale of MeanDecreaseGini is not important as it is a relative measure of variable importance.

Appendix A2 - Quantification of beachings as in water (beachings along shore) or on land (recoveries displaced)

In a preliminary analysis of the beaching locations identified in this study, we found that most beachings occurred in water, stranding close to the coast, as expected. However, we also found an unexpectedly large amount of beaching locations on land, mostly within small ports or coastal villages. To further explore that critical aspect of our work we first classified manually a randomly selected sample of 100 identified beaching locations based on a Google Map visualization and obtained 55 beachings occurring in water and 45 on land. Moreover, beachings identified in water showed two situations: (i) beachings that occurred in water only (35 cases, e.g., Fig. A2.1) and (ii) beachings that occurred in water first and then found beached again on land some days later (20 cases, e.g., Fig. A2.2). Also, beachings identified as occurring on land revealed two situations prior to beaching: (i) an apparently normal drift towards the coast (39 cases, e.g., Fig. A2.3) and (ii) a sudden change in the direction of the trajectory near the coast (6 cases, e.g., Fig. A2.4).

Subsequently, the whole dataset of ~ 10 000 identified beaching locations was classified automatically as “in water” or “on land” using an algorithm based on the OpenStreetMap (OSM) land polygons as mentioned in the main text. The automatic classification resulted in an overall percentage of ~53% of beachings in water and ~47% on land, which are very similar to the values obtained in our manual classification of 100 locations. Moreover, a direct comparison of the manual vs. automatic classification of these 100 cases showed that the results were identical except for 3 cases where the locations were actually difficult to determine as being in water or on land, such as in intertidal zones, a few meters from the coast.

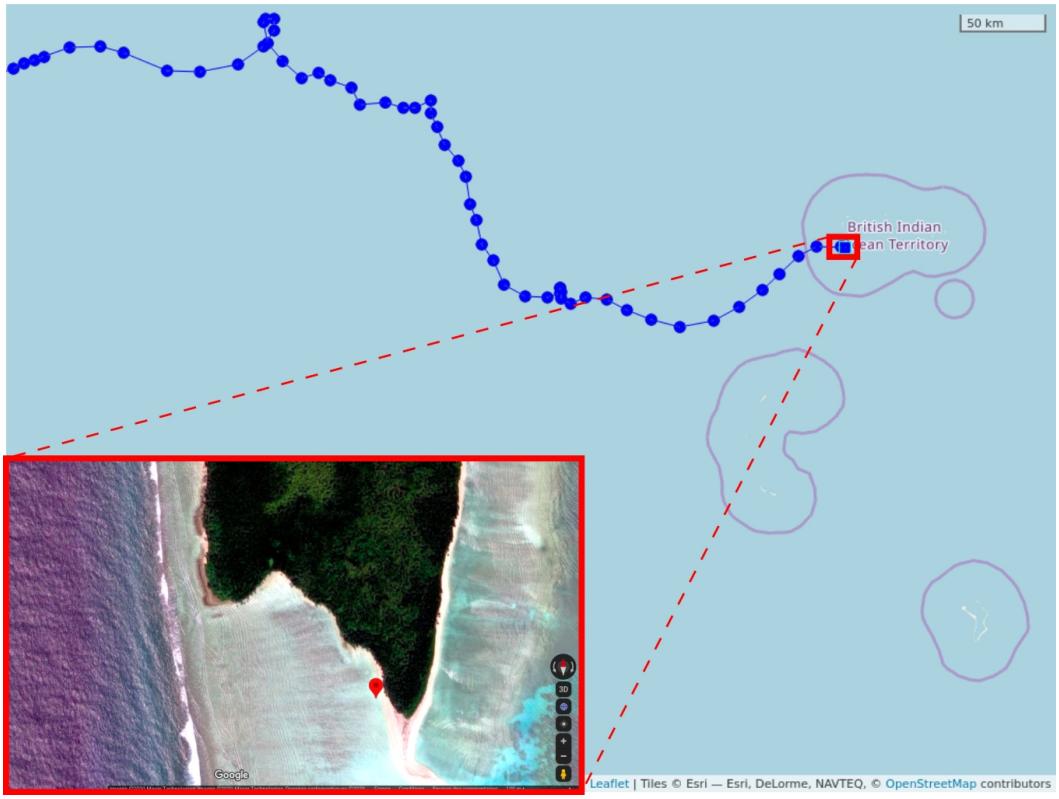

Figure A2.1: The end of the trajectory of buoy n° 50424 (in blue) and a zoom on its identified beaching location (71.7513°,-5.4148°) classified visually as in water.

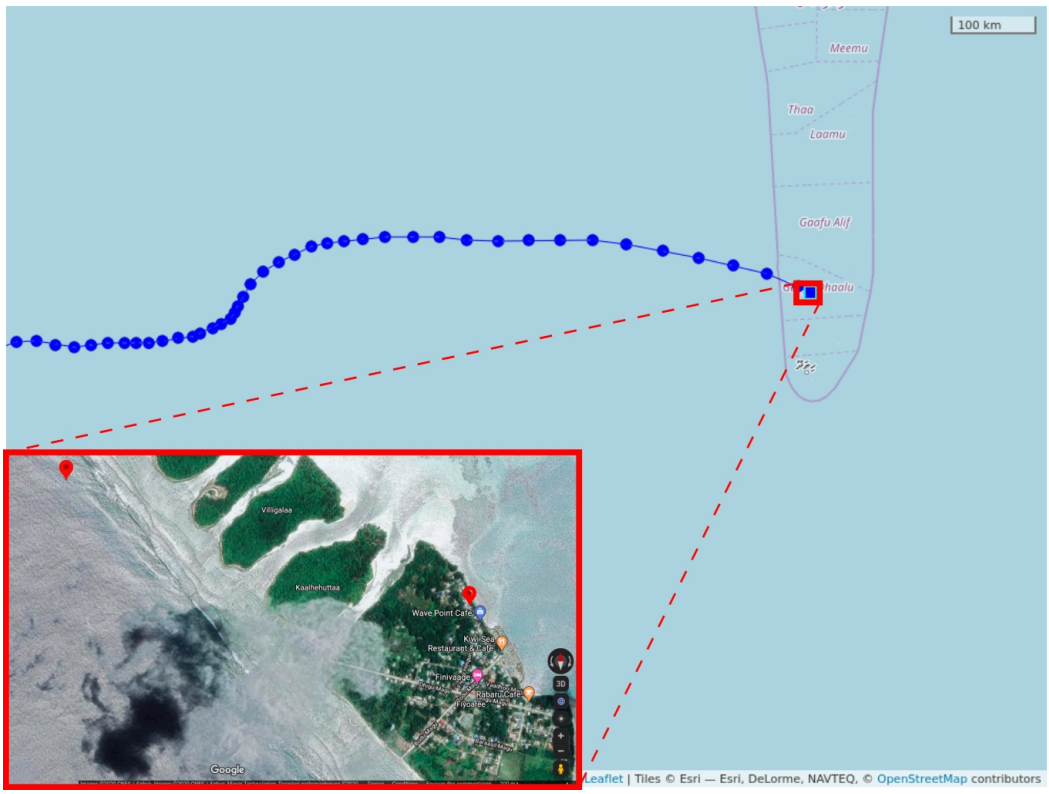

Figure A2.2: The end of the trajectory of buoy n° 9709 (in blue) and a zoom on two identified beaching locations classified visually as in water for the first one (73.1218°,0.2307°) and then on land for the second one (73.1365°,0.226°) 3 days later.

Figure A2.3: The end of the trajectory of buoy n° 30126 (in blue) and a zoom on its identified beaching location (-2.2013°, 4.8303°) classified visually as on land.

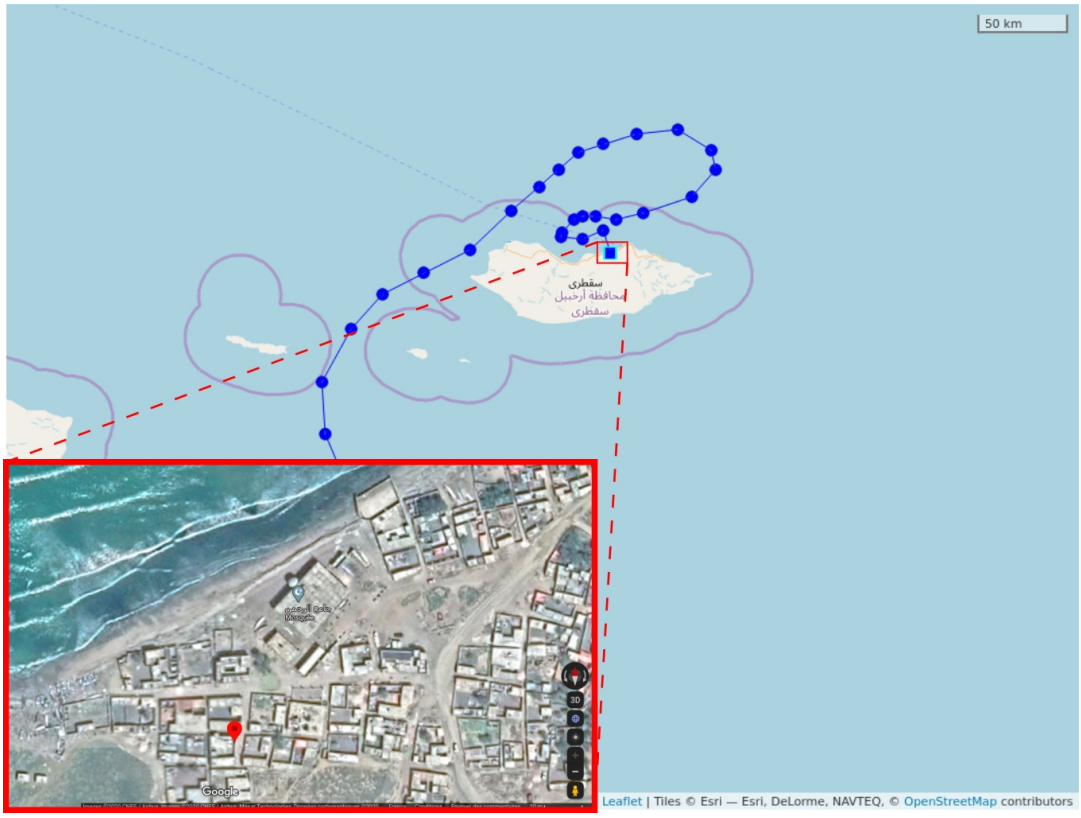

Figure A2.4: The end of the trajectory of buoy n° 15130 (in blue) and a zoom on its identified beaching location (54.016°,12.6522°) classified visually as on land. Note that here there was a sudden change in the trajectory prior to beaching, likely because the buoy was picked up by a boat.

Appendix A3 - Additional figures

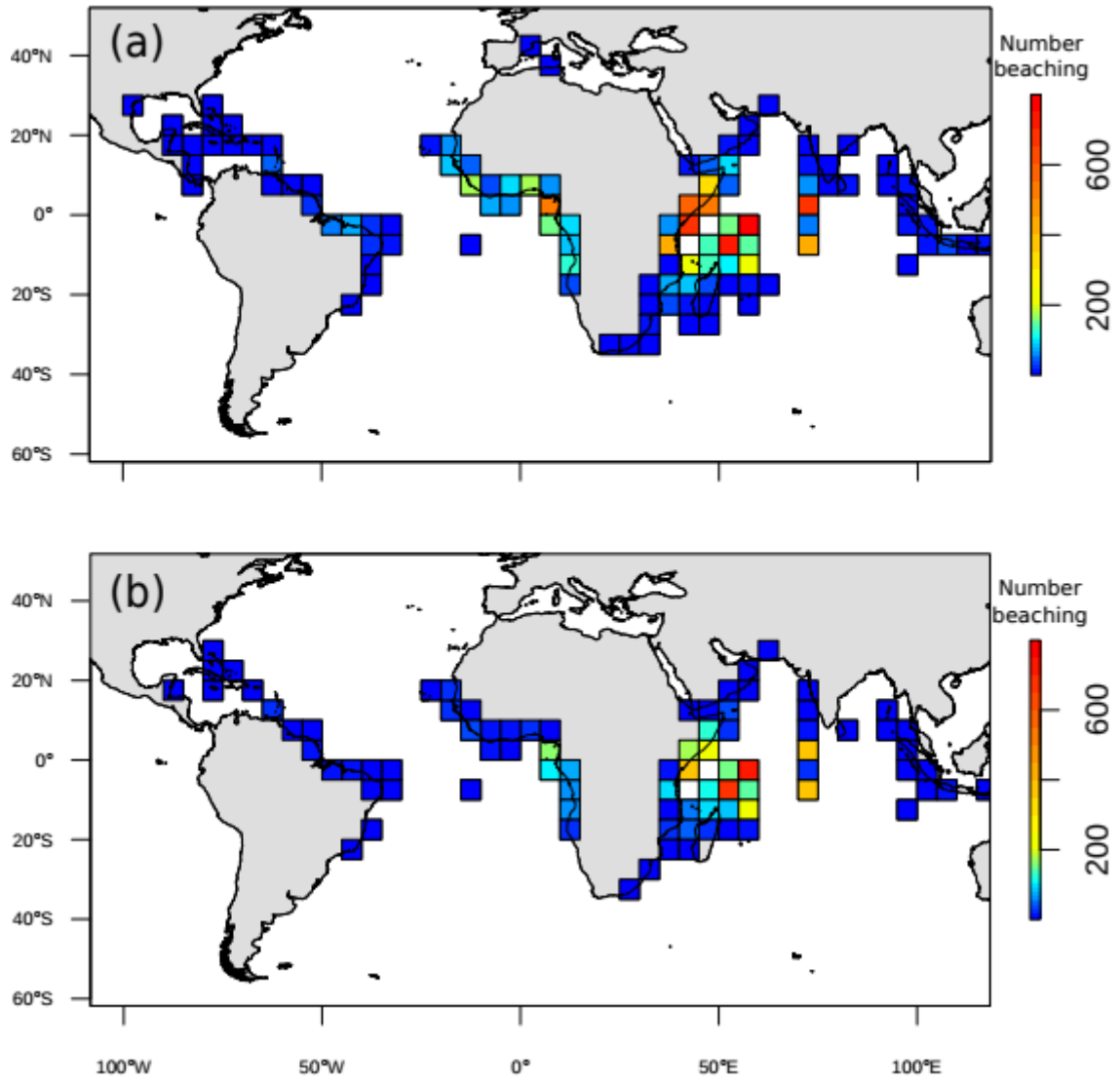

Figure A3.1 : The total number of dFADs beached in each 5°x5° grid cell for the period 2008-2017. Redder colors indicate higher numbers of beaching. In (a), all beachings are considered, whereas in (b) only beachings along shore are included. Beachings along shore and recoveries displaced to shore were separated via intersection with OpenStreetMap land polygons. Note that our dFAD trajectory data is incomplete before ~2010, so the absolute number of beachings is likely somewhat higher than values shown in the figure, though differences are likely to be small as the number of dFADs was far lower before 2010 than after 2010.

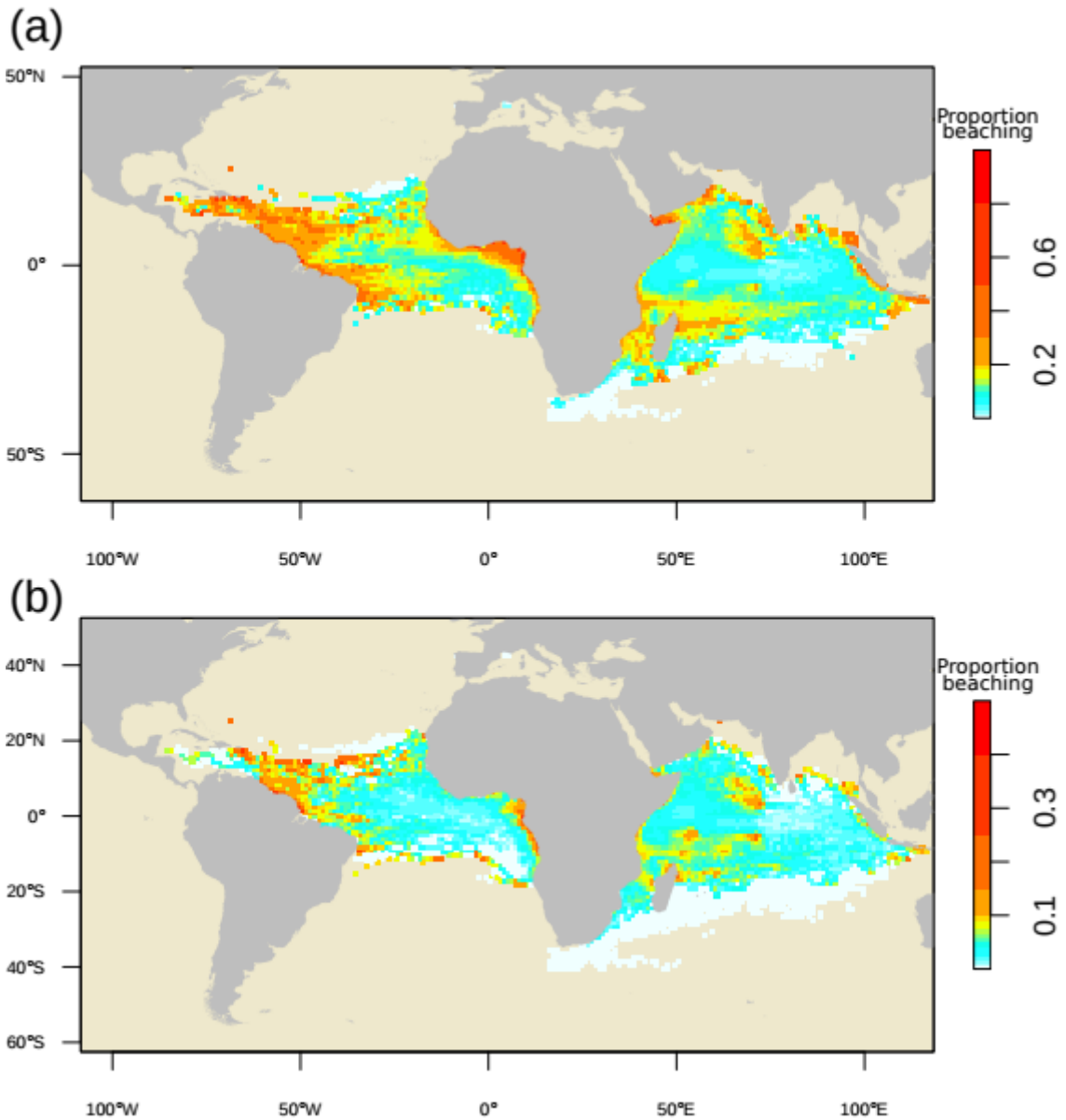

Figure A3.2: Maps of the proportion of dFADs that beached within 12 months after passing through each 1°x1° grid cell over the period 2008-2017. In (a), all beachings are considered, whereas in (b) only beachings along shore are included. The color intervals are unevenly distributed to highlight the low values.

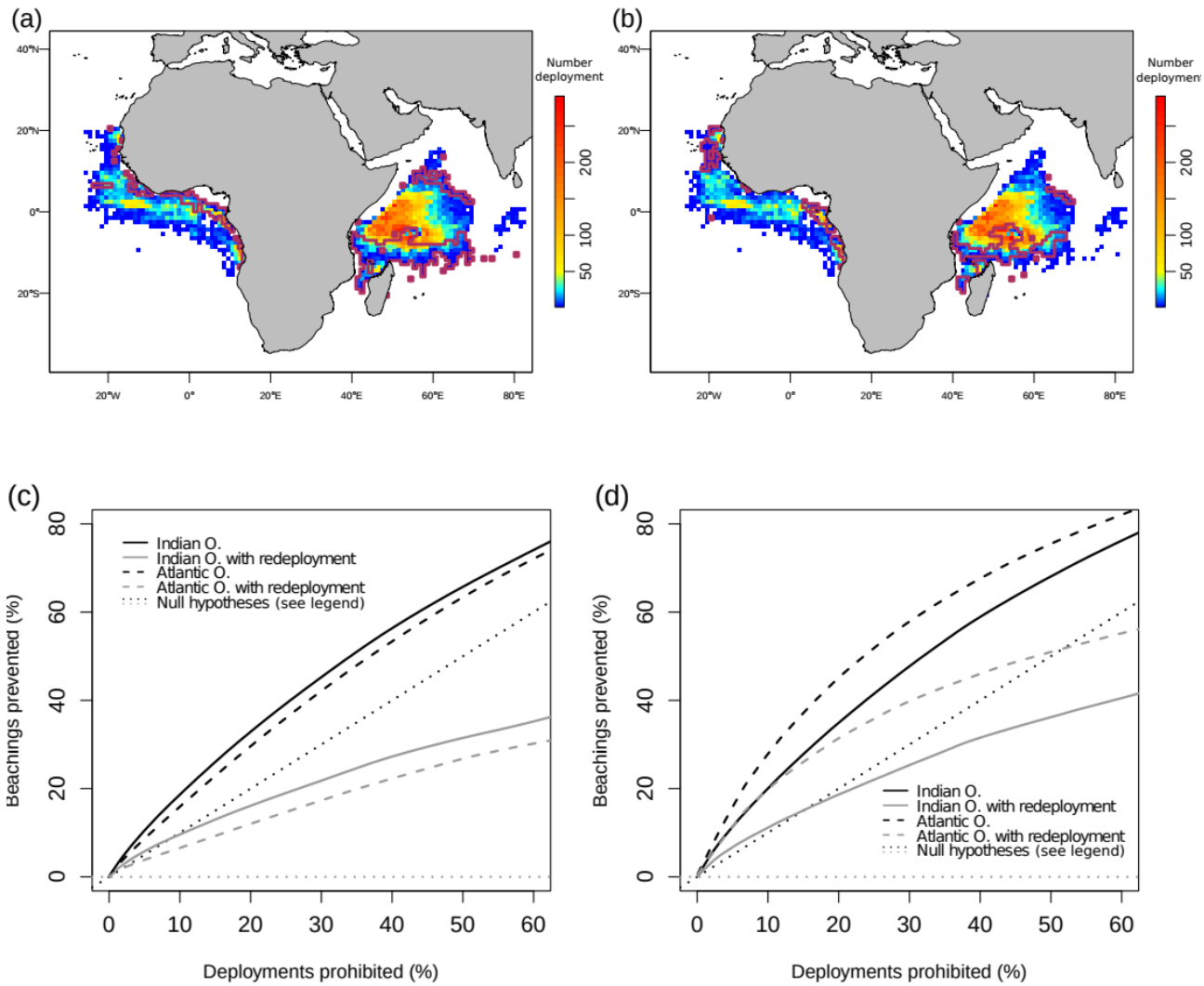

Figure A3.3: Density maps representing the number of dFAD deployments in each 1°x1° cell recorded in logbook data for the period 2013-2017. The purple curves delimit areas representing the 20% of deployments most likely to produce a beaching within 12 months of a dFAD passing through those areas (a-b). Predicted reduction in beaching rate as a function of the amount of area put aside in annual closures to dFAD deployments. Areas are closed from most likely to least likely to produce a beaching within 12 months of deployment (c-d), with area being quantified along the x-axis in terms of the fraction of deployments that occurred in closed areas prior to their closure. In (a-c), all beachings are considered, whereas in (b-d), only beachings along shore are included.

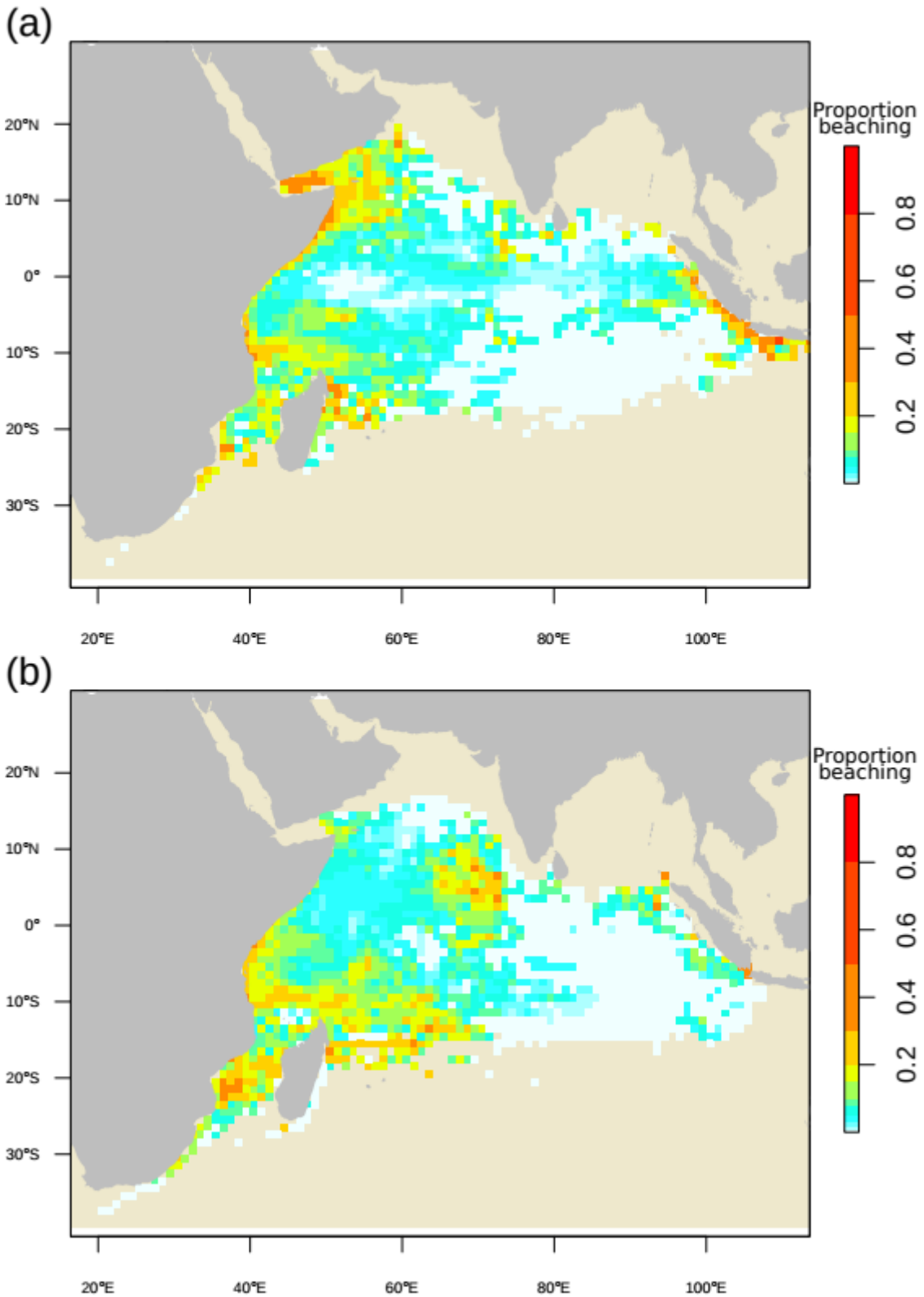

Figure A3.4: Seasonal maps of the proportion of dFADs that beached within 3 months after passing through each 1°x1° grid cell over the period 2008-2017. (a) October-March; (b) April-September. The color intervals are unevenly distributed to highlight the low values.

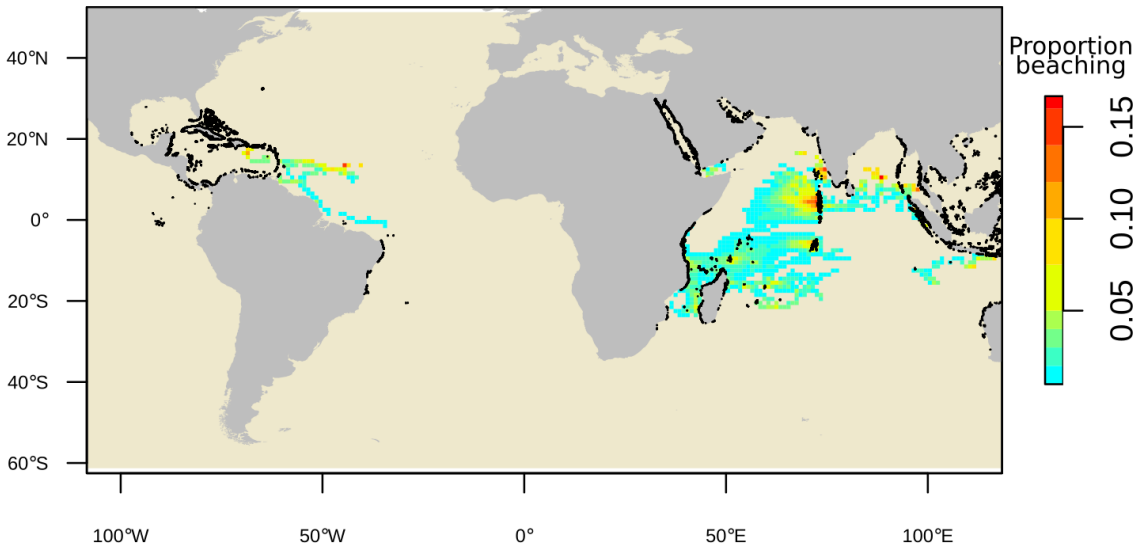

Figure A3.5: Map of the proportion of dFADs that beached in coral reefs within 3 months after passing through each 1°x1° grid cell over the period 2008-2017. The color intervals are unevenly distributed to highlight the low values.

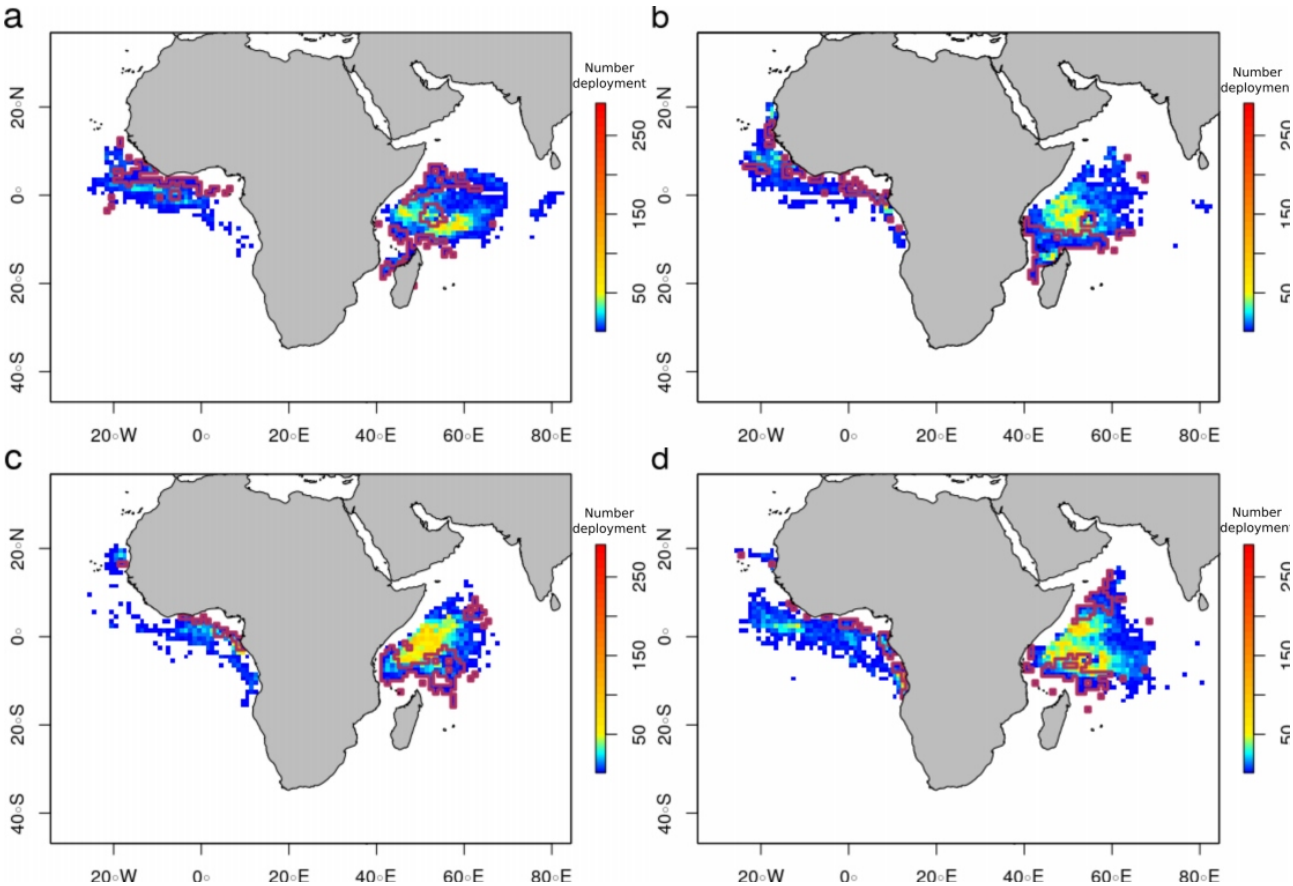

Figure A3.6: Density maps representing the number of dFAD deployments in each 1°x1° cell recorded in logbook data by quarter over the period 2013-2017 (a) Jan-March;(b) Apr-Jun;(c) Jul-Sep;(d) Oct-Dec. The purple curves delimit areas representing the 20% of deployments most likely to produce a beaching within 3 months of a dFAD passing through those areas.

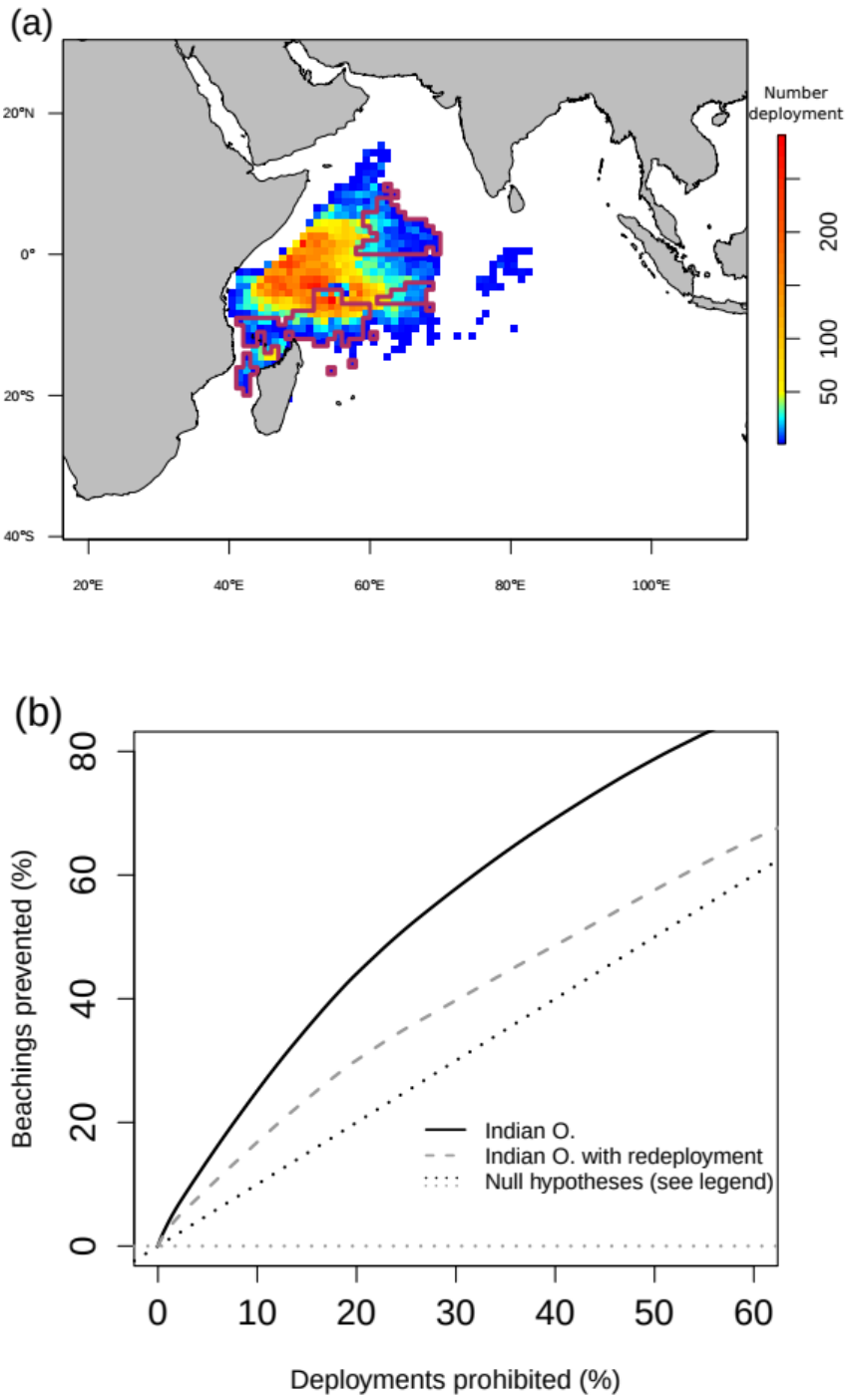

Figure A3.7: (a) Density maps representing the number of dFAD deployments in each 1°x1° cell recorded in logbook data for the period 2013-2017. The purple curves delimit areas representing the 20% of deployments most likely to produce a beaching in coral reefs within 3 months of a dFAD passing through those areas. (b) Predicted reduction in beaching rate as a function of the amount of area put aside in annual closures to dFAD deployments. Areas are closed from most likely to least likely to produce a beaching within 3 months of deployment, with area being quantified along the x-axis in terms of the fraction of deployments that occurred in closed areas prior to their closure.

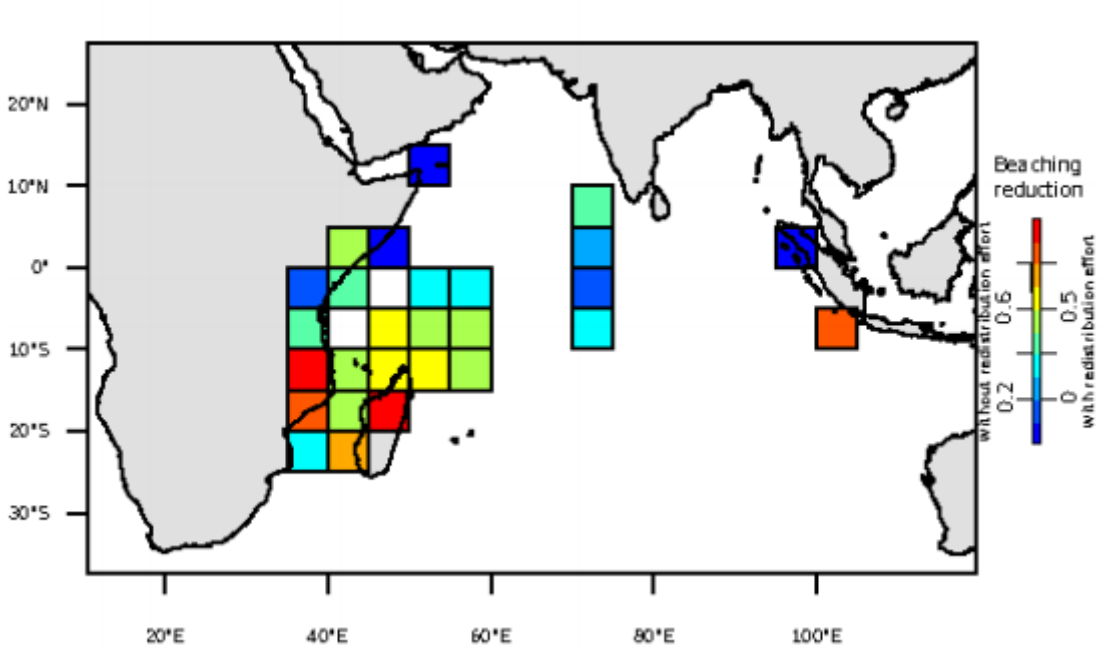

Figure A3.8: Map representing the predicted reduction in beaching when the 20% of dFAD deployments most likely to produce a beaching on coral reefs within 3 months are prohibited (see areas in Fig A3.7a), without (values on the left of the colorbar) and with (values on the right of the colorbar) dFAD deployment effort redistribution to non-prohibited areas.

CHAPITRE 2

Preventing the loss of derelict drifting fish aggregating devices through recovery at sea

Bien que le programme proposé dans le premier chapitre d'interdiction de déployer des DCP dans des zones risquant fortement de conduire à un échouage s'annonce prometteur, il semble être à même de protéger certaines zones plus que d'autres. En particulier, le Nord-Ouest de l'Océan Indien et le Nord du Golfe de Guinée, qui représentent pourtant de grandes zones d'échouage, sembleraient bénéficier peu de cette mesure. Dans ces zones, nos observations de taux élevés de récupération des bouées attachées aux DCP par ce qui semble être des petits pêcheurs suggèrent que des programmes de récupération des DCP en mer pourraient être une mesure complémentaire efficace à mettre en place. Dans ce chapitre 2, nous avons abordé cette problématique en analysant plus de 100,000 trajectoires de DCP dans les Océans Indien et Atlantique afin d'évaluer leur devenir. L'identification de zones où les DCP sortent massivement des zones de pêches, ainsi que le passage d'un nombre important de DCP à proximité de ports, ont mis en évidence que la mise en place d'un programme de récupération des DCP en mer serait efficace pour empêcher leur perte et échouage, notamment pour les zones qui bénéficieraient moins du premier programme.

Ce Chapitre 2 est en révision dans Nature Sustainability :

Imzilen T, Lett C, Chassot E, Maufroy A, Goujon M, Kaplan DM. Preventing the loss of derelict drifting fish aggregating devices through recovery at sea. Nature Sustainability (version révisée).

1. Introduction

In the last decade, concerns about plastic pollution in the world's seas and oceans have increased and attracted attention from managers and policymakers, with calls for an international agreement to address this issue (Borrelle et al., 2017). Oceans and coastal waters receive a large percentage of their waste and pollutants from land-based sources with an estimated 4.8–12.7 million metric tons of plastic entering the ocean annually (Jambeck et al., 2015; Haward, 2018). However, a non-negligible portion of marine plastic pollutants originates from sea-based sources, especially fisheries due to derelict, lost or otherwise discarded fishing equipment (United Nations Environment Programme, 2017; Richardson et al., 2019). In tropical tuna fisheries, purse seine vessels deploy large numbers of drifting Fish Aggregating Devices (dFADs) to aggregate fish and facilitate their capture (Maufroy et al., 2015; Imzilen et al., 2021), with the total number of such devices deployed annually worldwide exceeding 100,000 in recent years (Gershman et al., 2015; Escalle et al., 2021; Imzilen et al., 2021). A dFAD is typically made from a bamboo and/or metal raft equipped with plastic floats to ensure buoyancy, a submerged substructure stretching up to 100 m below the surface consisting mostly of ropes or rolled old purse seine nets (acting both as a fish aggregator and a drogue, connecting dFADs to the water column), and a satellite-transmitting GPS-tracking buoy. Many of these materials consist of plastics or metals that have a long lifespan in ocean conditions (Murua et al. 2017; Zudaire et al. 2020). Due to their efficiency in increasing fishery productivity, dFAD fishing has become the dominant fishing mode for tropical tuna purse seine fishers worldwide (Fonteneau et al., 2013), with a global annual catch exceeding 2 million metric tons in recent years. Most importantly for the context of this study, a large percentage of dFADs eventually end up drifting outside fishing grounds or are otherwise lost (e.g., beaching, breaking up, sinking), potentially threatening sensitive ecosystems, such as coral reefs (Maufroy et al., 2015; Escalle et al., 2019; Imzilen et al., 2021), and contributing non-biodegradable waste to the world's oceans (e.g. Burt et al., 2020).

Scientists, fishers and policymakers recognize that mitigation measures must be implemented to reduce dFAD loss and its associated environmental impacts (Davies et al., 2017; Maufroy et al., 2018; Hanich et al., 2019). In recent years, multiple management changes have been made to address the negative aspects of dFAD use. Tuna regional fisheries management organizations (RFMOs) currently limit the number of floating objects monitored by an individual purse seine vessel at any given time to 300 buoys in the Atlantic Ocean and Indian Ocean (ICCAT,

2019; IOTC, 2019a, respectively), though the extent to which these restrictions have actually led to a reduction in the number of dFADs is not clear (Imzilen et al., 2021). In the Atlantic Ocean, time-area closures have been extended from 2 to 3 months in 2021 to suspend dFAD activities (deployment, fishing, deployment of a buoy on a dFAD previously owned by another vessel) in the whole Atlantic Ocean from January to March. In addition, RMFOs encourage the use of biodegradable materials in the construction of dFADs (ICCAT, 2015; IOTC, 2019b; IATTC-WCPFC, 2020), which has become a systematic component of national FAD management plans (ORTHONGEL, 2021a, 2021b), ongoing Fisheries Improvement Projects and other sustainability projects of purse seine fishing companies and fleets (Zudaire et al., 2020). However, identifying and developing suitable materials to replace the non-biodegradable materials of dFADs has proven difficult and will likely take time (Zudaire et al., 2020; Lopez et al., 2019). In addition, a recent study showed that the dFAD beachings, which can lead to environmental damage even if dFADs are biodegradable, may be significantly reduced if closures to dFAD deployments strategies are adopted in the Indian and Atlantic Oceans (Imzilen et al., 2021). However, this study also showed that closures will not be uniformly effective in reducing beachings, with some areas being well protected and others receiving little benefit. Furthermore, the closures considered in Imzilen et al. (2021) only relate to beaching in coastal areas, and do not take into account other potential negative impacts, such as perturbations to the pelagic ecosystem, inefficient use of fishing resources and dFAD loss in the open ocean. Therefore, additional management options for reducing dFAD contributions to marine pollution and environmental damage are needed.

One promising approach to mitigate the negative impacts of dFADs consists in implementing recovery programs. In 2016, a component of the EU purse seine fishing industry, joined later by the rest of EU purse seine fishing companies, in collaboration with a local NGO and the Seychelles Fishing Authority (SFA), implemented a program, FAD Watch, to prevent dFAD beaching in certain coastal areas of the Seychelles archipelago (Zudaire et al., 2018). A dFAD detection system was set up to alert participants when dFADs arrived within 3 to 5 nm off 6 islands of the Seychelles archipelago. A total of 109 dFADs were collected in the period 2016-2017. Though promising, scaling up this type of program to an entire ocean basin is not evident, particularly in systems comprised of many small islands (Escalle et al., 2019). Nevertheless, a recent analysis in the Indian and Atlantic Oceans indicates that up to ~50% of “beached” dFADs may actually consist of GPS transmitting buoys being recovered by artisanal fishers in specific coastal areas (Imzilen et al., 2021), suggesting that beaching/loss early warning systems linked to dFAD recovery programs may be effective in reducing undesirable dFAD impacts.

The goal of this paper is to analyze the trajectories of dFADs in the Indian and Atlantic Oceans with respect to a set of factors that may facilitate the implementation of effective and efficient dFAD recovery programs to reduce the negative ecological impacts of lost dFADs. In addition to examining where and when dFADs exit main fishing zones, we identify typical transit paths outside of fishing zones and where they are likely to pass in close proximity to major ports that could potentially be used for organizing regional recovery programs.

2. Materials and methods

1.1. Data collection

This paper is based on a combination of European Union (EU) purse seine fishing effort data from 2012-2018, used to define core fishing grounds, and data on the trajectories of dFAD tracking buoys deployed by French and French-associated vessels over the same time period, used to identify where and when dFADs drift outside fishing zones. EU purse seine fishing effort data were obtained from public catch-effort datasets available from the Indian Ocean Tuna Commission[1] (IOTC) and the International Commission for the Conservation of Atlantic Tunas[2] (ICCAT). We used EU instead of just French effort data so as to have the most accurate description of zones where dFADs had a significant probability of being fished upon by any purse seine vessel. The average distribution of French fishing effort does not show strong differences from that of the entire EU, so this decision did not significantly impact the results.

The GPS locations of satellite-transmitting tracking buoys attached to dFADs used by the French and associated (Mauritius, Italy, Seychelles, Belize) purse seine and support vessels (i.e., vessels that do not fish, but simply deploy and maintain a network of dFADs for other fishing vessels) operating in the Indian and Atlantic Oceans are available from 2007 onward through a collaborative agreement between the French National Research Institute for Sustainable Development (IRD) and the French frozen tuna producers' organization ORTHONGEL (coverage 75–86% before 2010 and ~100% after that date; Maufroy et al., 2015). Though tracking buoys can be attached to any floating object (e.g., natural debris such as logs) and not just dFADs (i.e., floating objects built and deployed by fishers specifically to aggregate fish), the vast majority of floating objects encountered by purse seiners in recent years are dFADs (>90% based on observer

1 Data available at https://iotc.org/data/datasets/latest/CESurface, accessed 2020-05-27
2 Data available at https://iccat.int/Data/t2ce_PS91-18_bySchool.7z, accessed 2020-05-27

data; Maufroy et al., 2017). For simplicity, we will therefore use the term “dFAD” to refer to all types of floating objects to which tracking buoys are attached.

The sampling periodicity of dFAD positions varies from approximately 15 minutes to 2 days, with buoys deployed during the study period typically emitting between 2 and 4 positions per day. Raw position data includes a mix of ~90% positions in the water and 10% positions onboard a vessel (e.g., from transit periods preceding deployment or after recovery at sea). Onboard positions were removed so that individual buoy trajectories could be broken into a series of in-water trajectories using a Random Forest (onboard versus at sea) classification algorithm based primarily on buoy speed and speed variability (Imzilen et al., 2021). dFAD in-water trajectories were defined as series of uninterrupted successive positions classified as in water with no temporal gaps in location data exceeding 2 days.

In this study, we used dFAD trajectories from 2012 to 2018. This period was chosen as a representative recent period characterized by the deployment of large numbers of dFADs for which exhaustive position information is available. This data set consists of 97,353 Indian Ocean (in-water) trajectories representing a total of 43,047 distinct buoys and 26,839 Atlantic Ocean trajectories representing a total of 13,216 distinct buoys. dFAD trajectory data were stored in a PostgreSQL relational database (version 10.14-1) with the PostGIS extension for geospatial data (version 2.4.8).

Trajectories spanning less than 2 days were removed from analyses as these were likely to be associated with errors in the in-water-onboard position classification algorithm or corresponded to fast deployments and recoveries, neither of which are a concern for dFAD loss studied here (~23.48% of all in-water trajectories spanned <2 days, corresponding to 0.09% of the total drift time in the dataset).

Data on port locations, sizes and characteristics, used to assess proximity of dFADs to potential bases for recovery programs, were obtained from the World Port Index (WPI) database provided by the National Geospatial-Intelligence Agency[3].

Statistical analyses and data visualization were carried out using R (R Core Team, 2021)

3 Data available at https://msi.nga.mil/Publications/WPI, accessed 2020-06-01

with functionalities provided by the sf (Pebesma, 2018) and tmap (Tennekes, 2018) packages.

1.2. Definition of core fishing grounds

Core fishing grounds were characterized by first calculating the total number of "fishing hours", the standard effort unit considered to monitor purse seine fisheries (FAO 1997) available in public-domain catch-effort datasets, in each 1° x1° grid cell including all fish school types (free-swimming and object-associated tuna schools). Only cells with >200 fishing hours over the study time period were kept as the initial basis for defining core fishing grounds. Then we removed isolated, outlying cells, and filled in small gaps and irregularities in the remaining areas so as to have for each ocean a single, connected definition of "core fishing grounds" (hereafter referred to simply as "fishing grounds" when there is no possibility for confusion; Fig. 2.1 & Supplementary Fig. B1).

1.3. dFAD movements to and from fishing grounds

The positions within the core fishing grounds of each dFAD in-water trajectory were classified into one of three categories based on the eventual fate of the dFAD: (i) the dFAD remains in the fishing grounds throughout the remaining part of the trajectory, (ii) the dFAD leaves the fishing grounds at some point during the remaining part of the trajectory, but later drifts back into the fishing grounds, and (iii) the dFAD definitively leaves the fishing grounds never to return. Areas most likely to lead to a dFAD drifting away from fishing grounds and, subsequently, being lost or beached were identified by first breaking in-water trajectories into a series of "passages" through individual 1°x1° grid cells of the fishing grounds (composed of all sequential positions within a given grid cell). Probability of loss (by month or over the entire study period) was then assessed based on the percentages of these dFAD "passages" for a given cell assigned to each of the three fate categories mentioned above.

1.4. Proximity to ports

For the dFADs that definitively leave core fishing grounds, the proximity of their trajectories to world ports of different size categories was calculated to assess feasibility of local recovery programs. We calculated in each 1°x1° grid cell along the borders of the fishing grounds the proportion of those dFADs definitively leaving the fishing grounds that later passed within 50

km to a port in the WPI database. We chose the distance of 50 km to port as an approximate limit based on the feasibility of dFAD recoveries within a reasonable amount of time by the medium-sized vessels likely to be used for such operations. The passages of dFADs close to ports were broken down according to port size categories (small, medium and large as recorded in the WPI database) as size is potentially an important factor for the port to have the capacity to maintain a recovery vessel and/or be able to transport valuable dFAD components (e.g., the tracking buoy, the recovery of which is a potential source of revenue for such programs) to major purse-seine ports of call.

3. Results

EU purse seine fishing effort data show that fishing activities occur mainly in the western Indian Ocean and the eastern Atlantic Ocean (Fig. 2.1). Fishing activities are more homogeneous in space in the Indian Ocean than in the Atlantic Ocean, for which the fishing grounds are an elongated strip following the west coast of Africa with some notable gaps wherein effort is low despite being surrounded by areas of high fishing effort (some of these gaps are related to issues with obtaining a fishing agreement between the EU and coastal nations for EEZ access of EU purse seine vessels, such as for Sao Tomé and Principe and the Democratic Republic of Congo). The total number of fishing hours in our core fishing grounds (Fig. 2.1) represent 96.86% of all fishing hours in the Indian Ocean and 95.31% in the Atlantic Ocean.

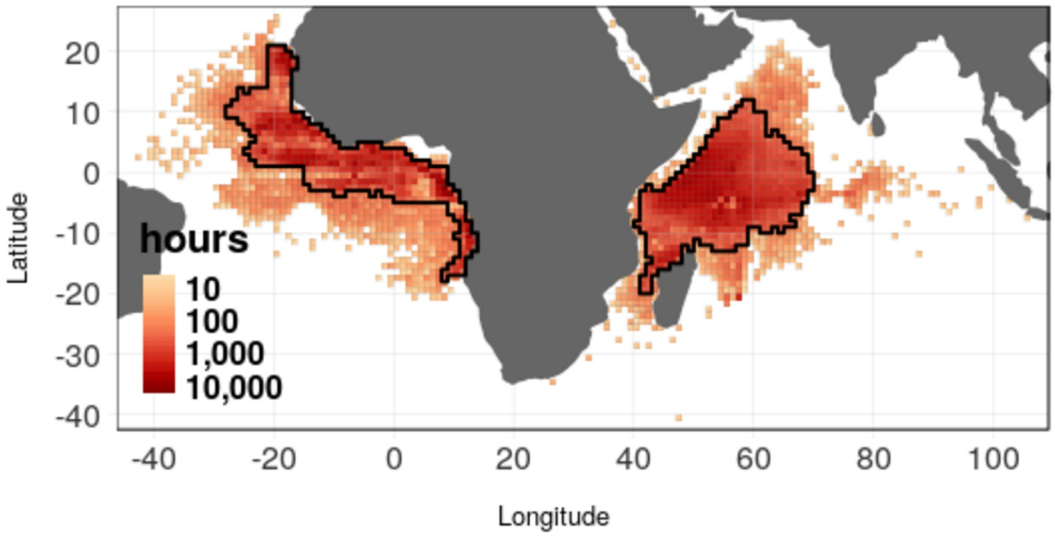

Figure 2.1: Total number of EU purse seine fishing hours in each 1°x1° grid cell for the period 2012-2018. The thick, solid curves delimit our definitions of core fishing grounds (primarily consisting of cells with more than 200 fishing hours over the study period).

Maps of the number of dFADs passages in each 1°x1° grid cell clearly identify dFAD hotspots within fishing grounds (Figs. 2.2 and 2.3). In the Indian Ocean, passages of dFADs are concentrated in the southern and northwestern parts of the fishing grounds. In the Atlantic Ocean, they occur most frequently in a longitudinal band located between 0° and 10°N (Fig. 2.2). Seasonal variability in the distribution of dFADs is most notable in the Indian Ocean where dFADs are concentrated in the southern part of the fishing grounds for the 6 months from November to April and in the northwestern parts (Somali upwelling zone) from May to October (Fig. 2.3), consistent with known monsoon-driven seasonality in Indian Ocean circulation and fishing activities (Kaplan et al., 2014; Davies et al., 2014).

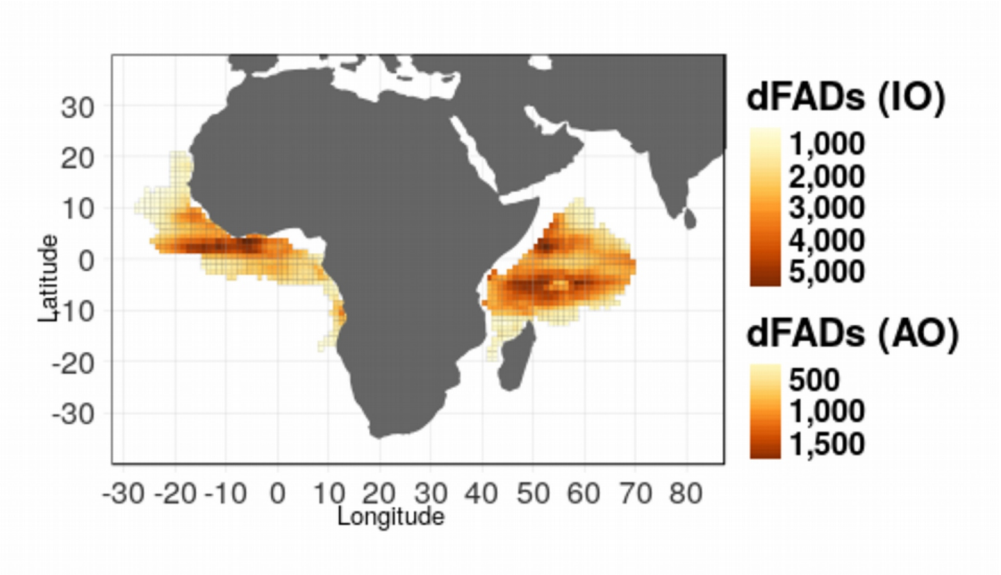

Figure 2.2: Total number of times dFADs passing through each 1°x1° grid cell within the fishing grounds of the Indian Ocean (IO) and Atlantic Ocean (AO) for the period 2012-2018.

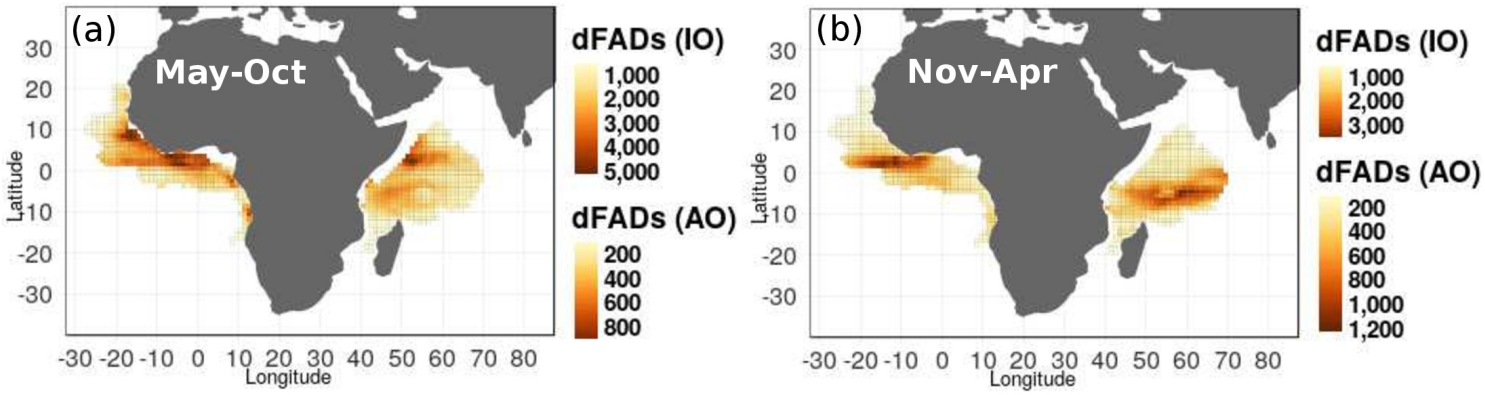

Figure 2.3: The total number of times dFADs passed through each 1°x1° grid cell within the fishing grounds in the Indian (IO) and Atlantic Oceans (AO) for the period 2012-2018 for the months of (a) May-October and (b) November-April.

Global analyses of dFAD movements in fishing grounds show that the proportions of dFADs that either remain within fishing grounds or definitively leave fishing grounds are roughly equal (40-50% each; Table 2.1) and considerably higher than those that leave and return (Table 2.1 and Fig. 2.4). Not surprisingly, dFADs that remain in fishing grounds are most often located in the interior of the fishing grounds (Fig. 2.4a-d). dFADs that leave and return, while infrequent, most often occur along the northwest and southeast borders of the fishing grounds in the Indian Ocean, and off West Africa and the Republic of Congo in the Atlantic Ocean (Fig. 2.4b-e). Even for dFAD passages in many interior areas of the fishing grounds, dFADs have a relatively high probability of definitively leaving fishing grounds (>40%), with higher values in the northeastern and southwestern areas in the Indian Ocean and the northwestern and southern areas in the Atlantic Ocean (Fig. 2.4c-f). Seasonal variability is most notable in the proportion of buoys leaving active fishing areas in the Indian Ocean. For example, the proportion is relatively low just west of the Maldives from June to August compared to other times of the year (supplementary Fig. B2) despite monsoon-driven eastward currents during these months, likely due to intense dFAD fishing activity during this time period (Kaplan et al. 2014).

Table 2.1: Total number and percentage of dFAD trajectories[a] that remain, leave and return, and definitively leave the fishing grounds of the purse seine fisheries of the Indian and Atlantic Oceans over the period 2012-2018.

dFAD trajectories	Indian Ocean		Atlantic Ocean	
	Number	Percentage	Number	Percentage
In the fishing grounds	67,412	-	16,940	-
Definitively leave	28,478	42.24%	7,047	41.60%
Remain	27,628	40.98%	7,721	45.58%
Leave and return	11,306	16.78%	2,172	12.82%

a Only in-water dFAD trajectories spanning more than 2 days were included in analyses.

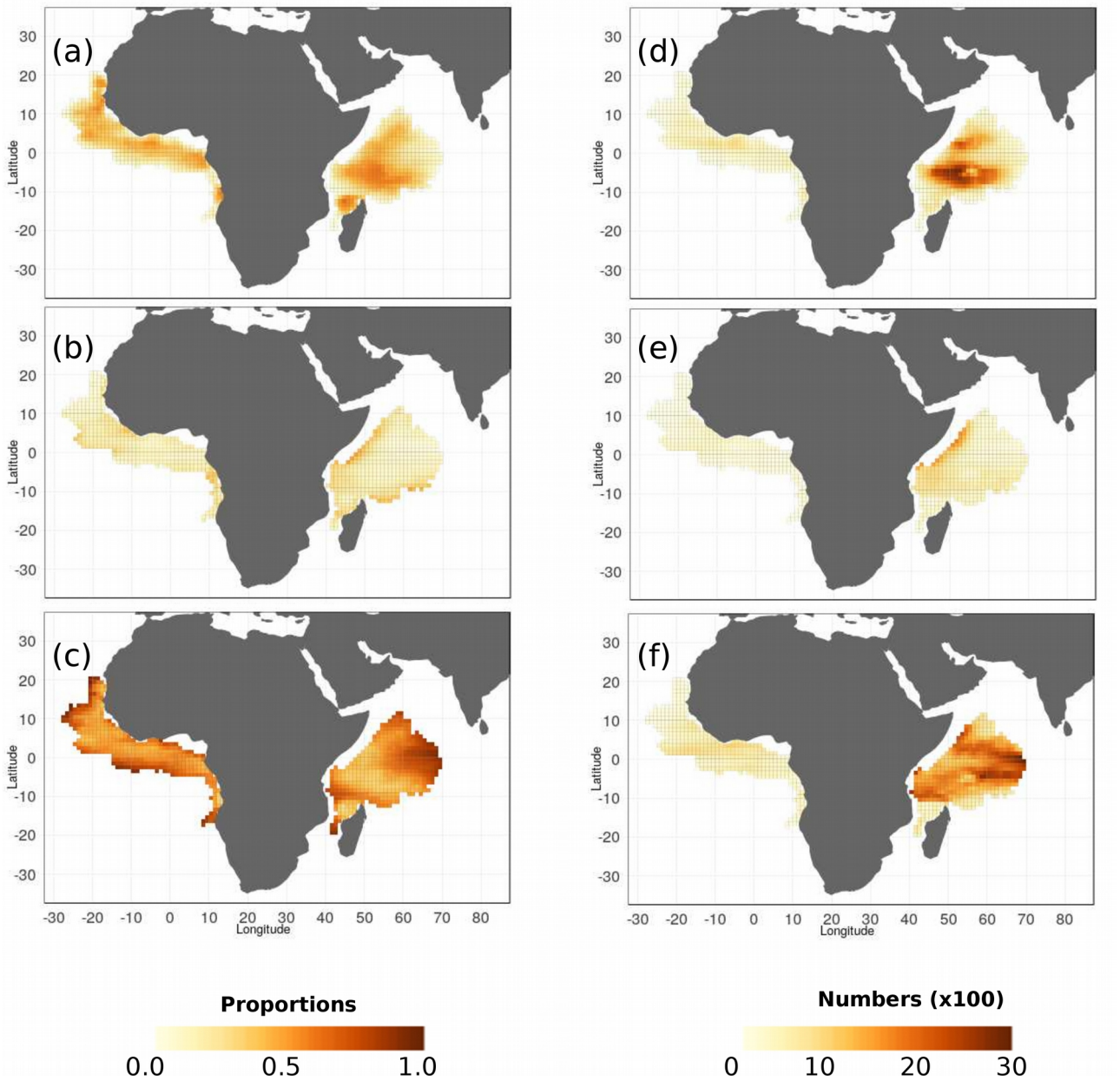

Figure 2.4: Maps of the proportion (a-c) and number (d-f) of passages of dFADs that remain (a, d), leave and return (b, e), and definitively leave (c, f) the fishing grounds after passing through each 1°x1° grid cell over the period 2012-2018.

There is bi-modal seasonality in the rate at which dFADs definitively leave fishing grounds in both oceans (Fig. 2.5). For the Indian Ocean, there is a dominant peak in dFAD loss around November, followed by a secondary peak in May, whereas the less marked seasonality in the Atlantic has broad peaks around July and around December. In both oceans, seasonality is primarily, but not exclusively, due to real differences in loss rates as opposed to differences in the number of deployments (i.e., the seasonality of the proportions in Fig. 2.5b are qualitatively quite similar to that of the absolute numbers in Fig. 2.5a).

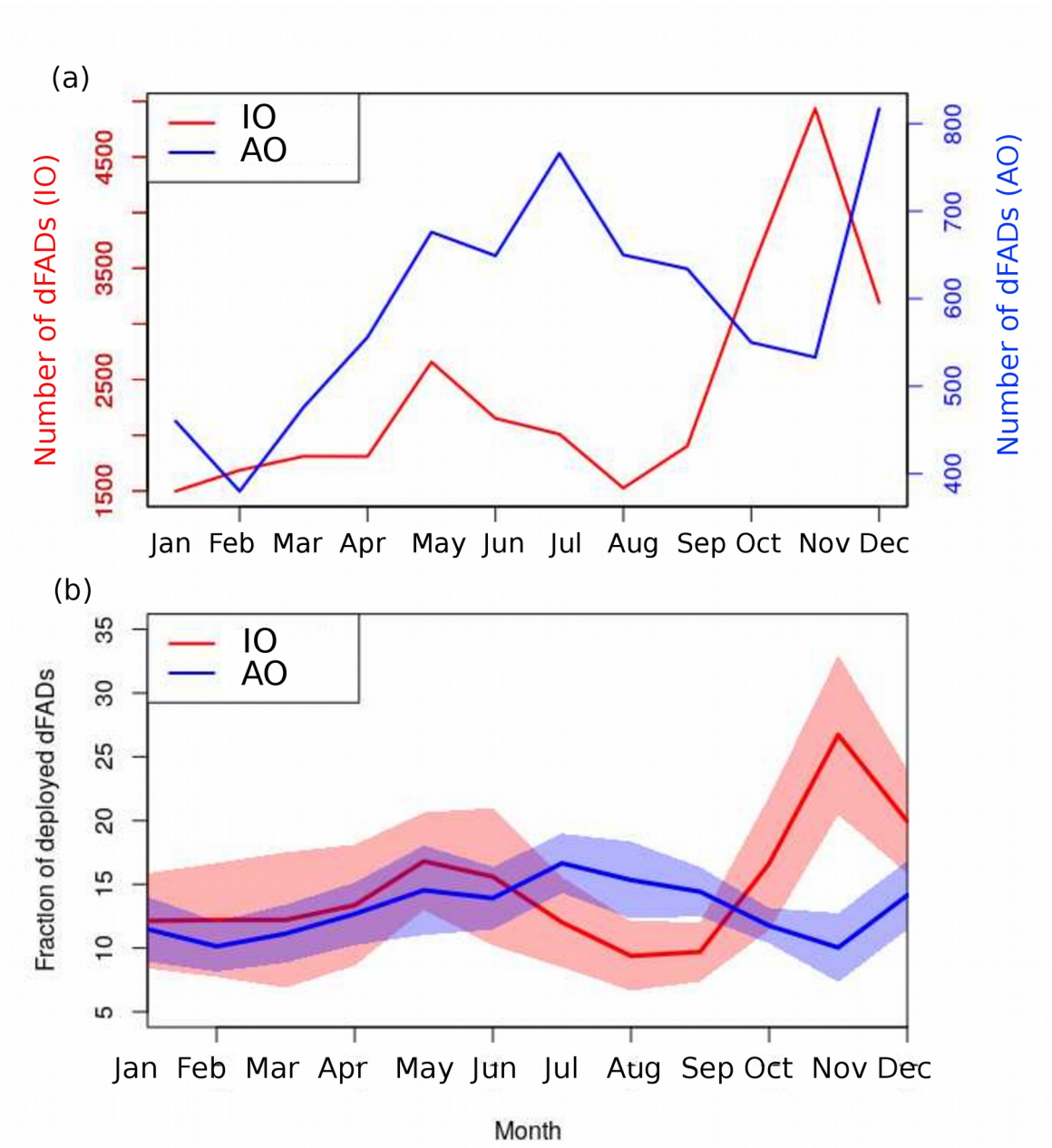

Figure 2.5: Monthly variability in the total number (a) and percentage (b) of dFADs that definitively leave the fishing grounds over the period 2012-2018 for the Indian (solid, blue curves) and Atlantic (red, dashed curves) Oceans. The central lines in (b) indicate the mean percentage leaving fishing grounds averaged over the seven years examined in this study, whereas the shaded regions around the central lines indicate one standard deviation around the mean. An indication of interannual variability was not included in (a) because the increasing tendency in the total number of deployed dFADs made it impossible to compare across years.

The final recorded positions of dFADs that definitively leave fishing grounds are consistent with major surface ocean currents (Bourles et al., 1999; Schott et al., 2009), with final positions concentrated away from fishing grounds near, for example, the coasts of the Maldives and Somalia in the Indian Ocean and Brazil and the Gulf of Guinea coasts in the Atlantic Ocean (Fig. 2.6).

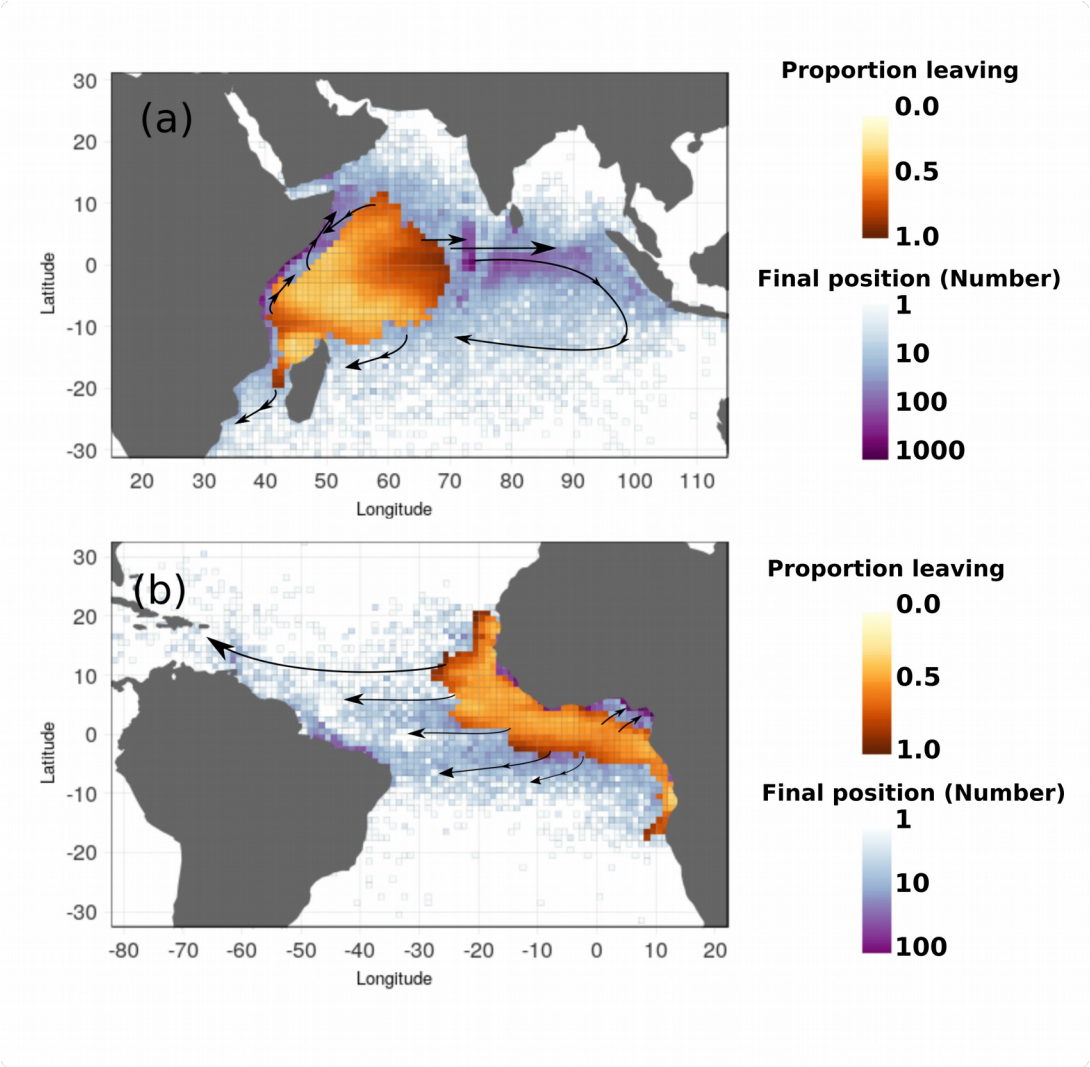

Figure 2.6: Schemes illustrating the dominant directions followed by dFADs after leaving the fishing grounds definitively in the Indian (a) and Atlantic (b) Oceans. Brown colors represent the proportion of dFADs passing through each 1°x1° grid cell of the fishing grounds that end up outside (same as in Fig. 2.4c), whereas blue colors represent the number of final positions of these dFADs in each grid cell (note that the blue color bar is on a log scale). Black arrows represent typical drift directions followed by dFADs as determined by a qualitative review of their trajectories.

Among the dFADs that definitively left the fishing grounds, about 18% in the Indian Ocean and 30% in the Atlantic Ocean passed within 50 km of a port (Table 2.2). The highest percentages were recorded in border areas immediately adjacent to the African coast, particularly, near Tanzania and Mozambique in the Indian Ocean, and in the Gulf of Guinea and Angola in the Atlantic Ocean (Fig. 2.7). In these areas, from 30% to 100% of dFADs leaving the fishing grounds passed near a port. In the Indian Ocean, most dFADs exiting along the northwestern boundary of the fishing grounds passed near the large port of Mogadishu, Somalia (1,641 dFADs), whereas dFADs leaving from the southwestern boundary passed primarily near 2 medium-sized ports: Mombasa, Kenya

(1,869 dFADs and Dar Es Salaam, Tanzania (276 dFADs), and 5 small ports (Fig. 2.8 and Table 2.3). In the Atlantic Ocean, dFADs definitively leaving fishing grounds via the eastern boundary passed primarily near Gulf of Guinea ports, especially the large port of Pennington Oil Terminal located off Nigeria (275 dFADs), 6 medium ports (92 to 273 dFADs) and 5 small ports (93 to 287 dFADs) (Fig. 2.8 and Table 2.3). Among the dFADs passing close to a port, one third (33.62%) eventually beach or have their tracking buoys recovered by coastal fishers (Imzilen et al., 2021).

Table 2.2: Total number and percentage of dFADs that leave definitively the purse seine fishing grounds of the Indian and Atlantic Oceans and pass close (i.e. within 50 km) to large, medium and small ports (50 km) over the period 2012-2018. Note that all dFADs are taken into account even if they pass near several port categories.

dFAD trajectories	Indian Ocean		Atlantic Ocean	
	Number	Percentage	Number	Percentage
All ports	5,007	17.58%	2,088	29.63%
Large ports	1,685	5,92%	273	3.87%
Medium ports	2,257	7,99%	1,032	14,64%
Small ports	3,247	11,39%	1,359	19,28%

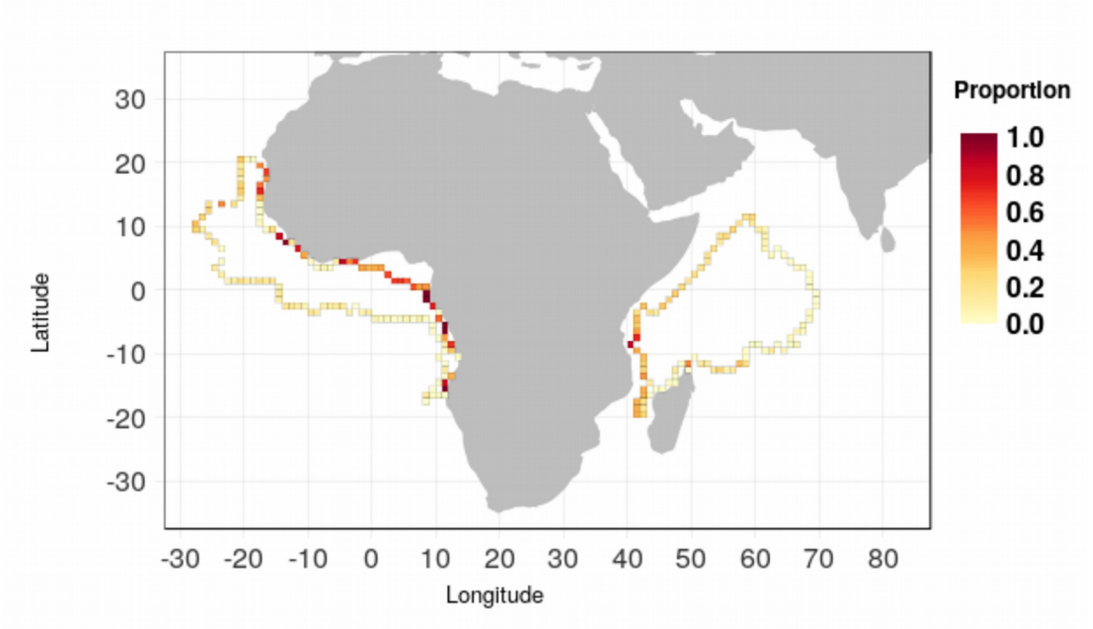

Figure 2.7: Proportion of dFADs at the border of the purse seine fishing grounds of the Indian and Atlantic oceans that definitively leave fishing grounds and that pass close (< 50 km) to ports.

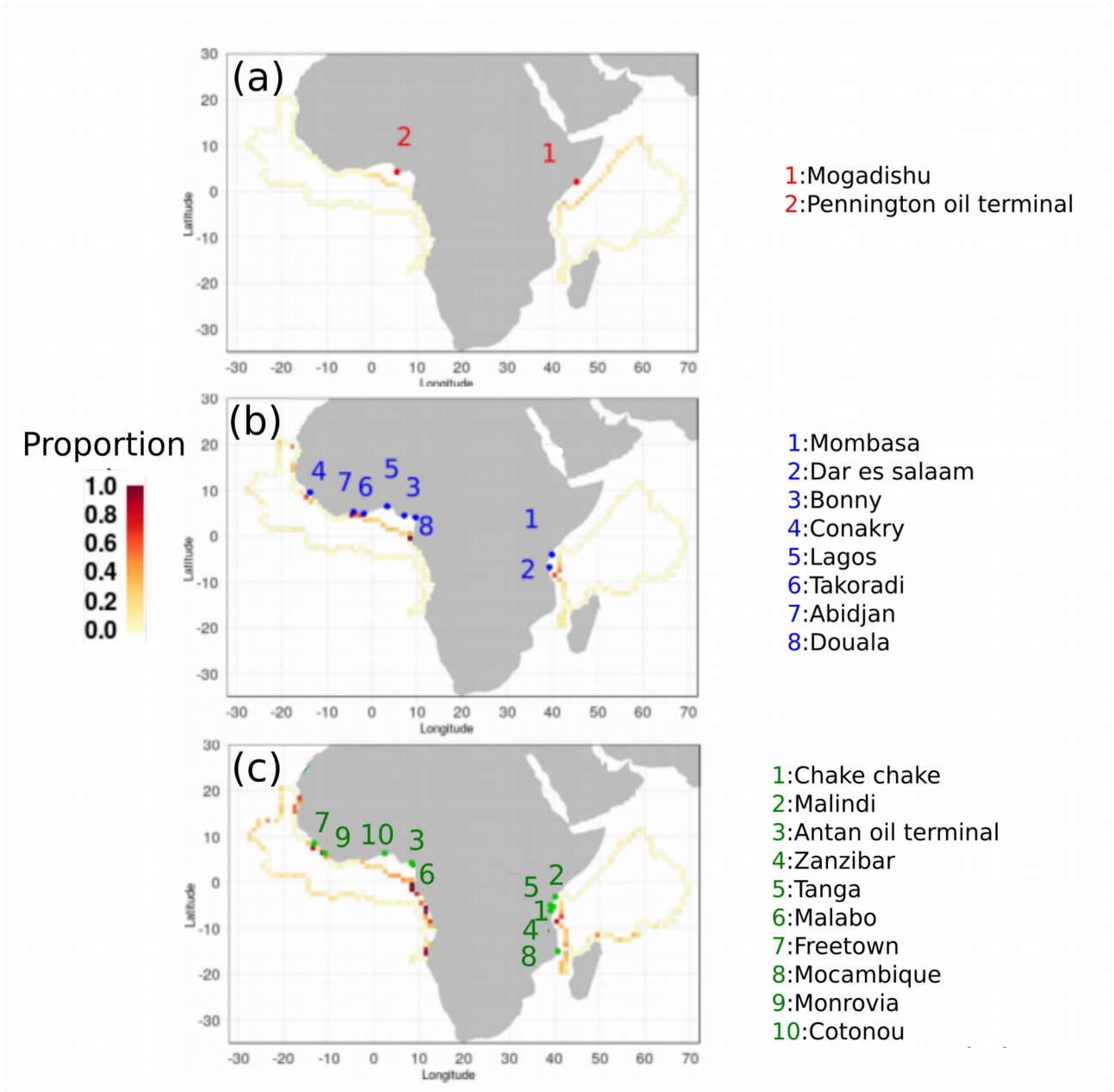

Figure 2.8: Proportion of dFADs at the border of fishing grounds that definitively leave fishing groups and that pass close (<50 km) to (a) large, (b) medium and (c) small ports. Note that all dFADs are taken into account even if they pass near several port categories and that only ports for which more than 90 dFADs passed within 50 km are indicated by name.

Table 2.3: Numbers and percentages of dFADs that definitively leave the purse seine fishing grounds of the Indian and Atlantic oceans and pass within 50 km of specific large, medium and small ports over the period 2012-2018.

Country[a]	Ocean	Port name[b]	Port size	Total dFAD passes[c]	Percentage of dFAD passes	Unique dFAD passes[d]
SO	Indian	Mogadishu	Large	1,641	5.76	1,641
NI	Atlantic	Pennington oil terminal	Large	275	0.97	275
KE	Indian	Mombasa	Medium	1,869	6.56	1,771
TZ	Indian	Dar es salaam	Medium	276	0.97	271
NI	Atlantic	Bonny	Medium	273	0.96	178
GV	Atlantic	Conakry	Medium	172	0.60	172
NI	Atlantic	Lagos	Medium	136	0.48	123
GH	Atlantic	Takoradi	Medium	134	0.47	130
IV	Atlantic	Abidjan	Medium	98	0.34	98
CM	Atlantic	Douala	Medium	92	0.32	88
TZ	Indian	Chake chake	Small	1,748	6.14	535
KE	Indian	Malindi	Small	520	1.83	36
NI	Atlantic	Antan oil terminal	Small	287	1.01	143
TZ	Indian	Zanzibar	Small	267	0.94	98
TZ	Indian	Tanga	Small	231	0.81	70
EK	Atlantic	Malabo	Small	157	0.55	82
SL	Atlantic	Freetown	Small	111	0.39	71
MZ	Indian	Mocambique	Small	108	0.38	101
LI	Atlantic	Monrovia	Small	102	0.36	100
BN	Indian	Cotonou	Small	93	0.33	12

a The country names corresponding to the postal abbreviations cited in the table are: SO= Somalia; NI=Nigeria; KE=Kenya; TZ=Tanzania; GV=Guinea; GH=Ghana; IV=Ivory coast; CM= Cameroon; EK=Equatorial Guinea; SL= Sierra Leone; MZ=Mozambique; LI=Liberia; BN= Benin.

b Only ports passed by more than 90 dFADs are presented in the table.

c All dFADs are taken into account even if they pass close to several port categories.

d dFADs are only taken into account if they do not pass close to other larger ports.

4. Discussion

Our results provide significant guidance for implementing effective dFAD recovery programs to mitigate the negative impacts of dFAD loss, which threatens vulnerable habitats and contributes to sea-based marine pollution in the Indian and Atlantic Oceans. We assessed the fates of over 84,253 trajectories of dFAD tracking buoys deployed by the French fleet throughout the

Indian and Atlantic Oceans' tropical tuna fishing grounds. More than 40% of dFAD trajectories ultimately drifted away from fishing grounds never to return, potentially later beaching in coastal areas (Balderson and Martin, 2015; Imzilen et al., 2021). More than 20% of these trajectories (7,095) passed within 50 km of a port over the period 2012-2018, indicating that coastal dFAD recovery programs could be effective complementary measures to other mitigation measures, such dFAD buoy limits implemented by RFMOs and as dFAD deployment closures (Imzilen et al., 2021). Indeed, Imzilen et al. (2021) showed that preventing dFAD deployments in areas particularly likely to lead to dFAD beachings would mostly protect coastal areas along the southwestern Indian Ocean and the eastern Gulf of Guinea. Here, we found that most dFADs exiting fishing grounds from the northwestern Indian Ocean and the northern Gulf of Guinea passed close to regional ports and could therefore potentially be recovered before beaching in these coastal areas. Though our results are specific to the French and associated purse-seine fishing fleet, available data indicate that other purse seine fishing fleets have similar spatio-temporal patterns of deployments in the Indian and Atlantic Oceans (Katara et al., 2018), suggesting that our results are applicable to the entire tropical tuna purse seine fishery in these oceans.

Recovery in the high sea could also be structured around the information provided in this paper. We identified areas where a significant percentage of buoys exit fishing grounds towards the high seas never to return. In the Indian Ocean, dFADs leaving from the eastern border (70°E) end up beached in or transiting through the Maldives and the eastern Indian Ocean. This happens relatively less frequently in the period from June to August and becomes much more frequent from October to December. Low loss rates June to August are consistent with known seasonal patterns in dFAD deployment and fishing during this period, that is traditionally used to prepare the main dFAD fishing season that occurs during the following months. At that time of the year, dFADs are deployed by fishers with the intent that they drift along the eastern African coast until they reach the main dFAD fishing ground off Somalia, while avoiding the strong monsoon-driven currents favorable to eastward export of dFADs from fishing grounds (Schott et al 2009). This is followed by a more intense dFAD fishing season from August to October during which dFADs exiting the main fishing ground may not be recovered to avoid impacting fishing operations. Finally, starting in November, a period of transition towards fishing further south in the Indian Ocean occurs, with relatively more focus on free-swimming school sets(Kaplan et al. 2014; Maufroy et al. 2017), likely contributing to abandonment of dFADs in the northern Indian Ocean to the high seas in the last quarter of the year. High loss rates in the fourth quarter are also consistent with the dominant

eastward transport of the South Equatorial Countercurrent during this time period (Schott et al., 2009).

In the Atlantic Ocean, dFADs lost to the high seas exit fishing grounds mostly from the northwestern border (between 10°-20°N) and southwestern border (2°-5°S), which is consistent with dominant transport directions of the North Equatorial Current and the South Equatorial Current (Bourles et al., 1999). Though the seasonality of loss is less marked in the Atlantic Ocean than in the Indian Ocean, the peak months of July and December are associated with transitions in the spatio-temporal distribution of deployments from principally deploying just north of the equator off of East Africa to focusing on the Gulf of Guinea further east (Maufroy et al. 2017). These transitions could lead to increased dFAD abandonment in areas highly susceptible to export of dFADs outside of fishing grounds, similar to that hypothesized for the Indian Ocean, though seasonality in currents may also play an important role.

While the information provided in this paper on spatio-temporal patterns of dFAD loss provides an essential foundation for implementing dFAD recovery strategies, there are a number of important practical challenges to the success of such efforts. Most efforts towards reducing marine debris have to date focused on beach clean-ups (Schneider et al., 2018; Duan et al., 2020). Such operations are costly, time-consuming and only capture a fraction of the overall debris (Chen, 2015; Burt et al., 2020). In order to prevent debris beaching, recovery at sea is a promising solution (Löhr et al., 2017) but this requires consolidating systems to observe these debris (Maximenko et al., 2019) and improving the understanding of their drift (van Sebille et al., 2020), as well as putting in place the appropriate socio-economic and political frameworks (Stafford and Jones, 2019). Combining observations and drift modeling, Sherman and van Sebille (2016) showed that collectors placed in appropriate locations could reduce the mass of floating microplastics significantly. However, in order to collect larger debris, such as lost dFADs, appropriately-sized and equipped vessels are required, necessarily imposing a number of complex organizational considerations and trade-offs (Duan et al., 2020). Broadly, the equipment required for recovery operations (e.g., boat size and gear), the type of recovery program (e.g., collaboration with local fishers, non-governmental organizations (NGOs) and/or nation-states, use of support vessels, and/or chartering of dFAD recovery vessels) and the funding solutions (e.g. reuse of recovered tracking buoys or dFAD plastic floats, and/or polluter-payer systems collected at dFAD and buoy deployment or manufacturing) need to be optimized to recover a maximum number of dFADs while minimizing costs and fishing impacts. These considerations highlight the importance of identifying areas

leading to losses and multiple ports of different sizes from which operations could potentially be conducted, as we have done above, as well as careful analysis of the possible impediments to the implementation of recovery programs, some initial thoughts for which we provide below.

Some possible impediments for dFAD recovery programs are environmental, strategic or geopolitical. For instance, even if the Somali coast is identified as a dFADs beaching hotspot in winter (Imzilen et al., 2021), and has potential for a port-based recovery program as we show here, recovering dFADs along this coast is unlikely to be a priority due to the area's relatively limited amount of sensitive habitats, such as coral reefs, and because of the difficult and dangerous socio-political situation in the country and its adjacent waters. On the other hand, the Maldives archipelago is likely to be a priority given that it is an area with high dFAD beaching rates in coral reefs (Imzilen et al., 2021) and also an area where many dFADs leave fishing grounds and never return. Implementing a recovery program in this area could be particularly valuable, especially given that the Maldives is well integrated into regional maritime transport and tuna fisheries. However, implementing such a program for a large island chain composed of > 1,000 individual islands is likely to be complex. Extensive collaboration with regional stakeholders, such as research institutes, fisher associations and NGOs, would be essential to operationalize a recovery program in the Maldives and elsewhere.

Another major challenge for at sea dFAD recovery is availability of appropriate vessels to remove dFADs from the water. The vertical subsurface structure of dFADs generally stretches from 50 to 80 m below the surface. The weight of the materials used to build dFADs and the numerous sessile organisms that attach to the "dFAD tail", eventuallymake dFAD very heavy (up to hundreds of kg) and therefore difficult to remove from the water. Complete removal is likely only possible for medium to large vessels with an appropriate crane or winch for hauling heavy material. For smaller vessels, it may only be possible to remove the parts of the dFAD that are exposed at the surface, such as the GPS buoy, plastic flotation devices and/or metallic or plastic structural elements. However, this could still be extremely useful as the remaining material will normally sink before reaching coastal environments, thereby potentially avoiding the most important environmental impacts. This strategy would be particularly valuable if the subsurface structure can be made of biodegradable materials (Zudaire et al., 2020; Lopez et al., 2019). Imzilen et al. (2021) suggested that the removal of GPS buoys by artisanal fishers is already occurring in coastal areas. Therefore, if dFAD tracking information can be made accessible and appropriate incentive mechanisms are put in place to encourage recovery of other non-biodegradable dFAD elements than just the buoy, this

strategy could significantly contribute to reducing marine pollution from dFADs. Other practical considerations should be taken into account once at port, such as the availability of a disposal facility for polluting components of dFADs and the potential to transport the tracking buoys and reusable dFAD components, which can be recycled and reused, to purse-seine vessel ports of call. All of these potential impediments can be addressed, but they will require active engagement from fishers, RFMOs, NGOs and coastal nations.

In addition to such recovery programs, existing complementary measures controlling the numbers of dFADs present at sea (e.g., limits on the number of operational GPS-tracking buoys, and limits on the use of support vessels) may need to be strengthened, as a greater number of dFADs obviously contributes to higher risks of marine pollution and beaching. However, oddly enough, such measures may aggravate problems of derelict dFADs if their consequences are not accurately anticipated. For example, limits on the per vessel number of tracked dFADs implemented by tuna RFMOs have modified the strategy of some components of the purse seine fishery, encouraging them to remotely deactivate satellite-transmitting GPS-tracking buoys when dFADs leave purse seine fishing grounds in order to lower operational costs associated with satellite transmission of tracking buoy data and maintain the total number of operational buoys below authorized limits (currently 300 per vessel at any instant for both oceans; ICCAT, 2019; IOTC, 2019a). The loss of position information prevents the tracking of dFADs outside fishing grounds and may result in under-estimation and spatial bias in estimates of the risks of beaching and loss (Baske and Adam, 2019; Imzilen et al. 2021). A potential solution would be to consider derelict dFADs as part of a stock of “recoverable dFADs” that are not counted as part of the individual vessel’s quota of operational buoys, but for whom position information is transmitted and made available to partners involved in recovery programs (Baske and Adam, 2019). The current RFMO-implemented reduction in the number of support vessels in the Indian Ocean also oddly may increase the loss of dFADs as these vessels may be used for the recovery of dFADs before they leave fishing grounds, highlighting the urgent need for complementary dFAD management and recovery approaches.

A final question about dFAD recovery programs is how they could be financed. The logistical challenges described above, such as chartering appropriate recovery vessels, involve significant costs that cannot be ignored. The most simple and logical financing scheme would be a polluter-payer program whereby vessels and/or fishing nations pay some monetary amount per derelict dFAD into an independently-run and verified clean-up fund dedicated to recovering dFADs

and otherwise reducing marine pollution. The basic elements for identifying what vessels, fishing companies and/or nations are deploying dFADs are largely in place via RFMO reporting requirements, dFAD vessel logbooks and purse-seine observer programs. The detailed spatio-temporal maps provided here and in Imzilen et al. (2021) identify where the losses and impacts are occurring, thereby providing a blueprint for apportioning such funds geographically. The missing elements are mostly political: facilitating access to tracking information for derelict dFADs, for which there is essentially no technical impediment; implementing requirements for appropriate disposal of derilect dFADs; and improving collaboration between industry and regional stakeholders that would be involved clean-up programs.

Though these missing elements may seem formidable, there are very promising precedents for rapidly addressing these types of issues. Throughout the 2010's, various initiatives of purse seine fleets, national scientists, and organizations such as the International Sustainable Seafood Foundation (ISSF), have allowed the rapid adoption of mitigation measures by t-RFMOs or by the fleets themselves. This was the case for non-entangling dFADs (Goujon et al., 2012), Best Practices guidelines for the release of sensitive species (Grande et al., 2019; Poisson et al., 2014, 2012), exhaustive observer coverage (Goujon et al., 2017a, 2017b) and FAD management plans, that are all required for ISSF participating fishing companies if they wish that tuna from their fishing vessels is accepted by ISSF member canneries. A similar approach could be used to address dFAD loss and pollution, using the fulcrums of the ISSF, MSC certification of certain purse-seine fisheries and EU environmental regulations to extend the commitments already made by some of the fleets (e.g. full provision of detailed dFAD tracking data to national scientists as in this study, tests of recovery mechanisms as in the frame of the FAD Watch project in Seychelles) to other fleets and other areas, and therefore rapidly transform the whole industry behaviour for the benefit of all. We hope that the information provided here will help policymakers engage with this issue and identify optimal management strategies.

Appendix B - Additional figures

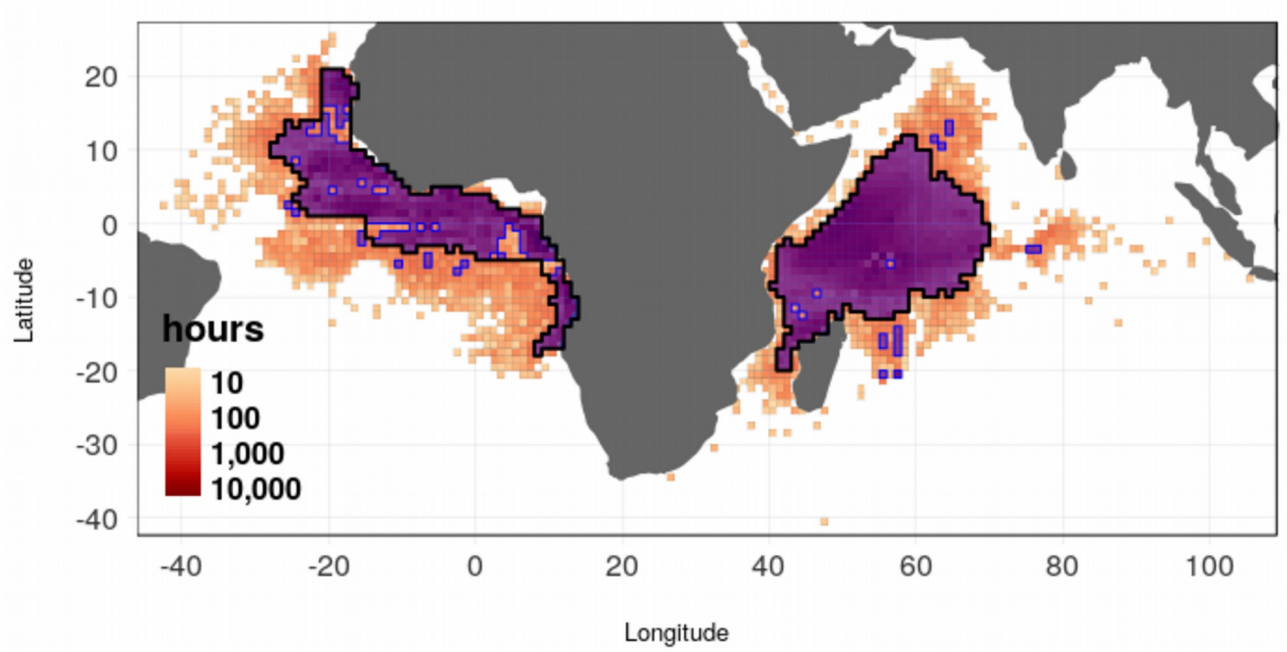

Figure B1: Total number of EU purse seine fishing hours in each 1°x1° grid cell for the period 2012-2018. The thick, solid curves delimit our definitions of core fishing grounds (primarily consisting of cells with more than 200 fishing hours over the study period). The purple colors represent exactly the cells with more than 200 hours of fishing.

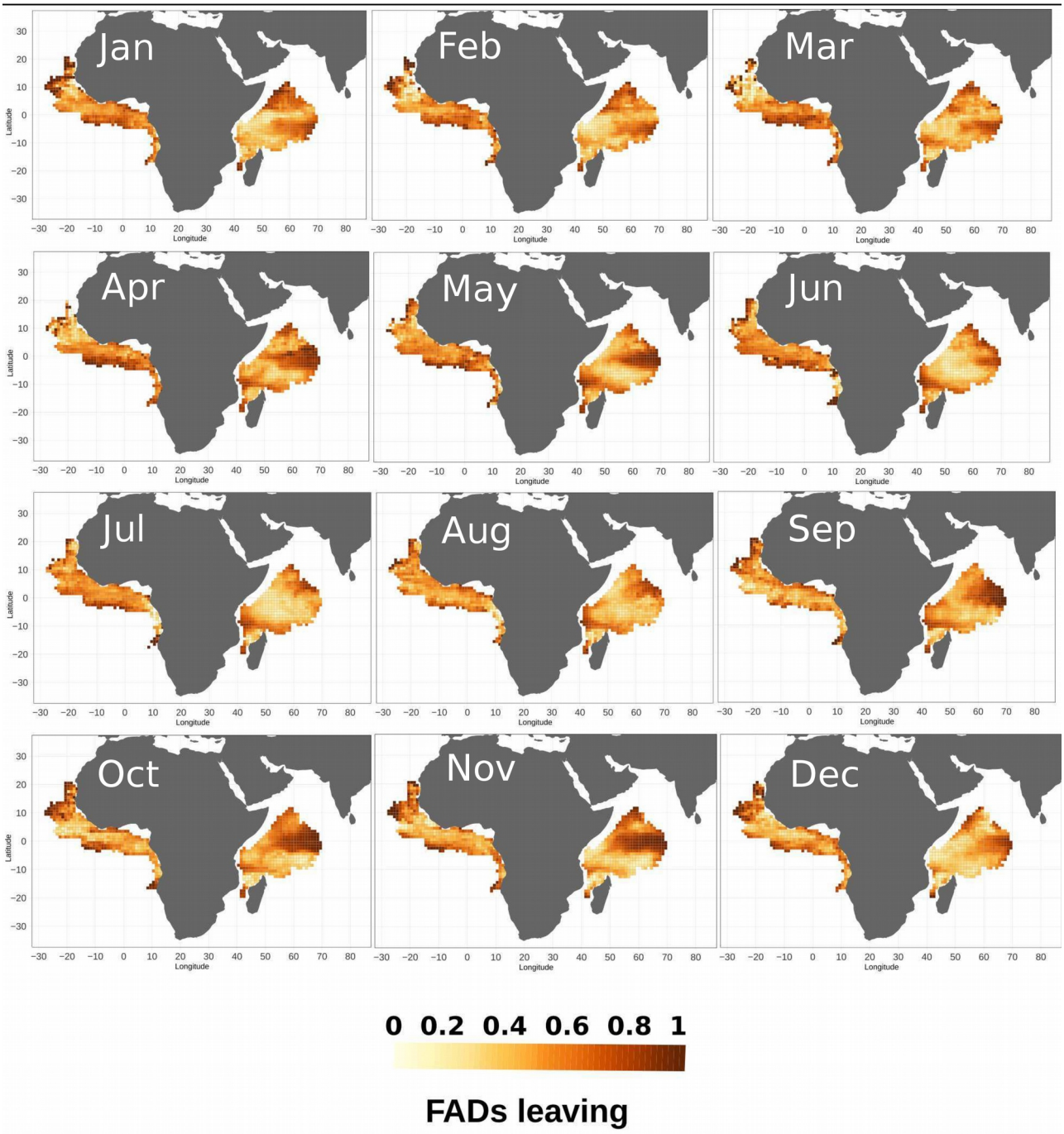

Figure B2: Monthly maps of the proportion of dFADs that definitively leave the fishing grounds after passing through each 1°x1° grid cell over the period 2012-2018. Months advance by rows from January in the top-left to December in the bottom-right panel.

CHAPITRE 3

Fish aggregating devices drift like oceanographic drifters in the near-surface currents of the Atlantic and Indian Oceans

Les deux premières mesures de mitigation proposées dans les chapitres précédents semblent efficaces et complémentaires pour diminuer la perte et l'échouage des DCP. Cependant, ces mesures sont globales et traitent le problème à l'échelle des bassins océaniques. Il nous a donc paru nécessaire d'évaluer la possibilité de compléter ces mesures par des outils permettant de prédire avec précision les trajectoires des DCP au niveau individuel. Pour cela il a fallu d'abord répondre à la question de savoir si les DCP suivaient plus ou moins les courants océaniques. À cette fin, nous avons comparé dans ce chapitre 3 les composantes de vitesse des DCP avec celles des drifters conçus en océanographie pour suivre les courants de la couche de surface. Les résultats ont montré que les DCP dérivent effectivement de manière similaire aux drifters, mais nous avons noté néanmoins que les DCP dérivaient un peu moins vite, en particulier dans l'Océan Atlantique. Cette étude a également révélé que la distribution spatiale des DCP est complémentaire à celle des drifters ce qui suggère que l'énorme volume de données collectées par les pêcheurs via leurs DCP pourrait contribuer aux observations océaniques par l'enrichissement des bases de données mondiales.

Ce Chapitre 3 a été publié dans Progress in Oceanography :

Imzilen T, Chassot E, Barde J, Demarcq H, Maufroy A, Roa-Pascuali L, Ternon J-F, Lett C. 2019. Fish aggregating devices drift like oceanographic drifters in the near-surface currents of the Atlantic and Indian Oceans. Progress in Oceanography ***171****:108–127.*
https://doi.org/10.1016/j.pocean.2018.11.007

1. Introduction

Oceans cover 70% of the Earth's surface and are much harder to observe than terrestrial systems (Richardson and Poloczanska, 2008). For centuries, mariners have been observing the states of oceans and the atmosphere by recording oceanographic and physical meteorological data near the ocean's surface (Woodruff et al., 1987). As early as the nineteenth century, international collaborative efforts were initiated to coordinate the collection and curation of ocean-atmosphere data from voluntary observing ships (VOS) and build large-scale marine data sets. Such data sets are now considered essential for oceanographic and climate studies (Woodruff et al., 1987; Kent et al., 2010; Freeman et al., 2017). From the 1970s, ocean data collection was revolutionized with the advent of satellite technology and the development of sensors that were capable of measuring a large range of oceanographic and atmospheric features (Martin, 2004).

Combining in situ and remotely-sensed satellite observations has proven to be an essential step to improving our understanding of how ocean circulation affects climate at regional and global scales through the transport of water and heat received from the sun (Maximenko et al., 2009; Lee et al., 2010). Remotely-sensed measurements of sea surface temperature, altimetry and vector winds provide a synoptic view of ocean surface current patterns at consistent and regular spatial and temporal scales (Lagerloef et al., 1999; Sudre and Morrow, 2008; Dohan and Maximenko, 2010). At a finer scale, in situ velocity measurements of near-surface currents are routinely collected by satellite-tracked drifters maintained by the Global Drifter Program (GDP), an operational component of the Global Ocean Observing System (GOOS) and the Global Climate Observing System (GCOS). This data provides a direct measurement of water properties and complements the satellite data by supplying information on high-frequency, small-scale oceanic processes (Niiler and Paduan, 1995; Reverdin et al., 2003; Lumpkin and Elipot, 2010). These drifters are floating devices that comprise a surface buoy equipped with a satellite transmitter and a subsurface sea anchor (Fig. 3.1). Since the 2010s, the GDP has maintained a global array of ∼1,200–1,500 drifters that have been deployed from VOS, research vessels and planes to cover the world's oceans (Joseph, 2013; Lumpkin and Johnson, 2013; Elipot et al., 2016). In addition to supporting oceanographic and climate research, the ocean circulation information acquired by these systems has been instrumental in supporting both military and civil applications, including search and rescue operations that use the data to improve their field of search predictions (Davidson et al., 2009). More recently, their role in tracking floating debris (Law et al., 2010; Cózar et al., 2014) has garnered attention as concerns about marine plastics pollution increase.

A knowledge of ocean dynamics is also key for fishermen who use it to both navigate and find fish resources. Monitoring surface water characteristics is essential in pelagic fisheries where the use of satellite remote-sensing has long been recognized as a fish harvesting aid (Simpson, 1992; Chassot et al., 2011). Modern fishing vessels are now equipped with a large range of sensors and electronic tools that constantly monitor the marine environment, enabling fishermen to identify the suitable habitats of target fish species (e.g. Torres-Irineo et al., 2014). Large-scale purse seiners are equipped with GPS and AIS positions systems, navigation compass, radars for both navigation and bird detection, sonars and lateral sounders for fish detection, current meters,wind sensors, and sea surface temperature (SST) thermometers. In addition, the vessels receive daily information on oceanographic features through commercial products derived from satellite imagery, i.e. meteorological and SST maps, sea-level anomaly data that allow identifying surface currents and temperature fronts as well as mesoscale features such as eddies and filaments, ocean-colour data, temperature data based on microwave imagery, and subsurface temperature maps (Saitoh et al., 2009). In tuna fisheries, the purse seine vessels that target fish schools have increasingly deployed satellite-tracked fish aggregating devices (FADs) over the last decades. Typically made of a bamboo raft equipped with floats to ensure buoyancy and a sea anchor built of old fishing nets (Fig. 3.1), these FADs attract tuna and increase fishery productivity (Fonteneau et al., 2013; Maufroy et al., 2017). In recent years, the number of GPS-buoy equipped FADs used globally in this fishery has increased markedly. Currently, it is estimated that more than 100,000 FADs are drifting around the globe at any given time (Baske et al., 2012; Scott and Lopez, 2014). While the average lifespan of a FAD at sea (40 days; Maufroy et al., 2015) is shorter than a typical drifter (450 days; Lumpkin et al., 2012), there are many more in circulation, particularly in the tropical areas where the purse seine fleets operate. Consequently, it is likely that FADs could provide the GDP with complementary data, particularly in equatorial regions. Given that these areas are currently under sampled due to factors such as infrequent deployment of drifters and equatorial divergence (Lumpkin and Pazos, 2007), this increased FAD data coverage is especially important. As an illustrative case, a few FAD positions were used to complement the drifter data and ocean model outputs analyzed to locate the wreckage of the Air France flight that crashed in 2009 en route from Rio de Janeiro to Paris (Drévillon et al., 2013).

The overarching objective of this study is to test to what extent FADs deployed by fishermen are surrogates for GDP drifters, providing estimates of upper-ocean current velocities that are

unbiased and of similar precision as those obtained from GDP drifters. To test this, we combined and analyzed large data sets from GDP drifters, a satellite-derived surface current product available from the Ocean Surface Currents Analyses Real-time (OSCAR) processing system and approximately 5 million FAD positions collected by French tuna fishing companies between 2008 and 2014 in the Atlantic and Indian Oceans.

2. Materials and methods

To begin with, we directly compared the velocities of FAD and drifter pairs observed in close proximity over similar time periods. We then used the OSCAR currents as an indirect comparison point for both the FAD and drifter data. For the large biogeographical provinces of the Atlantic and Indian Oceans (Longhurst, 2007), we estimated the correlations between the OSCAR currents and the observed FAD and drifter velocities. We then compared FAD and drifter movements with short-term OSCAR current projections.

2.1. Fish aggregating devices

The GPS locations of the buoys attached to the FADs used by the French fishing fleet operating in the Atlantic and Indian Oceans have been available since 2008 through a collaborative agreement between the Institut de Recherche pour le Développement (IRD) and the French frozen tuna producers' organization ORTHONGEL. The full methodology used to filter and process the raw GPS data to derive FAD trajectories at sea can be found in Maufroy et al. (2015). The current FAD data set consists of 4,777,524 positions, belonging to a total of 21,047 distinct buoys that were deployed at sea between 2008 and 2014. The sampling periodicity of FAD position varies from 15 min (minimum) to 2 days (maximum). It can be remotely modified to facilitate detection when a vessel is on its final approach to a FAD. Approximately 20% of the FAD data set consists of successive locations emitted within a time period of less than 6 h and most FADs emitted two successive signals within a 24-h period.

FADs used by the French purse seine fleets during 2008–2014 mostly consisted of rectangular bamboo rafts of about 4–6 m 2 covered in old pieces of purse seine nets (Franco et al., 2009). Bamboo is a light, floatable, natural composite material with a high strength-to-weight ratio that is resistant to water logging. Several floats made of ethylene vinyl acetate copolymer and used in the floatline of purse seine nets are generally attached under the surface structure of the raft to ensure buoyancy. In the late 2000s, a few Spanish vessels started using plastic trawl floats and PVC pipes for building FAD floating structures (Franco et al., 2009). The subsurface structure found

below FADs was composed of one or two hanging panels typically made out of old purse seine netting of mesh size varying between 90 mm and 200 mm. A weight made of old pieces of chain or cables was generally attached at the bottom of the net to keep it in vertical position (Fig. 3.1). Initially, nets under the FAD hung in ’curtains’ (Fig. 3.1 - upper middle left). From the early 2010s, newer design featuring ‘sausages’ of nets (Fig. 3.1 – upper middle right) were introduced to prevent accidental entanglements of turtles and sharks in the FAD’s netting (ISSF, 2012; Filmalter et al., 2013). Although most of the FADs have progressively been designed with ‘sausage’ type nets in the Indian Ocean over years, ‘curtain’ type nets have remained predominant in the Atlantic Ocean. French GPS buoys have also been deployed on floating objects of natural (e.g. palm trees, logs, Fig. 3.1 - upper right) or anthropogenic (e.g. ropes) origins that represented about 20% of all floating objects encountered at sea by observers on French purse seiners during 2008–2014, with the Mozambique Channel being characterized by a relatively high percentage of these natural objects (Maufroy et al., 2017).

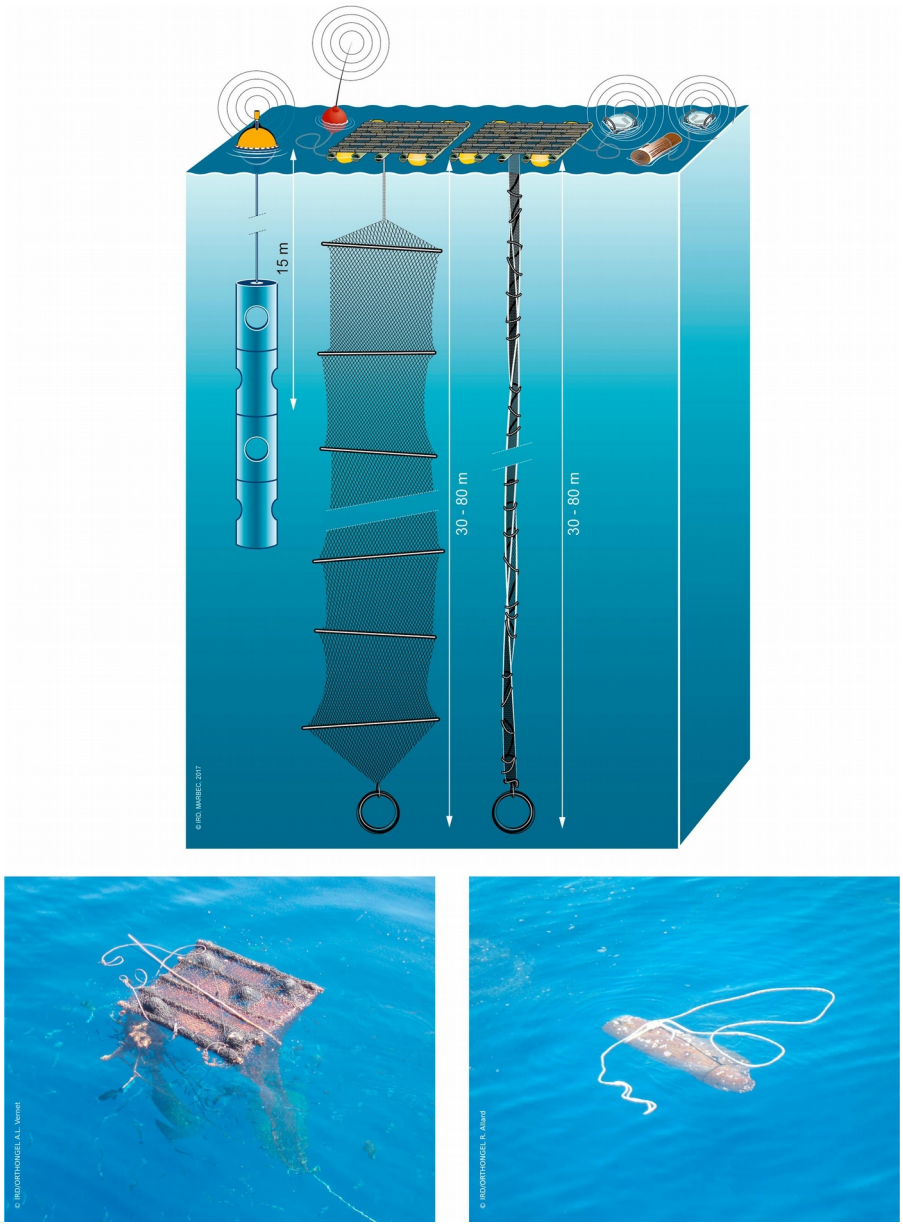

Figure 3.1: Description of the structure and design (in the water column) of a typical drifter (upper left) and of fish aggregating devices (FADs) used in purse seine fisheries including artificial rafts with a sea anchor made of 'curtain' nets (upper middle left, lower left photo) or 'sausage' nets (upper middle right) and natural logs (upper right, lower right photo).

2.2. Surface drifters

The drifters are made up of a surface buoy (30 cm diameter) that is attached by a long, thin tether to a holey sock drogue (sea anchor) that is centered at 15 m below the surface (Fig. 3.1 - upper left). The buoy measures sea surface temperature and other properties such as air pressure and wind direction and sends this information to passing satellites using an ARGOS transmitter (Lumpkin and Pazos, 2007). While the size of the buoy and drogue can vary, their drag area ratio is standardized, which acts to constrain their downwind slip (Niiler and Paduan, 1995). The GDP

archives most of the data collected by the drifters. We downloaded our data set (1,092,466 positions belonging to 2,285 distinct, drogued drifters having occurred in the Indian and Atlantic Oceans during 2008 2014) from ftp://ftp.aoml.noaa.gov/phod/pub/buoydata/. Hansen and Poulain (1996) detail the corrections that are applied to the raw data.

2.3. Data filtering

A very small number of velocity values collated from the FAD database were found to be inconsistent with the maximum speed expected for ocean currents (peak speeds of 2.6 m s^{-1} and 2.01 m s^{-1} reported in the Agulhas Current and Gulf Stream, respectively, by Lutjeharms (2006) and Rossby (2016); maximum speed in the drifter dataset 2.9 m s^{-1}). We therefore removed FAD data points that had velocity values higher than the 99.99% quantile value (471.6 cm s^{-1} , i.e. 9.17 knots). Only 0.01% of the remaining FAD velocity values were higher than 2.9 m s^{-1}.

2.4. Data distribution

There is twice as much data for the Indian Ocean as the Atlantic Ocean but overall, the number of FAD locations has increased markedly in both oceans over the study period while the amount of drifter data remained relatively constant (Table 3.1). This reflects the significant expansion in the FAD fishery that has taken place in both regions (Maufroy et al., 2017). In this study, we focused on eight large biogeographical provinces, four of which occurred in the Atlantic Ocean (i.e. Guinea Current Coastal (GUIN), Eastern Tropical (ETRA), North Atlantic Tropical (NATR), and Western Tropical Atlantic (WTRA)) and four in the Indian Ocean (East Africa Coastal (EAFR), North West Arabian Upwelling (ARAB), Indian Monsoon Gyres (MONS), and Indian Southern Subtropical Gyre (ISSG)) (Longhurst, 2007). The total number of FAD data points collated for these provinces was > 50,000 (Table 3.2).

Table 3.1: Annual number of fish aggregating device (FAD) and drifter observations analyzed in the Atlantic and Indian Ocean.

Device	Ocean	2008	2009	2010	2011	2012	2013	2014
FADs	Atlantic	17,849	45,469	102,216	153,990	286,156	322,490	464,930
FADs	Indian	105,356	149,211	200,983	382,315	580,547	784,130	1,181,882
Drifters	Atlantic	93,540	108,828	84,912	65,851	75,974	118,127	87,067
Drifters	Indian	51,482	38,311	48,314	46,669	52,378	80,788	140,225

Table 3.2: Total number of fish aggregating device (FAD) and drifter observations collected in the Longhurst biogeographical provinces between 2008 and 2014. Selected provinces are shaded.

Province description	Code	Drifters	FADs
Australia-Indonesia Coastal Province	AUSW	16,651	6,106
Benguela Current Coastal Province	BENG	6,431	1,858
Brazil Current Coastal Province	BRAZ	19,616	1,399
Canary Coastal Province	CNRY	13,085	21,399
China Sea Coastal Province	CHIN	4,216	0
E. Africa Coastal Province	EAFR	31,129	175,733
E. India Coastal Province	INDE	10,248	237
Guianas Coastal Province	GUIA	12,693	8,946
Guinea Current Coastal Province	GUIN	8,009	234,069
NW Arabian Upwelling Province	ARAB	23,477	367,690
Red Sea, Persian Gulf Province	REDS	39	10
Sunda-Arafura Shelves Province	SUND	6,872	83
SW Atlantic Shelves Province	FKLD	189	0
W. India Coastal Province	INDW	5,494	2,401
Archipelagic Deep Basins Province	ARCH	27,079	554
Caribbean Province	CARB	2,515	174
Eastern Tropical Atlantic Province	ETRA	59,360	780,874
Indian Monsoon Gyres Province	MONS	146,717	2,665,216
Indian S. Subtropical Gyre Province	ISSG	160,585	162,963
N. Atlantic Tropical Gyral Province	NATR	184,484	63,101
South Atlantic Gyral Province	SATL	260,199	47,029
Western Tropical Atlantic Province	WTRA	57,414	230,438
S. Subtropical Convergence Province	SSTC	34,406	805
Subantarctic Province	SANT	1,603	27
N. Atlantic Subtropical Gyral Province	NASE	0	87

2.5. Satellite currents

The satellite-derived surface current information produced by the OSCAR processing system is provided in near-real time from a combination of quasi-steady geostrophic and locally wind-driven dynamics (Lagerloef et al., 1999) (http://www.oscar.noaa.gov). The OSCAR product combines: (i) a geostrophic term computed from the gradient of ocean surface topography fields using several sources of spatial observation through time, (ii) a wind-driven velocity term computed

from an Ekman-Stommel formulation with variable eddy viscosity using QuikSCAT and National Centers for Environmental Prediction winds, and (iii) a thermal wind adjustment using Reynolds sea surface temperature (Reynolds and Rayner, 2002). Dohan and Maximenko (2010) provide a full description of the OSCAR product. In this study, we used the 1/3 degree grid and 5-day interval resolution of the OSCAR currents, which is designed to represent a 30 m surface layer average. The OSCAR currents have been validated with moored buoys, drifters, and shipboard acoustic Doppler current profilers (Johnson et al., 2007).

2.6. Direct comparison

To compare possible velocity differences between the floating devices, we selected every FAD and drifter pair that emitted a signal in near space and time. Thus, for each FAD location and 24-h time period, we searched for a drifter within a 1/6 degree radius (10 nm). If several drifters were identified, we selected the device that was closest in time. A sensitivity analysis, with time periods of 12 h and 2.5 days (consistent with the OSCAR temporal resolution), was then conducted. The correlation between the corresponding zonal and meridional velocity components for the FAD and drifter pairs was then considered using the Pearson's correlation coefficient (Johnson et al., 2007). We then used major axis regression models forced through the origin to assess the agreement between the two variables (Legendre and Legendre, 1998; Warton et al., 2006). This approach accounts for the measurement errors in both variables. Preliminary tests indicated that estimated intercepts were generally not significantly different from 0. Sensitivity of the results was assessed against this assumption, i.e. estimating both slopes and intercepts.

2.7. Indirect comparison

This comparative analysis was then extended to the full data set by undertaking an indirect comparison of FAD and drifter velocities using satellite measurements of near-surface current velocities. At each FAD and drifter position, we linearly interpolated the OSCAR current data in time and space to calculate the OSCAR velocities (Johnson et al., 2007; Dohan and Maximenko, 2010). To determine the correlation and agreement between the FADs and OSCAR and drifters and OSCAR, we used the methodology described in the previous section. This analysis was completed at both the basin and large biogeographical province scales to ensure that the different oceanographic regimes of the Indian and Atlantic Oceans were represented. The spatio-temporal autocorrelation of velocity values along the FAD and drifter trajectories was accounted for by subsampling the data at values that were close (5 days) and far above (15 days) the Lagrangian integral time scale estimated for drifters in the Indian Ocean (i.e. 2–7 days; Peng et al., 2014).

2.8. Projection of FAD and drifter locations using OSCAR

The OSCAR velocities were then used to project the FAD and drifter locations from one timestep to the next to compare their Lagrangian transport in near-surface waters. We computed the distance d between the projected location and the next observed location and the distance D between the current location and next observed location to estimate the index d / D for FADs and drifters. These indices were used to gauge the degree of departure of each floating device from the OSCAR currents predictions (Berta et al., 2014; Yaremchuk et al., 2016). Distributions were compared (i.e., for FADs and drifters) at both the basin and (selected) large biogeographical province scales.

3. Results

At the basin scale, the velocity distributions of FADs and drifters were similar in the Atlantic Ocean, where the first quartile, median, and third quartile values in the FAD and drifter velocity distributions were 11.45, 19.96, 32.8 cm s^{-1} , and 11.59, 19.34, 30.07 cm s^{-1} , respectively. In the Indian Ocean, the velocity distributions of both device types were found to be different and with higher values, 21.58, 35.13, 54 cm s^{-1} for FADs and 16.18, 26.39, 40.36 cm s^{-1} for drifters. At a regional scale, FAD and drifter velocities were similar in the ETRA, NATR, and WTRA biogeographical provinces of the inter-tropical Atlantic Ocean, but they differed in the GUIN province (Table 3.3). In that province, the number of drifter locations was the lowest, more than an order of magnitude lower than the number of FAD locations (Table 3.2).

Table 3.3: The first quartile, median, and third quartile values (cm s^{-1}) from the fish aggregating device (FAD) and drifter velocity distributions in selected Longhurst biogeographical provinces of the Atlantic (upper part of the table) and Indian (lower part) Oceans (see Table 3.2 for acronyms of the provinces and Fig. 3.2 for their location).

Device	Province	1st quartile	Median	3rd quartile
Drifters	ETRA	11.62	19.65	31.45
FADs	ETRA	12.08	20.29	31.91
Drifters	GUIN	13.07	23.05	38.60
FADs	GUIN	8.91	15.98	28.49
Drifters	NATR	8.36	13.39	19.95
FADs	NATR	9.03	15.09	24.42
Drifters	WTRA	15.47	26.73	42.99
FADs	WTRA	15.58	27.39	44.18
Drifters	ARAB	14.25	23.86	39.37
FADs	ARAB	27.17	45.67	75.87
Drifters	EAFR	18.77	33.29	56.81
FADs	EAFR	22.63	36.72	55.12
Drifters	ISSG	13.70	22.20	33.39
FADs	ISSG	18.36	28.56	40.73
Drifters	MONS	17.00	27.89	43.64
FADs	MONS	21.27	34.51	52.65

Within the four provinces that make up most of the south-western Indian Ocean, FAD velocities were substantially higher than drifter velocities (Table 3.3). Differences in velocities between FADs and drifters were attributed to differences in the spatio-temporal distribution between the two types of devices. In the Atlantic Ocean, the FAD data were concentrated in the central-eastern region (Fig. 3.2A) while the drifter data were more evenly distributed, although the northern area showed the highest concentrations (Fig. 3.2B). In the Indian Ocean, the FAD data were concentrated in the central-western region (Fig. 3.2A) while the drifter data were more evenly distributed over the entire basin (Fig. 3.2B). At a smaller, 1°×1° spatial scale, the FADs and drifters showed very similar patterns of velocity in the near-surface currents (Fig. 3.2C and D), revealing the major oceanographic features of both the tropical Atlantic Ocean (the South Equatorial and the North Brazil currents, the Equatorial countercurrent and the Guinea current) and the Indian Ocean (Somali, North Madagascar, and Agulhas currents, the Equatorial countercurrent and the South Equatorial current).

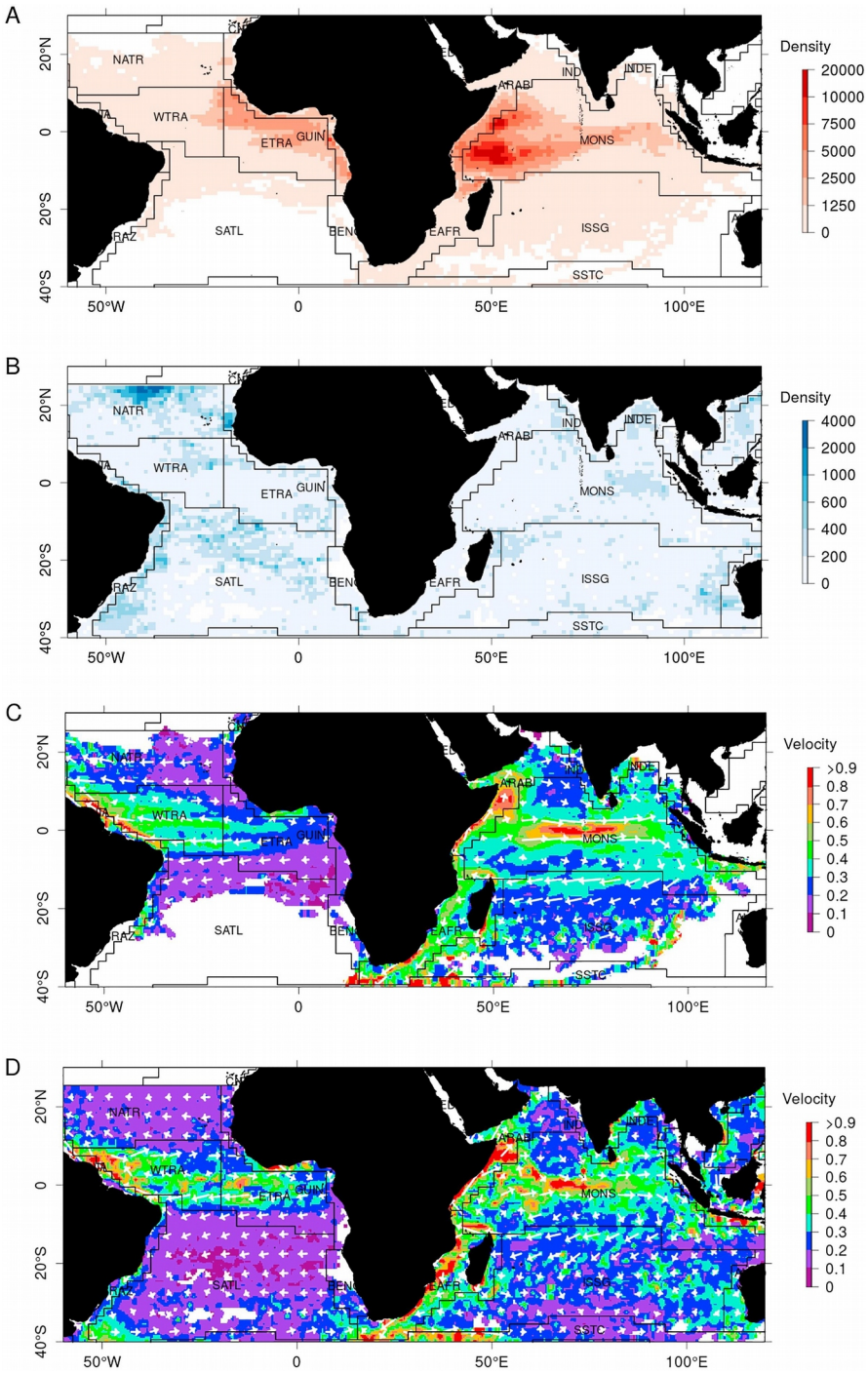

Figure 3.2: Spatial distribution of fish aggregating devices (FADs; A) and drifters (B) in the Atlantic and Indian Oceans. Density corresponds to the number of location points observed in each 1°x1° grid cell for the time period 2008–2014. Mean of near-surface ocean currents (m s^{-1}) for the period 2008–2014, derived from FAD (C) and drifter (D) movements. Solid lines indicate boundaries between biogeographical provinces (Longhurst, 2007) (see Table 3.2 for acronyms).

More than 18,000 pairs of FADs and drifters were detected across the Atlantic (n = 4,146) and Indian (n = 14,558) Oceans (Fig. 3.3). For these pairs, the zonal and meridional components of the FAD vs. drifter velocities were found to be significantly and highly correlated with Pearson's correlation coefficients between 0.68 and 0.93 (Fig. 3.4). This result was found to be robust to the

time period considered for the definition of pairs of floating devices (Table 3.4). We also found several pairs in both oceans that shared common trajectories over several weeks to months, e.g., two FADs deployed in the Indian Ocean in 2013 traveled with two drifters during several months (Fig. 3.5). In the Indian Ocean, the velocity of FAD and drifter pairs agreed remarkably well (Fig. 3.4 and Table 3.4). In the Atlantic Ocean, however, small but consistent systematic differences in the velocity components indicate that drifters move faster than FADs (2–37% higher velocity components, 10–21% higher overall velocity; Fig. 3.4 and Table 3.4). When major axis regressions were not forced through the origin, there was no change in these results except for the velocity component in the Atlantic Ocean, for which slopes came closer to 1 and intercepts were significantly different from 0 (Appendix Table C1.1).

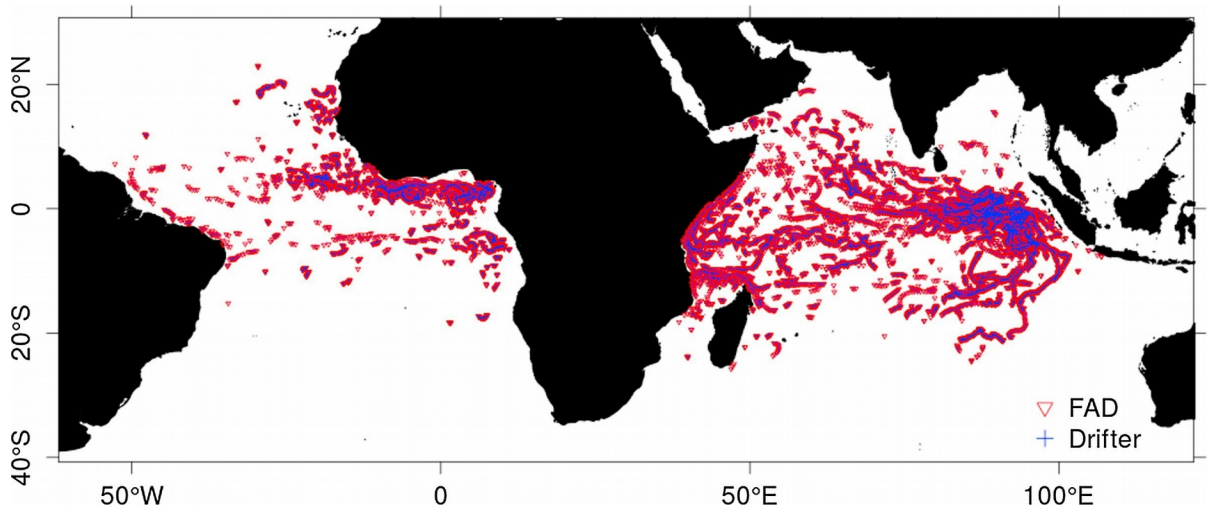

Figure 3.3: Spatial distribution of FADs (red triangles) and drifters (blue crosses) pairs that occurred within a 10 nm radius during 24-h periods in the Atlantic (n = 4,146) and Indian (n= 14,558) Oceans.

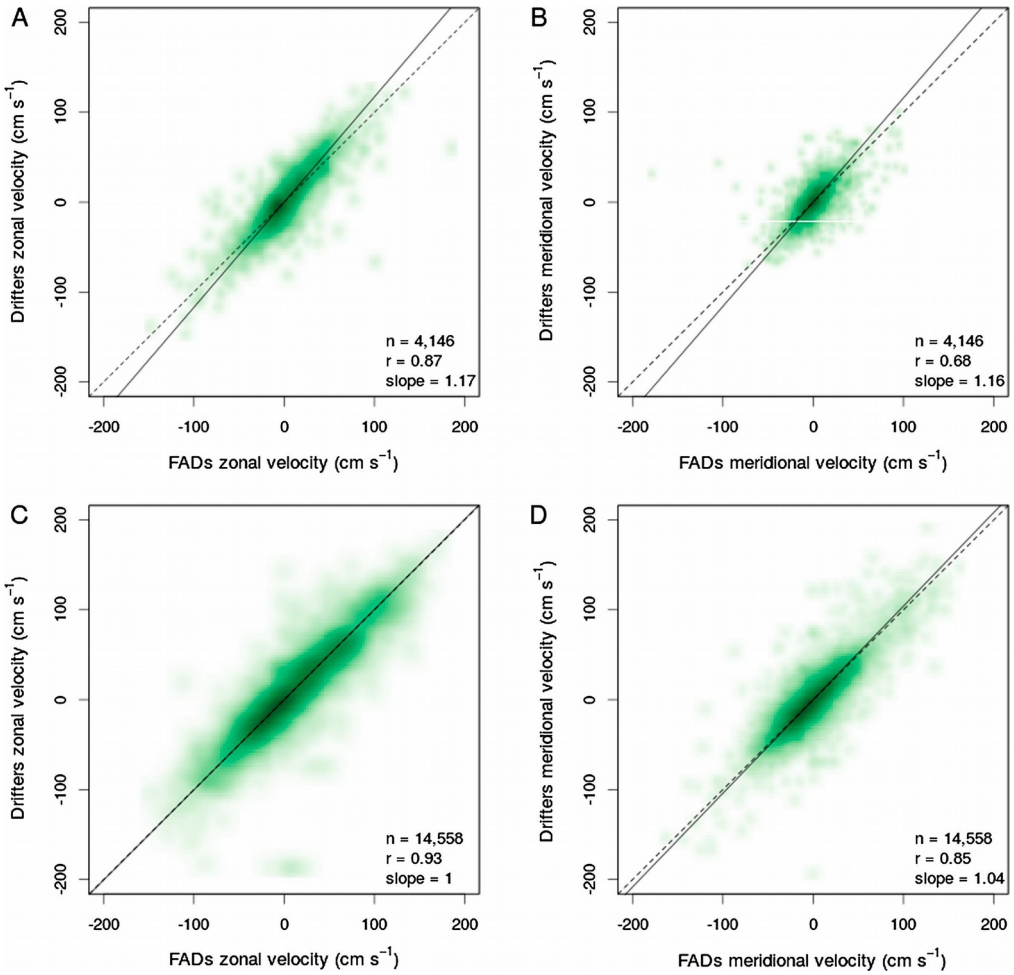

Figure 3.4: Velocity comparisons between the FAD and drifter pairs (A) zonal component in the Atlantic Ocean; (B) meridional component in the Atlantic Ocean; (C) zonal component in the Indian Ocean; and (D) meridional component in the Indian Ocean. The solid line indicates the major axis regression model and the dashed line indicates the 1:1 isoline.

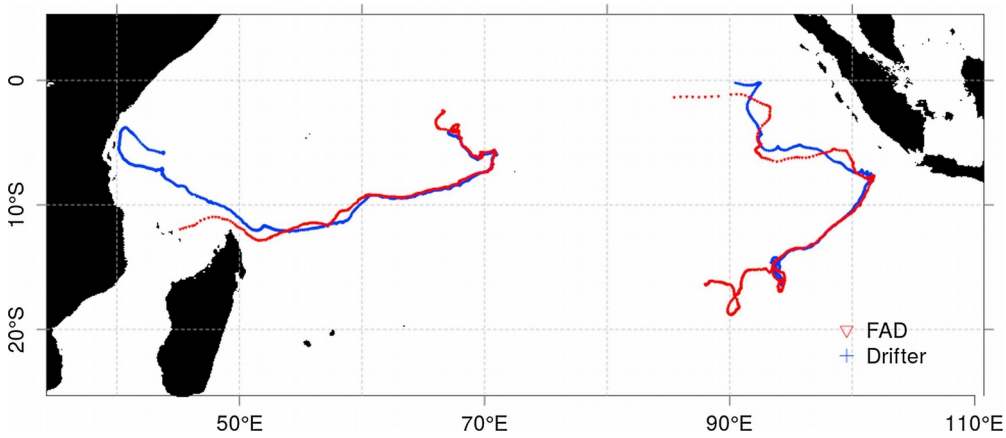

Figure 3.5: Examples of long-associated drift across the Indian Ocean featuring fish aggregating device (FAD) buoy n° 17179 (red triangles) and drifter n° 109550 (blue crosses) on the left, FAD buoy n° 16812 and drifter n° 109364 on the right, sharing similar trajectories between August and November 2013.

Table 3.4: The number of FADs and drifters pairs, correlation coefficients and slopes (with lower and upper bounds) of the velocity components for FAD vs. drifter at different spatio-temporal buffers in the Atlantic and Indian Oceans. Buffers are defined by radius deltaD_deg and time period deltaT_day (see text in section "Direct comparison").

Ocean	deltaD_deg	deltaT_day	Component	n	r	Slope	Slope low.	Slope upp.
Indian	1/6	0.5	Velocity	10,015	0.85	1.01	1.00	1.01
Indian	1/6	1	Velocity	14,558	0.83	1.01	1.01	1.02
Indian	1/6	2.5	Velocity	25,967	0.78	1.03	1.02	1.03
Atlantic	1/6	0.5	Velocity	2,842	0.73	1.12	1.10	1.14
Atlantic	1/6	1	Velocity	4,146	0.75	1.15	1.13	1.16
Atlantic	1/6	2.5	Velocity	7,739	0.71	1.20	1.18	1.21
Indian	1/6	0.5	u	10,015	0.93	1.00	0.99	1.01
Indian	1/6	1	u	14,558	0.93	1.00	1.00	1.01
Indian	1/6	2.5	u	25,967	0.90	1.01	1.01	1.02
Atlantic	1/6	0.5	u	2,842	0.87	1.16	1.14	1.19
Atlantic	1/6	1	u	4,146	0.87	1.17	1.15	1.19
Atlantic	1/6	2.5	u	7,739	0.85	1.21	1.19	1.22
Indian	1/6	0.5	v	10,015	0.88	1.02	1.01	1.03
Indian	1/6	1	v	14,558	0.85	1.04	1.03	1.05
Indian	1/6	2.5	v	25,967	0.76	1.08	1.07	1.09
Atlantic	1/6	0.5	v	2,842	0.69	1.06	1.02	1.10
Atlantic	1/6	1	v	4,146	0.68	1.16	1.12	1.20
Atlantic	1/6	2.5	v	7,739	0.58	1.33	1.29	1.37

The outcomes of the comparative analysis of FAD and drifter velocities with OSCAR satellite current products further supports the case for using FADs for monitoring ocean surface dynamics. Here, the spatial patterns in both FAD and drifter current velocities and directions were consistent with the remotely-sensed surface currents (Appendix Fig. C1.1). The correlation coefficients of velocity components between FADs and OSCAR and drifters and OSCAR were generally very similar (Fig. 3.6, Appendix Figs. C1.2–C1.5, Appendix Figs. C1.6 and C1.7 and Appendix Table C1.2). After accounting for autocorrelation in the data, these relationships were still highly significant (Appendix Table C1.3). However, the OSCAR currents appeared to be slower than the currents derived from the in situ data collected from the floating devices, as indicated by the slopes of the relationships between

the OSCAR currents and floating devices being lower than 1 in all cases but one (Appendix Fig. C1.8 and Appendix Table C1.2). At the biogeographical province scale, the large variability observed in these slopes (FADs: 0.2–0.9 and drifters: 0.3–1.2) shows that they are not representing the surface dynamics at the same spatio-temporal scale.

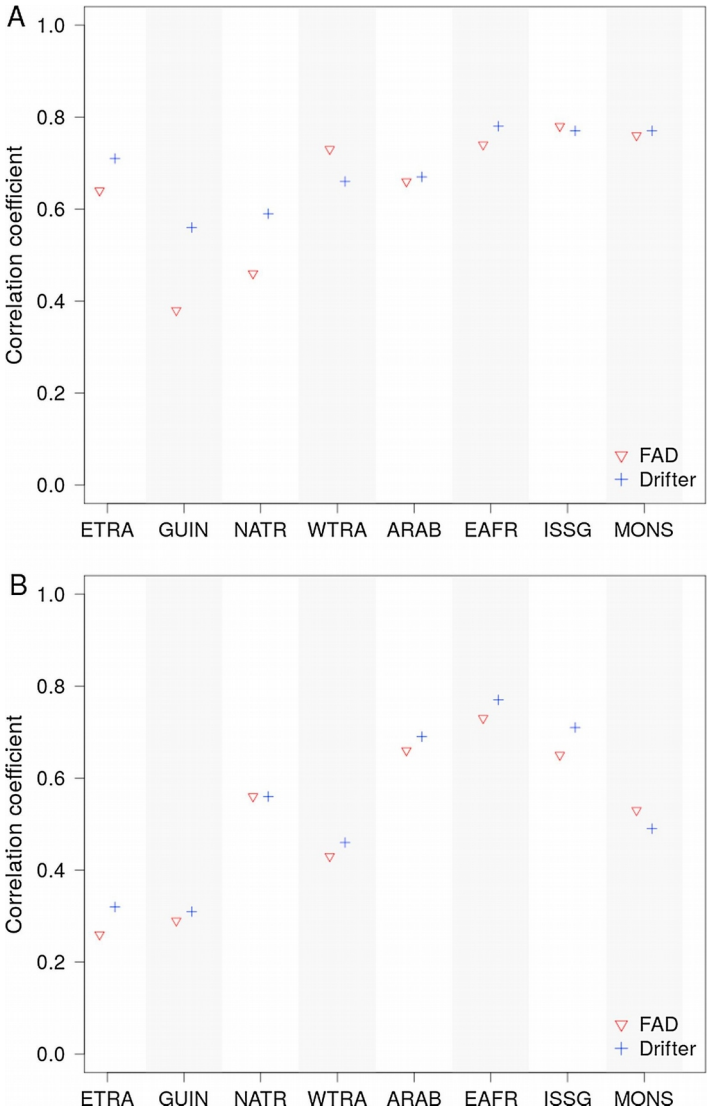

Figure 3.6: The comparison of correlation coefficients for the (A) zonal and (B) meridional components of velocity for the Ocean Surface Currents Analyses Real-time (OSCAR) versus fish aggregating devices (FADs) and OSCAR versus drifters in the selected Longhurst biogeographical provinces (see Table 3.2 for acronyms of the provinces and Fig. 3.2 for their location).

The distributions of the OSCAR-projection error index d / D for FADs and drifters were almost identical across all biogeographical provinces (Appendix Fig. C1.9), with the notable

exception in the south subtropical gyre province of the Indian Ocean (ISSG). Differences in spatial coverage explain this result, with FADs mostly occurring in the North of the ISSG province during the 2008–2014 period while drifters spanned the whole area (Fig. 3.2).

4. Discussion

We combined large data sets of remotely-sensed current speed with the GPS positions of thousands of satellite-tracked floating devices to show that the fish aggregating devices used in tuna fisheries and oceanographic drifters move similarly in near-surface ocean currents. This confirms that in tropical areas, the oceanographic information provided by satellite buoys on FADs could complement that gathered by the Global Ocean Observing System's drifter program. However, we highlighted some differences in the behaviour of FADs and drifters.

While drifters drogues are centered at 15 m below the surface, the FADs subsurface structure composed of curtain or sausage nets can go down to 50–60 m in the Indian Ocean, 80 m in the Atlantic Ocean. These differences in anchoring depth between the two types of floating devices, and between FADs, locate them in different current layers. Indeed, we noted some speed differences between the two types of floating devices, particularly in the Atlantic Ocean, which are likely related to differences in their drogue structures. In the absence of strong winds, the geostrophic balance dominates the upper ocean circulation. In this case, floating devices with different windage and drogues at different depths, or even without drogue, move at similar velocities. Conversely, higher and variable winds generate internal waves as well as Ekman currents. The former modify the mixed layer depth whereas the latter generate currents that quickly rotate with depth. In both cases, floating devices with different drogue lengths will move with different velocities and often in different directions (Poulain et al., 2009). At smaller scales, non-linear dynamics arising from wind-vorticity generate convergence and divergence regions where floating devices drogued at various depth will respond in different ways.

Velocities of drifter and FAD pairs compared remarkably well in the Indian Ocean, despite differences in their design. In that Ocean, velocities in the Equatorial countercurrent where many FADs occur have indeed been found to be relatively homogeneous along a 0–60 m depth range (Gnanaseelan and Deshpande, 2017), showing the same reversal pattern during monsoon periods. Depth homogeneous velocities were also reported along two modelled transects North of Madagascar and off Tanzania (Manyilizu et al., 2016), within two areas of high FAD occurrence.

By contrast, the eastern equatorial Atlantic Ocean is characterised by the prominence of the Equatorial Undercurrent (EUC), a strong permanent eastward flow located just below the westward South Equatorial current (Johns et al., 2014). FADs built and deployed in the Atlantic Ocean have tails going down to 80 m, longer than in the other oceans (Franco et al., 2009), and at a depth where the core of the EUC is found along the equator (Johns et al., 2014). These deep tails likely slow down the drift of the FADs as compared to the shallow subsurface structure of the drifters, explaining our results.

More generally and although the mechanisms of associative behavior of tuna to FADs remain poorly understood (Fréon and Dagorn, 2000), tuna fishermen consider that deeper tails increase the attraction of tunas by slowing down the FADs (Franco et al., 2009). The depth of FAD tails were also shown to affect the tuna species composition (Lennert-Cody et al., 2008) and the arrival of fish (Orúe et al., 2017) at FADs, with tunas arriving earlier with deeper tails. Consequently, the depth of FAD appendages has been increasing in recent years in all oceans (Murua et al., 2018). In the eastern Pacific Ocean for instance, data collected by observers showed a substantial deepening of the net webbing from a median depth < 10 m in the early 1990s to about 30m nowadays (Hall and Roman, 2017). However, the progressive adoption of sausage nets in place of curtain nets, aimed at reducing the entanglement of marine species, may incidentally decrease the anchoring effect of the FAD tail appendage. In this study, our data came from fishing companies that use very similar FAD designs made of bamboo rafts and recycled fishing nets of similar lengths. More broadly, information on the structural design of FADs and their components is now being systematically collected through the fisheries observer programs run in both oceans. This new information will be useful to determine the influence of the subsurface currents on FAD drift. In particular, a comparison of FAD velocity between natural floating objects (e.g. palm trees, logs), which do not have a subsurface structure, and artificial FADs, which do have, would provide insight into the effects of design on FADs drift. A comparison of the drift and separation of concurrently deployed drifter and FAD clusters would also provide insight into the extent to which design explains the observed differences in speed between the two types of floating devices.

Given that the FAD data we used in this study is open access, we expect that further analysis will be undertaken to fully validate the potential applications of FAD data for oceanographers, and that the results of this work will prompt long-term collaborations with the tuna fishing industry. The quantity of information available to the scientific community would strongly benefit from the

release of data from other purse seine fishing companies operating in the Atlantic and Indian Oceans since the French purse seine fleet only represented about 10% of the total drifting FADs in recent years (Maufroy et al., 2017). Recent availability of FAD GPS positions in the western and central Pacific Ocean shows a positive step in this direction (Escalle et al., 2017). It would also be beneficial to apply the GDP's quality control procedures (Hansen and Poulain, 1996; Lumpkin and Pazos, 2007) to the FAD data. This step may provide useful information that is currently missing such as FAD location errors.

The GPS buoys tracked in the present study were mostly deployed within the fishing grounds of the French purse seine fleet (Maufroy et al., 2015; Snouck-Hurgronje et al., 2018). Other purse seine fleets include some non-fishing support vessels that maintain the array of FADs and can deploy buoys outside fishing grounds, anticipating their drift in productive areas several weeks in advance (Arrizabalaga et al., 2001; Assan et al., 2015). In this context, GPS buoy data from fleets assisted by support vessels would greatly complement the French data set and provide a more complete picture of the near-surface ocean currents of the tropical areas covered in the present study.

More broadly, the conspicuous character of global changes presents some serious observational challenges. Effectively responding to these challenges requires better integration across individual networks and multiple platforms, to make the most of synergies between the different types of ocean observations (Roemmich et al., 2010). The development of standards for metadata and data formats, as well as access protocols (e.g., Web Services), has recently enhanced interoperability functions in information systems. Thus, these standards are better able to merge and process heterogeneous data sets stored in distributed infrastructures and promote integration across scientific disciplines (Reichman et al., 2011; Mooney et al., 2013; Robertson et al., 2014). Data management systems should also include well-described control procedures that aim to inform users about the best quality data sets available (Roemmich et al., 2010). In oceanography, the recent introduction of key standards contributes to this higher level of interoperability for physical and chemical parameters delivered as gridded data (e.g. model outputs, or satellite remote-sensing products) or time series of parameters retrieved from platforms at sea (Hankin et al., 2010). Like the data collected through citizen science initiatives (Lauro et al., 2014), the millions of data collected by fishermen could substantially increase the spatio-temporal coverage of ocean observations in a cost-efficient manner. Thus, the major contributions these data sets could potentially make to the

GOOS and GCOS calls for improved collaboration with the fishing industry (Gawarkiewicz and Mercer, 2018; Moreno et al., 2016) and the establishment of a system that adequately acknowledges the contributors and fosters a data sharing environment.

The openness of anonymized FAD tracking data has almost no cost for the fishing industry and provides an ideal opportunity to communicate in a transparent way about their practices. In particular, it shows willingness with regards to compliance and accountability on the limited number of active buoys per fishing vessel recently implemented by most tuna Regional Fisheries Management Organisations (RFMOs). Complying with Conservations and Management Measures of the RFMOs will increasingly become important for the allocation of stock quotas and access rights in the future (IOTC, 2018). In the Seychelles, access to some fishing grounds of the exclusive economic zone identified as part of the ongoing Management Spatial Planning will be restricted to sustainable fishing practices, which could include availability of FAD data for scientific and monitoring purpose. Globally, most purse seine fishing companies are now involved in Fisheries Improvement Projects with the objective of reaching the standards of the Marine Stewardship Certification (MSC) and increase benefits. The provision of information on FAD-related fishing practices is a key component of MSC assessment due to the growing concerns of FAD fishing (Fonteneau et al., 2013; Davies et al., 2017). Fishermen who voluntarily release data sets that are useful for advancing our understanding of ocean dynamics will benefit from their efforts through improved image and communication to the general public.

Appendix C1

Table C1.1: Same as Table 3.4 but with major axis regression not forced through the origin (the estimated intercept is added in the last column).

Ocean	deltaD_deg	deltaT_day	Component	n	r	Slope	Slope low.	Slope upp.	Intercept
Indian	1/6	0.5	Velocity	10,015	0.85	1.01	0.99	1.02	0
Indian	1/6	1	Velocity	14,558	0.83	1.01	1	1.02	0.37
Indian	1/6	2.5	Velocity	25,967	0.78	1	0.99	1.01	1.55
Atlantic	1/6	0.5	Velocity	2,842	0.73	1.01	0.98	1.05	3.62
Atlantic	1/6	1	Velocity	4,146	0.75	1.04	1.01	1.06	4.12
Atlantic	1/6	2.5	Velocity	7,739	0.71	1.09	1.06	1.11	4.05
Indian	1/6	0.5	u	10,015	0.93	1	0.99	1.01	−0.03
Indian	1/6	1	u	14,558	0.93	1	1	1.01	−0.22
Indian	1/6	2.5	u	25,967	0.9	1.02	1.01	1.02	−0.22
Atlantic	1/6	0.5	u	2,842	0.87	1.16	1.14	1.19	0
Atlantic	1/6	1	u	4,146	0.87	1.17	1.15	1.19	0.07
Atlantic	1/6	2.5	u	7,739	0.85	1.2	1.19	1.22	0.76
Indian	1/6	0.5	v	10,015	0.88	1.02	1.01	1.03	−0.28
Indian	1/6	1	v	14,558	0.85	1.04	1.03	1.05	−0.47
Indian	1/6	2.5	v	25,967	0.76	1.08	1.07	1.09	−0.67
Atlantic	1/6	0.5	v	2,842	0.69	1.06	1.02	1.1	−0.45
Atlantic	1/6	1	v	4,146	0.68	1.16	1.12	1.2	−0.37
Atlantic	1/6	2.5	v	7,739	0.58	1.33	1.29	1.37	−0.61

Table C1.2: Summary of the major axis regression models fitted to the velocity components of the Ocean Surface Currents Analyses Real-time (OSCAR) measurements versus fish aggregating devices (FADs) and OSCAR versus drifters in the selected Longhurst biogeographical provinces of the Atlantic and Indian Oceans. Slope low. = 2.5% quantile value used as the lower limit of the regression slope estimate; Slope upp. = 97.5% quantile value used as the upper limit of the regression slope estimate. r = Pearson's correlation coefficient.

Device	Component	Province	Slope low.	Slope	Slope upp.	r
FADs	Zonal	ETRA	0.769	0.771	0.773	0.64
FADs	Zonal	GUIN	0.710	0.717	0.725	0.38
FADs	Zonal	NATR	0.192	0.195	0.198	0.46
FADs	Zonal	WTRA	0.696	0.699	0.702	0.73
FADs	Zonal	ARAB	0.876	0.879	0.882	0.66
FADs	Zonal	EAFR	0.571	0.573	0.576	0.74
FADs	Zonal	ISSG	0.669	0.672	0.675	0.78
FADs	Zonal	MONS	0.739	0.739	0.740	0.76
Drifters	Zonal	ETRA	0.686	0.692	0.697	0.71
Drifters	Zonal	GUIN	0.630	0.651	0.673	0.56
Drifters	Zonal	NATR	0.369	0.371	0.373	0.59
Drifters	Zonal	WTRA	0.737	0.744	0.751	0.66
Drifters	Zonal	ARAB	0.717	0.728	0.738	0.67
Drifters	Zonal	EAFR	0.713	0.719	0.725	0.78
Drifters	Zonal	ISSG	0.615	0.617	0.620	0.77
Drifters	Zonal	MONS	0.767	0.770	0.773	0.77
FADs	Meridional	ETRA	0.506	0.511	0.515	0.26
FADs	Meridional	GUIN	0.668	0.677	0.686	0.29
FADs	Meridional	NATR	0.391	0.395	0.400	0.56
FADs	Meridional	WTRA	0.534	0.538	0.543	0.43
FADs	Meridional	ARAB	0.736	0.739	0.742	0.66
FADs	Meridional	EAFR	0.543	0.545	0.547	0.73
FADs	Meridional	ISSG	0.535	0.538	0.541	0.65
FADs	Meridional	MONS	0.664	0.666	0.667	0.53
Drifters	Meridional	ETRA	0.377	0.387	0.396	0.32
Drifters	Meridional	GUIN	1.068	1.144	1.227	0.31
Drifters	Meridional	NATR	0.349	0.351	0.353	0.56
Drifters	Meridional	WTRA	0.658	0.669	0.679	0.46
Drifters	Meridional	ARAB	0.627	0.635	0.644	0.69
Drifters	Meridional	EAFR	0.631	0.636	0.642	0.77
Drifters	Meridional	ISSG	0.534	0.537	0.539	0.71
Drifters	Meridional	MONS	0.673	0.680	0.686	0.49

Table C1.3: The number of observations and correlation coefficients of the velocity components of Ocean Surface Currents Analyses Real-time (OSCAR) versus fish aggregating devices (FADs) and OSCAR versus drifters for the entire dataset (n, Corr_u, Corr_v) and for the datasets subsampled every 5 days (n5, corr5_u, corr5_v) and 15 days (n15, corr15_u, corr15_v) in the Atlantic and Indian Oceans.

Device	Ocean	n	Corr_u	Corr_v	n5	corr5_u	corr5_v	n15	corr15_u	corr15_v
FADs	Atlantic	1,393,100	0.62	0.31	66,228	0.57	0.27	36,986	0.53	0.24
FADs	Indian	3,384,424	0.75	0.58	181,193	0.72	0.56	108,611	0.70	0.55
Drifters	Atlantic	634,297	0.58	0.49	32,303	0.58	0.47	11,211	0.57	0.49
Drifters	Indian	458,065	0.74	0.63	23,418	0.75	0.64	8,187	0.77	0.65

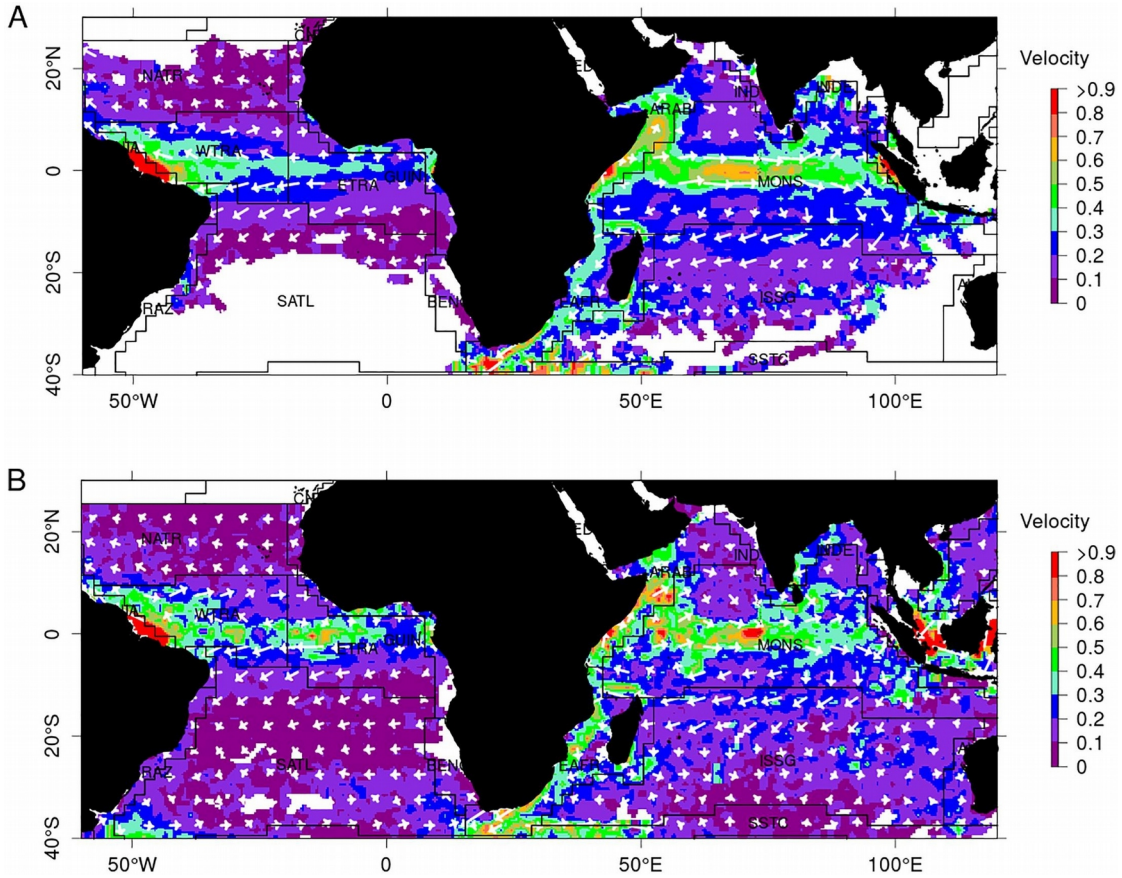

Figure C1.1: Mean of near-surface ocean currents (m s −1) for the period 2008–2014, derived from OSCAR at FADs (i.e., OSCAR data interpolated at the time and location of FAD data) (A) and OSCAR at drifters (i.e., OSCAR data interpolated at the time and location of drifter data) (B). Solid lines indicate boundaries between biogeographical provinces (Longhurst, 2007) (see Table 3.2 for acronyms).

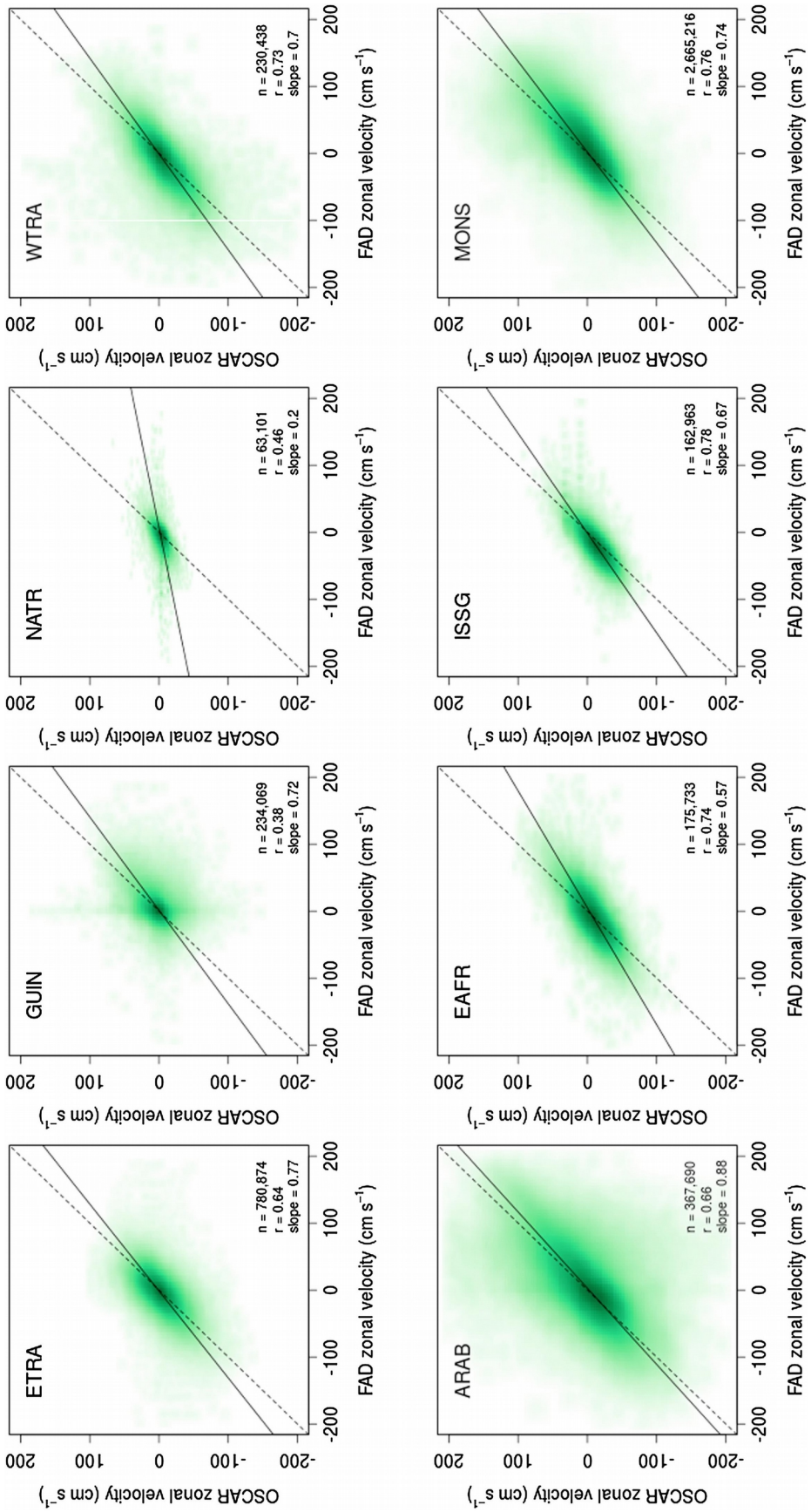

Figure C1.2: The comparison of zonal velocities between fish aggregating devices (FADs) and Ocean Surface Currents Analyses Real-time (OSCAR) in the selected Longhurst biogeographical provinces of the Atlantic Ocean (top) and Indian Ocean (bottom). The solid line indicates the major axis regression model and the dashed line indicates the 1:1 isoline.

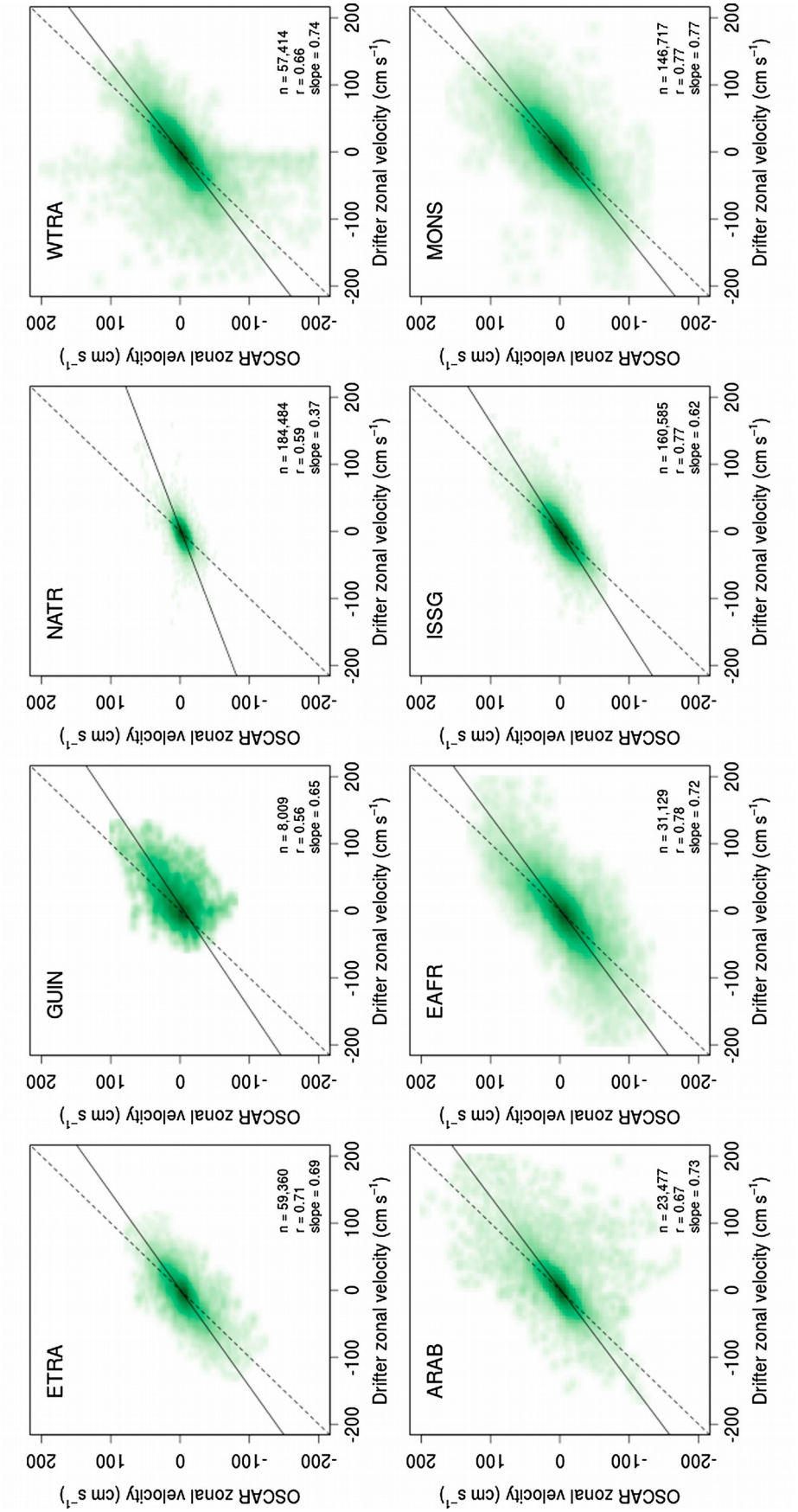

Figure C1.3. The comparison of zonal velocities between drifters and Ocean Surface Currents Analyses Real-time (OSCAR) in the selected Longhurst biogeographical provinces of the Atlantic Ocean (top) and Indian Ocean (bottom). The solid line indicates the major axis regression model and the dashed line indicates the 1:1 isoline.

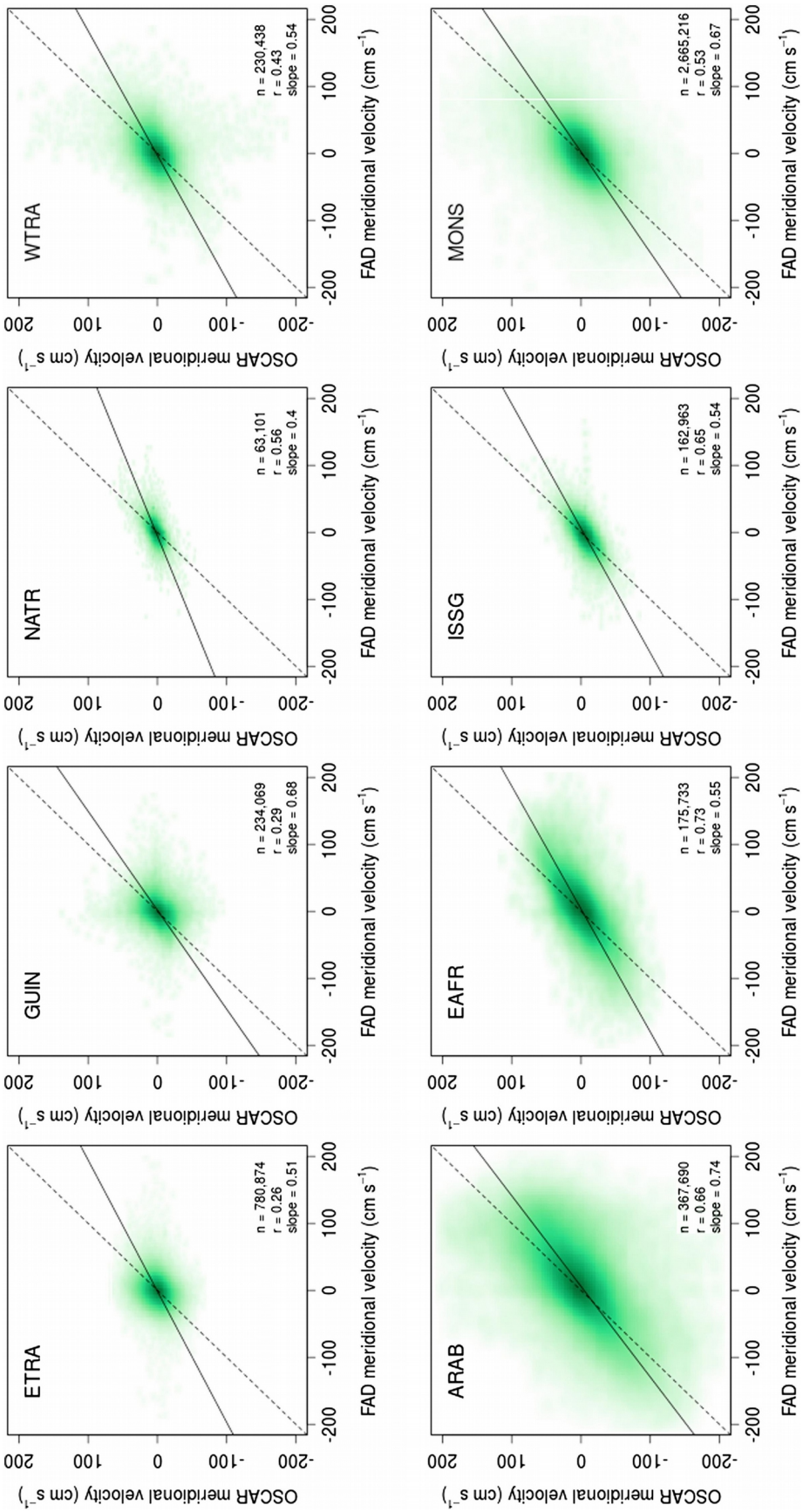

Figure C1.4: The comparison of meridional velocities between fish aggregating devices (FADs) and Ocean Surface Currents Analyses Real-time (OSCAR) in the selected Longhurst biogeographical provinces of the Atlantic Ocean (top) and Indian Ocean (bottom). The solid line indicates the major axis regression model and the dashed line indicates the 1:1 isoline.

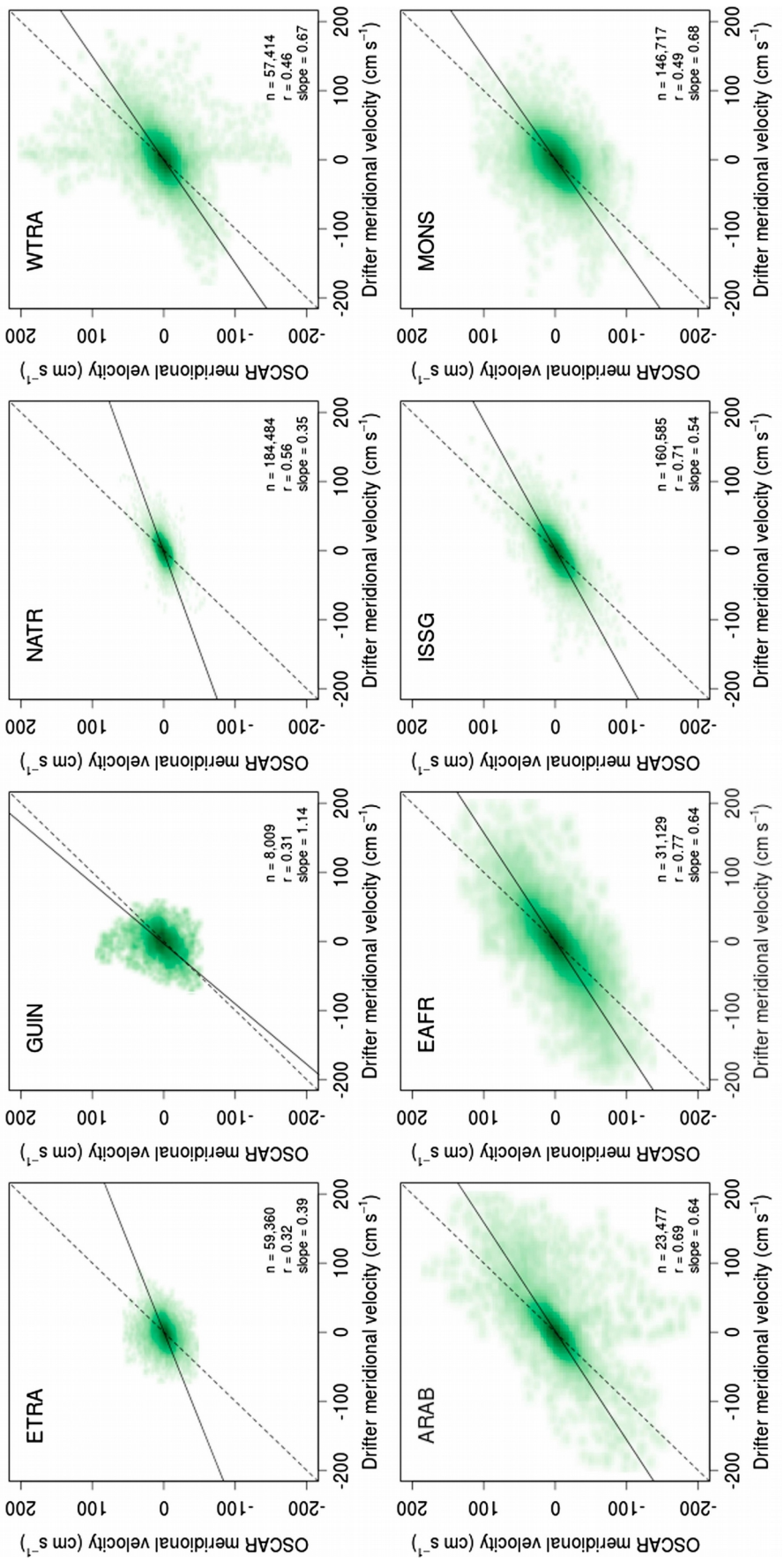

Figure C1.5: The comparison of meridional velocities between drifters and Ocean Surface Currents Analyses Real-time (OSCAR) in the selected Longhurst biogeographical provinces of the Atlantic Ocean (top) and Indian Ocean (bottom). The solid line indicates the major axis regression model and the dashed line indicates the 1:1 isoline.

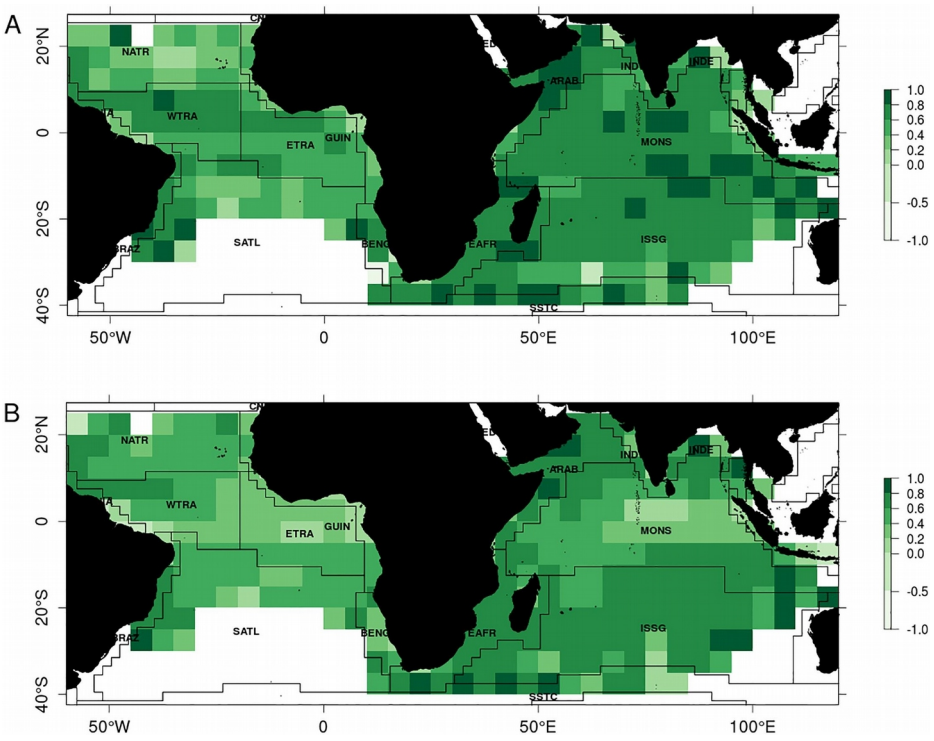

Figure C1.6: Correlation in each 5 ° × 5 ° grid cell of zonal (A) and meridional (B) velocity components between FADs and OSCAR.

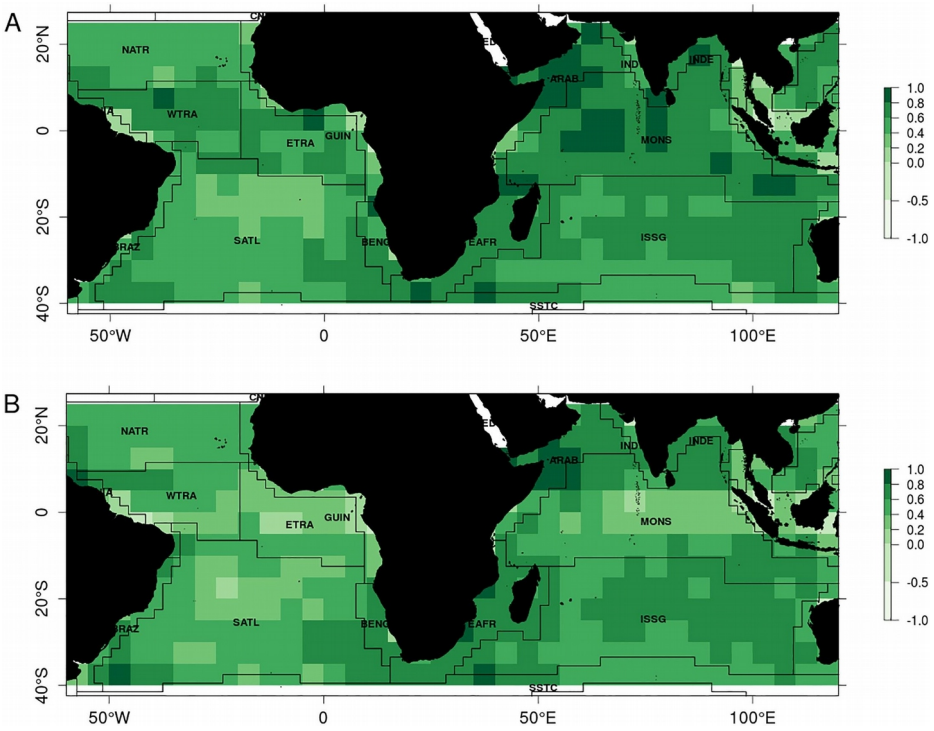

Figure C1.7: Correlation in each 5 ° × 5 ° grid cell of zonal (A) and meridional (B) velocity components between drifters and OSCAR.

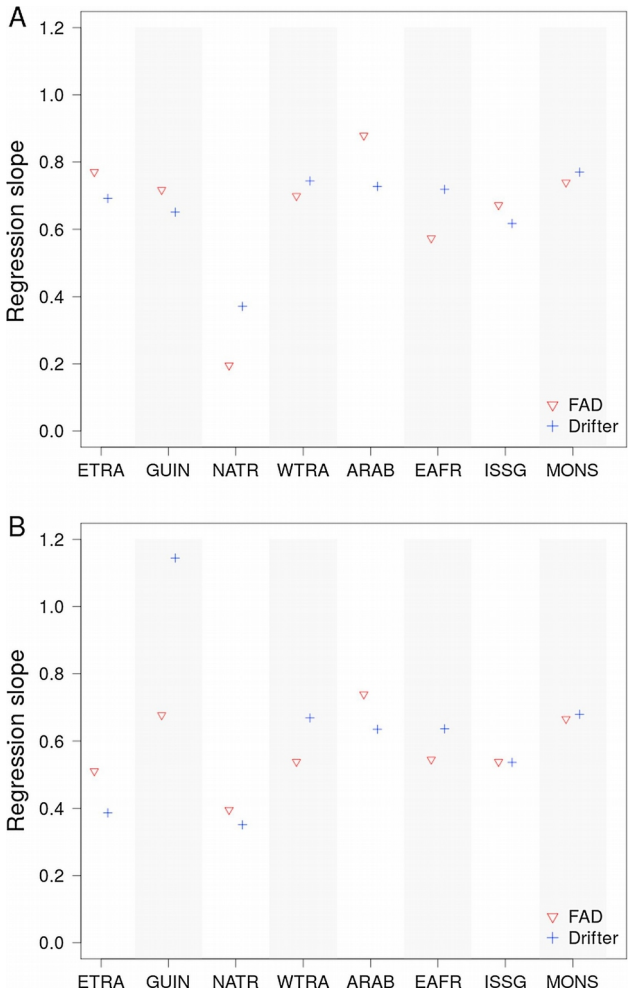

Figure C1.8: The comparison of slopes of major axis regression models fitted to the (A) zonal and (B) meridional velocity data of the Ocean Surface Currents Analyses Real-time (OSCAR) versus fish aggregating devices (FADs) and OSCAR versus drifters in the selected Longhurst biogeographical provinces.

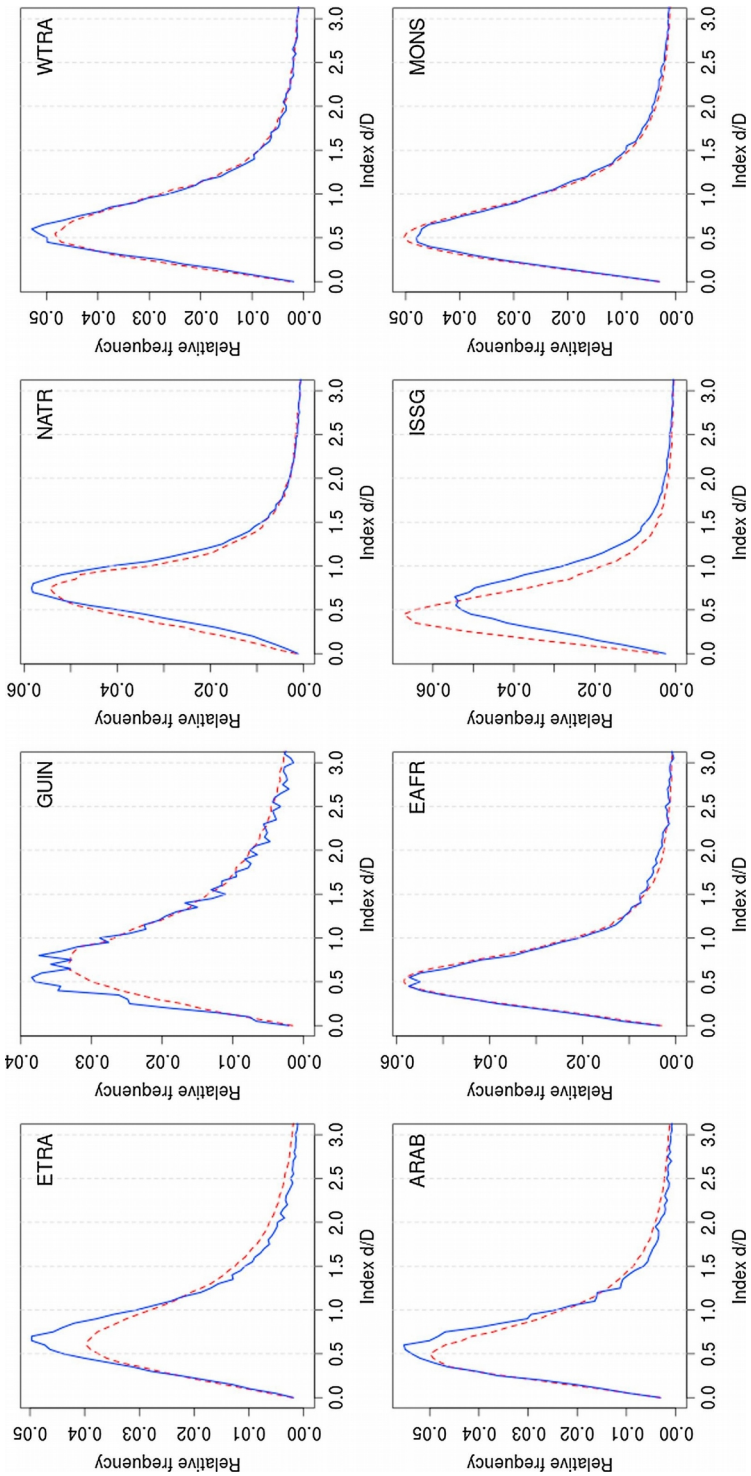

Figure C1.9: Relative frequency distributions of the index d / D that describe the prediction skill of fish aggregating devices (FADs; dashed red curves) and drifters (solid blue curves), with respect to the Ocean Surface Currents Analyses Real-time (OSCAR) velocities for the selected Longhurst biogeographical provinces, where d is the distance between the projected and observed location at the next time step and D is the distance between the current and next observed locations.

Appendix C2

All the datasets and scripts used to reproduce the analyses of this study are available in the open scientific repository Zenodo at: https://doi.org/10.5281/zenodo.1051023.

CHAPITRE 4

Simulations of drifting fish aggregating device (dFAD) trajectories in the Atlantic and Indian Oceans

Après avoir montré dans le chapitre précédent que les DCP dérivants suivaient les courants océaniques, l'utilisation d'un outil de transport Lagrangien pour simuler leurs trajectoires devenait envisageable. Dans ce chapitre 4, nous avons évalué l'efficacité de l'outil Lagrangien Ichthyop pour simuler les trajectoires des DCP. Pour forcer Ichthyop nous avons testé trois produits de courants océaniques et comparé la précision des trajectoires simulées. Les résultats ont montré que les simulations permettent de bien reproduire les densités de DCP observées à l'échelle des deux bassins océaniques Indien et Atlantique. Cependant, la capacité de simuler les trajectoires des DCP individuellement est meilleure dans l'Océan Indien que dans l'Océan Atlantique. Nous avons également constaté que la précision des simulations est sensible à la profondeur et à la résolution spatiale du produit de forçage en notant une meilleure précision obtenue avec les simulations forcées par le produit de plus haute résolution.

Ce Chapitre 4 est soumis à Progress in Oceanography :

Imzilen T, Kaplan DM, Barrier N, Lett C. Simulations of drifting fish aggregating device (dFAD) trajectories in the Atlantic and Indian Oceans. Progress in Oceanography (soumis).

1. Introduction

For centuries, fishers have been using drifting floating objects (FOBs) to attract fish and facilitate their capture (Fréon & Dagorn 2000; Castro et al. 2002). FOBs were historically natural items such as algae, wooden debris, or even marine mammals (Greenblatt 1979). In the 1980's, tropical tuna purse-seine fisheries began to manufacture and deploy human-made FOBs, commonly referred to as drifting Fish Aggregating Devices (dFADs). The use of dFADs has massively increased over the last decades due to use of GPS-equipped, satellite-transmitting tracking buoys that allow fishers to remotely know a dFAD's exact location and due to the more recent incorporation of echo-sounders into tracking buoys, allow fishers to remotely have an indication of tuna presence and fishable biomass (Chassot et al. 2014; Lopez et al. 2014). Currently, purse seiners fish predominantly on dFADs with more than 100,000 of these deployed annually worldwide (Fonteneau et al. 2013; Scott & Lopez 2014; Taconet et al. 2018). The use of dFADs poses a number of major concerns regarding overfishing of target and bycatch species and disturbance to pelagic and coastal ecosystems (Amandè et al. 2010; Dagorn et al. 2013; Filmalter et al. 2013; Maufroy et al. 2015). Furthermore, a large number of dFADs end up lost outside fishing areas and potentially beached (i.e., stranded in coastal areas), thereby contributing to marine debris and threatening sensitive marine habitats such as coral reefs (Balderson & Martin 2015; Stelfox et al. 2016; Zudaire et al. 2018; Imzilen et al. 2021).

Several management changes have been implemented by tuna regional fisheries management organizations (RFMOs) to mitigate these negative impacts of dFADs. These include limitations on the number of dFADs monitored by purse seine vessels (ICCAT 2019; IOTC 2019a) and guidelines encouraging the development and use of biodegradable dFADs (ICCAT 2015; IOTC 2019b; IATTC-WCPFC 2020). However, these restrictions and incentives remain insufficient or have not been fully implemented (development of biodegradable dFADs remains a challenging area of research) for adequately dealing with many of the negative impacts of dFADs use, especially their loss and beaching. To prevent and reduce environmental damage due to the loss and beaching of dFADs, additional management options were recently explored in the Indian and Atlantic Oceans. Imzilen et al. (2021) showed that preventing dFAD deployments in areas with high risk of eventual beaching could decrease beachings by up to 40%. As a complementary measure, Imzilen et al. (subm.) showed that implementing dFAD at-sea recovery programs could also decrease their loss and beaching. Nevertheless, these blanket measures would not identify dFAD loss and beaching risk

at the level of individual dFADs, potentially impeding deployment of or removing dFADs for which real risks are low, nor would they account for the impacts of dFADs for which the tracking buoy has been removed or remotely turned off by fishers. It is therefore necessary to complement these proposed measures with tools that allow one to accurately predict the drift trajectories of individual dFADs.

The present work was conducted in the context of another aspect of future dFADs that is still under investigation: the use of remotely controlled dFADs that could modify their trajectories in order to prevent beaching. In that perspective, one would need a model to anticipate dFAD beaching based on their drift trajectories. Here we explore the possibility of using a Lagrangian particle-tracking model to simulate the trajectories of dFADs. Lagrangian models have been largely used to understand many aspects of the ocean circulation (van Sebille et al. 2018) and to investigate the drift of marine organisms ranging from algae (Putman et al. 2020) to sea turtles (Putman & Mansfield 2015), and the drift of non-living matters from plastic debris (Lebreton et al. 2012) to oil spills (Ivichev et al. 2012). Lagrangian simulations have also recently been used for dFADs. A limited number of dFAD trajectories were simulated to explore the spatiotemporal dynamics of dFAD dispersal in the western Indian Ocean (Imzilen et al. 2016; Davies et al. 2017) and around the Chagos Archipelago in the central Indian Ocean (Curnick et al. 2021). Simulations of dFADs were also used to provide estimates of connectivity between exclusive economic zones (EEZ) in the Western and Central Pacific Ocean (Phillips et al. 2019), and to complement observed dFADs trajectories in order to quantify the link between dFAD deployment sources and beaching locations (Escalle et al. 2019). Nevertheless, only relatively limited attention has been paid to the accuracy of these simulations for simulating dFAD trajectories.

Amemou et al. (2020) performed simulations of dFAD trajectories using a Lagrangian model (Ichthyop, Lett et al. 2008) forced by different oceanic currents derived from remote sensing products (OSCAR, Lagerloef et al. 1999, and GlobCurrent, Johannessen et al. 2016) and from a hydrodynamic model (CROCO, Debreu et al. 2012), finding that simulations compared rather poorly to observations over the period 2008-2014 in the Atlantic Ocean. Multiple potential explanations exist for this poor performance, including insufficient spatio-temporal resolution of the forcing products and the dFAD vertical substructure leading to drift trajectories that are poorly reflected by surface transport patterns (Imzilen et al. 2019). Furthermore, given the differences in

the vertical structure of dFADs used in the Indian Ocean versus the Atlantic Ocean (Franco et al. 2009), as well as the significant increase in the number of dFADs deployed by purse seiners since 2014 (Maufroy et al. 2017; Imzilen et al. 2021), the extent to which this poor performance would be representative of models applied to current dFAD deployment patterns and other areas than the Atlantic Ocean is unclear. Moreover, as ocean current velocities at different depths may affect the drift of dFADs (Imzilen et al. 2019), the use of ocean currents at different depths should also be considered in the assessment of the accuracy of dFAD simulations. Winds could also possibly impact dFAD trajectories, but have not been taken into account in existing simulations. Several studies have yet showed that adding a windage component to ocean surface velocities was an important factor of accurately representing drift trajectories (Santos et al. 2018b, 2018a; Putman et al. 2020).

The aim of this study is to assess the accuracy of a Lagrangian model (Ichthyop, Lett et al. 2008) to simulate dFAD trajectories for an extensive dataset of > 100,000 trajectories of dFADs deployed in the Indian and Atlantic Oceans by the French tropical tuna purse seine fleet over the period 2010-2018. The Lagrangian model was forced by two satellite-derived ocean currents products, OSCAR (Lagerloef et al. 1999) and GEKCO (Sudre et al. 2013), and also by the NEMO (Madec et al. 2013) ocean model output GLORYS12V1 (Fernandez & Lellouche 2021; Drévillon et al. 2021) at multiple depths levels, in order to determine the most appropriate forcing product in terms of simulation accuracy. Finally, we assessed whether including a windage component to the ocean currents improved the simulation quality of dFAD trajectories. These simulation results are used to assess our capacity to accurately represent dFAD trajectories over spatial and temporal scales that are pertinent to tropical tuna resource management.

2. Material and methods

2.1. Observed dFAD trajectories

The locations of GPS-buoys attached to dFADs are available through a collaborative agreement between the French National Research Institute for Sustainable Development (“Institut de Recherche pour le Développement”, IRD) and the French frozen tuna producers’ organization ORTHONGEL. The observed dFAD trajectories used in this study were processed following Imzilen et al. (subm.). We also removed all positions included in the beaching events identified by

Imzilen et al. (2021), as it is not plausible, in this case, to simulate the drift of a buoy that probably snagged and stopped moving. dFAD locations are transmitted with a periodicity that varies along the buoy trajectory, typically emitting between 2 and 4 positions per day. For the sake of comparing simulated and observed trajectories, observed trajectories were linearly interpolated between observations at a 6-hour timestep. Also, the lifespan of the observed trajectories were limited to 100 days as we assumed based on prior literature (Amemou et al. 2020) that beyond this lifespan it was highly likely that the spatial separation between simulated and real trajectories would be sufficiently large to render comparisons uninteresting.

In this study, we used data of dFAD locations covering the period 2010–2018 representing 79,927 trajectories, corresponding to 45,513 distinct tracking buoys, in the Indian Ocean and 22,948 trajectories, corresponding to 14,207 distinct tracking buoys, in the Atlantic Ocean.

2.2. Simulated dFADs trajectories

dFAD trajectories were simulated using the Lagrangian model Ichthyop (Lett et al., 2008). Ichthyop is a free particle-tracking tool developed in Java mostly dedicated to simulate the trajectories of marine ichthyoplankton, but which can also be used as a Lagrangian model to track water masses or drifting entities. In the given study, Ichthyop 3.3.6 (10.5281/zenodo.4244484) was used, to which some minor changes have been made. These modifications include a different way to manage Netcdf time and the possibility to convert dataset coordinates from a Pacific system (longitudes ranging from 0 to 360) to an Atlantic one (longitudes between -180 and 180). The code used in the present study is available on Ichthyop's public GitHub repository (https://github.com/ichthyop/ichthyop/tree/feature/wind).

Ichthyop was forced by three different ocean current products, OSCAR, GEKCO and GLORYS12V1 and (in some simulations) by one wind product (Global Ocean Wind), as detailed in the next section. The displacement of each particle was given by the sum of an advective component due to the currents and a windage component (i.e., a vector in the same direction as and proportional to the winds) when wind was considered. Particle locations were updated at each time step (6 h) using the Runge-Kutta fourth order scheme.

Ichthyop simulations forced with GLORYS12V1, OSCAR and GEKCO are hereafter referred to as GLO, OSC and GEK, respectively.

2.3. Global ocean currents

OSCAR

Ocean Surface Current Analyses Real-time (OSCAR) is a NASA-funded research project that produces satellite-based global sea surface current maps combining geostrophy estimated from sea-surface height, surface wind speed computed from Ekman and Stommel shear dynamics, and a complementary term from the surface buoyancy gradient using sea-surface temperature (Lagerloef et al. 1999; Bonjean & Lagerloef 2002). OSCAR currents have been validated with drifters, shipboard acoustic Doppler current profilers and moored buoys (Johnson et al. 2007). In this study, we used the 1/3° grid and 5-day interval resolution of the OSCAR currents, which is designed to represent a 30 m surface layer average. The data is freely available through the NASA Physical Oceanography data center (https://podaac.jpl.nasa.gov).

GEKCO

Geostrophic and Ekman Current Observatory (GEKCO) is a satellite product developed by the Laboratoire d'Etudes en Géophysique et Océanographie Spatiales (LEGOS) in France. GEKCO provides an estimate of surface currents combining geostrophic and wind-driven components using observations of sea surface height and wind stress via satellite-derived measurements. GEKCO currents have been validated with independent observations from both Lagrangian and Eulerian perspectives using drifters, shipboard acoustic Doppler current profilers and moored buoys (Sudre et al. 2013). The data was requested from LEGOS (*https://www.legos.omp.eu*) and was provided at a 1/4° resolution with a time resolution of 1 day.

GLORYS

The Global Ocean Physical Reanalysis (GLORYS12V1, Fernandez & Lellouche 2021) product provided by The European Copernicus Marine Environment Monitoring Service (CMEMS) consists of a global ocean reanalysis dataset based on the NEMO model (Madec et al. 2013) driven at the surface by ECMWF ERA-Interim reanalysis until the end of 2018 and ERA5 reanalysis afterwards. This product provides 3D currents information defined on a regular grid with a 1/12º horizontal resolution (approx. 8km) and 50 fixed vertical levels describing the ocean from the surface to the bottom. The GLORYS12V1 product reproduces the main ocean currents well, and the upper layers equatorial vertical dynamics structures are in good accordance with moorings observations (Drévillon et al. 2021). In this study, we used the 1/12° grid and a time resolution of 1 day of the

GLORYS12V1 currents at different depths: 0m, 5m, 10m, 15m and 30m. The data is available through the CMEMS website (https://marine.copernicus.eu).

2.4. Global winds

We used the Global Ocean Wind data produced by IFREMER and distributed by CMEMS. This satellite L4 product uses scatterometers on board several satellites that measure the small waves at the surface of the ocean and estimate global sea surface winds at high spatial and temporal resolutions (Desbiolles et al. 2017). The Global Ocean Wind product is provided at 1/4° spatial resolution and every 6 hours on the CMEMS website (https://marine.copernicus.eu).

When simulating Lagrangian particle trajectories, windage values of 1%, 3% and 5% of wind strength were used to assess whether adding a windage component to ocean currents improved model performance.

2.5. Comparing observed and simulated dFAD trajectories

Spatial distributions

To have a global view of the differences between the observed distributions of dFADs and simulated particles in the Indian and Atlantic Oceans, we produced density maps representing the total number of times observed dFADs or simulated particles were located in each 1°x1° grid cell of the Indian and Atlantic Oceans over the study period (2010-2018).

Separation distance

The separation distance (or error distance) is a measure of the model accuracy often used in studies that assess the performance of particle-tracking models (e.g., Kaplan et al. 2005; Liu & Weisberg 2011). The separation distance is the distance between simulated and observed positions at each timestep along the trajectories:

$$D(t)=\sqrt{\left(x_p(t)-x_o(t)\right)^2+\left(y_p(t)-y_o(t)\right)^2}$$

where (x, y) are the geographic coordinates at time t and the indices o and p refer to the observed dFADs and simulated particles, respectively. We calculated the mean separation distances over all dFADs in each Ocean.

Skill score

The skill score (ss) is another index used to assess the accuracy of Lagrangian models (e.g., Liu & Weisberg 2011; Amemou et al. 2020) that is based on separation distances normalized by the net displacement of the object:

$$ss(t) = 1 - D(t)/D_o(t)$$

Where $D(t)$ is the separation distance described in the previous section, and $D_o(t)$ is the length of the observed trajectory measured along a straight line between the initial position and the position at time t, also called the observed absolute dispersion (Taylor 1921). The skill score, *ss*, is 0 or negative when the model is not efficient, and equals 1 for a perfect match between observed and simulated trajectories. We used the median of ss(t) values calculated over all considered dFADs, rather than the mean, because the mean was affected by extreme negative values corresponding to some rare cases when the observed trajectories lengths were very close to 0.

3. Results

We plotted an illustrative example of an observed dFAD trajectory and its corresponding simulated trajectories produced with the three forcing products (Fig. 4.1). The dFAD n° 25809 was deployed on May 21st 2015 in the Indian Ocean at (5.5°S , 59.38°E) and drifted more than 400 days. The corresponding simulated trajectory obtained with GLO was overall quite similar to the true trajectory, with first an eastward drift up to 85-90°E, then a long westward drift up to the North of Madagascar, and eventually drifting northwards along the eastern African coast. By contrast, the trajectories obtained with OSC and GEK compared less well to the observation as they diverged quickly to the South. In this example, GLO performed better than OSC and GEK (Fig. 4.1b), but this was not necessarily the case for simulations of other dFAD trajectories and there was no clear, consistent ranking of the relative performances of the different products when individual trajectories were examined.

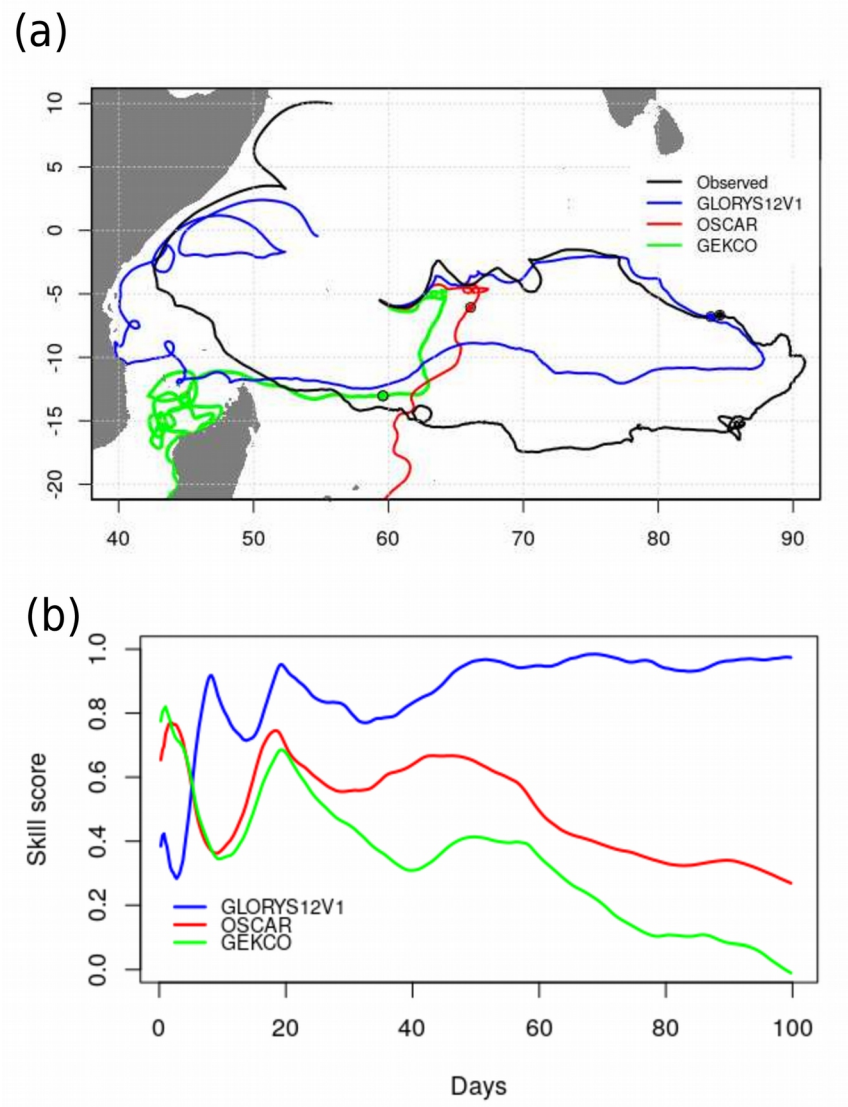

F*igure 4.1: (a) Example of an observed trajectory of dFAD (black) n° 25809 that was deployed on May 21st 2015 and drifted more than 400 days, and its corresponding simulated trajectories obtained with the Ichthyop Lagrangian model forced by GLORYS12V1-0m (blue), OSCAR (red) and GEKCO (green) currents. Black circles show the positions after 100 days of drift, the time period suggested for the trajectory comparisons in this study. (b) Skill scores corresponding to the simulated trajectories with the three forcing products over 100 days of drift.*

To get a global view of the differences between observed and simulated dFAD trajectories in the whole domain study, we plotted density maps (Fig. 4.2, Supplementary Fig . D1.1). Simulations produced overall similar patterns as observations with most of dFADs being concentrated in the western Indian Ocean and eastern Atlantic Ocean (Fig. 4.2). In both Oceans, a more realistic spatial distribution of dFADs was produced by GLO (Fig. 4.2b,f). For example, in the Indian Ocean, few particles simulated with OSC and GEK (Fig. 4.2g,h) reached the eastern side of the basin compared

to the observations (Fig. 4.2e). In addition, simulations with OSC tended to underestimate the density of dFADs in the northern part of the Indian Ocean and along the East African coast, whereas simulations with GEK tended to overestimate the density in the southern part of the Indian Ocean. In the Atlantic Ocean, simulations with GEK (Fig. 4.2d), particularly, but also OSC (Fig. 4.2c), showed hotspots of dFAD concentration that were not consistent with the observations (e.g., in the Gulf of Guinea, Fig. 4.2a).

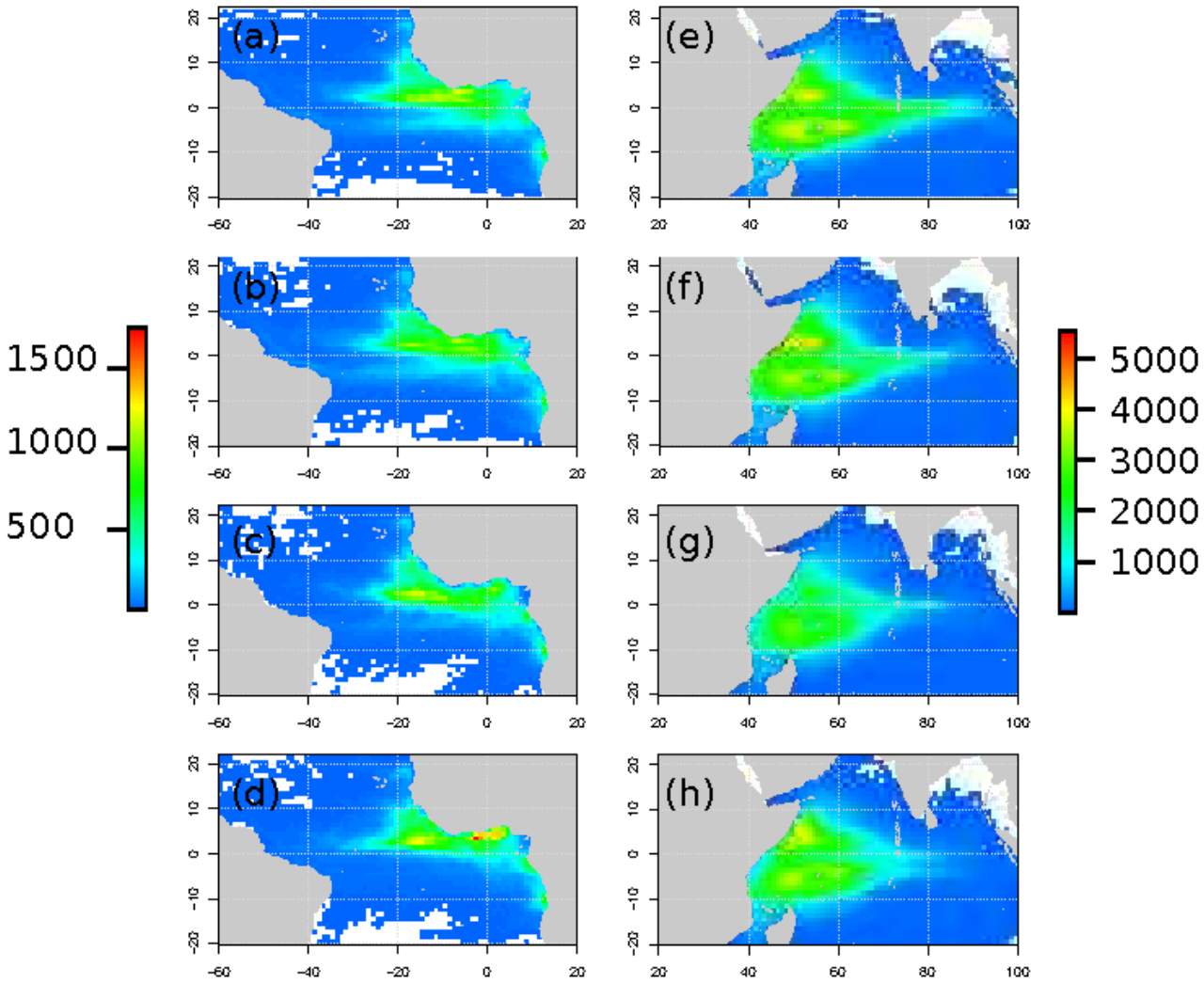

Figure 4.2: Densities of (a-e) observed dFADs and simulated particles using the Ichthyop Lagrangian model forced by (b-f) GLORYS12V1- 0m, (c-g) OSCAR and (d-h) GEKCO currents, computed as the total number of times dFADs or simulated particles were located in each of 1°x1° grid cells in the (left) Atlantic Ocean and (right) Indian Ocean, over the period 2010-2018.

Separation distances (i.e., error distances) between observations and simulations increased quickly with time, eventually reaching ~ 1000 km in 100 days. Error rates were quite similar for the three forcing products, with slightly larger errors obtained in the Indian Ocean than in the Atlantic Ocean, and generally the lowest separation distances being for the GLO simulations (Fig. 4.3). For the GLO simulations, timescales to reach a mean separation distance of 111 km (i.e., 1º of latitude, a typical spatial scale for statistical data for tropical tuna fisheries) were 8 days in the Atlantic Ocean and 6.5 days in the Indian Ocean, whereas to reach a mean separation of 370 km (i.e., 200 nm, the typical size of an EEZ) were 30 days in the Atlantic Ocean and 25.5 days in the Indian Ocean (Fig. 4.3). In the Indian Ocean, separation distances were significantly lower than observed traveled distances, whereas separation and observed travel distances were of similar orders of magnitude in the Atlantic Ocean (Supplementary Fig. D1.2).

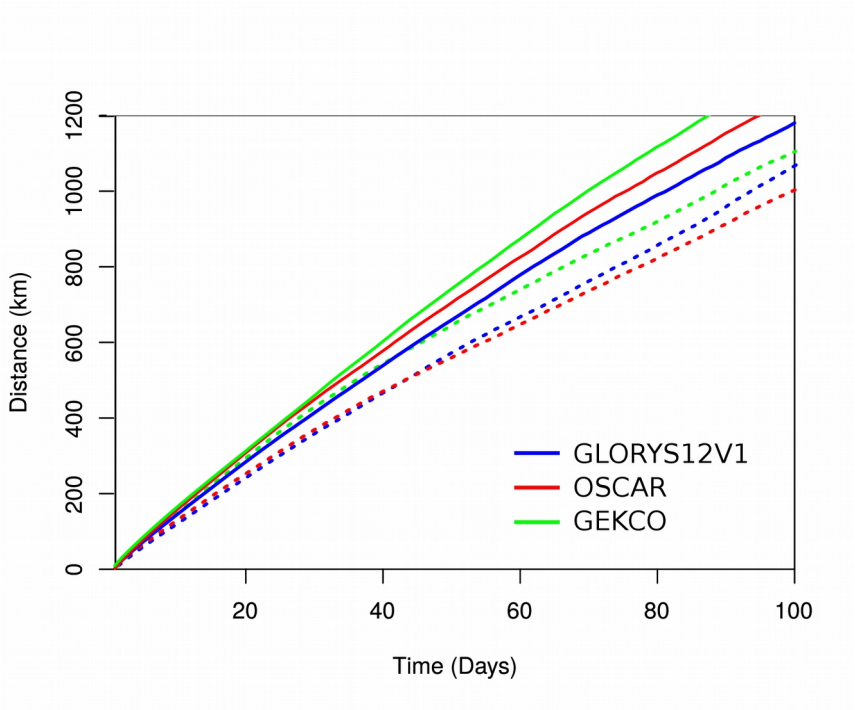

F*igure 4.3: Mean separation distance over time obtained between observed and simulated dFADsin the (solid lined) Indian and (dotted lines) Atlantic Oceans using (blue) GLORYS12V1-0m, (red) OSCAR and (green) GEKCO. Shaded regions were added in a separate figure (Supplementary Fig. D1.2) showing the 1st quartile and 3rd quartile to indicate the dispersion around the mean.*

When the error distances were normalized by the observed traveled distances (skill scores), then differences between forcing products and oceans became more apparent. First, for all forcing products and all depth levels for GLO, skill scores increased sharply in the first days and then dropped slowly over time (Figs. 4.4 and 4.5). Also, for all forcing products and all depth levels for

GLO, considerably higher skill scores were obtained in the Indian Ocean than in the Atlantic Ocean (Figs. 4.4 and 4.5). In both oceans, GLO had the highest skill scores (Fig. 4.5). In the Indian Ocean, the skill obtained with GLO 0 m was the highest compared to that for other depth levels (Fig. 4.4a), whereas in the Atlantic Ocean the highest skill score was obtained for GLO 5 m (Fig. 4.4b). Including windage improved the results spectacularly in some cases (Fig. 4.6), but it was detrimental on average (Fig. 4.7, Supplementary Fig. D1.3).

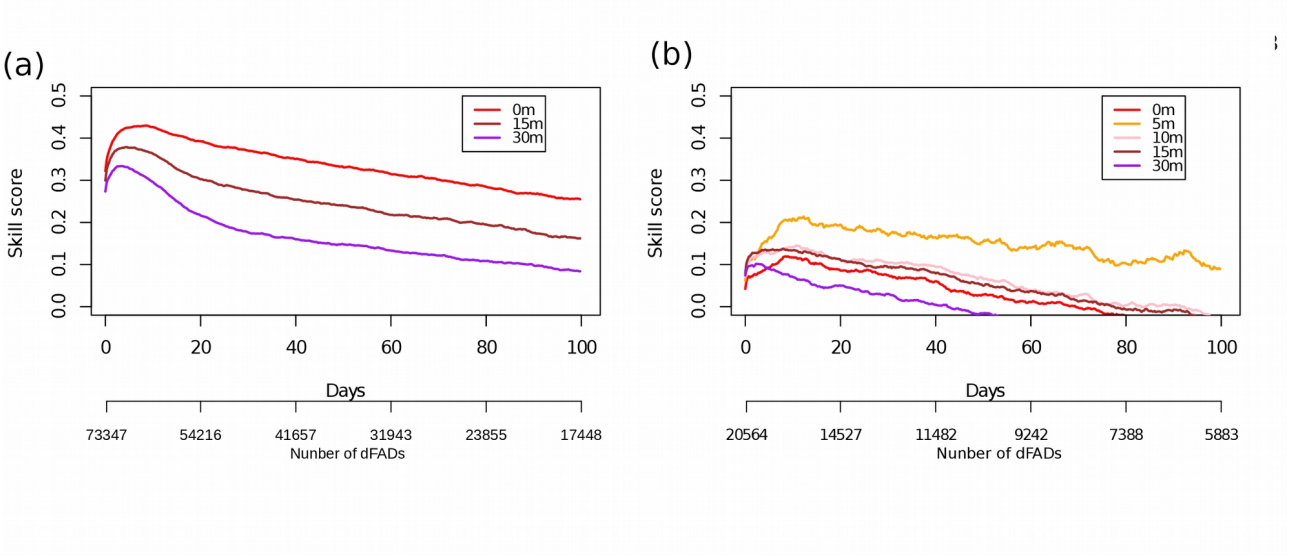

F*igure 4.4: Median skill score obtained over time with GLORYS12V1 for different depth levels (red) 0 m, (orange) 5 m,(pink) 10 m, (brown) 15 m, and (purple) 30 m in (a) the Indian and (b) Atlantic Oceans. The number of dFADs used in the median calculation is indicated in the lowest x-bar. Note than more depth values were used in (b) than in (a) for which the trend was clearer.*

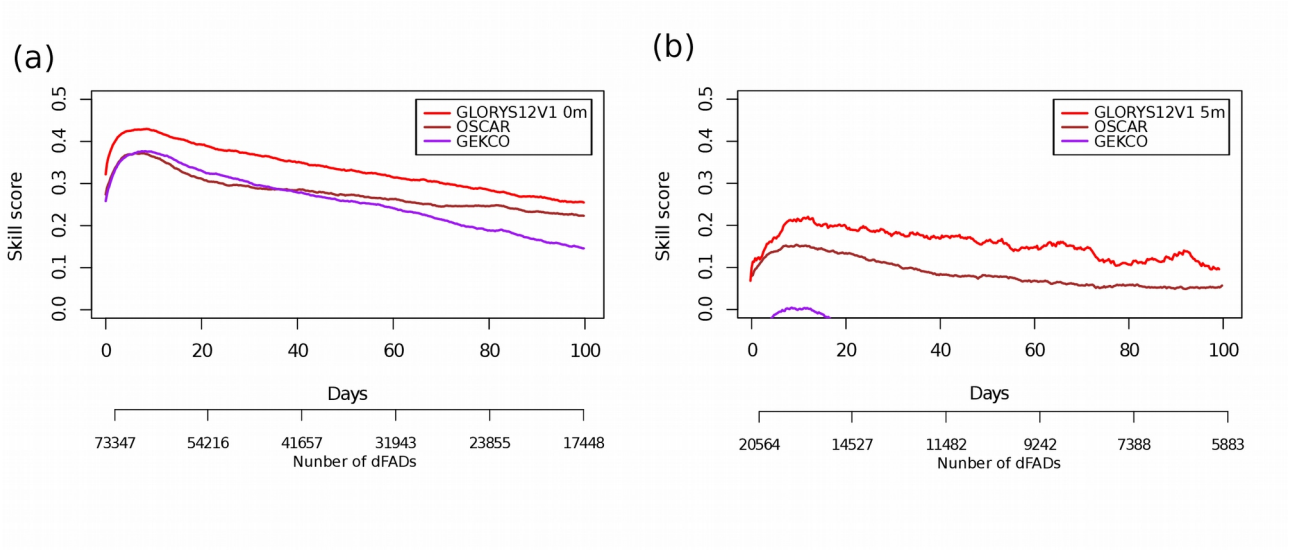

F*igure 4.5: Median skill score obtained over time with (red) GLORYS12V1, (brown) OSCAR and (purple) GEKCO in (a) the Indian and (b) Atlantic Oceans. Only the highest skill score curve obtained for GLORYS12V1 is represented (i.e. 0 m for the Indian Ocean and 5 m for the Atlantic Ocean, see Fig. 4.4). The number of dFADs used in the median calculation is indicated in the lowest x-bar.*

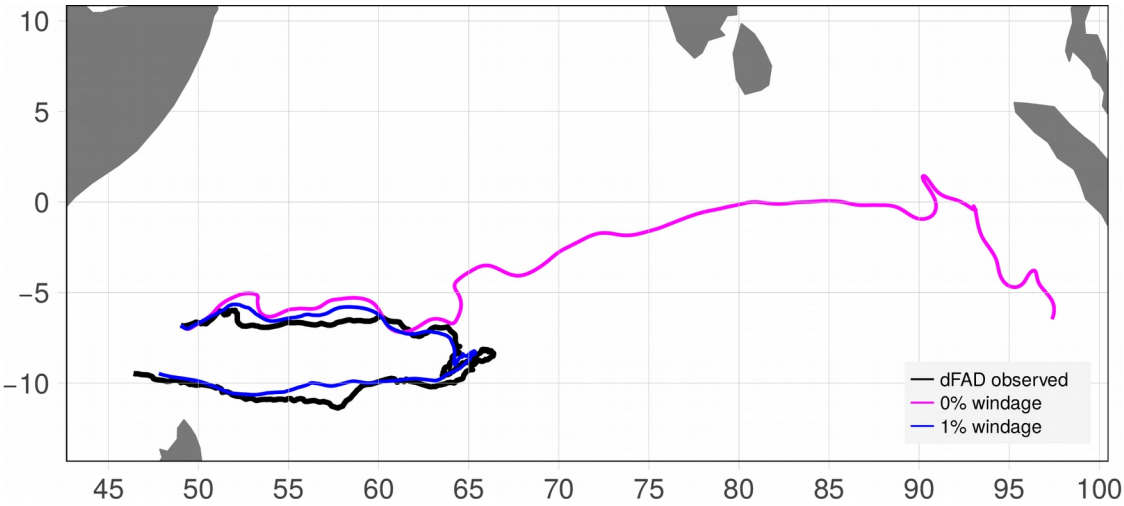

F*igure 4.6: Example of an observed trajectory of dFAD (black) n° 32357 that was deployed on December 14st 2015 and drifted more than 250 days, and its corresponding simulated trajectories obtained with the Ichthyop Lagrangian model forced by OSCAR including (pink) 0% and (blue) 1% of windage.*

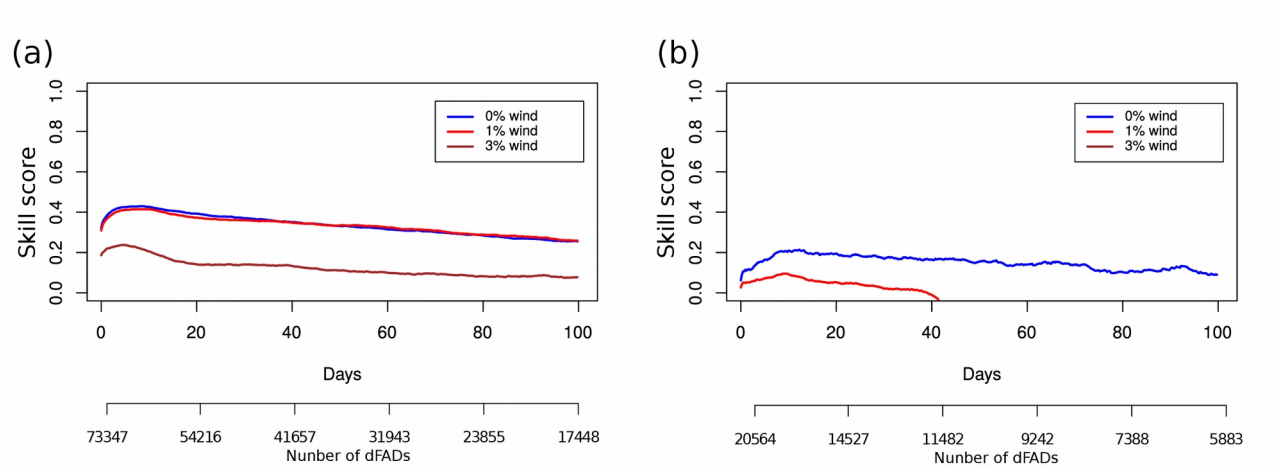

F*igure 4.7: Median skill score obtained with GLORYS12V1 including different values of windage factor (blue) 0%, (red) 1% and (brown) 3% in (a) the Indian and (b) Atlantic Oceans. Skill score obtained with 3% of windage in the Atlantic Ocean is negative indicating that the model is not efficient and therefore do not appear in the figure. The number of dFADs used in the median calculation is indicated in the lowest x-bar. The highest skill score GLORYS12V1 simulation was used (i.e. 0 m for the Indian Ocean and 5 m for the Atlantic Ocean, see Fig. 4.4).*

4. Discussion

We assessed the accuracy of a Lagrangian model, Ichthyop, forced with three different ocean currents products, GLORYS12V1, OSCAR and GEKCO, to simulate the trajectories of drifting fish aggregating devices (dFADs). We simulated > 100,000 dFAD trajectories in the Indian and Atlantic Oceans over the period 2010-2018, and compared all simulations to their corresponding observations. Simulations based on all three forcing fields were able to reproduce the large-scale spatial distribution of dFADs, though model performance was slightly higher with GLORYS12V1 that with the other two products. Amemou et al. (2020) also found good agreement between simulated and observed dFAD spatial distributions in the Atlantic Ocean over the period 2010-2014 using OSCAR and two other forcing fields that were not suitable for our study, the satellite-derived product GlobCurrent and outputs from a regional hydrodynamic model, CROCO. We also assessed model performance by calculating separation distances and skill scores. Simulations based on GLORYS12V1 had higher accuracy than those based on OSCAR and GEKCO. This may be due to the higher spatio-temporal resolutions of GLORYS12V1. Amemou et al. (2020) also found that CROCO model outputs performed better than the satellite-derived ocean current products, at least over the domain covered by a high-resolution zoom in the Gulf of Guinea.

We found notable differences between the Indian and Atlantic Oceans. Though separation distances were somewhat higher for the Indian Ocean (exceeding 100 km after 6 days) than for the Atlantic Ocean (100 km after 7.5 days), the performance of the model in terms of skill score was remarkably better in the Indian Ocean (skill scores in the range 0.3-0.4) than in the Atlantic Ocean (skill scores < 0.2), due to the higher transport rates in the former than in the latter. Comparisons of model performances forced with GLORYS12V1 at multiple depths showed that the skill score was highest at 0 m in the Indian Ocean, but at 5 m in the Atlantic Ocean. This difference may be related to the subsurface structure of dFADs. dFADs deployed in both oceans have subsurface ropes or rolled pieces of nets used by fishers to alter the tuna species composition (Lennert-Cody et al. 2008), the arrival of fish on the dFAD (Orúe et al. 2017) and to increase the attraction of tunas by anchoring the dFAD in slower subsurface currents and thereby lowering the drift speed of the dFAD (Franco et al. 2009). These dFADs hanging nets go down to 80 m below the surface in the Atlantic Ocean, more than in others oceans (e.g., typical lengths in the Indian Ocean are 50 m).

We examined whether the accuracy of the model was improved by including a windage component in simulations. Although windage appears to improve predictions of transport for other objects drifting in the upper layer of the ocean surface (Trinanes et al. 2016; Santos et al. 2018a; Putman et al. 2020), our results showed that adding a windage factor of 1%, 2% and 5% did not. We assume that this result is also due to the effect of the considerable vertical structures of dFADs, which is relatively large and heavy compared to the more limited surface exposure of dFADs. This result is consistent with previous works indicating that dFADs drift like oceanographic drogued drifters (Imzilen et al. 2019), as drogued drifters were also found to be unaffected by the windage component (Putman et al. 2020). Another physical process affecting surface particles movement is the wave-induced Stokes drift (Fraser et al. 2018; Villas Bôas et al. 2019; Dobler et al. 2019). Previous studies showed that Stokes drift influences the movement of undrogued drifters transported by ocean currents in the uppermost surface layer (Maximenko et al. 2012; Mheen et al. 2019). However, drogued drifters are transported by ocean currents at a nominal 15-m depth (Niiler et al. 1995) and are therefore less influenced by Stokes drift (Mheen et al. 2019). The impact of Stokes drift on dFAD trajectories was not directly assessed in this study, but given their considerable subsurface structure and transport patterns that closely resemble those of drogued drifters (Imzilen et al. 2019), we hypothesize that the effect will be minor.

Although the skill scores obtained in this study were not very high, they are consistent with the range of values reported in previous work on oceanographic drifters (De Dominicis et al. 2016; Amemou et al. 2020). Nevertheless, these values remain far below the normalized separations (an index equivalent to the skill score) calculated from observed pairs of dFADs opportunistically found to be close in space and time (0.6-0.8 in the Indian Ocean, 0.4-0.6 in the Atlantic Ocean, Appendix Figs. D2.1 and D2.2). Though it is unrealistic to expect that simulated trajectories will have the same accuracy as real close-by paired objects, our results indicated that using high-resolution, data-assimilating hydrodynamic models is likely the best avenue for improving model-data comparisons. Using online Lagrangian models run within hydrodynamic models, as opposed to offline tools such as Ichthyop, may also improve accuracy given that online models have access to the higher internal timestep of hydrodynamic models.

Given the large scale agreement of simulated and observed dFAD spatial distributions, simulated dFAD trajectories could be used as a complementary tool to the implementation of limits on dFAD numbers (ICCAT 2019; IOTC 2019a),spatial closures to reduce beaching of dFADs (Imzilen et al. 2021) and recovery programs to prevent dFAD loss (Zudaire et al. 2018; Imzilen et al,. Subm.) for anticipating the passage of dFADs through sensitive habitat areas, such as biologically diverse and fragile island archipelagos possessing coral reefs and marine protected areas (Curnick et al. 2021). At smaller scales of individual trajectories, our results indicate that existing models have the capacity to accurately predict the 1ºx1º cell (a typical statistical unit for management of tropical tuna purse-seine fisheries) for ~6.5-8 days and can determine the EEZ of a dFAD for ~25.5-30 days. While the prior may be too short for many management purposes, it could still be useful for directing dFADs over short time scales if motorized dFADs with directional capabilities become available and data-assimilating predictive ocean circulation models can be put in place. Furthermore, 30 days is on the order of typical soak times for dFADs (Maufroy et al. 2015) and therefore could be useful for assigning dFADs to larger spatial regions, for example for understanding regional spatial distributions of dFADs whose tracking buoys have been remotely turned off, examining impacts of dFADs on spatial closures and moratoria, and eventually predicting fishing activities in the EEZs of specific nations. It is our hope that the results in this manuscript can be leveraged to aide these management objectives and improve future predictive models of dFAD trajectories.

Appendix D1: Supplementary figures

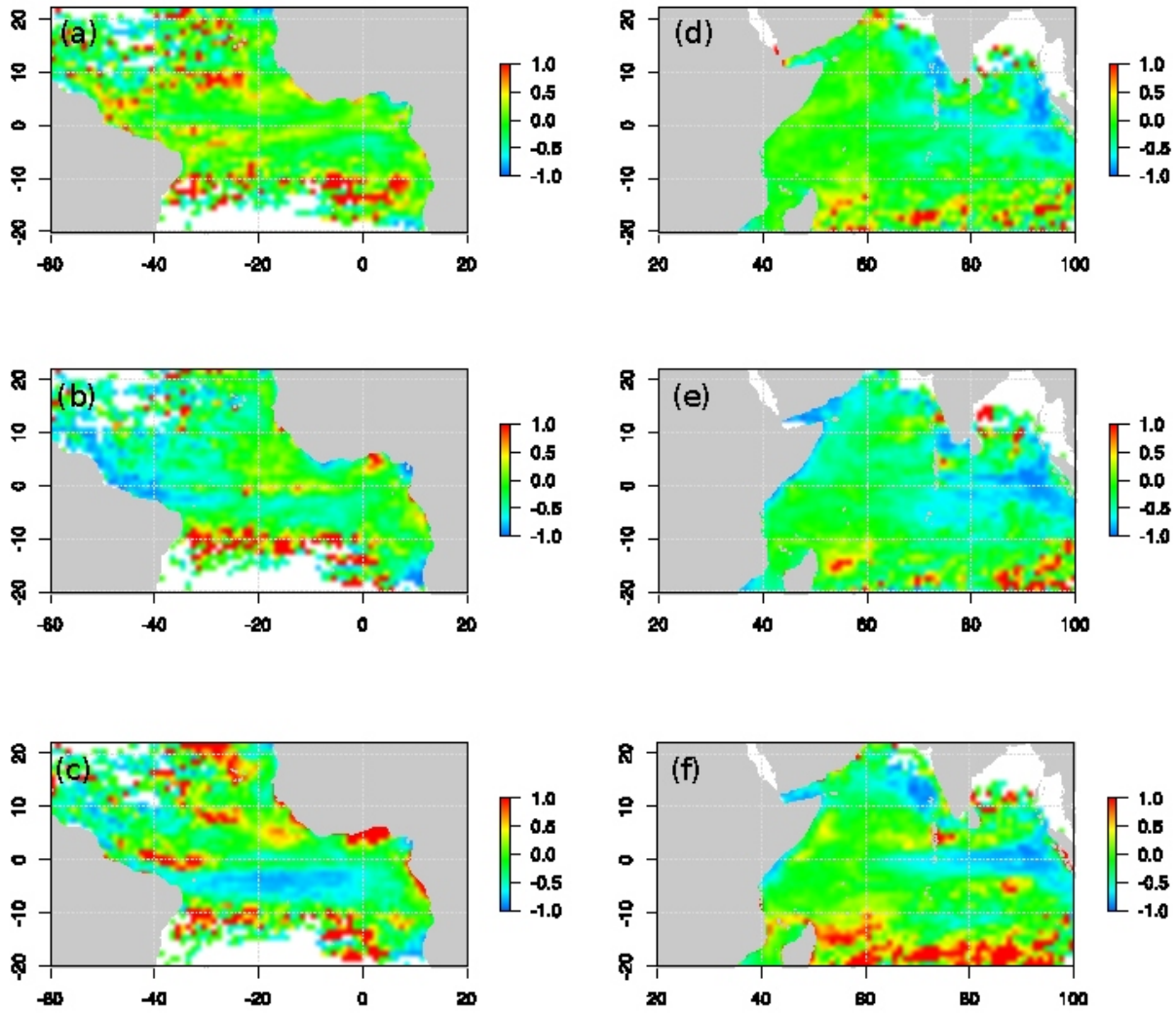

Figure D1.1: Maps of normalized density difference ((Dsimul – Dobs)/ Dobs) using the Ichthyop Lagrangian model forced by (a-d) GLORYS12V1- 0m, (b-e) OSCAR and (c-f) GEKCO currents, in (left) the Atlantic Ocean and (right) the Indian Ocean, over the period 2010-2018.

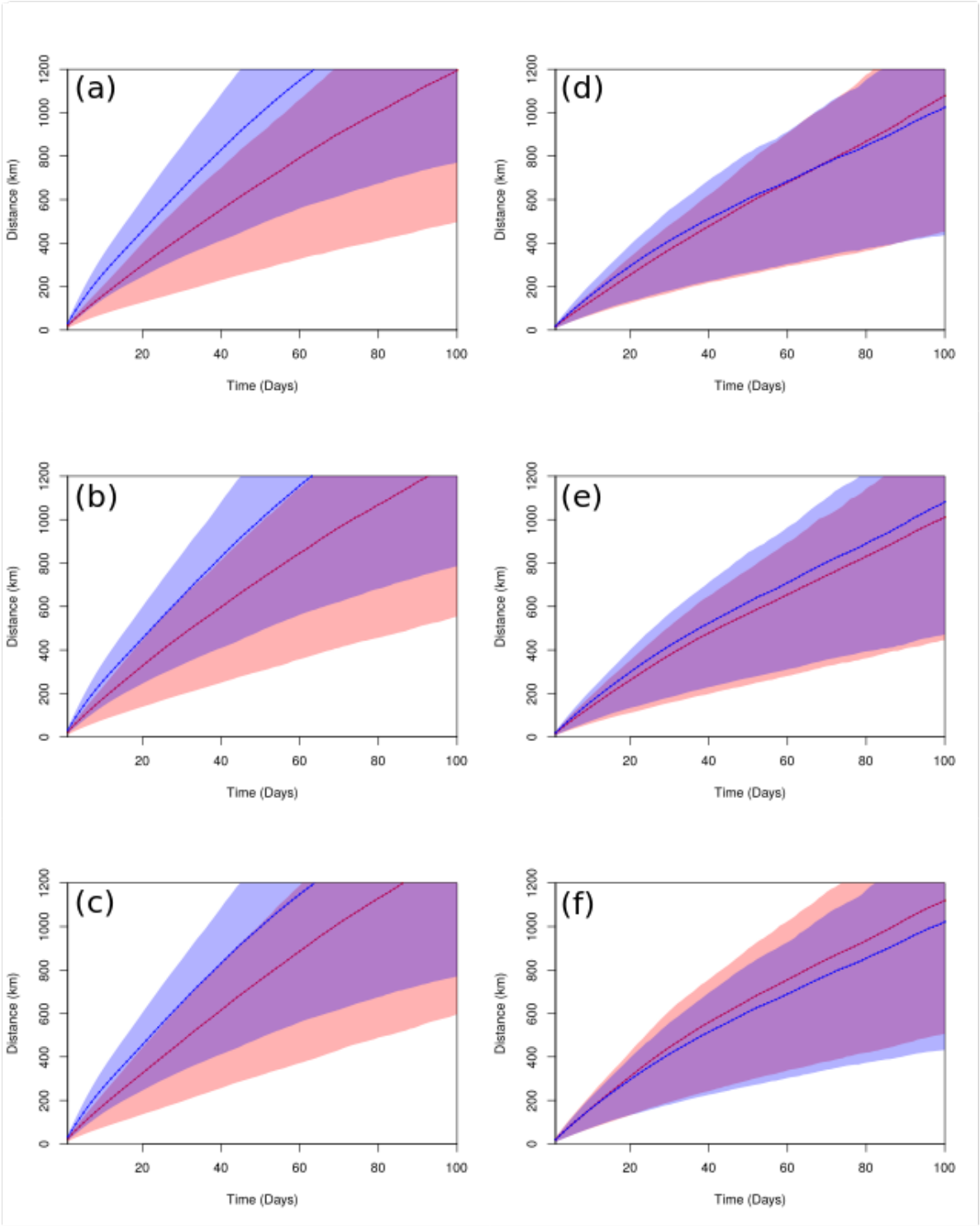

Figure D1.2: Mean separation distance over time obtained between observed and simulated dFADs in (a-b-c) the Indian and (e-f-g) Atlantic Oceans. The red lines indicate the mean separation distance with observed dFADs and simulated particles with (a-d) GLORYS12V1-0m , (b-e) OSCAR and (c-f) GEKCO. The blue lines indicate the mean distance traveled by the observed dFADs. The shaded regions around the central lines show the 1st quartile and 3rd quartile to indicate the dispersion around the mean.

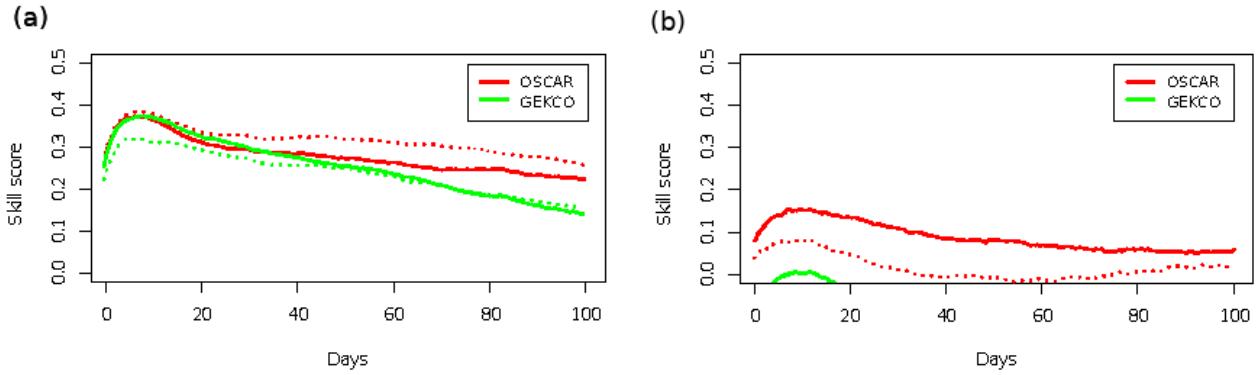

Figure D1.3: Median skill score obtained with (red) OSCAR and (green) GEKCO in (a) the Indian and (b) Atlantic Oceans(solid lines) without windage and (dotted lines) with 1% of windage. Negative values indicate that the model is not efficient and therefore do not appear in the figure.

Appendix D2 : Normalized separation for pairs of close dFADs

We identified pairs of dFADs found to be close in time and space (meeting points < 2 km and < 6 h)and found > 70,000 in the Indian Ocean and > 10,000 in the Atlantic ocean over the period 2010-2018. From the trajectories followed by the two dFADs of a pair from their meeting point, we calculated an index that we call ‘normalized separation’ , an equivalent to the skill score calculated from the simulations:

$$d(t)=\left\{1-\left(d_{separation}(t)/d_{traveled}(t)\right)\right\}$$

where d(t) represent the ‘normalized separation’, d_traveled(t) is the distance traveled from the meeting point by one (randomly chosen) of the two dFADs comprising the pair and d_(separation(t) is the distance between the two dFADs along the time after their meeting point.

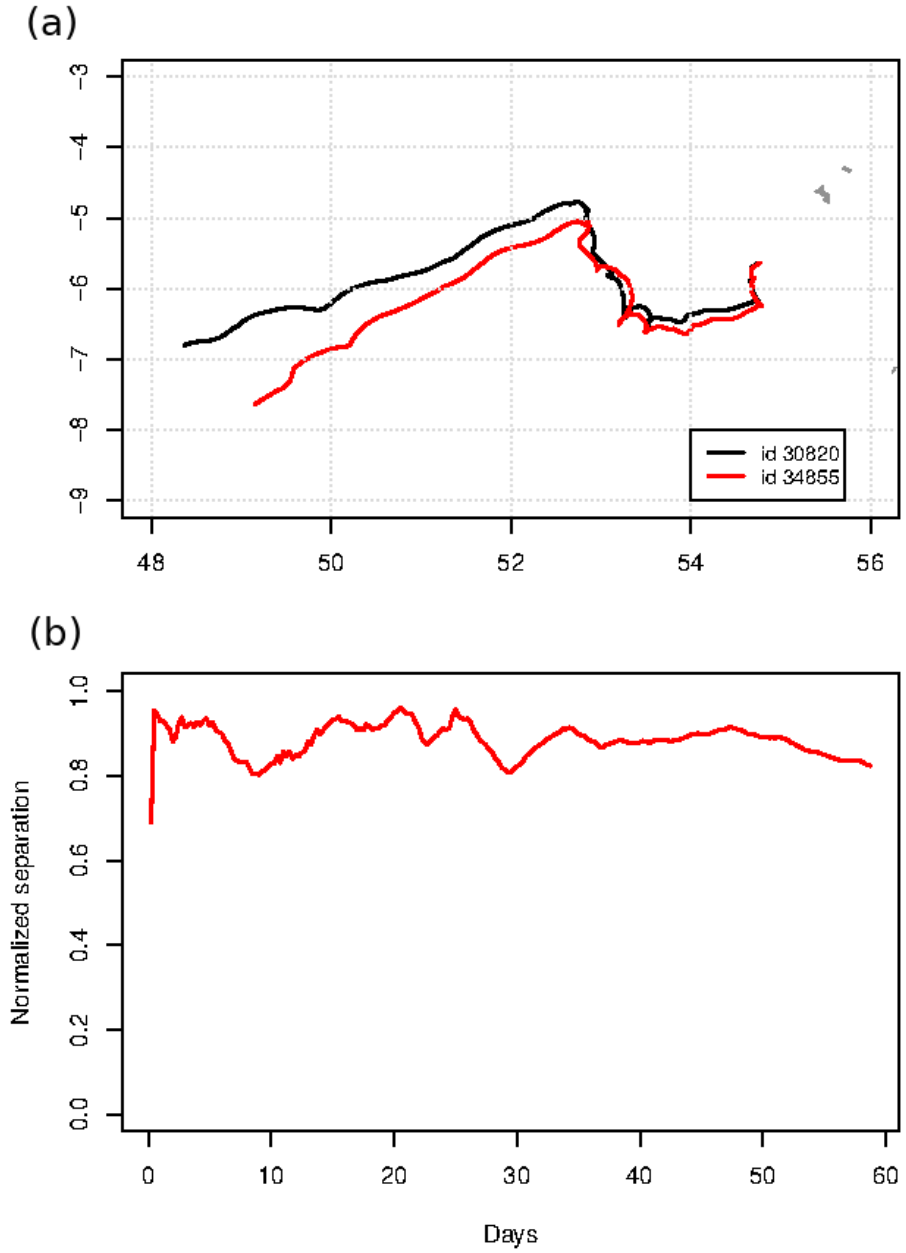

F*igure D2.1: Illustrative example of (a) the trajectories of a pair of dFADs found to be close in space and time (meeting points < 2 km and < 6 h) and its (b) corresponding normalized separation obtained over time. The dFADs met on July 26st 2011 and drifted closely during 60 days.*

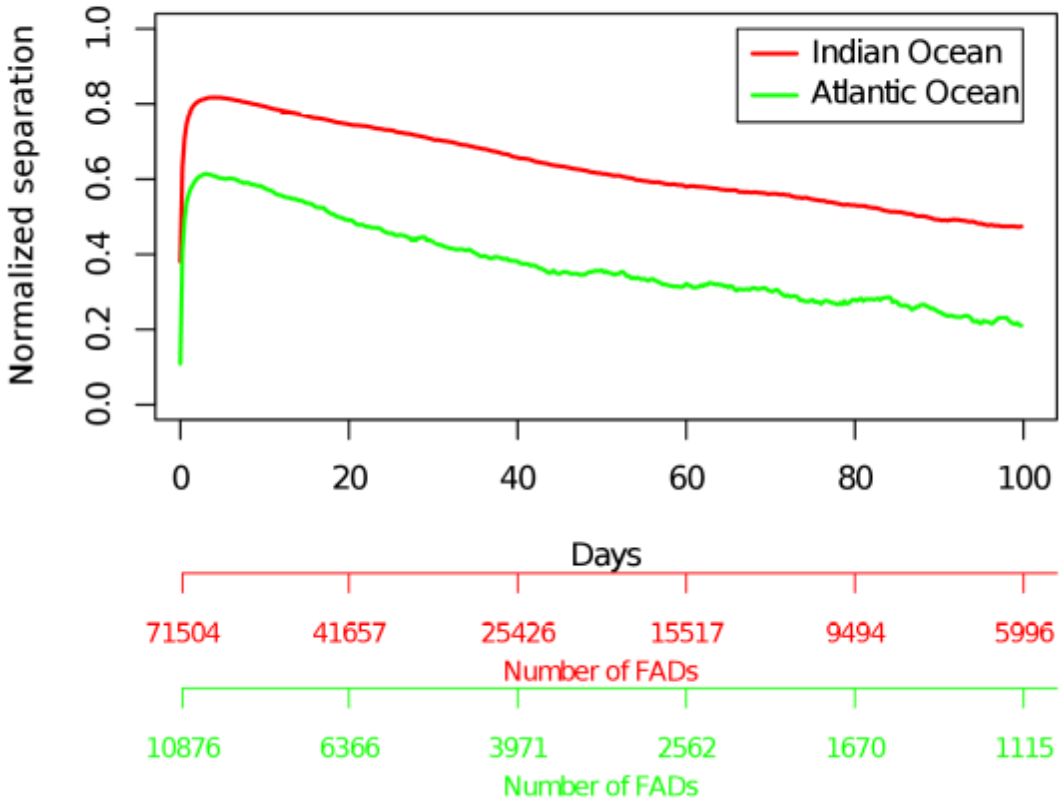

Figure D2.2: Median 'normalized separation' obtained over time for pairs of close dFAD trajectories observed in (red) the Indian Ocean and (green)the Atlantic Ocean over the period 2010-2018. The number of dFAD pairs used in the median calculation is indicated in the lowest x-bar.

Discussion générale

Les engins et dispositifs de pêche perdus, abandonnés ou rejetés en mer causent d'importants problèmes écologiques. Les dispositifs de Concentration de Poissons dérivants (DCP) utilisés dans les pêcheries thonières tropicales à la senne coulissante contribuent à ces problèmes. Ces dispositifs massivement déployés au cours de la dernière décennie ont augmenté l'efficacité de pêche des thoniers senneurs tropicaux.. Cependant, leur utilisation est associée à un certain nombre d'impacts négatifs, en particulier les événements de perte et d'échouage de DCP qui contribuent aux débris marins et représentent une menace pour les habitats fragiles tels que les récifs coralliens (Filmalter et al. 2013; Balderson & Martin 2015; Maufroy et al. 2015). Les Organisations Régionales de Gestion de la Pêche (ORGP) responsables de la gestion des stocks de thons tropicaux ont pris des mesures visant à réduire les impacts négatifs des DCP. Cependant, ces restrictions et incitations restent insuffisantes, en particulier pour les échouages et la perte des DCP. Ce travail de thèse a eu pour but d'explorer la possibilité de mettre en place trois mesures différentes de mitigation afin de permettre respectivement d'éviter, d'empêcher et d'anticiper la perte et l'échouage des DCP déployés par les flottilles françaises opérant dans l'Océan Atlantique et Indien.

Nous avons d'abord développé une méthode qui a permis d'estimer les taux d'échouages sur la période 2008-2017 (Chapitre 1). Les résultats ont montré que le nombre de DCP déployés dans les deux océans a considérablement augmenté au cours de la période d'étude, ce qui indique que la tendance observée précédemment (Maufroy et al. 2015; Floch et al. 2017, 2019) se poursuit. Le taux d'échouage a également augmenté significativement sur la période 2008-2013 avant de se stabiliser sur la période 2014-2017. Plusieurs hypothèses permettent d'expliquer cette augmentation, comme la contribution prédominante de la pêche sous DCP par rapport à la pêche sous bancs libres (Assan et al. 2019; Floch et al. 2019) et l'intégration des bouées échosondeurs (2010-2012) qui a permis d'augmenter l'efficacité de ce mode de pêche. Ces évolutions ont engendré un changement dans le comportement des pêcheurs, avec des déploiements plus importants de DCP, sans toutefois prévoir les mécanismes pour leur récupération en fin d'utilisation. La période de la piraterie au large de la Somalie (aux alentours des années 2007-2011) a eu également un effet néfaste suite à l'abandon des DCP qui entrent dans cette région et ce d'autant plus que cette région selon nos résultats est dans une zone à haut risque d'échouage. La période 2014-2017 coïncide avec plusieurs changements dans la pêcherie et il est donc difficile d'attribuer une cause spécifique à cette stagnation. La stabilisation du taux d'échouage à cette période est probablement partiellement liée à la mise en place de la limitation par les ORGP du nombre de bouées opérationelles par senneur (ICCAT 2019; IOTC 2019), poussant ainsi les pêcheurs à

désactiver à distance les DCP non productifs pour ne pas dépasser la limite imposée, cette désactivation entraîne une sous-estimation des taux d'échouage engendrée par la perte d'informations sur l'emplacement de ces DCP qui continuent de dériver en mer et qui peuvent plus tard s'échouer. Le changement dans la structure des DCP et le changements des distributions spatiales des déploiements des DCP peuvent également avoir un effet et contribuer à cette stabilisation.

Les estimations des taux d'échouage des DCP obtenues dans ce travail sont relativement similaire à celles estimées précédemment dans l'Océan Indien et Atlantique sur la période antérieur à 2011 (Maufroy et al. 2015). Cependant, ces estimation sont plus élevées que celles estimées pour des années plus récentes dans l'Océan Indien (Zudaire et al. 2018) et dans l'Océan Pacifique occidental et central (Escalle et al. 2019). En revanche, dans l'océan Indien, Zudaire et al. (2018) ont étudié principalement une petite région de l'archipel des Seychelles, qui est composée d'un grand ensemble de petites îles, expliquant peut-être des taux d'échouage plus faibles par rapport aux masses continentales bordant les Océans Indien et Atlantique que nous avons considérées. Escalle et al. (2019) ont examiné une zone du Pacifique qui est aussi caractérisée par de nombreuses petites chaînes d'îles, comme pour Zudaire et al. (2018). Par ailleurs ces études utilisaient des méthodologies un peu plus restrictives que la notre pour définir un échouage. Ces différences se figurent principalement du fait que Zudaire et al. (2018) considèrent un échouage quand la position d'un DCP intersecte la surface de la terre, Maufroy et al (2015) et Escalle et al (2019) considèrent un échouage quand un DCP s'arrête de bouger complètement (position du DCP qui se répète trois fois), tandis que dans notre étude on considère un échouage lorsque un DCP s'arrête complètement de bouger où légèrement dans un rayon qui ne dépasse pas 200m.

Nous avons ensuite évalué l'efficacité potentielle de la mise en place d'une mesure de atténuation pour éviter des échouages qui consisterait à interdire, ou grandement limiter, le déploiement des DCP dans certaines zones identifiées comme à risque car liées à un taux d'échouage élevé quand les DCP y sont déployés (Chapitre 1). L'analyse des trajectoires des DCP a permis d'identifier ces zones ainsi que les types (échouage en mer ou sur terre, sur récifs coralliens), les périodes et les origines de ces échouages. Les résultats ont montré qu'il y aurait beaucoup d'échouages à éviter en mettant en place un programme d'interdiction des déploiements, par exemple entre 20% et 40% des échouages si les déploiements étaient interdits dans l'Océan Indien au Sud du parallèle 8°N, dans la zone somalienne en hiver, et dans la zone située à l'Ouest des Maldives en été, et au niveau de la zone intertropicale longeant la côte Ouest de l'Afrique pour

l'Océan Atlantique. Ce programme permettrait d'éviter un nombre considérable d'échouages des DCP et par conséquent de contribuer à la protection des zones côtière et des récifs coralliens. De plus, les zones à haut risque proposées à la fermeture sont relativement homogènes, ce qui faciliterait la mise en place et la gestion d'un tel programme. Enfin, ces zones de fermeture ne sont pas des zones de forte activité de déploiement de DCP ou d'activités de pêche (Maufroy et al. 2015), ce qui suggère que ce programme pourrait être mis en œuvre avec un impact relativement faible sur la productivité des pêcheries concernées, bien qu'une étude approfondie pour quantifier cet impact sera nécessaire. Cependant, nos résultats suggèrent que certaines régions, en particulier le Nord-Ouest de l'Océan Indien et le Nord du Golfe de Guinée, qui représentent de grandes zones d'échouage, seraient moins protégées par cette mesure. Dans ces zones, les taux élevés de récupération des bouées de DCP par ce qui semble être des petits pêcheurs suggèrent que des systèmes d'alerte d'échouage et des programmes de récupération des DCP en mer pourraient être des mesures plus efficaces à mettre en place.

La mise en place potentielle d'un programme de récupération des DCP en mer est précisément l'aspect que nous avons abordé dans le Chapitre 2. Un tel programme (FAD Watch; Zudaire et al. 2018) a été déjà mis en œuvre en 2016 à petite échelle pour empêcher les échouages dans quelques îles de l'archipel des Seychelles. Ce programme a permis de collecter au total 109 DCP risquant l'échouage sur la période 2016-2017. Ici nous avons étudié la possibilité de mettre en œuvre un programme de récupération des DCP à l'échelle des bassins océaniques. Les résultats ont montré que plus de 40% des trajectoires des DCP dérivent loin des zones de pêche et finissent perdus au milieu de l'Océan ou échoués dans des zones côtières. Les premieres analyses ont permis d'identifier des zones où un grand nombre de DCP dérivaient loin des zones de pêche vers le large où un programme de récupération en mer serait approprié. Dans l'Océan Indien, les DCP quittant la zone de pêche par l'est finissent par échouer ou transiter par les Maldives et dériver vers l'est de l'Océan. Cela se produit plus fréquemment du mois d'octobre à décembre ce qui est cohérent avec le Contre Courant Équatorial Sud qui s'écoule vers l'est pendant cette période (Schott et al. 2009), mais aussi à la transition des activités de pêche vers le sud (qui commence au mois de novembre) qui ciblent plus des thons en bancs libres contribuant probablement à plus d'abandon des DCP dans le nord à cette période (Kaplan et al. 2014; Maufroy et al. 2017). Dans l'Océan Atlantique, les DCP perdus en haute mer quittent principalement du nord-ouest (entre 10°-20°N) et du sud-ouest (2°-5°S) de la zone de pêche, ce qui est cohérent avec les directions de transport dominantes du Courant Équatorial Nord et du Courant Équatorial Sud. La saisonnalité dans la perte des DCP est moins

marquée dans l'océan Atlantique bien que les mois de juillet et décembre marquent une légère augmentation qui pourrait être liée aux transitions dans la distribution spatio-temporelle des déploiements, passant principalement du déploiement au nord de la zone à une concentration vers l'est du Golfe de Guinée (Maufroy et al. 2017). Ces transitions pourraient conduire à une augmentation de perte et d'abandon des DCP dans des zones favorables à l'export en dehors de la zone de pêche, comme supposé pour l'océan Indien. Nous avons également trouvé que 20% de ces DCP passent relativement proches (< 50 km) d'un port et donc la mise en place de programmes de récupération depuis ces ports pourrait être efficace pour réduire la perte et l'échouage des DCP. En outre, nous avons montré que les zones moins protégées par la première mesure de mitigation proposée dans ce travail (Chapitre 1) bénéficieraient bien de cette deuxième mesure (Chapitre 2), montrant que la mise en place d'un programme de récupération des DCP en mer pourrait être une mesure efficace et complémentaire à la fermeture de zones aux déploiements.

Les deux premières mesures proposées pour diminuer la perte et l'échouage des DCP (Chapitre 1 et Chapitre 2) sont globales et traitent le problème à l'échelle des bassins océaniques. Les résultats que nous avons obtenus permettent d'estimer qu'un DCP passant dans telle zone à telle saison a statistiquement telle probabilité d'être perdu ou de s'échouer, mais ils ne fournissent pas d'information qui pourrait permettre d'estimer en temps réel cette probabilité pour un DCP donné selon sa localisation. Il nous a donc paru nécessaire d'évaluer la possibilité de compléter les mesures proposées précédemment par des outils permettant de prédire avec précision les trajectoires des DCP individuellement. Pour cela il a fallu d'abord répondre à la question de savoir si les DCP suivent plus ou moins les courants océaniques de surface. Pour cela nous avons comparé les composantes de vitesse des DCP de notre jeu de données avec celles de drifters utilisés en océanographie conçus pour suivre les courants de la couche de surface (Chapitre 3). Les résultats ont montré que les DCP dérivent de la manière similaire aux drifters, mais nous avons noté néanmoins que les DCP dérivaient un peu moins vite, en particulier dans l'Océan Atlantique. Ce ralentissement est potentiellement du à la structure verticale des DCP qui contribue à les freiner et, qui est plus longue pour les DCP déployés dans l'Océan Atlantique (> 80 m) que dans l'Océan Indien (50-60 m) (Franco et al. 2009). La structuration verticale des courants pourrait aussi avoir un rôle dans ce ralentissement et dans la distinction entre Océans Indien et Atlantique, puisque dans la partie de l'Océan Indien dans laquelle se trouvent des DCP la structure verticale des courants est relativement homogène (Manyilizu et al. 2016; Gnanaseelan & Deshpande 2017) alors que dans l'Océan Atlantique un fort courant permanent vers l'est est situé juste en dessous du Courant

Équatorial Sud qui s'écoule vers l'Ouest (Johns et al. 2014). Cette étude a également révélé que la distribution spatiale des DCP est complémentaire à celle des drifters ce qui suggère que l'énorme volume de données collectées par les pêcheurs via les DCP pourrait contribuer aux observations océaniques par l'enrichissement des bases de données mondiales.

Après avoir montré que les DCP dérivants dérivent plus ou moins de manière similaire aux drifters utilisés en océanographie, l'utilisation d'un outil de transport Lagrangien pour simuler leurs trajectoires devenait envisageable. Dans cette dernière partie de ce travail de thèse (Chapitre 4), nous avons utilisé un outil Lagrangien Ichthyop forcé par trois produits de courants océaniques afin de comparer et d'évaluer la précision des trajectoires simulées. Les résultats ont montré que l'efficacité de cet outil pour représenter les densités des DCP à l'échelle du bassin est relativement bonne et similaire dans les deux océans. Cependant, la capacité de simuler les trajectoires des DCP individuellement est meilleure dans l'Océan Indien que dans l'Océan Atlantique. Nous avons également constaté que la précision des simulations est sensible à la résolution spatiale du produit de forçage en notant une meilleure précision pour les simulations forcées par le produit de plus haute résolution. Ce constat a été également fait par Amemou et al. (2020) qui ont utilisé le même outil Lagrangien forcé par d'autres produits de courants. La précision des simulations est également liée à la profondeur des courants utilisés pour le forçage. Dans le cas où l'effet de la profondeur pouvait être testé, les meilleurs résultats ont été obtenus en utilisant les courants de surface dans l'Océan Indien et les courants pour la profondeur 5 m dans l'Océan Atlantique. Cette différence est petite mais pourrait être aussi liée à la différence dans les longueurs de la structure verticale des DCP dans les deux océans, comme expliqué précédemment. L'effet du vent a également été examiné, mais les résultats ont montré que la prise en compte de l'effet direct du vent sur la dérive n'améliore pas la précision des simulations des trajectoires des DCP, contrairement à ce qui a été montré pour d'autres cas dans des études précédentes comme pour les drifters sans drogue, les tortues et les sargasses (Trinanes et al. 2016; Santos et al. 2018; Putman et al. 2020). Bien que les performances obtenues dans la simulation des trajectoires au niveau individuel ne sont pas très élevées, elles sont cohérentes avec les résultats rapportés dans des travaux antérieurs sur les drifters océanographiques (De Dominicis et al. 2016; Amemou et al. 2020). Finalement, compte tenu de la similarité des distributions spatiales des DCP simulées et observées à grande échelle, cet outil en mode opérationnel dans le futur pourrait être utilisé pour prédire les zones à grand risque de perte et d'échouage des DCP et donc être utilisé comme une mesure de mitigation complémentaire

optimisant l’efficacité de la fermeture des zones pour éviter l'échouage des DCP (Chapitre 1) et aux programmes de récupération pour empêcher la perte des DCP (Chapitre 2).

Les informations fournies dans ce manuscrit pourraient constituer une base solide pour définir de nouvelles recommandations permettant d’atténuer les risques de perte et d’échouage des DCP. Toutefois, il existe un certain nombre de défis importants en terme d'application et d’organisation pour la réalisation et le succès de ces programmes. Le programme de récupération en mer des DCP, en particulier, nécessite une réflexion approfondie autour de sa mise en œuvre. À ce jour, la plupart des efforts visant à réduire les débris marins se sont concentrés sur le nettoyage des plages (Schneider et al. 2018; Duan et al. 2020). De telles opérations sont coûteuses, prennent du temps et ne récupèrent qu'une fraction de l'ensemble des débris (Chen 2015; Burt et al. 2020). En combinant observations et modélisations de dérive, Sherman et van Sebille (2016) ont montré que des collecteurs placés à des endroits appropriés pouvaient réduire considérablement la masse de micro-plastiques flottants. Cependant, afin de collecter des débris de plus grande taille, tels que des DCP perdus, des navires de taille et d'équipement appropriés sont nécessaires, imposant un certain nombre de considérations et de compromis complexes. De manière générale, l'équipement requis pour les opérations de récupération (par exemple, la taille des bateaux), le type de programme de récupération (par exemple, la collaboration avec les pêcheurs locaux et senneurs et/ou les organisations non gouvernementales -ONG-, l'utilisation de navires de support et /ou l’affrètement de navires de récupération) et les solutions de financement (par exemple la réutilisation des bouées GPS récupérées et des flotteurs en plastique, et/ou le développement d’un système pollueur-payeur appliqué lors du déploiement ou de la fabrication des DCP) doivent être optimisés pour récupérer un maximum de DCP tout en minimisant les coûts et les impacts sur la pêcherie.

Outre les défis logistiques, certains obstacles aux programmes de récupération des DCP sont environnementaux, stratégiques ou géopolitiques. Par exemple, même si la côte somalienne est identifiée comme une zone à haut risque d'échouage des DCP en hiver (Chapitre 1) et a un potentiel pour le succès d’un programme de récupération des DCP depuis les ports de la région (Chapitre 2), la récupération des DCP le long de cette côte est moins prioritaire en raison de l’absence relative d'habitats sensibles, tels que les récifs coralliens, et particulièrement délicate à mettre en place du fait de la situation sociopolitique difficile et dangereuse du pays et de ses eaux adjacentes. D'un autre côté, l'archipel des Maldives est susceptible d'être une priorité étant donné qu'il s'agit d'une zone avec des taux d'échouage de DCP élevés dans les récifs coralliens (Chapitre 1) et également d’une zone où de nombreux DCP quittent les zones de pêche (Chapitre 2). La mise en œuvre d'un

programme de récupération dans cette zone pourrait être particulièrement précieuse. Cependant, la mise en œuvre d'un tel programme pour un archipel composé de plus de 1,000 îles est susceptible d'être complexe. Une collaboration approfondie entre les différentes parties prenantes de cette région, telles que les instituts de recherche, les associations de pêcheurs et les ONG, serait donc essentielle pour mettre en place un programme de récupération efficace aux Maldives, et ailleurs.

D'autres considérations logistiques doivent être prises en compte une fois les DCP ramenés au port, telles que la disponibilité d'une installation de traitement et d'élimination de leurs composants polluants ainsi que la possibilité de transporter les bouées GPS et les autres composants réutilisables vers les senneurs pour leur donner une seconde vie.

Nous soulignons qu'un nombre des DCP perdus peut également couler et nuire aux habitats benthiques (Derraik 2002; Macfadyen et al. 2009), cependant les données de positions pour ce type d'éventement ne sont pas disponibles. De telle données pourraient permettre d'aborder cet événement et venir compléter nos résultats dans de futurs travaux.

Nos résultats sont spécifiques à la flottille de pêcherie à la senne coulissante française et des pays associés (Île Maurice, Italie, Seychelles, Belize), cependant les données disponibles indiquent que d'autres flottilles de pêche à la senne coulissante ont des activités de déploiement de DCP similaires dans les Océans Indien et Atlantique (Katara et al. 2018), suggérant que nos résultats sont applicables à l'ensemble de la pêcherie thonière tropicale à la senne coulissante dans ces océans. Nous avons également montré que les DCP suivent plus ou moins les courants océaniques de surface. Sachant que les déchets marins issus de la pêche sont constitués d'autres engins de pêche abandonnés en mer qui suivent également les courants océaniques et dont la quantité, la distribution et les effets ont considérablement augmenté au cours des dernières décennies (Derraik 2002; Macfadyen et al. 2009; Gilman 2016), les résultats de ce travail pourraient donc également constituer une base d'étude pour réduire les déchets marins issus de la pêche de façon générale.

Pour conclure, ce travail de thèse a proposé et a évalué l'efficacité de trois mesures de mitigation pour atténuer les risques de perte et échouage des DCP dans les Océans Indien et Atlantique. Les résultats obtenus sont prometteurs et pourraient constituer une base solide pour préserver nos océans et nos littoraux de cet impact négatif. Bien que les difficultés de mise en place

de ces différentes mesures existent, les obstacles rencontrés peuvent être surmontés si les efforts des pêcheurs, ONG, ORGP et toute autre instance liée aux pêcheries tropicales thonières se réunissent.

Références bibliographique

Amandè, M.J., Ariz, J., Chassot, E., Delgado de Molina, A., Gaertner, D., Murua, H., Pianet, R., Ruiz, J., Chavance, P., 2010. Bycatch of the European purse seine tuna fishery in the Atlantic Ocean for the 2003–2007 period. Aquat. Living Resour. 23, 353–362. https://doi.org/10.1051/alr/2011003

Amemou, H., Koné, V., Aman, A., Lett, C., 2020. Assessment of a Lagrangian model using trajectories of oceanographic drifters and fishing devices in the Tropical Atlantic Ocean. Progress in Oceanography 188, 102426. https://doi.org/10.1016/j.pocean.2020.102426

Anderson, R.C., 2009. Entanglement of Olive Ridley Turtles Lepidochelys olivacea in ghost nets in the equatorial Indian Ocean. | IOTC [WWW Document]. URL https://www.iotc.org/documents/entanglement-olive-ridley-turtles-lepidochelys-olivacea-ghost-nets-equatorial-indian-ocean (accessed 10.5.21).

Ariz, J., Delgado de Molina, A., Fonteneau, A., Gonzales Costas, F., Pallarés, P., 1999. Logs and tunas in the eastern tropical Atlantic: a review of present knowledge and uncertainties, Proceedings of the International Workshop on the Ecology and Fisheries for Tunas Associated with Floating Objects. February pp11-13, 1992. Inter-American Tropical Tuna Commission Special Report 11, La Jolla, California, pp. 21–65.

Arrizabalaga, H., Ariz, J., Mina, X., Delgado de Molina, A., Artetxe, I., Pallarés, P., Iriondo, A., 2001. Analysis of the activities of supply vessels in the Indian Ocean from observers data, in: IOTC Proceedings. IOTC, Victoria, Seychelles, 19-27 June 2001, pp. 390–401.

Assan, C., Lucas, J., Chassot, E., 2019. Statistics of the Seychelles purse seine fleet targeting tropical tunas in the Indian Ocean (2000-2018). Presented at the Twenty first session of the Working Party on Tropical Tunas, IOTC, San Sebastian, Spain, 21-26 October 2019, p. 18p.

Assan, C., Lucas, J., Maufroy, A., Chassot, E., Delgado de Molina, A., 2015. Seychelles auxiliary vessels in support of purse seine fishing in the Indian Ocean during 2005-2014, in: IOTC Proceedings. CTOI, Montpellier, France, 23-28 October 2015, p. 12.

Baidai, Y., Dagorn, L., Amandè, M.J., Gaertner, D., Capello, M., 2020. Tuna aggregation dynamics at Drifting Fish Aggregating Devices: a view through the eyes of commercial echosounder buoys. ICES Journal of Marine Science 77, 2960–2970. https://doi.org/10.1093/icesjms/fsaa178

Balderson, S.D., Martin, L.E.C., 2015. Environmental impacts and causation of “beached” drifting fish aggregating devices around Seychelles Islands: A preliminary report on data collected by Island Conservation Society. Presented at the Eleventh Session of the IOTC Working Party on Ecosystems and Bycatch, Indian Ocean Tuna Commission, Olhao, Portugal, 7-11 September 2015, p. 15.

Bard, F.-X., Stretta, J.-M., Slepoukha, M., 1985. Les épaves artificielles comme auxiliaires de la pêche thonière en océan Atlantique : quel avenir ?

Baske, A., Adam, M.S., 2019. Options for Improving dFAD Recovery and Accountability to Minimize Coastal Habitat Damage and Marine Litter 6.

Baske, A., Gibbon, J., Benn, J., Nickson, A., 2012. Estimating the use of drifting Fish Aggregation Devices (FADs) around the globe (Discussion Paper). PEW Environment Group.

Bell, J.D., Kronen, M., Vunisea, A., Nash, W.J., Keeble, G., Demmke, A., Pontifex, S., Andréfouët, S., 2009. Planning the use of fish for food security in the Pacific. Marine Policy 33, 64–76. https://doi.org/10.1016/j.marpol.2008.04.002

Berta, M., Bellomo, L., Magaldi, M.G., Griffa, A., Molcard, A., Marmain, J., Borghini, M., Taillandier, V., 2014. Estimating Lagrangian transport blending drifters with HF radar data and models: Results from the TOSCA experiment in the Ligurian Current (North Western Mediterranean Sea). Progress in Oceanography 128, 15–29. https://doi.org/10.1016/j.pocean.2014.08.004

Bonjean, F., Lagerloef, G.S.E., 2002. Diagnostic Model and Analysis of the Surface Currents in the Tropical Pacific Ocean. Journal of Physical Oceanography 32, 2938–2954. https://doi.org/10.1175/1520-0485(2002)032<2938:DMAAOT>2.0.CO;2

Borrelle, S.B., Rochman, C.M., Liboiron, M., Bond, A.L., Lusher, A., Bradshaw, H., Provencher, J.F., 2017a. Opinion: Why we need an international agreement on marine plastic pollution. PNAS 114, 9994–9997. https://doi.org/10.1073/pnas.1714450114

Borrelle, S.B., Rochman, C.M., Liboiron, M., Bond, A.L., Lusher, A., Bradshaw, H., Provencher, J.F., 2017b. Opinion: Why we need an international agreement on marine plastic pollution. PNAS 114, 9994–9997. https://doi.org/10.1073/pnas.1714450114

Bourles, B., Molinari, R.L., Johns, E., Wilson, W.D., Leaman, K.D., 1999. Upper layer currents in the western tropical North Atlantic (1989–1991). Journal of Geophysical Research: Oceans 104, 1361–1375. https://doi.org/10.1029/1998JC900025

Bromhead, D., Foster, Findlay, Kalish, 2003. A review of the impact of fish aggregating devices (fads) on tuna fisheries: Final report to the fisheries resources research fund [WWW Document]. URL https://scholar.google.com/citations?view_op=view_citation&hl=en&user=EPrnt-IAAAAJ&citation_for_view=EPrnt-IAAAAJ:2osOgNQ5qMEC (accessed 9.29.21).

Burt, A.J., Raguain, J., Sanchez, C., Brice, J., Fleischer-Dogley, F., Goldberg, R., Talma, S., Syposz, M., Mahony, J., Letori, J., Quanz, C., Ramkalawan, S., Francourt, C., Capricieuse, I., Antao, A., Belle, K., Zillhardt, T., Moumou, J., Roseline, M., Bonne, J., Marie, R., Constance, E., Suleman, J., Turnbull, L.A., 2020. The costs of removing the unsanctioned import of marine plastic litter to small island states. Scientific Reports 10, 14458. https://doi.org/10.1038/s41598-020-71444-6

Caddy, J.F., Majkowski, J., 1996. Tuna and trees: a reflection on a long-term perspective for tuna fishing around floating logs. Fisheries Research 25, 369–376. https://doi.org/10.1016/0165-7836(95)00449-1

Castro, J., Santiago, J., Santana-Ortega, A., 2002. A general theory on fish aggregation to floating objects: An alternative to the meeting point hypothesis. Rev. Fish. Biol. Fish. 11, 255–277. https://doi.org/10.1023/A:1020302414472

Chassot, E., Bonhommeau, S., Reygondeau, G., Nieto, K., Polovina, J.J., Huret, M., Dulvy, N.K., Demarcq, H., 2011. Satellite remote sensing for an ecosystem approach to fisheries management. ICES Journal of Marine Science 68, 651–666. https://doi.org/10.1093/icesjms/fsq195

Chassot, E., Goujon, M., Maufroy, A., Cauquil, P., Fonteneau, A., Gaertner, D., 2014. The use of artificial fish aggregating devices by the French tropical tuna purse seine fleet: historical perspective and current practice in the Indian Ocean, in: Sixteenth Session of the Working Party on Tropical Tunas. Presented at the Bali, Indonesia, 15-19 November 2014, IOTC, Victoria, p. 17p.

Chen, C.-L., 2015. Regulation and Management of Marine Litter, in: Bergmann, M., Gutow, L., Klages, M. (Eds.), Marine Anthropogenic Litter. Springer International Publishing, Cham, pp. 395–428. https://doi.org/10.1007/978-3-319-16510-3_15

Consoli, P., Sinopoli, M., Deidun, A., Canese, S., Berti, C., Andaloro, F., Romeo, T., 2020. The impact of marine litter from fish aggregation devices on vulnerable marine benthic habitats of the central Mediterranean Sea. Marine Pollution Bulletin 152, 110928. https://doi.org/10.1016/j.marpolbul.2020.110928

Cózar, A., Echevarría, F., González-Gordillo, J.I., Irigoien, X., Úbeda, B., Hernández-León, S., Palma, Á.T., Navarro, S., García-de-Lomas, J., Ruiz, A., Fernández-de-Puelles, M.L., Duarte, C.M., 2014. Plastic debris in the open ocean. Proceedings of the National Academy of Sciences 111, 10239–10244. https://doi.org/10.1073/pnas.1314705111

Curnick, D.J., Feary, D.A., Cavalcante, G.H., 2021. Risks to large marine protected areas posed by drifting fish aggregation devices. Conservation Biology 35, 1222–1232. https://doi.org/10.1111/cobi.13684

Dagorn, L., Fréon, P., 1999. Tropical tuna associated with floating objects: A simulation study of the meeting point hypothesis. Canadian Journal of Fisheries and Aquatic Sciences - CAN J FISHERIES AQUAT SCI 56, 984–993. https://doi.org/10.1139/cjfas-56-6-984

Dagorn, L., Holland, K.N., Restrepo, V., Moreno, G., 2013. Is it good or bad to fish with FADs? What are the real impacts of the use of drifting FADs on pelagic marine ecosystems? Fish and Fisheries 14, 391–415. https://doi.org/10.1111/j.1467-2979.2012.00478.x

Davidson, F., Allen, A., Brassington, G., Breivik, Ø., Daniel, P., Kamachi, M., Sato, S., King, B., Lefevre, F., Sutton, M., 2009. Applications of GODAE ocean current forecasts

to search and rescue and ship routing. Oceanography 22, 176–181. https://doi.org/10.5670/oceanog.2009.76

Davies, T., Curnick, D., Barde, J., Chassot, E., IOTC ad hoc Working Group on FADs (WGFAD), 1., Madrid (ESP), 2017/04/18, 2017a. Potential environmental impacts caused by beaching or drifting fish aggregating devices and identification of management solutions and uncertainties. CTOI, Victoria Mahé.

Davies, T., Curnick, D., Barde, J., Chassot, E., IOTC ad hoc Working Group on FADs (WGFAD), 1., Madrid (ESP), 2017/04/18, IOTC ad hoc Working Group on FADs (WGFAD), 1., Madrid (ESP), 2017/04/18, 2017b. Potential environmental impacts caused by beaching or drifting fish aggregating devices and identification of management solutions and uncertainties. CTOI, Victoria Mahé.

Davies, Tim, Skerritt, D., Mees, C., Pearce, J., Franklin, T., 2017. An analysis of the uses, impacts and benefits of fish aggregating devices (FADs) in the global tuna industry Final Report.

Davies, T.K., Mees, C.C., Milner-Gulland, E.J., 2014. Modelling the Spatial Behaviour of a Tropical Tuna Purse Seine Fleet. PLOS ONE 9, e114037. https://doi.org/10.1371/journal.pone.0114037

De Dominicis, M., Bruciaferri, D., Gerin, R., Pinardi, N., Poulain, P.M., Garreau, P., Zodiatis, G., Perivoliotis, L., Fazioli, L., Sorgente, R., Manganiello, C., 2016. A multi-model assessment of the impact of currents, waves and wind in modelling surface drifters and oil spill. Deep Sea Research Part II: Topical Studies in Oceanography, Physical, chemical and biological observations and modelling of oil spills in the Mediterranean Sea 133, 21–38. https://doi.org/10.1016/j.dsr2.2016.04.002

Debreu, L., Marchesiello, P., Penven, P., Cambon, G., 2012. Two-way nesting in split-explicit ocean models: Algorithms, implementation and validation. Ocean Modelling 49–50, 1–21. https://doi.org/10.1016/j.ocemod.2012.03.003

Dempster, T., Taquet, M., 2004. Fish aggregation device (FAD) research: gaps in current knowledge and future directions for ecological studies. Rev Fish Biol Fisheries 14, 21–42. https://doi.org/10.1007/s11160-004-3151-x

Derraik, J.G.B., 2002. The pollution of the marine environment by plastic debris: a review. Marine Pollution Bulletin 44, 842–852. https://doi.org/10.1016/S0025-326X(02)00220-5

Desbiolles, F., Bentamy, A., Blanke, B., Roy, C., Mestas-Nuñez, A.M., Grodsky, S.A., Herbette, S., Cambon, G., Maes, C., 2017. Two decades [1992–2012] of surface wind analyses based on satellite scatterometer observations. Journal of Marine Systems 168, 38–56. https://doi.org/10.1016/j.jmarsys.2017.01.003

Dobler, D., Huck, T., Maes, C., Grima, N., Blanke, B., Martinez, E., Ardhuin, F., 2019. Large impact of Stokes drift on the fate of surface floating debris in the South Indian Basin. Marine Pollution Bulletin 148, 202–209. https://doi.org/10.1016/j.marpolbul.2019.07.057

Dohan, K., Maximenko, N., 2010. Monitoring ocean currents with satellite sensors. Oceanography 23, 94–103. https://doi.org/10.5670/oceanog.2010.08

Drévillon, M., Greiner, E., Paradis, D., Payan, C., Lellouche, J.-M., Reffray, G., Durand, E., Law-Chune, S., Cailleau, S., 2013. A strategy for producing refined currents in the Equatorial Atlantic in the context of the search of the AF447 wreckage. Ocean Dynamics 63, 63–82. https://doi.org/10.1007/s10236-012-0580-2

Drévillon, M., Lellouche, J.-M., Régnier, C., Garric, G., Bricaud, C., Bourdallé-Badie, R., 2021. QUALITY INFORMATION DOCUMENT For Global Ocean Reanalysis Products GLOBAL_REANALYSIS_PHY_001_030 52.

Duan, G., Nur, F., Alizadeh, M., Chen, L., Marufuzzaman, M., Ma, J., 2020. Vessel routing and optimization for marine debris collection with consideration of carbon cap. Journal of Cleaner Production 263, 121399. https://doi.org/10.1016/j.jclepro.2020.121399

Elipot, S., Lumpkin, R., Perez, R.C., Lilly, J.M., Early, J.J., Sykulski, A.M., 2016. A global surface drifter data set at hourly resolution. Journal of Geophysical Research: Oceans 121, 2937–2966.

Environment, U.N., 2017. The First Global Integrated Marine Assessment: World Ocean Assessment I [WWW Document]. UNEP - UN Environment Programme. URL http://www.unep.org/resources/report/first-global-integrated-marine-assessment-world-ocean-assessment-i (accessed 9.22.21).

Escalle, L., Brouwer, S., Scutt Philipps, J., Pilling, G., office, P.N.A., 2017. Preliminary analysis of PNA FAD tracking data from 2016 and 2017. WCPFC, Rarotonga, Cook Islands, p. 21p.

Escalle, L., Hare, S.R., Vidal, T., Brownjohn, M., Hamer, P., Pilling, G., 2021. Quantifying drifting Fish Aggregating Device use by the world's largest tuna fishery. ICES Journal of Marine Science. https://doi.org/10.1093/icesjms/fsab116

Escalle, L., Muller, B., Hare, S., Hamer, P., Pilling, G., Office, P., 2020. Report on analyses of the 2016/2020 PNA FAD tracking programme.

Escalle, L., Phillips, J.S., Brownjohn, M., Brouwer, S., Gupta, A.S., Sebille, E.V., Hampton, J., Pilling, G., 2019. Environmental versus operational drivers of drifting FAD beaching in the Western and Central Pacific Ocean. Sci Rep 9, 1–12. https://doi.org/10.1038/s41598-019-50364-0

Fernandez, E., Lellouche, J.M., 2021. Product User Manual for the Global Ocean Physical Reanalysis Product Global_reanalysis_ Phy_001_030.

Filmalter, J.D., Capello, M., Deneubourg, J.-L., Cowley, P.D., Dagorn, L., 2013a. Looking behind the curtain: quantifying massive shark mortality in fish aggregating devices. Front. Ecol. Env. 130627131409009. https://doi.org/10.1890/130045

Filmalter, J.D., Capello, M., Deneubourg, J.-L., Cowley, P.D., Dagorn, L., 2013b. Looking behind the curtain: quantifying massive shark mortality in fish aggregating devices. Frontiers in Ecology and the Environment 11, 291–296. https://doi.org/10.1890/130045

Floch, L., Billet, N., Dewals, P., Irié, D., Cauquil, P., Gaertner, D., Chassot, E., 2017. Statistics of the French purse seine fishing fleet targeting tropical tunas in the Atlantic Ocean (1962-2015). ICCAT Col. Vol. Sci. Pap. 73, 755–778.

Floch, L., Depetris, M., Dewals, P., Duparc, A., Kaplan, D.M., Lebranchu, J., Marsac, F., Pernak, M., Bach, P., 2019. Statistics of the French purse seine fishing fleet targeting tropical tunas in the Indian Ocean (1981-2018). Presented at the Twenty first sesstion of the Working Party on Tropical Tunas, San Sebastian, Spain, 21-26 October 2019, p. 27p.

Fonteneau, A., Chassot, E., Bodin, N., 2013. Global spatio-temporal patterns in tropical tuna purse seine fisheries on drifting fish aggregating devices (DFADs): Taking a historical perspective to inform current challenges. Aquatic Living Resources 26, 37–48. https://doi.org/10.1051/alr/2013046

Fonteneau, A., Pallares, P., Pianet, R., 2000. A worldwide review of purse seine fisheries on FADs. Presented at the Pêche thonière et dispositifs de concentration de poissons, Caribbean-Martinique, 15-19 Oct 1999.

Franco, J., Dagorn, L., Sancristobal, I., Moreno, G., 2009. Design of ecological FADs. IOTC, Mombasa, Kenya, 12-14 October 2009, p. 22.

Fraser, C.I., Morrison, A.K., Hogg, A.M., Macaya, E.C., van Sebille, E., Ryan, P.G., Padovan, A., Jack, C., Valdivia, N., Waters, J.M., 2018. Antarctica's ecological isolation will be broken by storm-driven dispersal and warming. Nature Clim Change 8, 704–708. https://doi.org/10.1038/s41558-018-0209-7

Freeman, E., Woodruff, S.D., Worley, S.J., Lubker, S.J., Kent, E.C., Angel, W.E., Berry, D.I., Brohan, P., Eastman, R., Gates, L., Gloeden, W., Ji, Z., Lawrimore, J., Rayner, N.A., Rosenhagen, G., Smith, S.R., 2017. ICOADS Release 3.0: a major update to the historical marine climate record. International Journal of Climatology 37, 2211–2232. https://doi.org/10.1002/joc.4775

Fréon, P., Dagorn, L., 2000a. Review of fish associative behaviour: Toward a generalisation of the meeting point hypothesis. Reviews in Fish Biology and Fisheries 10, 183–207. https://doi.org/10.1023/A:1016666108540

Fréon, P., Dagorn, L., 2000b. Review of fish associative behaviour: Toward a generalisation of the meeting point hypothesis. Rev Fish Biol Fisheries 10, 183–207. https://doi.org/10.1023/A:1016666108540

Galgani, F., Fleet, D., Van Franeker, J., Katsanevakis, S., Maes, T., J, M., L, O., Poitou, I., Hanke, G., R, T., Amato, E., A, B., Janssen, C., 2010. Marine Strategy Framework Directive: Task Group 10 Report Marine litter. https://doi.org/10.2788/86941

Galland, G., Rogers, A., Nickson, A., 2016a. Netting billions: a global valuation of tuna. URL http://pew.org/1VVZLVj (accessed 9.24.21).

Galland, G., Rogers, A., Nickson, A., 2016b. Netting billions: A global valuation of tuna. The PEW Charitable Trusts, Washington D.C., U.S.A.

Gawarkiewicz, G., Malek Mercer, A., 2018. Partnering with Fishing Fleets to Monitor Ocean Conditions. Annual Review of Marine Science. https://doi.org/10.1146/annurev-marine-010318-095201

Gershman, D., Nickson, A., O'Toole, M., 2015. Estimating The Use of FADs Around the World 24.

Gilman, E., 2016. Biodegradable fishing gear: part of the solution to ghost fishing and marine pollution. Animal Conservation 19, 320–321. https://doi.org/10.1111/acv.12298

Gnanaseelan, C., Deshpande, A., 2017. Equatorial Indian Ocean subsurface current variability in an Ocean General Circulation Model. Climate Dynamics 1–13. https://doi.org/10.1007/s00382-017-3716-8

Gooding, R.M., Magnuson, J.J., 1967. Ecological Significance of a Drifting Object to Pelagic Fishes.

Goujon, M., Maufroy, A., Relot-Stirnemann, A., Moëc, E., Amandè, M.J., Bach, P., Cauquil, P., Sebarros, P., 2017a. Collecting data on board French and Italian tropical tuna purse seiners with common observers: results of Orthongel's voluntary observer program OCUP (2013-2017) in the Atlantic Ocean (No. SCRS/2017/212A).

Goujon, M., Maufroy, A., Relot-Stirnemann, A., Moëc, E., Bach, P., Cauquil, P., Sebarros, P., 2017b. Collecting data on board French and Italian tropical tuna purse seiners with common observers: results of Orthongel's voluntary observer program OCUP (2013-2017) in the Indian Ocean (No. IOTC-2017-WPDCS13-22_Rev1).

Goujon, M., Vernet, A.-L., Dagorn, L., 2012. Preliminary results of the Orthongel program eco-FAD" as June 30th 2012 " | IOTC (Groupe de travail sur les écosystèmes et les prises accessoires (GTEPA) No. IOTC-2012-WPEB08-INF21). IOTC.

Grande, M., Murua, H., Zudaire, I., Goñi, N., Bodin, N., 2014. Reproductive timing and reproductive capacity of the Skipjack Tuna (Katsuwonus pelamis) in the western Indian Ocean. Fisheries Research 156, 14–22. https://doi.org/10.1016/j.fishres.2014.04.011

Grande, M., Ruiz, J., Murua, H., Murua, J., Goñi, N., Krug, I., Arregui, I., Salgado, A., Zudaire, I., Santiago, J., 2019. Progress on the code of good practices on the tropical tuna purse seine fishery in the Indian Ocean (No. IOTC-2019-WPEB15-33).

Greenblatt, P.R., 1979. Associations of tuna with flotsam in the eastern tropical pacific.

Gurvan, M., Benshila, R., Bricaud, C., Coward, A., Dobricic, S., Furner, R., Oddo, P., 2013. NEMO ocean engine. Notes du Pôle de modélisation de l'Institut Pierre-Simon Laplace (IPSL): (27). https://doi.org/10.5281/zenodo.1464817

Hall, M., 1992. The association of tunas with floating objects and dolphins in the Eastern Pacific Ocean. 1992. Part VII. Some hypotheses on the mechanisms governing the association of tunas with floating objects and dolphins.

Hall, M., Roman, M.H., 2017. The fishery on fish-aggregating devices (FADs) in the Eastern Pacific Ocean - Update. IATTC, La Jolla, California, U.S.A., p. 19p.

Hallier, J.-P., Gaertner, D., 2008. Drifting fish aggregation devices could act as an ecological trap for tropical tuna species. Marine Ecology Progress Series 353, 255–264. https://doi.org/10.3354/meps07180

Halpern, B.S., Gaines, S.D., Warner, R.R., 2004. Confounding Effects of the Export of Production and the Displacement of Fishing Effort from Marine Reserves. Ecological Applications 14, 1248–1256. https://doi.org/10.1890/03-5136

Hanich, Q., Davis, R., Holmes, G., Amidjogbe, E.-R., Campbell, B., 2019. Drifting Fish Aggregating Devices (FADs): Deploying, Soaking and Setting – When Is a FAD 'Fishing'? The International Journal of Marine and Coastal Law 34, 731–754. https://doi.org/10.1163/15718085-23441103

Hankin, S.C., Blower, J.D., Carval, T., Casey, K.S., Donlon, C., Lauret, O., Loubrieu, T., Srinivasan, A., Trinanes, J., Godoy, O., Mendelssohn, R., Signell, R., de la Beaujardiere, J., Cornillon, P., Blanc, F., Rew, R., Harlan, J., 2010. NetCDF-CF-OPeNDAP: Standards for ocean data interoperability and object lessons for community data standards processes, in: Proceedings of OceanObs'09: Sustained Ocean Observations and Information for Society. Hall, J., Harrison, D.E. & Stammer, D, 21-25 septembre 2009, Venice, Italy. https://doi.org/10.5270/OceanObs09.cwp.41

Hansen, D.V., Poulain, P.-M., 1996. Quality control and interpolations of WOCE-TOGA drifter data. Journal of Atmospheric and Oceanic Technology 13, 900–909. https://doi.org/10.1175/1520-0426(1996)013<0900:QCAIOW>2.0.CO;2

Haward, M., 2018. Plastic pollution of the world's seas and oceans as a contemporary challenge in ocean governance. Nature Communications 9, 1–3. https://doi.org/10.1038/s41467-018-03104-3

Hunter, J.R., Mitchell, C.T., 1967. Association of fishes with flotsam in the offshore waters of Central America. Fishery Bulletin 66, 13–29.

IATTC-WCPFC, 2020. Guidelines for non-entangling and biodegradable FAD materials-final | wcpfc [WWW Document]. URL https://www.wcpfc.int/node/48435 (accessed 4.9.21).

ICCAT, 2019. Compendium management recommendations and resolutions adopted by iccat for the conservation of atlantic tunas and tuna-like species.

ICCAT, 2015. Recommendation by ICCAT on a multi-annual conservation and management program for tropical tunas.

Imzilen, T., Chassot, E., Barde, J., Demarcq, H., Maufroy, A., Roa-Pascuali, L., Ternon, J.-F., Lett, C., 2019. Fish aggregating devices drift like oceanographic drifters in the near-surface currents of the Atlantic and Indian Oceans. Progress in Oceanography 171, 108–127. https://doi.org/10.1016/j.pocean.2018.11.007

Imzilen, T., Lett, C., Chassot, E., Barde, J., 2016. Modeling trajectories of fish aggregating devices with satellite images : use cases related to fisheries.

Imzilen, T., Lett, C., Chassot, E., Kaplan, D.M., 2021a. Spatial management can significantly reduce dFAD beachings in Indian and Atlantic Ocean tropical tuna purse seine fisheries. Biological Conservation 254, 108939. https://doi.org/10.1016/j.biocon.2020.108939

Imzilen, T., Lett, C., Chassot, E., Kaplan, D.M., 2021b. Spatial management can significantly reduce dFAD beachings in Indian and Atlantic Ocean tropical tuna purse seine fisheries. Biological Conservation 254, 108939. https://doi.org/10.1016/j.biocon.2020.108939

IOTC, 2019a. On an interim plan for rebuilding the indian ocean yellowfin tuna stock in the IOTC area of competence, 19/01.

IOTC, 2019b. Procedures on a Fish Aggregating Devices (FADs) management plan, 19/02.

IOTC, 2018. Report of the 4th Technical Committee on Allocation Criteria (No. IOTC-2018-TCAC04-R[E]). IOTC, Victoria, Seychelles, 5-7 February 2018.

ISSF, 2019a. Non-Entangling FADs. International Seafood Sustainability Foundation. URL https://iss-foundation.org/knowledge-tools/guides-best-practices/non-entangling-fads/ (accessed 10.7.21).

ISSF, 2019b. Status of the World Fisheries for Tuna: October 2019 [WWW Document]. FundingtheOcean.org. URL https://fundingtheocean.org/reports/status-of-the-world-fisheries-for-tuna-october-2019 (accessed 10.8.21).

ISSF, 2014. Report of the ISSF Workshop on FADs as Ecological Traps (ISSF Technical Report 2014-03). International Seafood Sustainability Foundation,Washington,D.C.,USA.

ISSF, 2012. ISSF Guide to non-entangling FADs \textbar IOTC.

Itano, D.G., Fukofuka, S., Brogan, D., 2004. The development, design and recent status of anchored and drifting fads in the wcpo, 17tk Meeting of the Standing Committee on Tuna and Billfish (9-18 August 2004). Majuro, Marshall Islands.

Ivichev, I., Hole, L.R., Karlin, L., Wettre, C., Röhrs, J., 2012. Comparison of operational oil spill trajectory forecasts with surface drifter trajectories in the barents sea. J. Geol. Geosci. 1.

Jambeck, J.R., Geyer, R., Wilcox, C., Siegler, T.R., Perryman, M., Andrady, A., Narayan, R., Law, K.L., 2015. Plastic waste inputs from land into the ocean. Science 347, 768–771. https://doi.org/10.1126/science.1260352

Johannessen, J.A., Chapron, B., Collard, F., Rio, M.H., Piollé, J.F., Gaultier, L., Quartly, G., Shutler, J., Escola, R., Raj, R., Donlon, C., Danielson, R., Korosov, A., Nencioli, F., Kudryavtsev, V., Roca, M., Tournadre, J., Larnicol, G., Guitton, G., Miller, P.I., Warren, M., Hansen, M., 2016. GlobCurrent : Multisensor synergy for surface current estimation. Presented at the Living Planet Symposium 2016, ESA, Proceedings of Living Planet Symposium 2016.

Johns, W.E., Brandt, P., Bourlès, B., Tantet, A., Papapostolou, A., Houk, A., 2014. Zonal structure and seasonal variability of the Atlantic Equatorial Undercurrent. Climate Dynamics 43, 3047–3069. https://doi.org/10.1007/s00382-014-2136-2

Johnson, E.S., Bonjean, F., Lagerloef, G.S.E., Gunn, J.T., Mitchum, G.T., 2007. Validation and error analysis of OSCAR sea surface currents. Journal of Atmospheric and Oceanic Technology 24, 688–701. https://doi.org/10.1175/JTECH1971.1

Joseph, A., 2013. Measuring Ocean Currents: Tools, Technologies, and Data. Newnes.

Kaplan, D.M., Chassot, E., Amandé, J.M., Dueri, S., Demarcq, H., Dagorn, L., Fonteneau, A., 2014. Spatial management of Indian Ocean tropical tuna fisheries: potential and perspectives. ICES Journal of Marine Science 71, 1728–1749. https://doi.org/10.1093/icesjms/fst233

Kaplan, D.M., Largier, J., Botsford, L.W., 2005. HF radar observations of surface circulation off Bodega Bay (northern California, USA). Journal of Geophysical Research: Oceans 110. https://doi.org/10.1029/2005JC002959

Katara, I., Gaertner, D., Marsac, F., Grande, M., Kaplan, D.M., Urtizberea, A., Guery, L., Depetris, M., Duparc, A., Floch, L., Lopez, J., Abascal, F., 2018. Standardisation of yellowfin tuna CPUE for the EU purse seine fleet operating in the Indian Ocean (No. IOTC–2018–WPTT20–36_Rev1). Indian Ocean Tuna Commission 20th Working Party on Tropical Tunas (WPTT), Mahé, Seychelles.

Kent, E.C., Ball, G., Berry, D.I., Fletcher, J., Hall, A., North, S., Woodruff, S.D., 2010. The Voluntary Observing Ship (VOS) scheme, in: Proceedings of OceanObs'09, ESA Special Publication, WPP-306. Hall, J., Harrison, D.E. & Stammer, D, Venice, Italy, 21-25 September 2009, pp. 551–561.

Lagerloef, G.S.E., Mitchum, G.T., Lukas, R.B., Niiler, P.P., 1999. Tropical Pacific near-surface currents estimated from altimeter, wind, and drifter data. Journal of Geophysical Research: Oceans 104, 23313–23326. https://doi.org/10.1029/1999JC900197

Lauro, F.M., Senstius, S.J., Cullen, J., Neches, R., Jensen, R.M., Brown, M.V., Darling, A.E., Givskov, M., McDougald, D., Hoeke, R., Ostrowski, M., Philip, G.K., Paulsen, I.T., Grzymski, J.J., 2014. The common oceanographer: Crowdsourcing the collection of oceanographic data. PLOS Biology 12, e1001947. https://doi.org/10.1371/journal.pbio.1001947

Law, K.L., Morét-Ferguson, S., Maximenko, N.A., Proskurowski, G., Peacock, E.E., Hafner, J., Reddy, C.M., 2010. Plastic accumulation in the North Atlantic subtropical gyre. Science 329, 1185–1188. https://doi.org/10.1126/science.1192321

Lebreton, L., Slat, B., Ferrari, F., Sainte-Rose, B., Aitken, J., Marthouse, R., Hajbane, S., Cunsolo, S., Schwarz, A., Levivier, A., Noble, K., Debeljak, P., Maral, H., Schoeneich-Argent, R., Brambini, R., Reisser, J., 2018. Evidence that the Great Pacific Garbage Patch is rapidly accumulating plastic. Sci Rep 8, 1–15. https://doi.org/10.1038/s41598-018-22939-w

Lebreton, L.C.-M., Greer, S.D., Borrero, J.C., 2012. Numerical modelling of floating debris in the world's oceans. Marine Pollution Bulletin 64, 653–661. https://doi.org/10.1016/j.marpolbul.2011.10.027

Lee, T., Hakkinen, S., Kelly, K., Qiu, B., Bonekamp, H., Lindstrom, E.J., 2010. Satellite observations of ocean circulation changes associated with climate variability. Oceanography 23, 70.

Legendre, P., Legendre, L., 1998. Numerical ecology. Elsevier Science, New York, USA.

Lennert-Cody, C.E., Roberts, J.J., Stephenson, R.J., 2008. Effects of gear characteristics on the presence of bigeye tuna (*Thunnus obesus*) in the catches of the purse-seine fishery of the eastern Pacific Ocean. ICES Journal of Marine Science 65, 970–978. https://doi.org/10.1093/icesjms/fsn075

Lett, C., Verley, P., Mullon, C., Parada, C., Brochier, T., Penven, P., Blanke, B., 2008. A Lagrangian tool for modelling ichthyoplankton dynamics. Environmental Modelling & Software 23, 1210–1214. https://doi.org/10.1016/j.envsoft.2008.02.005

Liu, Y., Weisberg, R.H., 2011. Evaluation of trajectory modeling in different dynamic regions using normalized cumulative Lagrangian separation. Journal of Geophysical Research: Oceans 116. https://doi.org/10.1029/2010JC006837

Löhr, A., Savelli, H., Beunen, R., Kalz, M., Ragas, A., Van Belleghem, F., 2017. Solutions for global marine litter pollution. Current Opinion in Environmental Sustainability, Sustainability governance 28, 90–99. https://doi.org/10.1016/j.cosust.2017.08.009

Longhurst, A.R., 2007. Ecological geography of the sea. Academic Press, London, UK.

Lopez, J., Ferarios, J.M., Santiago, J., Ubis, M., Moreno, G., Murua, H., 2019. Evaluating potential biodegradable twines for use in the tropical tuna FAD fishery. Fisheries Research 219, 105321. https://doi.org/10.1016/j.fishres.2019.105321

Lopez, J., Moreno, G., Sancristobal, I., Murua, J., 2014. Evolution and current state of the technology of echo-sounder buoys used by Spanish tropical tuna purse seiners in the Atlantic, Indian and Pacific Oceans. Fisheries Research 155, 127–137. https://doi.org/10.1016/j.fishres.2014.02.033

Lumpkin, R., Elipot, S., 2010. Surface driter pair spreading in the North Atlantic. Journal of Geophysical Research 115, C12017. https://doi.org/10.1029/2010JC006338

Lumpkin, R., Johnson, G.C., 2013. Global ocean surface velocities from drifters: Mean, variance, El Niño–Southern Oscillation response, and seasonal cycle. Journal of Geophysical Research: Oceans 118, 2992–3006. https://doi.org/10.1002/jgrc.20210

Lumpkin, R., Maximenko, N., Pazos, M., 2012. Evaluating where and why drifters die. Journal of Atmospheric and Oceanic Technology 29, 300–308. https://doi.org/10.1175/JTECH-D-11-00100.1

Lumpkin, R., Pazos, M., 2007. Measuring surface currents with Surface Velocity Program drifters: the instrument, its data, and some recent results, in: Lagrangian Analysis and Prediction of Coastal and Ocean Dynamics. Cambridge University Press, pp. 39–67.

Lutjeharms, J.R.E., 2006. The Agulhas Current. Springer-Verlag, Berlin Heidelberg.

Macfadyen, G., Huntington, T., Cappell, R., 2009. Abandoned, lost or otherwise discarded fishing gear, FAO fisheries and aquaculture technical paper. United Nations Environment Programme : Food and Agriculture Organization of the United Nations, Rome.

Manyilizu, M., Penven, P., Reason, C.J.C., 2016. Annual cycle of the upper-ocean circulation and properties in the tropical western Indian Ocean. African Journal of Marine Science 38, 81–99. https://doi.org/10.2989/1814232X.2016.1158123

Marsac, F., Fonteneau, A., Menard, F., 2000. Drifting FADs used in tuna fisheries: an ecological trap? Presented at the Pêche thonière et dispositifs de concentration de poissons, Caribbean-Martinique, 15-19 Oct 1999, In Pêche thonière et dispositifs de concentration de poissons, Caribbean-Martinique, 15-19 Oct 1999.

Martin, S., 2004. An introduction to ocean remote sensing. Cambridge University Press.

Maufroy, A., 2016. Drifting Fish Aggregating Devices of the Atlantic and Indian Oceans : modalities of use, fishing efficiency and potential management (thèse de doctorat, Écologie fonctionnelle et sciences agronomiques, sous la direction de Bez, Nicolas Chassot, Emmanuel). Université de Montpellier, Montpellier.

Maufroy, A., Chassot, E., Joo, R., Kaplan, D.M., 2015a. Large-scale examination of spatio-temporal patterns of drifting fish aggregating devices (dFADs) from tropical tuna fisheries of the Indian and Atlantic oceans. PLoS ONE 10, e0128023. https://doi.org/10.1371/journal.pone.0128023

Maufroy, A., Chassot, E., Joo, R., Kaplan, D.M., 2015b. Large-scale examination of spatio-temporal patterns of drifting Fish Aggregating Devices (dFADs) from tropical tuna fisheries of the Indian and Atlantic Oceans. PLOS ONE 10, e0128023. https://doi.org/10.1371/journal.pone.0128023

Maufroy, A., Kaplan, D., Chassot, E., Goujon, M., 2018. Drifting fish aggregating devices (dFADs) beaching in the Atlantic Ocean: an estimate for the French purse seine fleet (2007-2015). ICCAT Col. Vol. Sci. Pap. 74, 2219–2229.

Maufroy, A., Kaplan, D.M., Bez, N., Molina, D., Delgado, A., Murua, H., Floch, L., Chassot, E., 2017a. Massive increase in the use of drifting Fish Aggregating Devices (dFADs) by tropical tuna purse seine fisheries in the Atlantic and Indian oceans. ICES Journal of Marine Science 74, 215–225. https://doi.org/10.1093/icesjms/fsw175

Maufroy, A., Kaplan, D.M., Bez, N., Molina, D., Delgado, A., Murua, H., Floch, L., Chassot, E., 2017b. Massive increase in the use of drifting Fish Aggregating Devices (dFADs) by tropical tuna purse seine fisheries in the Atlantic and Indian oceans. ICES J Mar Sci 74, 215–225. https://doi.org/10.1093/icesjms/fsw175

Maximenko, N., Corradi, P., Law, K.L., Van Sebille, E., Garaba, S.P., Lampitt, R.S., Galgani, F., Martinez-Vicente, V., Goddijn-Murphy, L., Veiga, J.M., Thompson, R.C., Maes, C., Moller, D., Löscher, C.R., Addamo, A.M., Lamson, M.R., Centurioni, L.R., Posth, N.R., Lumpkin, R., Vinci, M., Martins, A.M., Pieper, C.D., Isobe, A., Hanke, G., Edwards, M., Chubarenko, I.P., Rodriguez, E., Aliani, S., Arias, M., Asner, G.P., Brosich, A., Carlton, J.T., Chao, Y., Cook, A.-M., Cundy, A.B., Galloway, T.S., Giorgetti, A., Goni, G.J., Guichoux, Y., Haram, L.E., Hardesty, B.D., Holdsworth, N., Lebreton, L., Leslie, H.A., Macadam-Somer, I., Mace, T., Manuel, M., Marsh, R., Martinez, E., Mayor, D.J., Le Moigne, M., Molina Jack, M.E., Mowlem, M.C., Obbard, R.W., Pabortsava, K., Robberson, B., Rotaru, A.-E., Ruiz, G.M., Spedicato, M.T., Thiel, M., Turra, A., Wilcox, C., 2019. Toward the Integrated Marine Debris Observing System. Front. Mar. Sci. 6. https://doi.org/10.3389/fmars.2019.00447

Maximenko, N., Hafner, J., Niiler, P., 2012. Pathways of marine debris derived from trajectories of Lagrangian drifters. Marine Pollution Bulletin, At-sea Detection of Derelict Fishing Gear 65, 51–62. https://doi.org/10.1016/j.marpolbul.2011.04.016

Maximenko, N., Niiler, P., Centurioni, L., Rio, M.-H., Melnichenko, O., Chambers, D., Zlotnicki, V., Galperin, B., 2009. Mean Dynamic Topography of the Ocean Derived from Satellite and Drifting Buoy Data Using Three Different Techniques. Journal of Atmospheric and Oceanic Technology 26, 1910–1919. https://doi.org/10.1175/2009JTECHO672.1

Mheen, M. van der, Pattiaratchi, C., Sebille, E. van, 2019. Role of Indian Ocean Dynamics on Accumulation of Buoyant Debris. Journal of Geophysical Research: Oceans 124, 2571–2590. https://doi.org/10.1029/2018JC014806

Miyake, M., Miyabe, N., Nakano, H., Nations, F. and A.O. of the U., 2004. Historical Trends of Tuna Catches in the World. Food & Agriculture Org.

Mooney, H.A., Duraiappah, A., Larigauderie, A., 2013. Evolution of natural and social science interactions in global change research programs. Proceedings of the National Academy of Sciences of the United States of America 110, 3665–3672.

Moreno, G., Dagorn, L., Capello, M., Lopez, J., Filmalter, J., Forget, F., Sancristobal, I., Holland, K., 2016. Fish aggregating devices (FADs) as scientific platforms. Fisheries

Research, The use of fishing vessels as scientific platforms 178, 122–129. https://doi.org/10.1016/j.fishres.2015.09.021

Moreno, G., Murua, J., Dagorn, L., Hall, M., Altamirano, E., Cuevas, N., Grande, M., Moniz, I., Sancristobal, I., Santiago, J., Uriarte, I., Zudaire, I., Restrepo, V., 2018. Workshop for the reduction of the impact of Fish Aggregating Devices´structure´ on the ecosystem, ISSF Technical Report 2018-19A. International Seafood Sustainability Foundation, Washington, D.C., USA. https://doi.org/10.13140/RG.2.2.11384.49925

Moreno, G., Salvador, J., Murua, H., Uranga, J., Zudaire, I., Murua, J., Grande, M., Cabezas, O., Restrepo, V., 2021. The JellyFAD: a paradigm shift in bio-FAD design (No. IOTC-2021-WGFAD02-10).

Murua, J., Moreno, G., Hall, M., Dagorn, L., Itano, D., Restrepo, V., 2017. Towards global non-entangling fish aggregating device (FAD) use in tropical tuna purse seine fisheries through a participatory approach (No. ISSF Technical Report 2017–07). International Seafood Sustainability Foundation, Washington, D.C., USA.

Murua, J., Moreno, G., Itano, D., Hall, M., Dagorn, L., Restrepo, V., 2018. ISSF Skippers' Workshops Round 7 (ISSF Technical Report No. 2018– 01). ISSF, Washington D.C., U.S.A.

Niiler, P.P., Paduan, J.D., 1995. Wind-Driven Motions in the Northeast Pacific as Measured by Lagrangian Drifters. Journal of Physical Oceanography 25, 2819–2830. https://doi.org/10.1175/1520-0485(1995)025<2819:WDMITN>2.0.CO;2

Niiler, P.P., Sybrandy, A.S., Bi, K., Poulain, P.M., Bitterman, D., 1995. Measurements of the water-following capability of holey-sock and TRISTAR drifters. Deep Sea Research Part I: Oceanographic Research Papers 42, 1951–1964. https://doi.org/10.1016/0967-0637(95)00076-3

ORTHONGEL, 2021a. Décision n° 21 du 29 juin 2021 relative au plan de gestion des DCP en Océan Indien pour 2021. Organisation française des producteurs de thon congelé et surgelé.

ORTHONGEL, 2021b. Décision n° 22 du 29 juin 2021 relative au plan de gestion des DCP en Atlantique pour 2021. Organisation française des producteurs de thon congelé et surgelé.

Orúe, B., Lopez, J., Moreno, G., Santiago, J., Soto, M., Murua, H., 2017. Colonization of drifting fish aggregating devices (DFADs) in the Western Indian Ocean, assessed by fishers' echo sounder, in: Http://Www.Iotc.Org/Meetings/13th-Working-Party-Ecosystems-and-Bycatch-Wpeb13.

Parton, K., Galloway, T., Godley, B., 2019. Global review of shark and ray entanglement in anthropogenic marine debris. Endangered Species Research 39. https://doi.org/10.3354/esr00964

Pebesma, E., 2018. Simple Features for R: Standardized Support for Spatial Vector Data. The R Journal 10, 439--446. https://doi.org/10.32614/RJ-2018-009

Peliz, A., Marchesiello, P., Dubert, J., Marta-Almeida, M., Roy, C., Queiroga, H., 2007. A study of crab larvae dispersal on the Western Iberian Shelf: Physical processes. Journal of Marine Systems 68, 215–236. https://doi.org/10.1016/j.jmarsys.2006.11.007

Peng, S., Qian, Y.-K., Lumpkin, R., Du, Y., Wang, D., Li, P., 2014. Characteristics of the near-surface currents in the Indian Ocean as deduced from satellite-tracked surface drifters. part i: pseudo-Eulerian statistics. Journal of Physical Oceanography 45, 441–458. https://doi.org/10.1175/JPO-D-14-0050.1

Phillips, J.S., Escalle, L., Pilling, G., Gupta, A.S., Sebille, E. van, 2019. Regional connectivity and spatial densities of drifting fish aggregating devices, simulated from fishing events in the Western and Central Pacific Ocean. Environ. Res. Commun. 1, 055001. https://doi.org/10.1088/2515-7620/ab21e9

Poisson, F., Séret, B., Vernet, A.-L., Goujon, M., Dagorn, L., 2014. Collaborative research: Development of a manual on elasmobranch handling and release best practices in tropical tuna purse-seine fisheries (No. IOTC-2014-WPEB10-INF15).

Poisson, F., Vernet, A.L., Seret, B., Dagorn, L., 2012. Good practices to reduce the mortality of sharks and rays caught incidentally by the tropical tuna purse seiners., http://ebfmtuna-2012.sciencesconf.org/conference/ebfmtuna-2012/pages/D6.2_Practices_to_reduce_shark_mortality_purse_seiners.pdf.

Poulain, P.-M., Gerin, R., Mauri, E., Pennel, R., 2009. Wind effects on drogued and undrogued drifters in the Eastern Mediterranean. Journal of Atmospheric and Oceanic Technology 26, 1144–1156. https://doi.org/10.1175/2008JTECHO618.1

Putman, N.F., Lumpkin, R., Olascoaga, M.J., Trinanes, J., Goni, G.J., 2020. Improving transport predictions of pelagic Sargassum. Journal of Experimental Marine Biology and Ecology 529, 151398. https://doi.org/10.1016/j.jembe.2020.151398

Putman, N.F., Mansfield, K.L., 2015. Direct Evidence of Swimming Demonstrates Active Dispersal in the Sea Turtle “Lost Years.” Current Biology 25, 1221–1227. https://doi.org/10.1016/j.cub.2015.03.014

R Core Team, 2021. R: A Language and Environment for Statistical Computing. R Foundation for Statistical Computing, Vienna, Austria.

Reichman, O.J., Jones, M.B., Schildhauer, M.P., 2011. Challenges and opportunities of open data in ecology. Science 331, 703–705.

Reverdin, G., Niiler, P.P., Valdimarsson, H., 2003. North Atlantic Ocean surface currents. Journal of Geophysical Research: Oceans 108, 3002. https://doi.org/10.1029/2001JC001020

Reynolds, R.W., Rayner, N.A., 2002. An improved in situ and satellite SST analysis for climate. Journal of Climate 15, 1609–1625.

Richardson, A.J., Poloczanska, E.S., 2008. Under-resourced, under threat. Science 320, 1294.

Richardson, K., Asmutis-Silvia, R., Drinkwin, J., Gilardi, K.V.K., Giskes, I., Jones, G., O'Brien, K., Pragnell-Raasch, H., Ludwig, L., Antonelis, K., Barco, S., Henry, A., Knowlton, A., Landry, S., Mattila, D., MacDonald, K., Moore, M., Morgan, J., Robbins, J., van der Hoop, J., Hogan, E., 2019. Building evidence around ghost gear: Global trends and analysis for sustainable solutions at scale. Marine Pollution Bulletin 138, 222–229. https://doi.org/10.1016/j.marpolbul.2018.11.031

Robertson, T., Döring, M., Guralnick, R., Bloom, D., Wieczorek, J., Braak, K., Otegui, J., Russell, L., Desmet, P., 2014. The GBIF Integrated Publishing Toolkit: Facilitating the efficient publishing of biodiversity data on the internet. PLOS ONE 9, e102623. https://doi.org/10.1371/journal.pone.0102623

Roemmich, D., Boehme, L., Claustre, H., Freeland, H., Fukasawa, M., Goni, G., Gould, W.G., Gruber, N., Hood, M., Kent, E., Lumpkin, R., Smith, S., Testor, P., 2010. Integrating the ocean observing system: Mobile platforms, in: Proceedings of OceanObs'09: Sustained Ocean Observations and Information for Society. Hall, J., Harrison, D.E. & Stammer, D., Venice, Italy, 21-25 September 2009, pp. 377–394. https://doi.org/10.5270/OceanObs09.pp.33

Rossby, H., 2016. Visualizing and Quantifying Oceanic Motion. Annual review of marine science 8. https://doi.org/10.1146/annurev-marine-122414-033849

Ruiz, J., Abascal, F.J., Bach, P., Baez, J.C., Cauquil4, P., Grande1, M., Krug, I., Lucas, J., Murua, H., Alonso, M.L.R., Sabarros, P.S., 2018. Bycatch of the European, and assocated flag, purse-seine tuna fishery in the indian ocean for the period 2008-2017 (No. IOTC-2018-WPEB14-15). IOTC Working Party on Ecosystems and Bycatch (WPEB), Cape Town, South Africa.

Saitoh, S.-I., Chassot, E., Dwivedi, Fonteneau, Kiyofuji, H., Kumari, Kuno, Matsumura, S., Platt, Raman, Sathyendranath, Solanki, H., Fumihiro, T., 2009. Remote sensing applications to fish harvesting. pp. 57–76.

Santos, B.S., Friedrichs, M.A.M., Rose, S.A., Barco, S.G., Kaplan, D.M., 2018a. Likely locations of sea turtle stranding mortality using experimentally-calibrated, time and space-specific drift models. Biological Conservation 226, 127–143. https://doi.org/10.1016/j.biocon.2018.06.029

Santos, B.S., Kaplan, D.M., Friedrichs, M.A.M., Barco, S.G., Mansfield, K.L., Manning, J.P., 2018b. Consequences of drift and carcass decomposition for estimating sea turtle mortality hotspots. Ecological Indicators 84, 319–336. https://doi.org/10.1016/j.ecolind.2017.08.064

Schneider, F., Parsons, S., Clift, S., Stolte, A., McManus, M.C., 2018. Collected marine litter — A growing waste challenge. Marine Pollution Bulletin 128, 162–174. https://doi.org/10.1016/j.marpolbul.2018.01.011

Schott, F.A., McCreary, J.P., 2001. The monsoon circulation of the Indian Ocean. Progress in Oceanography 51, 1–123. https://doi.org/10.1016/S0079-6611(01)00083-0

Schott, F.A., Xie, S.-P., McCreary Jr., J.P., 2009. Indian Ocean circulation and climate variability. Reviews of Geophysics 47. https://doi.org/10.1029/2007RG000245

Scott, G., Lopez, J., 2014. The use of FADs in tuna fisheries (Directorate-General for internal policies No. IP/B/PECH/IC/2013-123). European Union.

Scott, G.P., Lopez, J., 2014. The Use of Fads in Tuna Fisheries. Brussels: European parliament.

Sherman, P., Sebille, E. van, 2016. Modeling marine surface microplastic transport to assess optimal removal locations. Environ. Res. Lett. 11, 014006. https://doi.org/10.1088/1748-9326/11/1/014006

Simpson, J.J., 1992. Remote sensing and geographical information systems: Their past, present and future use in global marine fisheries. Fisheries Oceanography 1, 238–280.

Snouck-Hurgronje, J.E., Kaplan, D.M., Chassot, E., Maufroy, A., Gaertner, D., 2018. Fishing on floating objects (FOBs): how French tropical tuna purse seiners split fishing effort between GPS-monitored and unmonitored FOBs. Can. J. Fish. Aquat. Sci. 75, 1849–1858. https://doi.org/10.1139/cjfas-2017-0152

Stafford, R., Jones, P.J.S., 2019. Viewpoint – Ocean plastic pollution: A convenient but distracting truth? Marine Policy 103, 187–191. https://doi.org/10.1016/j.marpol.2019.02.003

Stelfox, M., Hudgins, J., Sweet, M., 2016. A review of ghost gear entanglement amongst marine mammals, reptiles and elasmobranchs. Marine Pollution Bulletin 111, 6–17. https://doi.org/10.1016/j.marpolbul.2016.06.034

Sudre, J., Maes, C., Garçon, V., 2013a. On the global estimates of geostrophic and Ekman surface currents. Limnology and Oceanography: Fluis and Environments 3, 1–20. https://doi.org/10.1215/21573689-2071927

Sudre, J., Maes, C., Garçon, V., 2013b. On the global estimates of geostrophic and Ekman surface currents. Limnology and Oceanography: Fluids and Environments 3, 1–20. https://doi.org/10.1215/21573689-2071927

Sudre, J., Morrow, R.A., 2008. Global surface currents: a high-resolution product for investigating ocean dynamics. Ocean Dynamics 58, 101. https://doi.org/10.1007/s10236-008-0134-9

Sun, C.L., Yeh, S.Z., Chang, Y.J., Chang, H.Y., Chu, S.L., 2013. Reproductive biology of female bigeye tuna Thunnus obesus in the western Pacific Ocean. J Fish Biol 83, 250–271. https://doi.org/10.1111/jfb.12161

Taconet, P., Chassot, E., Barde, J., 2018. Global monthly catch of tuna, tuna-like and shark species (1950-2015) aggregated by 1° or 5° squares (IRD level 2). https://doi.org/10.5281/zenodo.1164128

Tavares, D., de Moura, J., Merico, A., Siciliano, S., 2017. Incidence of marine debris in seabirds feeding at different water depths. Mar Pollut Bull 119, 68–73. https://doi.org/10.1016/j.marpolbul.2017.04.012

Taylor, G.I., 1921. Diffusion by Continuous Movements. Proceedings of the London Mathematical Society s2-20, 196–212. https://doi.org/10.1112/plms/s2-20.1.196

Tennekes, M., 2018. tmap: Thematic Maps in R. Journal of Statistical Software 84, 1--39. https://doi.org/10.18637/jss.v084.i06

Torres-Irineo, E., Gaertner, D., Chassot, E., Dreyfus-León, M., 2014a. Changes in fishing power and fishing strategies driven by new technologies: The case of tropical tuna purse seiners in the eastern Atlantic Ocean. Fisheries Research 155, 10–19. https://doi.org/10.1016/j.fishres.2014.02.017

Torres-Irineo, E., Gaertner, D., Chassot, E., Dreyfus-León, M., 2014b. Changes in fishing power and fishing strategies driven by new technologies: The case of tropical tuna purse seiners in the eastern Atlantic Ocean. Fisheries Research 155, 10–19. https://doi.org/10.1016/j.fishres.2014.02.017

Trinanes, J.A., Olascoaga, M.J., Goni, G.J., Maximenko, N.A., Griffin, D.A., Hafner, J., 2016. Analysis of flight MH370 potential debris trajectories using ocean observations and numerical model results. Journal of Operational Oceanography 9, 126–138. https://doi.org/10.1080/1755876X.2016.1248149

United Nations Environment Programme, 2017. Towards a pollution-free planet: background report. United Nations Environment Programme, Nairobi, Kenya.

United Nations Environment Programme, 2005. Marine letter, an analytical overview.

van Sebille, E., Aliani, S., Law, K.L., Maximenko, N., Alsina, J.M., Bagaev, A., Bergmann, M., Chapron, B., Chubarenko, I., Cózar, A., Delandmeter, P., Egger, M., Fox-Kemper, B., Garaba, S.P., Goddijn-Murphy, L., Hardesty, B.D., Hoffman, M.J., Isobe, A., Jongedijk, C.E., Kaandorp, M.L.A., Khatmullina, L., Koelmans, A.A., Kukulka, T., Laufkötter, C., Lebreton, L., Lobelle, D., Maes, C., Martinez-Vicente, V., Maqueda, M.A.M., Poulain-Zarcos, M., Rodríguez, E., Ryan, P.G., Shanks, A.L., Shim, W.J., Suaria, G., Thiel, M., Bremer, T.S. van den, Wichmann, D., 2020. The physical oceanography of the transport of floating marine debris. Environ. Res. Lett. 15, 023003. https://doi.org/10.1088/1748-9326/ab6d7d

van Sebille, E., Griffies, S.M., Abernathey, R., Adams, T.P., Berloff, P., Biastoch, A., Blanke, B., Chassignet, E.P., Cheng, Y., Cotter, C.J., Deleersnijder, E., Döös, K., Drake, H.F., Drijfhout, S., Gary, S.F., Heemink, A.W., Kjellsson, J., Koszalka, I.M., Lange, M., Lique, C., MacGilchrist, G.A., Marsh, R., Mayorga Adame, C.G., McAdam, R., Nencioli, F., Paris, C.B., Piggott, M.D., Polton, J.A., Rühs, S., Shah, S.H.A.M., Thomas, M.D., Wang, J., Wolfram, P.J., Zanna, L., Zika, J.D., 2018. Lagrangian ocean analysis: Fundamentals and practices. Ocean Modelling 121, 49–75. https://doi.org/10.1016/j.ocemod.2017.11.008

Villas Bôas, A.B., Ardhuin, F., Ayet, A., Bourassa, M.A., Brandt, P., Chapron, B., Cornuelle, B.D., Farrar, J.T., Fewings, M.R., Fox-Kemper, B., Gille, S.T., Gommenginger, C., Heimbach, P., Hell, M.C., Li, Q., Mazloff, M.R., Merrifield, S.T., Mouche, A., Rio, M.H., Rodriguez, E., Shutler, J.D., Subramanian, A.C., Terrill, E.J., Tsamados, M., Ubelmann, C., van Sebille, E., 2019. Integrated Observations of Global Surface Winds, Currents, and Waves: Requirements and Challenges for the Next Decade. Frontiers in Marine Science 6, 425. https://doi.org/10.3389/fmars.2019.00425

Viñuales-Solé, J., 1996. Los Etruscos amantes de la vida de Italia, Time Life Books Inc. Time Life Books Inc, Ediciones Folio, SA, Barcelona.

Warton, D.I., Wright, I.J., Falster, D.S., Westoby, M., 2006. Bivariate line-fitting methods for allometry. Biological Reviews 81, 259–291. https://doi.org/10.1017/S1464793106007007

Woodruff, S.D., Slutz, R.J., Jenne, R.L., Steurer, P.M., 1987. A Comprehensive Ocean-Atmosphere Data Set. Bulletin of the American Meteorological Society 68, 1239–1250. https://doi.org/10.1175/1520-0477(1987)068<1239:ACOADS>2.0.CO;2

Yaremchuk, M., Spence, P., Wei, M., Jacobs, G., 2016. Lagrangian predictability in the DWH region from HF radar observations and model output. Deep Sea Research Part II: Topical Studies in Oceanography, The Gulf of Mexico Ecosystem - before, during and after the Macondo Blowout 129, 394–400. https://doi.org/10.1016/j.dsr2.2013.05.035

Yellen, J.E., Brooks, A.S., Cornelissen, E., Mehlman, M.J., Stewart, K., 1995. A middle stone age worked bone industry from Katanda, Upper Semliki Valley, Zaire. Science 268, 553–556. https://doi.org/10.1126/science.7725100

Zudaire, I., Moreno, G., Murua, J., Murua, H., Tolotti, M.T., Roman, M., Hall, M., Lopez, J., Grande, M., Merino, G., Escalle, L., Hamer, P., Basurko, O.C., Capello, M., Dagorn, L., Ramos, M.L., Abascal, F.J., Báez, J.C., Pascual-Alayón, P., Déniz, S., Santiago, J., 2021. Biodegradable DFADs: Current Status and Prospects | IOTC (No. IOTC-2021-WGFAD02-09).

Zudaire, I., Santiago, J., Grande, M., Murua, H., Adam, P.-A., Nogués, P., Collier, T., Morgan, M., Kahn, N., Baguette, F., Moron, J., Moniz, I., Herrera, M., 2018. FAD Watch: a collaborative initiative to minimize the impact of FADs in coastal ecosystems.

Zudaire, I., Tolotti, M., Murua, J., Capello, M., Andrés, M., Basurko, Krug, I., Grande, M., Arregui, I., Uranga, J., Goñi, N., Sabarros, P., Ferarios, J.M., Ruiz, J., Baidai, Y., Floch, L., Ramos, M., Báez, J., Abascal, F., Moreno, G., Santiago, J., Dagorn, L., Arrizabalaga, H., Murua, H., 2020. Testing designs and identify options to mitigate impacts of drifting FADs on the ecosystem : final report. (No. Second Interim Report). European Commission.

Index des illustrations

Introduction générale

Chapitre 1

Chapitre 2

Chapitre 3

Chapitre 4

Index des tableaux

Publications découlant de ce travail de thèse

Articles "peer-reviewed" publiés:

*Imzilen T, Lett C, Chassot E, Kaplan DM. 2021. Spatial management can significantly reduce dFAD beachings in Indian and Atlantic Ocean tropical tuna purse seine fisheries. Biological Conservation **254**:108939. https://doi.org/10.1016/j.biocon.2020.108939* (Chapitre 1)

*Imzilen T, Chassot E, Barde J, Demarcq H, Maufroy A, Roa-Pascuali L, Ternon J-F, Lett C. 2019. Fish aggregating devices drift like oceanographic drifters in the near-surface currents of the Atlantic and Indian Oceans. Progress in Oceanography **171**:108–127. https://doi.org/10.1016/j.pocean.2018.11.007* (Chapitre 3)

Article en révision :

Imzilen T, Lett C, Chassot E, Maufroy A, Goujon M, Kaplan DM. Preventing the loss of derelict drifting fish aggregating devices through recovery at sea. Nature Sustainability (version révisée). (Chapitre 2)

Article soumis:

Imzilen T, Kaplan DM, Barrier N, Lett C. Simulations of drifting fish aggregating device (dFAD) trajectories in the Atlantic and Indian Oceans. Progress in Oceanography (soumis).(Chapitre4)

Conférences et groupes de travail:

*Imzilen T, Lett C, Chassot E and Kaplan DM. 2021 October. Spatial management can significantly reduce dFAD beachings in Indian and Atlantic Ocean tropical tuna purse seine fisheries. IOTC-2021-WGFAD02-07(*https://www.iotc.org*)*

Imzilen T, Lett C, Chassot E and Kaplan DM. 2021 May. Spatial options for reducing dFAD loss and beaching. 71st TUNA CONFERENCE AGENDA. https://www.tunaconference.org/proceedings-

Imzilen T, Lett C, Chassot E and Kaplan DM. 2019. Global analysis of beaching events in French dFAD trajectory data for impacts on sensitive habitats and proximity to ports. 2nd Meeting of the Joint Tuna RFMOs Working Group on FADs- 08-10 May, 2019 - San Diego, California, USA (https://www.iattc.org)

Résumé

La pollution marine est l'une des principales menaces qui pèsent sur les océans. Une partie importante des déchets et polluants marins provient des activités maritimes, en particulier la pêche, en raison d'équipements jetés, abandonnés, ou perdus. La pêche au thon tropical à la senne contribue à ce problème en construisant et déployant un nombre important de Dispositifs de Concentration de Poissons dérivants (DCP), dont de nombreux sont perdus ou s'échouent en endommageant des habitats fragiles tels que les récifs coralliens. L'objectif général de cette thèse est de proposer trois mesures pour atténuer ces problèmes dans les Océans Indien et Atlantique.

Tout d'abord, l'interdiction de déployer des DCP dans les zones risquées permettrait d'éviter un nombre considérable d'échouages. Entre 20% et 40% des échouages pourraient être évités si les déploiements étaient interdits dans l'Océan Indien au sud de 8°N de latitude, dans la zone somalienne en hiver, mais également dans la zone située à l'Ouest des Maldives en été, et au niveau de la zone intertropicale longeant la côte Ouest de l'Afrique pour l'Océan Atlantique. Ensuite, l'identification de régions où les DCP sortent massivement des zones de pêches, ainsi que le passage d'un grand nombre de DCP à proximité de ports, ont mis en évidence que la mise en place d'un programme de récupération des DCP en mer serait efficace pour diminuer considérablement leur perte. Ces deux mesures (interdiction de déploiement et récupération en mer) apparaissent complémentaires puisque les zones qui bénéficieraient moins du premier programme seraient davantage protégées par le second, en particulier au niveau du Nord-Ouest de l'Océan Indien et du Nord du Golfe de Guinée. Enfin, l'évaluation d'un outil de transport Lagrangien pour simuler les trajectoires des DCP a montré que l'efficacité de cet outil à l'échelle du bassin est relativement bonne dans les deux océans, que la capacité à simuler les trajectoires est meilleure dans l'Océan Indien que dans l'Océan atlantique, et que cette capacité dépend de la profondeur et de la résolution spatiale du produit de courant de forçage utilisé. Cet outil pourrait être utilisé en mode opérationnel dans le futur pour anticiper les trajectoires des DCP pouvant conduire à une perte ou à un échouage et donc être utilisé comme un programme de mitigation complémentaire aux deux autres programmes. Les résultats obtenus au cours de ces différents travaux constituent ainsi une base solide pour définir de nouvelles recommandations permettant d'atténuer les risques de perte et d'échouage des DCP et ainsi contribuer à la préservation de nos océans et de nos littoraux.

Mots clés : Pollution marine, Océan Atlantique, Océan Indien, Débris de pêche, Thons tropicaux, Dispositifs de Concentration de Poissons, courants océaniques, Transport Lagrangien

Abstract

Marine pollution has increased over time, becoming a major source of concern. A non-negligible proportion of these waste and pollutants are from sea-based sources, especially fisheries, due to derelict fishing equipment. Tropical tuna purse seine fishing vessels contribute to this problem by deploying large numbers of drifting Fish Aggregating Devices (dFADs), as a significant portion of these floating objects eventually end up derelict, potentially contributing to marine pollution and threatening sensitive ecosystems such as coral reefs. The general objective of this thesis is to use scientific analyses of dFAD trajectory and fishing data to propose mitigation measures to reduce these problems in the Indian and Atlantic Oceans. First, it is demonstrated that prohibiting deployments in areas most likely to lead to beachings has the potential to be effective for reducing the beaching rate. Results indicate that 21% to 40% of beachings could be prevented if deployments were prohibited in high risk areas, roughly delimited by the areas south of 8°S latitude, the Somali zone in winter, and the western Maldives in summer for the Indian Ocean, and in an elongated strip of areas adjacent to the western African coast for the Atlantic Ocean. Next, the identification of areas within the fishing ground where most dFADs exit, as well as the passage of a large number of dFADs close to ports, provides support for the implementation of recovery programs to collect these dFADs at sea and reduce their loss. These two measures appear to be complementary since areas predicted to benefit less from closures are more likely to benefit from recovery programs, particularly in the northwestern Indian Ocean and the northern Gulf of Guinea. Finally, the evaluation of a Lagrangian transport tool to simulate the trajectories of dFADs shows that the efficiency of this tool at the basin scale is relatively good in the two oceans, that the accuracy to simulate the trajectories is better in the Indian Ocean than in the Atlantic Ocean, and that this accuracy depends on the depth and the spatial resolution of the forcing currents product used. This tool could be used in an operational mode in the future to anticipate the trajectories of dFADs that could lead to loss or beaching and therefore be used as a complementary mitigation program to the other two measures described above (prohibiting deployments and recovery at sea). The results obtained during these various works thus constitute a solid basis to define new recommendations to mitigate the risks of loss and beachings of dFADs and thus contribute to the preservation of our oceans and our coasts.

Keywords : Marine pollution; Atlantic Ocean; Indian Ocean; Fishing debris; Tropical Tuna; fish aggregating devices; Ocean currents; Lagrangian transport